SPATIO-TEMPORAL PROBABILISTIC METHODOLOGY TO ESTIMATE LOCATION-SPECIFIC LOSS-OF-COOLANT ACCIDENT FREQUENCIES FOR RISK-INFORMED ANALYSIS OF NUCLEAR POWER PLANTS

BY

NICHOLAS O'SHEA

THESIS

Submitted in partial fulfillment of the requirements
for the degree of Master of Science in Nuclear, Plasma, and Radiological Engineering
in the Graduate College of the
University of Illinois at Urbana-Champaign, 2017

Urbana, Illinois

Master's Committee:

Assistant Professor Zahra Mohaghegh, Chair
Professor Rizwan Uddin

ABSTRACT

The United States Nuclear Regulatory Commission (NRC) has promoted the use of Probabilistic Risk Assessment (PRA) in nuclear regulatory activities. Since loss-of-coolant accidents (LOCAs) are critical initiating events for many PRA applications, the NRC has taken steps towards the quantification of LOCA frequencies for use in risk-informed applications. This research develops the Spatio-Temporal Probabilistic methodology to explicitly incorporate the underlying physics of failure mechanisms into the location-specific estimation of LOCA frequencies that are required for risk-informed regulatory applications such as risk-informed resolution of generic Safety Issue 191 (GSI-191).

The essence of the risk-informed resolution of GSI-191 is that location-specific LOCA frequencies drive the risk. The most recent NRC-sponsored estimations of LOCA frequencies were developed through an expert elicitation approach, provided in NUREG-1829. These estimations provided an *implicit* incorporation of underlying physics, space, and time. In support of the South Texas Project Nuclear Operating Company (STPNOC) risk-informed pilot project to resolve GSI-191, Fleming and Lydell developed a study which laid the groundwork for the location-specific estimations of LOCA frequencies. This research performs a critical review and a step-by-step quantitative verification of Fleming and Lydell's methodology and, thus, two key methodological gaps are identified: (a) lack of inclusion of non-piping reactor coolant system components, and (b) lack of explicit incorporation of the underlying physics of failure that lead to the occurrence of a LOCA. To address these gaps, first, this research qualitatively examines the significance of including the contributions of non-piping components into the estimations of LOCA frequencies by conducting industry-academia evidence seeking and screening processes.

Then, the Spatio-Temporal Probabilistic methodology is developed that can be used to quantitatively compare non-piping and piping components with respect to LOCA frequencies. The proposed Spatio-Temporal Probabilistic methodology also integrates the following two types of modeling:

(1) The Markov modeling technique to depict the renewal processes of components' repair due to periodic maintenance after degradations;

(2) Probabilistic Physics of failure (PPoF) models to explicitly incorporate the failure mechanisms, associated with the location and age of components, into the estimation of LOCA frequencies. PPoF models integrate the underlying mechanisms related to degradation into the Markov modeling technique and, subsequently, into location-specific LOCA frequency estimations.

In most of Markov models developed in this area of research, transition rates are developed using solely data-driven approaches and utilizing service data. The main problems with the Markov models with the solely data-driven transition rates are (1) inaccuracy due to insufficient data and (2) the lack of explicit connections with location-specific physics of failure mechanisms associated with transition rates. There is only one existing research that combines the Markov modeling technique with a stress-strength model of erosion corrosion for the piping components of Pressurized Heavy Water Reactors (PHWR); however due to the underlying assumptions of the methodology, this study does not adequately provide explicit incorporation of physical factors associated with locations. The Spatio-Temporal probabilistic methodology is the first research that combines the Markov technique with PPoF models for LOCA frequency estimations and, has four key tasks including:

- Task #1: Defining Markov States of Degradation
- Task #2: Modeling and Quantification of the Transition Rates of Degradation
  - Task # 2.1: Developing and quantifying physics of failure causal models
  - Task #2.2: Propagating uncertainties in the physics of failure causal models to develop Probabilistic Physics of failure (PPoF) models
  - Task #2.3: Calculating transition rates of degradation based on the output of Probabilistic Physics of failure (PPoF) models
  - Task # 2.4: Bayesian integration of the estimated transition rate from PPoF models and the ones from solely data-oriented approaches
- Task #3: Modeling and Quantification of the Transition Rates of Repair
- Task #4: Developing the Time-dependent Distributions of State Probabilities

The Spatio-Temporal Probabilistic methodology provides the possibility for explicitly including the effects of location-specific causal factors, such as operating conditions (e.g., temperature, pressure, pH), maintenance quality, and material properties (e.g., yield strength and corrosion resistance) on the probability of LOCA occurrence. This methodology is beneficial, not only for estimation of location-specific LOCA frequencies, but also for incorporation of spatio-temporal physics of failure into Probabilistic Risk Assessment (PRA); therefore, it helps advance risk estimation and risk prevention. The explicit incorporation of failure mechanisms helps more accurately estimate the likelihood of LOCA occurrences, dealing with limited historical data. Additionally, the explicit incorporation of the causal factors enables the use of sensitivity analyses, which allow the physical causal factors to be ranked in order of their risk significance. Ranking of causal factors helps optimize maintenance practices by indicating the most resource-efficient methods to reduce risks.

To show the feasibility, the spatio-temporal probabilistic methodology is implemented to examine the effects of Stress Corrosion Cracking (SCC) on the rupture probability of steam generator tubes. This case study demonstrates the comparative capabilities of the methodology by showing the variation in rupture probability based on the selection of Stainless Steel and Alloy 690 materials for fabrication of the expansion-transition region of the steam generator tubes. Although the tasks in this case study are explained based on SCC, which is a dominant mechanism associated with LOCA in nuclear power plants, the Spatio-Temporal Probabilistic methodology can be applied for other failure mechanisms (e.g., wear, creep) and for any high-consequence industry that deals with containment of flowing liquids or gases, such as the oil and gas industry.

ACKNOWLEDGEMENTS

I would like to express deep gratitude to the following individuals and organizations who made this research possible (in alphabetical order):

Department of Energy Office of Nuclear Energy:

This material is based upon work supported under an Integrated University Program Graduate Fellowship. Any opinions, findings, conclusions or recommendations expressed in this publication are those of the author and do not necessarily reflect the views of the Department of Energy Office of Nuclear Energy.

Mr. Karl Fleming:

Thank you for providing information regarding your methodology.

Mr. Ernie Kee:

Thank you for providing me with valuable industry insight. This research could not have been performed without your help as an expert reviewer for the investigative research regarding the non-piping components. Additionally, your insights enabled my research to be advanced with a practical industry perspective.

Mr. Bengt Lydell:

Thank you for providing information regarding your methodology.

Assistant Professor Zahra Mohaghegh:

I would like to express my sincerest gratitude to you, as my advisor, for the continuous support of me while I was performing this research. This research could not be possible without your patience, motivation, knowledge, and guidance. Thank you for all your intellectual support and encouragement.

Nuclear Plasma and Radiological Engineering Department at the University of Illinois Urbana-Champaign:

Thank you for being the home for my undergraduate and graduate studies.

Dr. Seyed Reihani:

Thank you for the help and guidance through the entire research process. Thank you for not only being a reviewer for the investigative research but also for providing your valuable insight to advance every stage of this research.

The Socio-Technical Risk Analysis (SoTeRiA) Research Laboratory at the University of Illinois Urbana-Champaign (http://soteria.npre.illinois.edu):

Thank you for supporting this research by creating a welcoming research environment and for providing constructive criticism through the whole process. Special thanks to the undergraduate researcher, Ethan Graven, for his help on Chapter 4 by supporting the runs of the code on the campus cluster; to Ph.D. student, Justin Pence, for his collaboration on the generation of Data-Theoretic idea in Chapter 4; to undergraduate intern, John Simmons, for his support on the evidence-seeking activities related to Chapter 3.

South Texas Project Nuclear Operating Company:

Thank you for providing data for the implementation of the methodology and for supporting the risk-informed GSI-191 project, which generated valuable insight for this research.

Professor Jim Stubbins

Your feedback and criticisms, as well as the time you dedicated to read and review my research as the head of the department are very much appreciated.

Professor Rizwan Uddin:

Your feedback and criticisms, as well as the time you dedicated to read and review my research as a member of my Master's committee are very much appreciated.

Finally, I would like to thank my family and friends for their unending love and support.

CONTENTS

LIST OF ACRONYMS

ANS	American Nuclear Society
ASME	American Society of Mechanical Engineers
BWR	Boiling Water Reactor
CBP	Conditional Break Probability
CCF	Common Cause Failure
CDF	Core Damage Frequency
CPR	Crack Propagation Rate
CRP	Conditional Rupture Probability
CVCS	Chemical Volume and Control System
D&C	Design and Construction Flaws
DEGB	Double-Ended Guillotine Break
DM	Damage Mechanism
E-C	Erosion-Corrosion
ECCS	Emergency Core Cooling System
EPRI	Electric Power Research Institute
ET	Event Tree
FT	Fault Tree
GRP	Generalized Renewal Process
HRA	Human Reliability Analysis
IE	Initiating Event
LB	Large Break
LERF	Large Early Release Frequency
LOCA	Loss-of-Coolant Accident
LSF	Limit State Function
MB	Medium Break
NHPP	Non-Homogenous Poisson Process

NPP	Nuclear Power Plant
NPSH	Net Positive Suction Head
NRC	United States Nuclear Regulatory Commission
PFM	Probabilistic Fracture Mechanics
PoF	Physics-of-Failure
PORV	Power-Operated Relief Valve
PPoF	Probabilistic Physics-of-Failure
PRA	Probabilistic Risk Assessment
PWR	Pressurized Water Reactor
PWSCC	Primary Water Stress Corrosion Cracking
PZR	Pressurizer
QHO	Quantitative Health Objective
RCP	Reactor Coolant Pump
RCS	Reactor Coolant System
RHRS	Residual Heat Removal System
RIDM	Risk-Informed Decision-Making
RI-ISI	Risk-Informed In-Service Inspection
RP	Renewal Process
RSS	Reactor Safety Study
SB	Small Break
SCC	Stress Corrosion Cracking
SEM	Standard Error of the Mean
SG	Steam Generator
SIR	Safety Injection and Recirculation Systems
SIS	Safety Injection System
SoTeRiA	Socio-Technical Risk Analysis Laboratory
SS	Stainless Steel
STPNOC	South Texas Project Nuclear Operating Company

TF	Thermal Fatigue

CHAPTER 1 : INTRODUCTION

1.1 INTRODUCTION AND STATEMENT OF OBJECTIVES

The United States Nuclear Regulatory Commission (NRC) promotes the use of Probabilistic Risk Assessment (PRA) in nuclear regulatory activities[1]. Section 1.2 of this thesis consists of the background on PRA and, Section 1.3 explains its application to regulatory Risk-Informed Decision-Making (RIDM). Since loss-of-coolant accidents (LOCAs) are critical initiating events for many PRA applications, the NRC has taken steps towards the quantification of LOCA frequencies [2, 3] for use in risk-informed applications. This research develops the Spatio-Temporal Probabilistic methodology to explicitly incorporate the underlying physics of failure mechanisms into the location-specific estimation of LOCA frequencies that are required for risk-informed regulatory applications such as the risk-informed resolution of Generic Safety Issue 191 (GSI-191)[4]. Section 1.4.2 briefly explains the South Texas Project Nuclear Operating Company (STPNOC) risk-informed resolution to this issue.

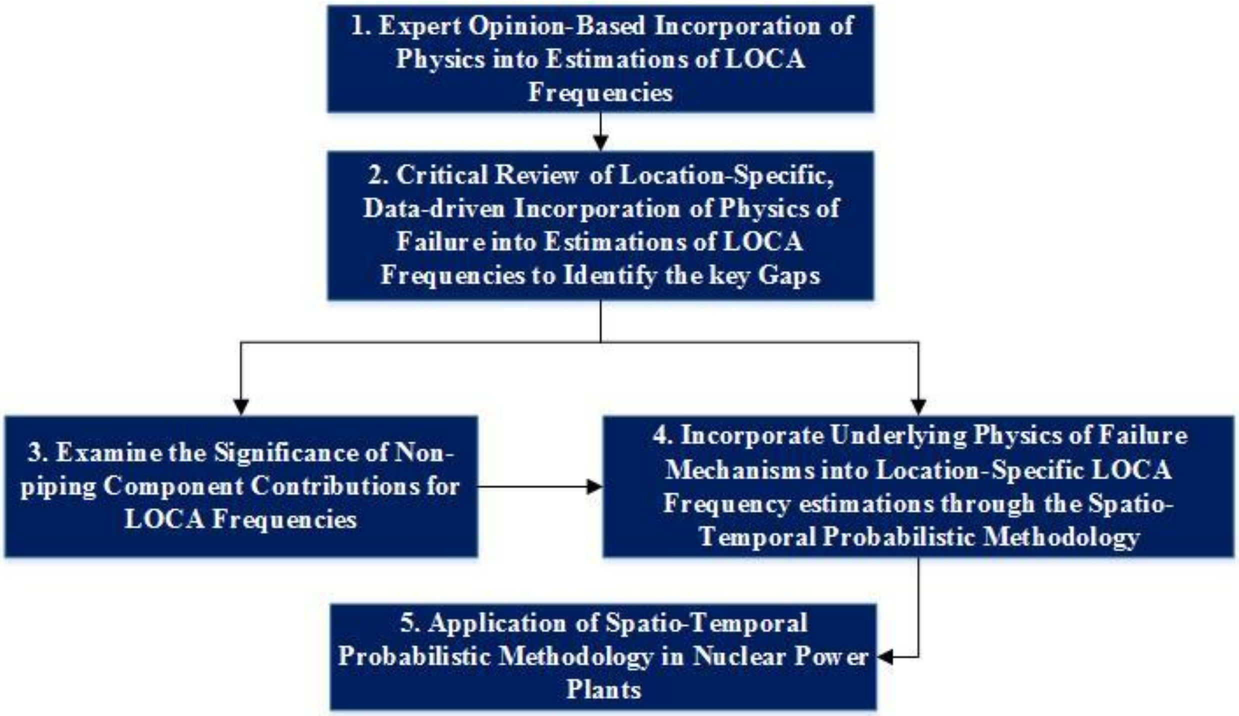

Figure 1.1 Roadmap of the Research

The premise of the risk-informed resolution of GSI-191 is that location-specific LOCA frequencies drive the risk of GSI-191 related failure. Therefore, Step #1 of the roadmap of this research, presented in Figure 1.1, begins with the most recent NRC-sponsored estimations of LOCA frequencies provided in NUREG-1829. These estimations are only *implicit* functions of underlying physics, space, and time. This indicates that the experts who developed the NUREG-1829 estimations understood how the underlying physical failure mechanisms could cause the occurrence of a LOCA; however, they did not develop an *explicit* model to incorporate these effects. The experts considered how LOCA frequencies changed, based on both the reactor-age and the location within the reactor coolant system (RCS), but they did not provide an *explicit* model incorporating these spatio-temporal effects. The experts performing the analysis documented in NUREG-1829 provided "multipliers" for the distributions of LOCA frequencies. These multipliers allow for the estimates to be adjusted from 25 years of reactor life to 40- or 60-

year estimates; however, these multipliers mask the mechanisms that, over time, change the LOCA frequencies. In other words, the temporal effects on LOCA frequencies are only *implicitly* considered. The NUREG-1829 estimations of LOCA frequencies are provided as a function of flow rates of escaping coolant, which are then converted to component break size. These frequencies represent a simple summation of the contributions to LOCA frequencies from all locations across the RCS, but the estimations of LOCA frequencies provided in NUREG-1829 do not *explicitly* provide the contribution for each individual location to the total of LOCA frequencies across the RCS. While the experts incorporated their knowledge of how contributions to LOCA frequencies vary by location in the RCS, this knowledge of spatial variation is only *implicitly* incorporated into the final NUREG-1829 results. A brief history of NRC-sponsored estimations of LOCA frequencies is provided in Section 1.4.3.

Step #2 of the roadmap of this research, presented in Figure 1.1, focuses on the critical review of the location-specific estimation of LOCA frequencies, developed by Fleming and Lydell[5] for the STPNOC risk-informed resolution of GSI-191. Fleming and Lydell's study laid the groundwork for the *explicit* incorporation of both underlying failure mechanisms and spatial variation into the estimation of LOCA frequencies. Fleming and Lydell, however, used a solely data-driven approach for the incorporation of the underlying failure mechanisms at each location across the RCS. Fleming and Lydell developed surrogate failure rates for each of the major failure mechanisms that affected a PWR RCS by attributing historical operating experience to dominant failure mechanisms across broad categories of welds. The temporal variation of LOCA frequencies in Fleming and Lydell's work was *implicitly* considered because they used the same generic "multipliers" developed by the experts for the NUREG-1829 elicitation. The probability of an RCS component experiencing a rupture changes as components degrade and, as they degrade, they are more likely to rupture and make an increased contribution to the estimation of LOCA frequencies. Therefore, to *explicitly* incorporate this temporal variation into LOCA frequencies, the states of degradation of the components in the RCS need to be considered.

Chapter 2 summarizes a critical review on the location-specific, data-driven incorporation of physics of failure mechanisms into the estimation of LOCA frequencies developed by Fleming & Lydell. The step-by-step quantitative verification of the results, critical review of the methodology, and implementation are provided. The author's contributions to the improvement of the Fleming & Lydell's report are detailed and the methodological gaps are identified and cover the (a) lack of incorporation of non-piping RCS components, (b) the implicit incorporation of reactor-age and lack of explicit incorporation of time and space, and the lack of explicit incorporation of the underlying physics of failure that lead to the occurrence of a LOCA.

Step #3 of the roadmap of this research, presented in Figure 1.1, further analyzes the criticality of one of the gaps, which is the lack of incorporating non-piping RCS components. The results of this investigation are reported in Chapter 3 of the thesis. Chapter 3 examines an evidence-seeking procedure and expert elicitation process to determine the significance of the contributions of non-piping reactor coolant system (RCS) components to the estimation of LOCA frequencies that was first presented in [6, 7]. Some estimations of LOCA frequencies have included contributions from non-piping RCS components[3], while other estimations have focused on the contributions from RCS piping components[2, 5].

Step #4 of the roadmap of this research, presented in Figure 1.1, focuses on other gaps in Fleming & Lydell's approach by developing the spatio-temporal probabilistic methodology which *explicitly* incorporates underlying physical failure mechanisms into the estimation of location-specific LOCA frequencies. In this methodology, the Markov modeling technique, which is based on the renewal process theory, is integrated with Probabilistic Physics of Failure models to estimate RCS LOCA frequencies as a function of location and age and with considerations of periodic degradation and repair phenomena. This idea was first presented in [8]. Probabilistic Physics of Failure models are used to develop a probability model directly from the physical failure mechanisms, building off the work presented in [9]. The underlying physics replace the need for statistical data[10, 11]. The methodology enables the effects of operating conditions, maintenance programs, and material selection to be compared with respect to their contributions to LOCA frequencies. This methodology will assist with the generation of a more efficient prevention strategy by identifying the most risk-significant causal factors. Improved prevention strategies will lead to more efficient maintenance programs allowing for a more efficient allocation of resources for improving safety and increasing system performance. Chapter 4 of this thesis explains the spatio-temporal probabilistic methodology.

Step #5 of the roadmap of this research, presented in Figure 1.1, focuses on a case study for the implementation of the spatio-temporal probabilistic methodology to examine the effects of stress corrosion cracking (SCC) on the rupture probability of steam generator tubes. This case study demonstrates the comparative capabilities of the methodology by showing the variation in rupture probability based on the selection of Stainless Steel and Alloy 690 materials for the fabrication of the expansion-transition region of the steam generator tubes. Chapter 5 of this thesis demonstrates the case study and its results. Chapter 6 of the thesis covers the conclusions and makes recommendations for the direction of future work.

1.2 PROBABILISTIC RISK ASSESSMENT

The NRC relies on PRA as one of the main pillars of its risk-informed regulatory and oversight functions[12, 13]. PRA (summarized in WASH-1400, also known as the Reactor Safety Study (RSS)[14] is a systematic methodology used to quantify the risks, in terms of frequencies of catastrophic failures, associated with complex engineering systems that are sometimes referred to as a system of systems. A nuclear power plant (NPP) is one example of a complex system of systems.

The PRA methodology integrates design and operation aspects of an NPP in a logical framework that, when solved, helps provide information for analyzing plant-specific and generic safety issues[15]. PRA can be developed down to individual system components at different levels of granularity. PRA helps disclose scenarios of events requiring analysis, as well as the sequences of events contributing to risk in terms of core damage frequency, large early release frequency, and property damage, injury, and death frequencies. The most common definition of risk, the triplet definition, asks three questions [16]:

- What can go wrong?
- What is the likelihood?
- What are the consequences?

Based on the triplet definition of risk, risk can be calculated as a frequency by using Equation (1.1) [16]:

$$Risk(R) = Frequency(f) \cdot Consequence(C) \tag{1.1}$$

Kaplan and Garrick[16] caution that Equation (1.1) may be misleading. By multiplying the frequency and consequence of events, a low-probability high-damage scenario is equivalent to a high-probability low-damage scenario quantitatively. These cases are qualitatively quite different, however, since the risks calculated may contain multiple scenarios of varying frequencies and consequences and these scenarios would generate a distribution of risk. Equation (1.1) would only provide an expected or average value of the distribution. Therefore, it might be beneficial to think of and describe risk as being comprised of frequencies and consequences, and to keep these two elements separate[16].

Since the commercial nuclear power industry has a very good safety record, it does not have a large database of events available for the purpose of quantifying accident scenario frequencies for use in Equation (1.1). Therefore, the assessment of plant design, operation, and safety is accomplished by identifying the sequences of potential events that dominate risk. The standard approach for modeling the possible sequences of events is to use event trees (ETs). ETs are inductive models that follow a chronological sequence of events that may lead to undesirable consequences. In other words, ETs implicitly incorporate time into the model of events leading to scenarios. The first event in an ET is known as the initiating event (IE). Once the analyst has become familiarized with the plant design and method of operation, the initiating events are defined and grouped. One type of initiating events is a loss-of-coolant accident (LOCA). After the initiating event occurs, the ET models a series of “top events” to determine to which “end state” the system will proceed. End states for PRAs of NPPs generally range from “no damage” to “maximum core damage”[17]. The event tree is functionalized using Boolean logic, which means that each top event has a probability of occurrence. The success or failure of each event determines which branching of the ET is to be followed and, consequently, which end state the system will reach. Separate event trees are generally constructed for each initiating event.

The probability for the occurrence of each top event in the ET must be quantified to determine the overall frequency for each of the end states. One approach to quantify the top event probability is to use a statistical estimate from available data. There is often insufficient data to draw a reliable statistical estimate; therefore, the system or sub-system associated with each top event can be modeled as a summation of its components. The classical approach for modeling the components of a system is to develop fault trees (FTs). FTs are deductive models that use Boolean logic gates, primarily “AND” and “OR” gates, to generate logical statements regarding the failure of a system. The failure of the system will correspond to the occurrence (failure) or nonoccurrence (success) of a top event. FTs are used to break-down the analysis of complex systems, for which there are insufficient data to develop a failure probability, into the components for which there are sufficient data available [18]. An example of ET and a corresponding FT can be found in Figure 1.2.

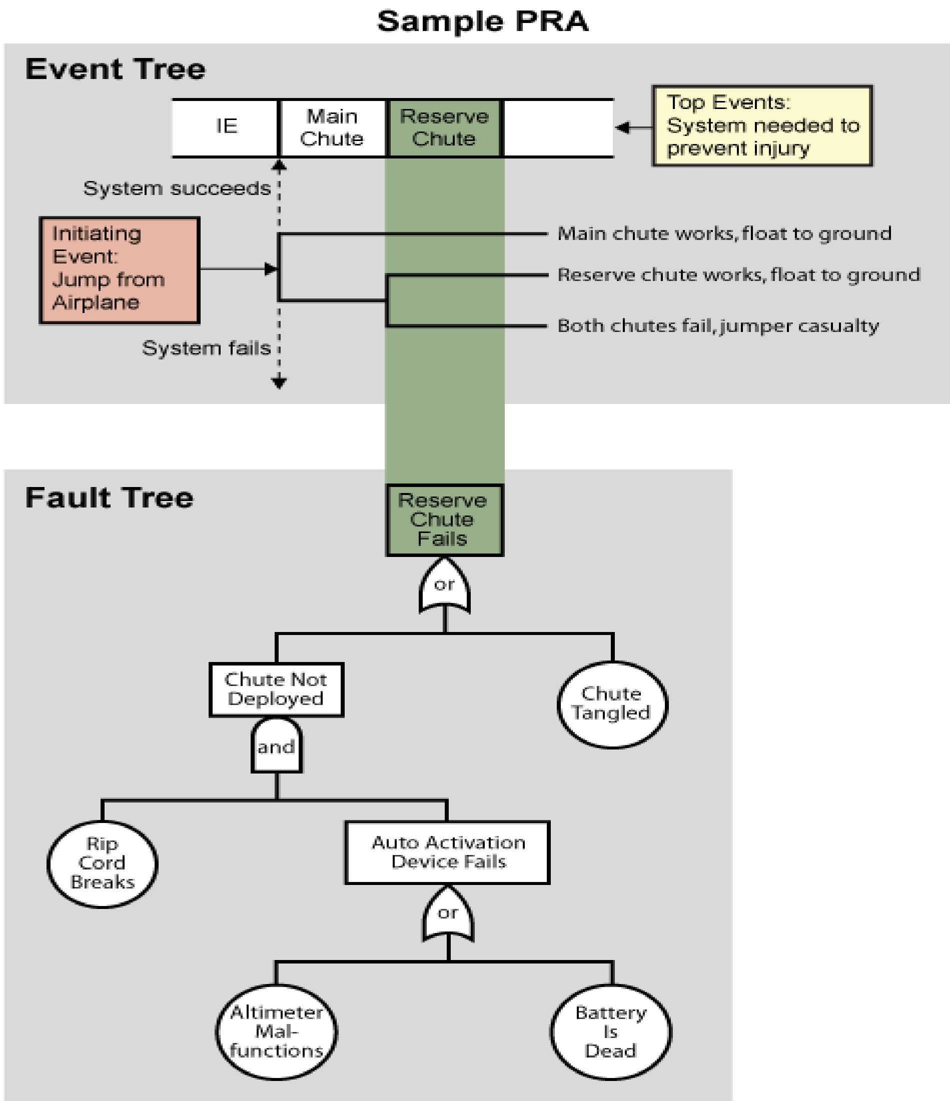

Figure 1.2 Event Tree and Connected Fault Tree Example [19]

It is important to note that the use of ETs and FTs will provide “surrogate frequencies” for each end state. Since there are insufficient data available to draw a statistical estimation of these end state frequencies, the surrogate frequencies are extracted from information from the components that build the system (or from partially relevant information utilizing Bayesian analysis) and are connected through a logical framework. However, the development of the surrogate frequencies has an additional benefit. By modeling the system at the component level, the contributions from individual components are no longer grouped under the performance of the system. This enables to the modeler to see which components make the most significant contributions to the end state frequencies.

Fault trees must be constructed in the context of the evaluation being performed. The depth of the fault tree analysis depends on the level of component or sub-system data available. The structure of the fault trees depends on how failure dependence between components is addressed in the analysis. Identification and analysis of dependent failures are extremely important in PRA studies, because such dependencies can increase the frequency of multiple failures; therefore, dependent failures must be considered throughout the probabilistic analysis[15]. PRA studies, through common-cause failure (CCF) analysis[20], are capable of modeling those dependent failure mechanisms that create an increase in overall risk.

Past PRAs have shown the importance of the incorporation of operator error. This error should be included in the system analysis to ensure that the true value of risk for an NPP is determined. Incorporation of operator error is performed using human reliability analysis (HRA). Error due to human action can significantly contribute to the overall risk experienced in a power plant[21].

The incorporation of uncertainty into PRA is integral. There are uncertainties associated with every step of a PRA and some of them may be significant. These uncertainties can stem from the available data at any level of analysis. Uncertainties are also associated with every simplifying assumption made throughout the analysis. These uncertainties must be propagated through the analysis in order to find the true uncertainty associated with the outputs of the model[15]. Uncertainties are captured by distributions of risk or frequency, and can be categorized as either aleatory or epistemic. Aleatory uncertainty is the portion of uncertainty associated with the randomness of the world, such as the roll of dice. Epistemic uncertainty is due to limited data and knowledge. For example, epistemic uncertainty may come from the measurement of an amount. If ten scientists take a measurement of a length or volume, those scientists may arrive at ten different answers. This uncertainty is called epistemic. Increasing the knowledge of system should reduce epistemic uncertainty, but aleatory uncertainty is essentially uncontrollable. Unless substantial effort is put into uncertainty quantification[22], it is often difficult to distinguish between these two types of uncertainties.

PRA models provide a wide variety of benefits. Primarily, they can be used to assess the risk significance of operational occurrences at NPPs. These models enable the analysts to evaluate alternative design changes to improve safety or reduce costs. Because these models incorporate both plant design and operational aspects, they can be useful in the training of plant operators and engineers. Additionally, PRA helps integrate different disciplines, such as engineering and behavioral sciences, into the study of human reliability. One of the most important aspects of PRA is that it provides decision-makers with information to make decisions about phenomena affecting intricate technical systems by identifying the dominant accident scenarios and contributing factors to risk[23].

1.3 RISK-INFORMED DECISION-MAKING

Traditionally, the United States Nuclear Regulatory Commission (NRC) has utilized a deterministic approach to answer two primary questions for assessing public safety:

- What can go wrong?
- What are the consequences?

In recent years, the NRC has implemented a risk-informed performance-based approach which also seeks to answer two additional questions:

- How likely is it that something will go wrong?
- What performance is required?

The NRC uses the triplet definition of risk, defined in Section 1.2, and the system performance requirements to combine the probability or likelihood of an event with the consequences of the event[24].

In 1995, the NRC established an overall policy for consistency on the use of PRA methods in nuclear regulatory activities across potential applications of PRA by issuing “Use of Probabilistic Risk Assessment Methods in Nuclear Regulatory Activities; Final Policy Statement[1]. This policy statement concludes with four points regarding the expanded use of PRA in NRC activities:

1) PRA technology should be increased in all regulatory matters, using state-of-the-art PRA methods, in a way that complements the NRC’s deterministic approach and supports defense-in-depth philosophy.
2) PRA and associated analysis should be used in regulatory matters, within the state-of-the-art, to reduce unnecessary conservatisms.
3) PRA evaluations should be as realistic as possible and the supporting data should be publicly available for review.

4) Appropriate consideration of uncertainties should be used for making regulatory judgements.

These four points are used as the basis for establishing the regulatory framework for making risk-informed decisions at the NRC. This process of integrated decision-making has been widely incorporated into the U.S. nuclear safety systems and procedures.

In 1998, the NRC published Regulatory Guide 1.174: An Approach for Using Probabilistic Risk Assessment in Risk-Informed Decisions on Plant-Specific Changes to the Licensing Basis[12]. The purpose of this regulatory guide is to improve the consistency with which regulatory decisions are made in areas using risk analyses to justify actions, specifically regarding the plant licensing basis. In this guide, an acceptable approach to risk-informed decision-making was established based on five principles, depicted in Figure 1.3:

1) The proposed change meets the current regulations unless it is explicitly related to a requested exemption or rule change
2) The proposed change is consistent with the defense-in-depth philosophy
3) The proposed change maintains sufficient safety margins
4) When proposed changes result in an increase in core damage frequency or risk, the increases should be small and consistent with the intent of the Commission's Safety Goal Policy Statement
5) The impact of the proposed change should be monitored using performance measure strategies

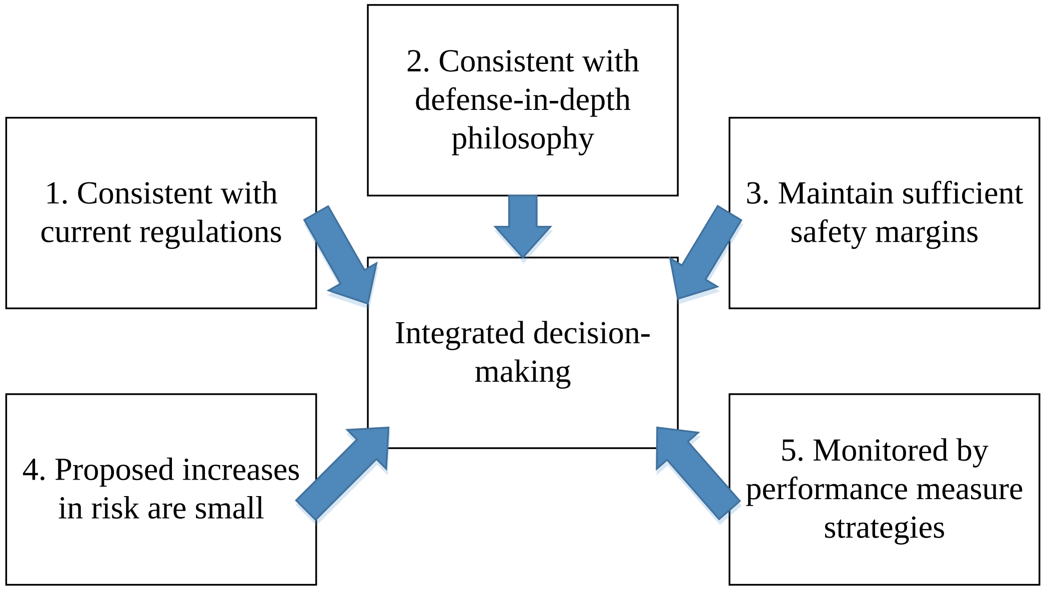

Figure 1.3 Principles of Risk-Informed Integrated Decision-Making, modified from [12]

Risk-informed decision-making should not be confused with risk-based decision-making. In risk-informed decision-making, risk is one of the five inputs of the decision-making process. The risk input is associated with the fourth box in Figure 1.3. A risk-based process would exclusively make decisions based on the risk analysis information[25]. However, a risk-informed decision takes into consideration the risk analysis information in addition to the current regulations, defense-in-depth philosophy, sufficient safety margins, and performance measure strategies. The motivation for implementing a risk-informed decision-making process is that with this, all the PRAs have ways to expose and reduce risk that, probably would not have been possible without the implementation of the PRA methodologies[26].

The risk information from PRAs is traditionally divided into three levels[15]:

- Level 1: Determination of core damage frequency (CDF) through the assessment of plant failures (hardware, software, and human).

- Level 2: Determination of large early release frequency (LERF) and severity through assessment of containment response of released radiation.
- Level 3: Development of risk curves for prompt fatalities and latent cancer fatalities through the assessment of off-site consequences to the public.

NPP license holders each develop a plant-specific Level 1 PRA[27]. Level 1 PRAs use information regarding initiating events and scenario development to quantify a CDF. Level 1 PRAs do not distinguish between the severity of the consequences beyond core damage.

Level 2 PRA expands upon a Level 1 PRA to consider containment response to an accident sequence. Level 2 PRA predicts the time and mode of containment failure, as well as the radionuclides released to the environment[15]. While Level 1 PRA only seeks to quantify the frequency of a scenario (core damage), Level 2 PRA seeks to quantify both the frequency and consequence of a scenario (radionuclide release).

Level 3 PRA uses the radionuclide information generated by the Level 2 PRA and assesses the transport of radionuclides through the environment. Level 3 PRA calculates the final consequences to the public and, therefore, completes the calculation provided in Equation (1.1) [15].

The source of risk information used in the NRC's decision-making process, represented by Figure 1.3, is the contribution of a proposed regulatory change to CDF and LERF. Using Level 1 and Level 2 PRAs, the inputs can be changed to see what the results of a regulatory change would be on CDF and LERF. There is a standard released by The American Society for Mechanical Engineers (ASME) for Level 1 and limited Level 2 PRA for full-power operations proposed in 2002[28]. There are no ASME or American Nuclear Society (ANS) standards, beyond the calculation of LERF[29], for either Level 2 or Level 3 PRA. According to the 2009 ASME standards, Level 1 PRA must contain[30]:

- Initiating event analysis
- Accident sequence analysis
- Success criteria analysis
- Systems analysis
- Human reliability analysis
- Data analysis
- Quantification

In addition to CDF and LERF, risk information also includes contributions from quantitative health objectives (QHOs). For the United States, QHOs ensure that prompt fatalities and cancer fatalities do not exceed 0.1% of the sum of prompt-fatality risks from other accidents to which the U.S. population is exposed and 0.1% of the sum of cancer fatality risks resulting from other causes[25]. While CDF and LERF are the main measures of risk in the risk-informed decision-making process, this does not mean that Level 3 PRA results regarding prompt and latent cancer risks should be ignored. The NRC has developed three major full-scope PRA studies [14, 31, 32] and another full-scope PRA project is in progress [33].

1.4 RISK-INFORMED RESOLUTION OF GENERIC SAFETY ISSUE 191

One risk-informed decision-making application which requires the location-specific estimation of LOCA frequencies is the risk-informed resolution of Generic Safety Issue 191 (GSI-191). Section 1.4.1 briefly explains the history of GSI-191 and Section 1.4.2 demonstrates the risk-informed resolution of GSI-191, which was started under the STPNOC pilot project. Section 1.4.3 provides a background on the location-specific frequency estimation for the risk informed GSI-191 project.

1.4.1 BACKGROUND ON GENERIC SAFETY ISSUE 191

The ECCS is designed to supply coolant to the reactor if a LOCA occurs. One of the legal requirements of title 10 of the Code of Federal Regulations (CFR) 50.46, "Acceptance Criteria for Emergency Core Cooling System (ECCS) for Light-water Nuclear Power Reactors," demands that a loss of long-term core cooling event must be mitigated with high probability[4]. Therefore, in September 1996, the U.S. NRC issued Generic Safety Issue 191 (GSI-191), which is titled "Assessment of Debris Accumulation on Pressurized Water Reactor Sump Performance." GSI-191 was issued to help alleviate concerns regarding the performance of the sump after the occurrence of a LOCA.

The concerns regarding PWR sump clogging due to debris date back to 1979 when the NRC opened Unresolved Safety Issue A-43, "Containment Emergency Sump Performance". In 1985, the NRC sent a generic letter to all licensees explaining the problem, but did not require action[34]. However, the concerns became more urgent when on July 28, 1992, an event occurred at a Swedish BWR. The event involved the clogging of two containment vessel spray system suction strainers, which are synonymous with ECCS sump screens, by previously dislodged mineral wool. The insulation material plugging occurred during a routine test[35]. In January and April of 1993, two similar events occurred at the Perry Nuclear Power Plant in North Perry, Ohio. The first event resulted from fibrous debris and the second event resulted from latent debris in the suppression pool. In the first event at Perry, the fibrous debris accumulated corrosion products more efficiently than the metal screen, resulting in a larger pressure drop (of flowing coolant water) through the sump screen due to the clogging at the screen[4]. An illustration of a typical PWR containment sump can be found in Figure 1.4.

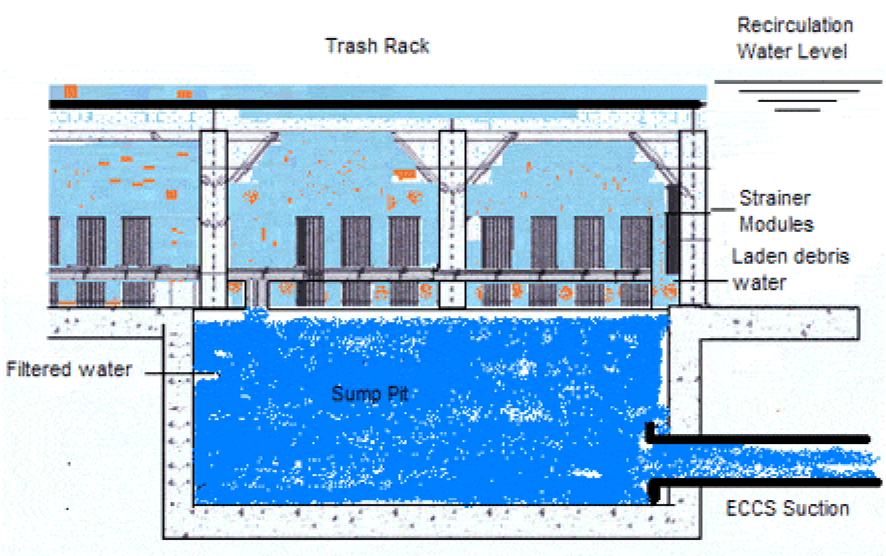

Figure 1.4 Illustration of Containment Sump from [36]

The NRC communicated these issues with the nuclear industry and they responded by modifying their strainers to minimize the potential for ECCS strainer clogging following a LOCA. The strainer issue for BWRs was eventually resolved through wide-scale strainer replacement[37]. However, after several years of testing, the NRC decided that the same approach was insufficient to resolve the issue for PWRs[4]. In response to the continued concerns regarding the PWR sump designs, the NRC issued Generic Letter 2004-02[38] requesting PWR plants to evaluate the recirculation functions of their ECCS and containment spray systems.

This proved to be quite challenging, as the combination of fibrous debris and chemical precipitates were found to cause a significant head loss in post-LOCA environments[39]. The head loss could lead to a net positive suction head (NPSH) for ECCS and containment spray pumps, which could prevent them from maintaining a cool core during a LOCA. Additionally, it was discovered that some of the finer debris could penetrate the strainer and inhibit coolant flow inside the reactor vessel. With these discoveries, it became clear that the GSI-191 issue presents two major questions[40]:

1. Would the debris that is carried with the coolant to the containment sump plug up the suction strainers of the ECCS pumps?
2. Would the debris that penetrates the strainers cause blockage of the fuel channels within the reactor core?

Despite early recognition for the need of risk quantification[41], and even after some thought had been given to it[42], both industry and the NRC opted for a classical deterministic approach for resolving GSI-191. Due to the complexities of the issue, the classical deterministic approach for resolving GSI-191 proved to be insufficient. Therefore, in 2010, the NRC commissioners directed the staff to consider new and innovative approaches for resolution. One of the options in the staff requirement memorandum[43] was the use of a risk-informed approach for evaluating the impact of debris on both sump blockage and in-vessel effects. Therefore, in

2011, the South Texas Project Nuclear Operating Company (STPNOC) initiated a risk-informed project to resolve GSI-191 by characterizing the risk significance of sump blockage[44].

1.4.2 STPNOC RISK-INFORMED PILOT PROJECT

The STPNOC pilot project implemented an integrative risk framework (i.e., integration of classical PRA with simulation-based modeling) to explicitly provide failure probabilities for the plant-specific PRA basic events, associated with GSI-191, that were related to post-LOCA phenomena. The STPNOC risk framework included a simulation module, known as CASA (Containment Accident Stochastic Analysis) Grande[45], to provide estimated probabilities and associated uncertainties to the plant-specific basic events. These probabilities and associated uncertainties are quantified using the time-dependent physical models inside CASA Grande. The phenomena modeled in the risk-informed GSI-191 project include the estimation of location-specific LOCA frequencies, jet formation physics, generation and transport of debris, effects of chemicals on head loss in debris beds, strainer head loss, degasification, and reactor thermal-hydraulics. The STPNOC risk-informed methodology consists of the following steps[46]:

1. Identify accident sequences relevant to GSI-191
2. Identify debris-related failure modes in those accident sequences
3. Identify the debris sources and locations
4. Ensure accident sequences have enough detail to measure impact on failure modes
5. Model the debris transport
6. Perform Monte Carlo simulations to determine the conditional probability of sump and in-vessel failures for various LOCA sizes and plant configurations

7. Pass these probabilities to the plant-specific PRA module to determine the risk from debris and compare to acceptance guidelines.

Figure 1.5 depicts the two elements of the integrated risk-informed GSI-191 framework at a high level of abstraction[44].

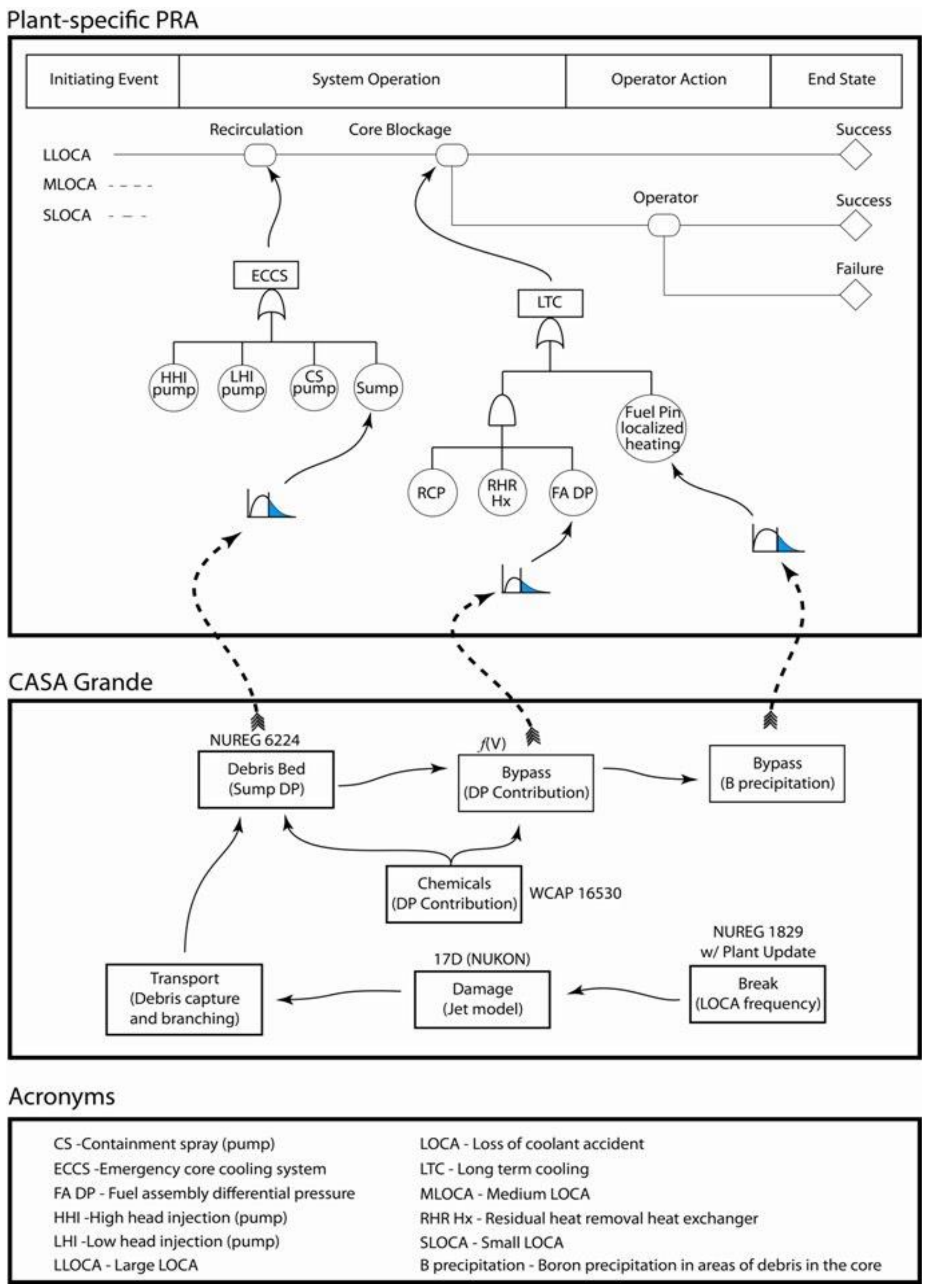

Figure 1.5 Illustration of the Integrated Framework for Risk-Informed GSI-191 [44]

The top element in Figure 1.5 illustrates the plant-specific PRA (referring to classical PRA) that includes ET risk scenarios and their associated FTs. The second element contains models of the underlying physical phenomena associated with the basic events in the top module. In other words, CASA Grande provides estimated probabilities, with consideration of the physical phenomena and the associated uncertainties, for the basic events to interface with the PRA module. These probabilities are based on the time-dependent physical models that have been developed for the basic events[44].

STPNOC developed extensive models to simulate the underlying physical phenomena associated with GSI-191[44]. In CASA, uncertainties in the physical parameters are propagated from break initiation to potential core damage precursors:

- Strainer head loss
- Core blockage
- Boron precipitation
- Air ingestion
- Mechanical collapse
- Flashing
- Air Intrusion
- Net positive suction head (NPSH)
- Boron precipitation
- Core flow

The output from these simulations was fed directly into the plant-specific PRA to calculate the change in CDF and LERF. The scope of the phenomena modeled by STPNOC includes[44]:

- Location-specific LOCA frequencies
- Jet formation physics
- Debris generation
- Debris transport
- Effects of chemicals on head loss in debris beds
- Strainer head loss
- Degasification
- Downstream or in-vessel effects
- Reactor thermal-hydraulics

The risk-informed approach for the resolution of GSI-191 has both advantages and disadvantages. The main disadvantage for the risk-informed approach is that a significant amount of effort is required for determining the probability distributions for the design inputs, quantifying uncertainties, and developing realistic physical models. The advantages to using the risk-informed approach include the following[47]:

1. Using realistic inputs and models that consider time-dependent factors can reduce conservatism in the results
2. The risk-informed approach is a holistic plant-specific assessment for GSI-191
3. Plant modifications such as insulation replacement can easily be evaluated to select the most efficient method to improve safety
4. Newly emerging issues can be quickly and easily addressed within the CASA Grande model

As Figure 1.5 shows, the initiating element of CASA Grande relates to the development of location-specific LOCA frequencies. Section 1.4.3 provides a background on LOCA frequency estimation and for the need to undertake the STPNOC project.

1.4.3 DEVELOPMENT OF LOCATION-SPECIFIC LOCA FREQUENCIES

The most recent NRC-sponsored estimations of LOCA frequencies were documented in NUREG-1829[3]. The LOCA frequencies provided in NUREG-1829 represent a summation of the frequencies as a function of component break size of all potential primary-side break locations. However, since two equivalent-size breaks in different locations may have a significantly different likelihood of occurrence and effect on GSI-191 related phenomena (e.g., quantity of debris generated, transport fractions, in-vessel flow paths, etc.), for the STPNOC risk-informed project, the total frequencies for all possible break locations had to be separated into the specific frequencies for each break location[44]. Section 1.4.3.1 summarizes the NRC-sponsored estimation of LOCA. Section 1.4.3.2 briefly highlights the location-specific LOCA estimation for the STPNOC project that can be more adequately explained and advanced in Chapter 2 to 4.

1.4.3.1 NRC-SPONSORED ESTIMATIONS OF LOCA FREQUENCIES

NPPs in the United States have been designed and constructed using traditional engineering methods. This means that the components in a nuclear plant were built based on various industry codes (e.g., the ASME code for heat exchangers). These codes are tailored so that the NPPs can withstand design basis accidents with high assurance. It does not matter how the design basis accident occurs, it is just assumed that the design basis accident is the initiating event and the NPP must be able to maintain the core cooling during such an event[48].

The Emergency Core Cooling System (ECCS) in NPPs is designed to ensure that the system can successfully mitigate postulated loss-of-coolant accidents (LOCAs). For this thesis, LOCA has the same definition utilized in NUREG-1829[3]:

> *"A breach of the reactor coolant pressure boundary which results in a leak rate beyond the normal makeup capability of the plant."*

The limiting condition, or design basis accident, considers that the largest pipe in the pressurized RCS suddenly ruptures, which is known as a double-ended guillotine break (DEGB). The occurrence of a DEGB would cause all the primary coolant to rapidly escape from the system. A

DEGB is generally accepted as an extremely unlikely event. To establish a risk-informed revision of this design basis, the understanding of LOCA frequencies as a function of component break size is a critical consideration. Therefore, the estimation of LOCA frequencies is necessary as an input for an assortment of risk-informed regulatory applications, including for the PRA of NPPs and for risk-informed in-service inspections (RI-ISI). Occurrence of LOCAs is rare; therefore, estimation of LOCA frequencies can be challenging. There are two main categories of approaches for estimating LOCA frequencies: operating experience-based estimations and probabilistic fracture mechanics (PFM) analyses[3].

In 1975, WASH-1400[14] developed the first operating experience-based study on piping failures for the nuclear power industry. This study provided the first LOCA frequencies. The estimations from WASH-1400 were separated into three categories based upon the size of the break in the component: 0.5-2.0 inches, 2.0-6.0 inches, and 6.0+ inches, which were eventually referred to as small break (SB), medium break (MB), and large break (LB). At the time of WASH-1400, a small amount of commercial NPP service data was available. Therefore, WASH-1400 used failure data from other industries, both U.S. and foreign, such as the oil and gas industry, to inform the estimations of LOCA frequencies. WASH-1400 LOCA frequencies were conservative estimates since the materials, in-service inspections, operating conditions, and environments of the nuclear industry - compared to the oil and gas industry[14] - were superior. One of the significant findings from WASH-1400 was the significance of SB LOCAs compared to LB LOCAs. Before WASH-1400, most of the nuclear safety efforts focused on LB LOCAs[49]. The only LOCA to occur in the U.S. commercial nuclear program was a SB LOCA, which occurred at Three Mile Island Unit 2, near Middletown, PA. This was the most serious accident in U.S. commercial nuclear power plant history, although the small radioactive releases had no detectable health effects to plant workers or to the public[50].

In 1990, the WASH-1400 estimates were used as the basis for the estimates of LOCA frequencies used in NUREG-1150[31]. NUREG-1150 utilized the same break size categories for PWRs as established in WASH-1400. However, due to differences in engineering characteristics, different break size categories were developed for liquid and steam piping for BWRs[51]. The NUREG-1150 estimations of LOCA frequencies were updated using Bayes' theory with WASH-1400 LOCA frequencies as the prior distribution. These estimates were updated using the additional evidence that zero LOCAs occurred in the United States after the WASH-1400 estimations were published. A detailed explanation of Bayesian theory will be covered in Chapter 4 of this thesis. Ultimately, by updating the WASH-1400 estimations with zero occurrences of LOCAs, the LOCA frequencies were reduced, thus making the estimations less conservative.

In 1999, NUREG/CR-5750, titled "*Rates of Initiating Events at U.S. Nuclear Power Plants: 1987-1995*", provided the next NRC-sponsored, operating experience-based evaluation of pipe break LOCA frequencies[2]. Using the same break size categories from NUREG-1150, NUREG/CR-5750 utilized two distinct approaches for estimating LOCA frequencies. SB LOCA frequencies were estimated using the additional U.S. operating experience since WASH-1400 to perform a simple Bayes update of the WASH-1400 SB LOCA frequency. This approach also combined PWR and BWR SB LOCA data into one set, because no significant difference could be found in the dominant failure mechanisms between the two plant types.

However, the approach for estimated MB and LB LOCA frequencies consisted of separating LOCA frequencies into a multiplication of precursor leak frequencies and a conditional pipe break probability (CBP). Precursor leak frequencies, for each BWR and PWR separately, are developed to incorporate information regarding leaks, or through-wall cracks, which had challenged piping integrity, but did not cause the occurrence of a LOCA. Additionally, conservative estimates were used for CBPs based upon information from fracture mechanics, high-energy pipe failure, and crack data. The conservative estimate used for the CBPs was developed by Beliczey and Schulz as shown in Equation (1.2) [52].

$$CBP = \frac{2.5}{DN} \tag{1.2}$$

where: DN is the nominal diameter of a piping component in millimeters. Using this new approach, the resulting MB and LB LOCA frequencies were reduced by over a factor of ten from the WASH-1400 and NUREG-1150 methods[2].

One of the primary advantages to separating LOCA frequencies into leak frequencies and CBPs is that leak frequencies can be calculated using past operating experience; thus, the analysts were only required to estimate the CBPs. However, the NRC determined that the NUREG/CR-5750 estimates were insufficient for design basis break size selection because they did not address all passive-system degradation concerns, nor did they differentiate between component break sizes greater than 6 inches[53].

The concerns regarding the NUREG/CR-5750 estimations of LOCA frequencies led to the most recent NRC-sponsored estimations of LOCA frequencies, documented in NUREG-

1829[3]. Since neither PFM nor the statistical analysis of operating experience are well suited to estimate LOCA frequencies due to the modeling complexity and the rareness of LOCA events, the NUREG-1829 estimations of LOCA frequencies were developed utilizing an expert elicitation approach to encompass insights from both methodologies. The expert elicitation approach developed separate BWR and PWR piping and non-piping passive system estimations of LOCA frequencies as a function of effective break size at three time periods:

- Current-day: Fleet average of 25 operational years for U.S. NPPs
- End-of-plant-license: Fleet average of 40 operational years for U.S. NPPs
- End-of-plant-license-renewal: Fleet average of 60 operational years for U.S. NPPs

The expert elicitation estimations were formed from the responses of an expert panel whose primary goal was to represent a group consensus while reflecting the uncertainty in each panelist's estimates and the diversity among the estimates. The NUREG-1829 estimations were developed for a set of 6 LOCA categories, which can be found in Table 1.1. These categories alleviate previous NRC concerns regarding the lack of differentiation between component break sizes larger than 6 inches in NUREG/CR-5750[3].

Table 1.1 LOCA Break Size Category Definitions from [3]

LOCA Category	Flow Rate (gpm)	BWR: Steam		BWR: Liquid		PWR: Liquid	
		Flow Rate Flux (gpm/in^2)	Effective Break Size (in)	Flow Rate Flux (gpm/in^2)	Effective Break Size (in)	Flow Rate Flux (gpm/in^2)	Effective Break Size (in)
1	100	355	0.5	595	0.5	687	0.5
2	1,500	355	2.25	595	1.75	687	1.5
3	5,000	355	4.25	595	3.25	687	3.5
4	25,000	355	9.5	595	7.25	687	6.75
5	100,000	355	19	375	18.5	641	14
6	500,000	355	42.25	375	41.25	641	31.5

NUREG-1829 was developed to produce estimates of total LOCA frequencies at U.S. NPPs. While the expert elicitation approach has provided the most recent NRC-sponsored generic estimations of LOCA frequencies, there are still some questions that remain regarding their interpretation. These questions include whether the NUREG-1829 results provide a justification for using a fixed set of LOCA frequencies for all U.S. PWRs, [54].

1.4.3.2 LOCATION-SPECIFIC ESTIMATIONS OF LOCA FREQUENCIES FOR STPNOC PILOT PROJECT

In support of the STPNOC risk-informed pilot project, Fleming and Lydell[5] developed a location-specific and break size-dependent estimation LOCA frequencies. Fleming and Lydell implemented a model, having a similar structure to the approach implemented in NUREG/CR-5750, that expressed LOCA frequencies as a function of precursor failure rates and conditional rupture probabilities (CRPs).

Fleming and Lydell chose to use a "bottom-up" approach; thus, estimates of LOCA frequencies were found by adding the LOCA frequency contributions from individual pipe weld components throughout the RCS. Fleming and Lydell aimed to build upon the risk-informed in-service inspection methodology developed by the Electric Power Research Institute (EPRI)[55] to develop location-specific LOCA frequencies. The individual LOCA frequencies were found as a function of component break size at each weld location. Fleming and Lydell utilized the expert analysis from NUREG-1829 as well as service data from the PIPExp database[56] in order to calculate these location-specific LOCA frequencies. The approach used by Fleming and Lydell accounted for the appropriate failure mechanisms at each pipe weld by applying damage mechanisms uniformly across broad categories of welds due to insufficient data from the

NUREG-1829 report regarding the effects of the individual damage mechanisms. Additionally, Fleming and Lydell made an approximate quantification of uncertainties associated with the LOCA frequency calculations.

The model used by Fleming and Lydell calculates LOCA initiating event frequencies as a function of pipe failure rates and conditional rupture probabilities for a given break size. This model is based on the following key assumptions. The first assumption is that LOCAs are most likely to occur at or near a field weld. LOCAs with larger break sizes generally result in more debris, which can potentially compromise the ECCS upon recirculation. After analyzing the available data, Fleming and Lydell concluded that these LOCAs with larger break sizes are dominated by pipe weld failures. Therefore, only pipe weld failures are analyzed in their report. The second key assumption is that any pipe failure such as a non-through wall flaw, crack, or leak that needs to be repaired or replaced is regarded as a precursor to more severe failures such as ruptures. They also assumed that the total LOCA frequency for a given break size can be found by taking the linear sum of the independent LOCA frequency contributions of all pipes large enough to support that break size.

With these three assumptions, data from NUREG-1829, and service data from the PIPExp database, the LOCA frequencies were calculated following three main steps:

1. Pipe failure rates were developed from pipe failure service data
2. CRP distributions were formed using expert unconditional LOCA frequencies found in NUREG-1829 and updated with service data of experienced failures and ruptures using Bayesian analysis

3. The results from the first two steps were combined to give the desired LOCA frequencies

Chapter 2 reports on the step-by-step critical review that has been conducted in this research regarding the Fleming and Lydell's methodology and concludes with the key gaps. To address the gaps, this research develops a qualitative analysis (See Chapter 3) and a new spatio-temporal probabilistic methodology (See Chapter 4) that provides more explicit incorporation of physical failure mechanisms associated with location and time into LOCA frequency estimations.

REFERENCES

1. Bates, A., *Use of Probabilistic Risk Assessment Methods in Nuclear Regulatory Activities; Final Policy Statement*, U. S. Nuclear Regulatory Commission, Editor. 1995: Federal Register. p. 42622-42629.

2. Poloski, J.P. and D.G. Marksberry, *Rates of Initiating Events at US Nuclear Power Plants: 1987-1995 (NUREG/CR-5750).* Washington, DC: US Nuclear Regulatory Commission, 1998. **12**.

3. Tregoning, R., L. Abramson, and P. Scott. *Estimating Loss-of-Coolant Accident (LOCA) Frequencies Through the Elicitation Process*, NUREG-1829, 2008.

4. Kee, E., Z. Mohaghegh, R. Kazemi, S.A. Reihani, B. Letellier, and R. Grantom. *Risk-Informed Decision Making: Application in Nuclear Power Plant Design & Operation*. in *American Nuclear Society Winter Meeting and Technology Expo*. 2013. Washington D.C.: American Nuclear Society.

5. Fleming, K., B. Lydell, and D. Chrun. *Development of LOCA Initiating Event Frequencies for South Texas Project GSI-191*, 2011.

6. O'Shea, N., Z. Mohaghegh, S.A. Reihani, E. Kee, K. Fleming, and B. Lydell. *Analyzing Non-Piping Location-Specifc LOCA Frequency For Risk-Informed Resolution of Generic Safety Issue 191*. in *International Topical Meeting on Probabilistic Safety Assessment and Analysis*. 2015. Sun Valley, ID, USA: American Nuclear Society.

7. O'Shea, N., S.A. Reihani, and Z. Mohaghegh. *Collaboration in Expert Elicitation on Non-Piping Component Contribution to the GSI-191*, Report, 2015.

8. O'Shea, N., Z. Mohaghegh, S.A. Reihani, and E. Kee, *Estimating Loss-of-coolant Accident (LOCA) Frequencies Via Spatio-Temporal Methodology*, in *13th International*

Conference on Probabilistic Safety Assessment and Management (PSAM 13). 2016: Seoul, Korea.

9. O'Shea, N., J. Pence, Z. Mohaghegh, and E. Kee. *Physics of Failure, Predictive Modeling and Data Analytics for LOCA Frequency*. in *Annual Reliability & Maintainability Symposium (RAMS)*. 2015. IEEE.
10. Mendel, M., *The Case for Probabilistic Physics of Failure*, in *Reliability and Maintenance of Complex Systems*, N.A.S.S.F.C.a.S. Sciences), Editor. 1996, Springer: Berlin, Heidelberg.
11. Chookah, M., M. Nuhi, and M. Modarres, *A probabilistic physics-of-failure model for prognostic health management of structures subject to pitting and corrosion-fatigue.* Reliability Engineering & System Safety, 2011. **96**: p. 1601-1610.
12. U.S. Nuclear Regulatory Commission, *An Approach for Using Probabilistic Risk Assessment in Risk-Informed Decisions on Plant-Specific Changes to the Licensing Basis*, U.S. Nuclear Regulatory Commission, Editor. 1998.
13. Apostolakis, G. *A Proposed Risk Management Regulatory Framework*, 2012.
14. U.S. Nuclear Regulatory Commission. *Reactor Safety Study: An Assessment of Accident Risks in U.S. Commercial Nuclear Power Plants*, WASH-1400 (NUREG 75/014), 1975.
15. American Nuclear Society. *PRA Procedures Guide*, NUREG/CR-2300, 1983.
16. Kaplan, S. and B.J. Garrick, *On the Quantitative Definition of Risk.* Risk Analysis, 1981. **1**(1): p. 11-27.
17. Modarres, M., *Risk Analysis in Engineering: Techniques, Tools, and Trends*. 2006, Boca Rator, FL: Taylor & Francis Group, LLC.

18. Modarres, M., M. Kaminskiy, and V. Krivtsov, *Reliability Engineering and Risk Analysis: A Practical Guide*. Second ed. 2010, Boca Raton, FL: Taylor & Francis Group.

19. Nuclear Regulatory Commission. July 17, 2013; Available from: http://www.nrc.gov/about-nrc/regulatory/risk-informed/pra.html.

20. Stamatelatos, M. *Probabilistic Risk Assessment: What Is It And Why Is It Worth Performing It?*, 2000.

21. Lee, J. and N. McCormick, *Risk and Safety Analysis of Nuclear Systems*. 2012: John Wiley & Sons.

22. Hora, S., *Aleatory and Epistemic Uncertainty in Probability Elicitaiton with an Example from Hazardous Waste Management.* Reliability Engineering & System Safety, 1996. **54**(2): p. 217-223.

23. Apostolakis, G. *How Useful is Quantitative Risk Assessment*, 2004.

24. U.S. Nuclear Regulatory Commission. *Risk Assessment in Regulation*. 2014; Available from: http://www.nrc.gov/about-nrc/regulatory/risk-informed.html.

25. Kumamoto, H., *Probabilistic Risk Assessment: PRA*, in *Satisfying Safety Goals by Probabilistic Risk Assessment*. 2007.

26. Garrick, B.J., *PRA-based risk management: History and perspectives.* Nuclear News, 2014(July 2014): p. 48-53.

27. Nuclear Regulatory Commission. *Nuclear Regulatory Commission Regulations Title 10, Code of Federal Regulations, Part 50, Section 50.71*, 1999.

28. Nuclear Regulatory Commission. *An Approach for Plant-Specific Risk-Informed Decision-making for In-service Inspection of Piping*, 2002.

29. Nuclear Regulatory Commission. *Issues and recommendations for advancement of PRA technology in risk-informed decision-making*, NUREG/CR-6813, 2003.

30. ASME/ANS RA-SA-2009. *Standard for Level 1/Large Early Release Freqeuncy Probabilistic Risk Assessment for Nuclear Power Plant Applications*. in *American Nuclear Society*. 2009. La Grange Park, Illinois: ASME.

31. Nuclear Regulatory Commission. *Severe Accident Risks: An Assessment for Five U.S. Nuclear Power Plants (NUREG-1150)*, 1990.

32. Chang, R. *State-of-the-art-reactor Consequence Analyses (SOARCA) Report*, 2012.

33. Nuclear Regulatory Commission. *Update on Staff Plans to Apply Full-Scope Site Level 3 PRA Project Results to the NRC's Regulatory Framework*, SECY-12-0123, 2012.

34. Nuclear Regulatory Commission, *Potential for Loss of Post-LOCA Recirculation Capability Due to Insulation Debris Blockage (Generic Letter No. 85-22)*. 1985: Washington, D.C.

35. Nuclear Regulatory Commission. *NRC Bulletin 96-03: Potential Plugging of Emergency Core Cooling Suction Strainers by Debris in Boiling Water Reactors*, 1996.

36. Nuclear Regulatory Commission. *Function of the Containment Sump*. 2013 May 9, 2013; Available from: http://www.nrc.gov/reactors/operating/ops-experience/pwr-sump-performance/function-containment-sump.html.

37. Zigler, G., J. Brideau, D.V. Rao, C. Shaffer, F. Souto, and W. Thomas. *Parametric Study of the Potential for BWR ECCS Strainer Blockage Due to LOCA Generated Debris*, Report, 1995.

38. Boger, B.A., *NRC Generic Letter 2004-02: Potential Impact of Debris Blockage on Emergency Recirculation During Design Basis Accidents at Pressurized-Water Reactors*. 2004.

39. Natesan, K., A. Moisseytsev, C. Bahn, D. Diercks, and C. Shaffer. *Knowledge Base Report on Emergency Core Cooling Sump Performance in Operating Light Water Reactors,* NUREG/CR-7172, 2014.

40. Nuclear Regulatory Commission. *Closure Options for Generic Safety Issue - 191, Assessent of Debris Accumulation on Pressurized Water Reactor Sump Performance*, SECY-10-0113, 2010.

41. Darby, J., D. Rao, and B. Letellier. *Technical Letter Report GSI-191 Study: Technical Approach for Risk Assessment of PWR Sump-Screen Blockage*, Report, 2000.

42. Teolis, D., R. Lutz, and H. Detar. *PRA Modeling of Debris-Induced Failure of Long Term Cooling via Recirculation Sumps*, 2009.

43. Vietti-Cook, A.L., *Assessment of Debris Accumulation on Pressurized Water Reactor Sump Performance[memorandum]*, in *Staff Reguirements - SECY-10-0113 - Closure Options For Generic Safety Issue-191*. 2010.

44. Mohaghegh, Z., E. Kee, S.A. Reihani, R. Kazemi, D. Johnson, R. Grantom, K. Fleming, T. Sande, B. Letellier, G. Zigler, D. Morton, J. Tejada, K. Howe, J. Leavitt, Y. Hassan, R. Vaghetto, S. Lee, and S. Blossom. *Risk-Informed Resolution of Generic Safety Issue 191*. in *International Topical Meeting on Probabilistic Safety Assessment and Analysis*. 2013. LaGrange Park, IL, USA: American Nuclear Society.

45. Alion Science & Technology, *CASA Grande Theory Manual*, in *ALION-SPP ALION-I009-10, STP STI 34179370*. 2015, Alion Science & Technology: Albuquerque, NM.

46. Fong, C.J. *Overview and Comparison of Risk-Informed Efforts to Resolve Generic Safety Issue 191*. in *International Topical Meeting on Probabilistic Safety Assessment and Analysis*. 2015. Sun Valley, ID: American Nuclear Society.

47. Sande, T., G. Zigler, E. Kee, B. Letellier, C.R. Grantom, and Z. Mohaghegh, *The Benefits of Using a Risk-Informed Approach to Resolve GSI-191*, in *20th International Conference on Nuclear Engineering*. 2012, ASME: Anaheim, California.

48. Budnitz, R. *Dr. Robert Budnitz explains Probabilistic Risk Analysis for Nuclear Power Plants*. 2014; Available from: https://www.youtube.com/watch?v=cf9G8vddUjk.

49. Bartel, R. *WASH-1400: The Reactor Safety Study: The Introduction of Risk Assessment to the Regulation of Nuclear Reactors*, NUREG/KM-0010, 2016.

50. Nuclear Regulatory Commission. *Backgrounder on the Three Mile Island Accident*. 2013 December 12, 2014; Available from: http://www.nrc.gov/reading-rm/doc-collections/fact-sheets/3mile-isle.html#summary.

51. Poloski, J.P., D.G. Marksberry, C.L. Atwood, and W.J. Galyean. *Appendix J - LOCA Frequency Estimates*, NUREG/CR-5750, 1999.

52. Beliczey, S. and H. Shulze, *Comments on Probabilities of Leaks and Breaks of Safety-Related Piping in PWR Plants.* International Journal of Pressure Vessels and Piping, 1990. **43**: p. 219-227.

53. Tregoning, R., L. Abramson, P. Scott, and N. Chokshi, *LOCA Frequency Evaluation Using Expert Elicitation.* Nuclear Engineering and Design, 2007. **237**: p. 1429-1436.

54. Fleming, K. and B. Lydell, *Insights Into Location Dependent Loss-of-Coolant Accident (LOCA) Frequency Assessment for GSI-191 Risk-Informed Applications.* Manuscript Submitted to Nuclear Engineering and Design, 2016.

55. Electric Power Research Institute. *Revised Risk-Informed In-Service Inspection Procedure*, TR 112657 Revision B-A, 1999.

56. Lydell, B.O.Y., *Pipexp-2011: Monthly summary of database content (status as of 31-july-2011)*, S.-P. Inc., Editor. 2011: Vail AZ.

CHAPTER 2 : CRITICAL REVIEW AND QUANTITATIVE VERIFICATION OF THE EXISTING LOCATION-SPECIFIC LOCA FREQUENCY ESTIMATION METHODOLOGY

This chapter relates to Step #2 in the roadmap of the research presented in Figure 2.1. Chapter 1 introduces the STPNOC risk-informed Generic Safety Issue 191 (GSI-191)[1], which is an example of a risk-informed industry-regulatory project and requires estimations of location-specific LOCA frequencies. Fleming and Lydell [2] developed a methodology for location-specific LOCA frequency estimation in the risk-informed GSI-191 project.

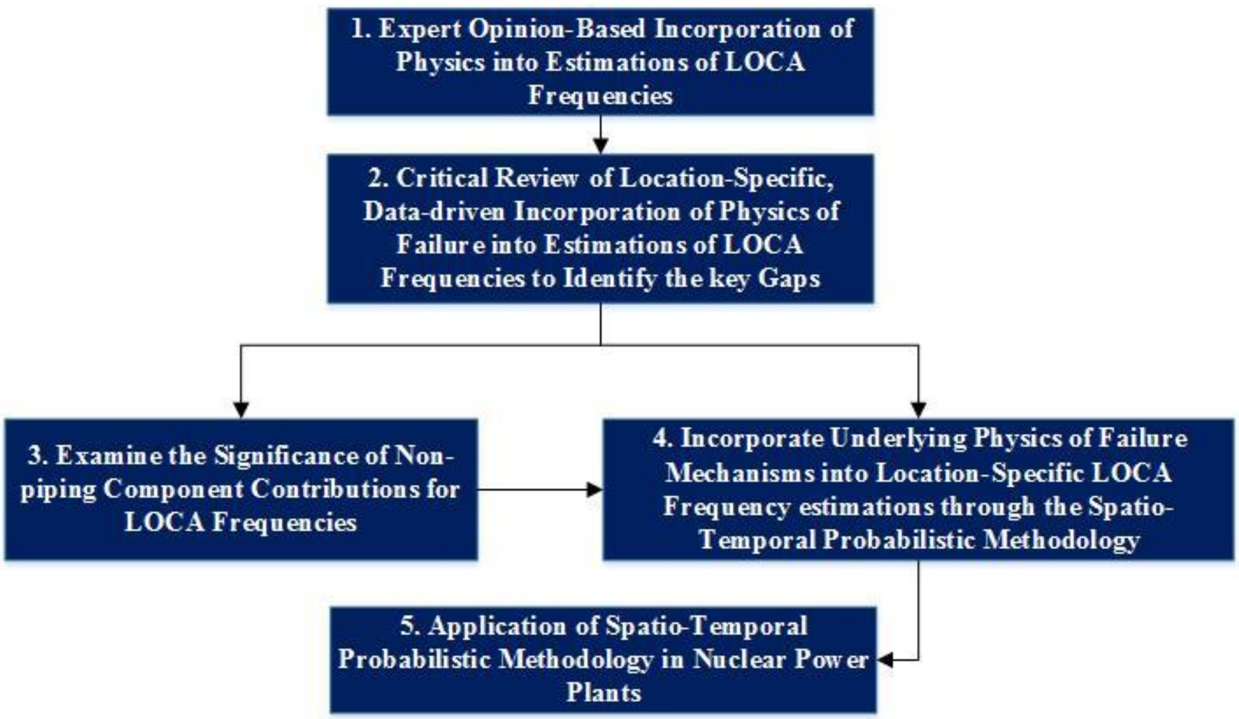

Figure 2.1 Research Roadmap

This chapter briefly explains Fleming and Lydell's methodology. Two contributions of this research thesis with respect to Fleming and Lydell's methodology are listed as follows:

(1) A quantitative verification process is run on their methodology and implementation. In some cases, their quantitative procedure is reproduced and, in other cases, additional quantification

procedures are done to scientifically verify their methodology and implementation. The quantitative verification process is done step-by-step (e.g., uncertainty quantification, Bayesian updating, failure rate estimation) and in parallel with direct communications with Fleming and Lydell, generating comments and resolutions sets, which are documented as parts of the oversight processes of the risk-informed GSI-191 project. The quantitative verification processes are demonstrated in Section 2.1. During the attempted recalculation of the results published by Fleming and Lydell, many comments and resolutions arose concerning various details. The communications with Karl Fleming regarding these questions can be found in Appendix A.

(2) Key gaps in Fleming and Lydell's methodology are highlighted in Section 2.2. Those gaps set the stage for the directions of a new investigation process (demonstrated in Chapter 3) and a new methodology (demonstrated in Chapter 4 and applied in Chapter 5) for location-specific LOCA frequency estimations.

2.1 CRITICAL REVIEW & QUANTITATIVE VERIFICATION

The purpose of Fleming and Lydell's work is to develop a location- and break size-dependent estimation of LOCA frequencies and their associated uncertainties to identify the most risk-significant break sizes and locations for GSI-191. Fleming and Lydell's work considered LOCAs initiating at or near the location of pipe and nozzle welds. The evaluation is limited to the ASME III Class 1 piping system pressure boundary failures, which consists of all hot leg, cold leg, crossover leg piping, pressurizer surge, spray, auxiliary spray, relief valve, safety valve and vent lines, a drain line, branch piping to the safety injection system (SIS), chemical & volume control system (CVCS), and residual heat removal system (RHRS).

Isolable LOCAs, seismically induced LOCAs, and LOCAs due to failures of components other than pipes are not included. Isolable LOCAs are not considered because they have a very high probability of isolation which leads to a very low risk significance level for such failures. Also, seismic events that are large enough to cause a LOCA would also have a high probability of seismic induced failure to mitigate the LOCA. The high probability of mitigation failure was judged by Fleming and Lydell to dominate the debris-induced failures related to the GSI-191; therefore, seismic events are not considered.

Fleming and Lydell's report estimates LOCA frequencies for each of the location-specific categories of welds. Additionally, the LOCA frequencies estimated by Fleming and Lydell are a function of the break-size of the RCS component. Fleming and Lydell adopt the same 6 LOCA break size categories that are implemented in NUREG-1829. These categories are discussed in Chapter 1 in Table 1.1. The STPNOC reactors are pressurized water reactors (PWRs); therefore, Fleming and Lydell utilized the effective break size numbers provided in the last column of Table 1.1.

Fleming and Lydell's report centers around the use of the model, found in Equations (2.1) and (2.2), which incorporates the location and break-size dependence of the LOCA frequencies,

$$F\left(LOCA_x\right) = \sum_i m_i \rho_{ix} \tag{2.1}$$

$$\rho_{ix} = \sum_k \lambda_{ik} P\left(R_x \mid F_{ik}\right) I_{ik} \tag{2.2}$$

where: $F(LOCA_x)$ is the LOCA frequency for a break size in category x (i.e., 1,2,3,4,5,6), per calendar year; m_i the number of pipe welds of category i; ρ_{ix} is the frequency of rupture of a component in category i with a break size in category x, λ_{ik} is the failure rate per weld-year for pipe component category i due to failure mechanism k; $P(R_x|F_{ik})$ is the conditional probability (CRP) of rupture of size x given failure of pipe component type i due to failure mechanism type k; and I_{ik} is the integrity management factor for weld type i and failure mechanism k. Equations (2.1) and (2.2) demonstrate that the estimation of LOCA frequencies is divided into two parts, the failure rate for each category of welds, λ_{ik}, and the CRP, $P(R_x|F_{ik})$. The total LOCA frequency for each break size category is equal to the LOCA frequency for each weld category location multiplied by the number of welds in that location category. The failure rate for each location category, i, and failure mechanism, k, can be found in Equation (2.3).

$$\lambda_{ik} = \frac{n_{ik}}{\tau_{ik}} = \frac{n_{ik}}{f_{ik} N_i T_i} \tag{2.3}$$

where: n_{ik} is the number of failures in pipe component category i from failure mechanism k; τ_{ik} is the population of welds in category i exposed to the failure mechanism k; f_{ik} is the fraction of the exposed weld population of i that is susceptible to failure mechanism k; Ni s the number of pipe welds of category i per reactor, T_i is the total exposure in reactor-years for the component type i.

The following sub-sections report on the results of critical reviews and quantitative verifications for the step-by-step procedure Fleming and Lydell utilized to develop the location-specific estimation of LOCA frequencies. Section 2.1.1 contains the critical review of the failure rate development for each category of all the applicable failure mechanisms. Section 2.1.2 includes the critical reviews on the development of the CRPs and Section 2.1.3 reviews the development of the location-specific LOCA frequencies.

2.1.1 CRITICAL REVIEW & QUANTITATIVE VERIFICATION ON FAILURE RATE DEVELOPMENT FOR EACH PIPING CATEGORY

The section examines the approach used by Fleming and Lydell to develop failure rates for each weld category. These failure rates incorporate surrogate failure data and degradation mechanism susceptibility information which allow the statistical analysis to be guided by the underlying physics. The procedure used by Fleming and Lydell consists of the following steps:

1. Define component/weld categories
2. Gather component failure information
3. Estimate component population exposure
4. Develop failure rate prior distributions and perform Bayesian updating for each calculation case
5. Calculate total failure rate for each component/weld category

The first step in the development of the location-specific failure rate is to group all the components, which are just welds in this report, into homogenous component categories that have distinct failure rates and rupture distributions. While it would be optimal to develop a unique failure rate for every weld location, there are approximately 775 weld locations within the Class 1 RCS pressure boundary at STPNOC; thus, there have not been enough failures at each location in the RCS to develop meaningful failure rates. Therefore, these categories provide a practical simplified assumption that every weld in a category has an identical failure rate. Fleming and Lydell first divided the welds into eight piping system categories:

1. RCS hot leg excluding steam generator (SG) inlet
2. RCS cold leg

3. RCS hot leg SG inlet
4. Pressurizer (PZR) surge line
5. PZR medium bore piping
6. Class 1 small bore piping
7. Class 1 medium bore safety injection and recirculation system (SIR) piping
8. Class 1 medium bore CVCS piping

These eight piping system categories were then subdivided into 45 calculation cases which consider weld types, damage mechanisms, and pipe sizes. It is assumed that the maximum break size of a component is equivalent to that of a double-ended guillotine break (DEGB).

As a first step, Fleming and Lydell's developed the surrogate failure rates. They developed 45 calculation categories that include the 775 Class 1 piping system welds. Fleming and Lydell define the term "pipe failure" to include any condition that leads to repair or replacement of an affected piping component. In this thesis, surrogate failure will be used in place of the term pipe failure to distinguish between the surrogate event and a true pipe rupture event, such as the ones discussed in Chapter 4. Databases on the piping service experience collect information spanning the full range of degradation conditions such as flaws that exceed ASME Section XI criteria for repair or replacement, cracks, leaks, and ruptures. Fleming and Lydell used surrogate failure information for Westinghouse, Mitsubishi Heavy Industries, and Framatome PWR plant operating experience from 1970 to 2010 from the PIPExp database[3]. One hundred sixty-three failures were identified and each one was sorted into a failure mechanism category for various plant systems.

The next step in the development of the surrogate failure rates is to determine the component population exposure for each calculation case. Component exposure is the cumulative amount of time responsible for the identified failures for which all the components were operational in the service experience database. The exposure is estimated using both the number of reactor-years of service experience and an estimated total of the number of components, or welds, per plant. Fleming and Lydell chose to use years of operation since first connected to the electrical grid. Ultimately, there were 3816.6 reactor-years of service experience for Westinghouse-type PWRs. Since each of the operational plants accounting for the service experience have varying numbers of welds and the exact numbers are unknown to the public, Fleming and Lydell developed an uncertainty distribution for the component exposure. For this purpose, they defined a three-point discrete distribution to characterize the uncertainty in the total reactor year population by reviewing isometric drawings for a selected sample of PWR plants.

Once the weld uncertainty distributions are developed for each calculation case, the failure mechanism-specific exposure estimations are developed. The failure mechanism-specific exposure estimations represent the number of years that welds, susceptible to a specific failure mechanism, were exposed to that failure mechanism. For example, if only half of the welds for a specific calculation case were exposed to a given failure mechanism, then the failure mechanism-specific exposure would be equal to one half of the total exposure. All welds are susceptible to design and construction flaws (D&C), so the D&C-specific exposure is equivalent to the total exposure.

The failure mechanism susceptibility fractions were developed based on Electric Power Research Institute (EPRI) documents[4, 5], NUREG/CR-6923[6], SCAP-SCC Working Group[7, 8], and the OECD Nuclear Energy Agency topical report[9]. Additionally, Fleming and Lydell developed failure mechanism failure rate prior distributions using work based on their previous works regarding failure rate development[4, 10-13]. These fractions are associated with uncertainty. Each failure mechanism fraction has a three-point uncertainty distribution representing high, medium, and low estimates.

The calculation case 1C for BJ welds exposed to thermal fatigue has a three-point uncertainty distribution for the number of welds in the reactors and a three-point uncertainty distribution for the thermal fatigue susceptibility fraction. To run a quantitative verification on the Fleming and Lydell's work on this step, the uncertainty distributions are combined to develop a nine-point discrete uncertainty distribution for the thermal fatigue-specific exposure estimation. The results of the recalculation for the reactor coolant system hot leg B-J welds for thermal fatigue can be found in Figure 2.2. Each branch of the uncertainty tree developed in Figure 2.2 corresponds to one of the possible values from the discrete uncertainty distributions for weld counts and the fraction of welds susceptible to thermal fatigue. The medium value for each possible result is assigned a probability of 0.5. The high and low values for each possible result is assigned a probability of 0.25. The exposure multiplier is the multiplication of the weld count uncertainty multiplier and the fraction of welds susceptible to the failure mechanism, in this case thermal fatigue. The final discrete uncertainty distribution consists of each value in the exposure column with a probability of occurrence listed in the exposure case probability. The recreated results shown in Figure 2.2 are in exact agreement with the results Fleming and Lydell [2] published for the B-J welds susceptible to thermal fatigue.

Welds/Loop	Number	Number/Average
Average	2.675	1
Minimum	2	0.75
Maximum	3	1.12

Welds/Loop	Loops	Rx-years	Weld-years
2.675	2	570	3050
2.675	3	2053	16472
2.675	4	1194	12775
Base Exposure			32297

	Weld Count Uncertainty	Fraction of B-J Welds Susceptible to Thermal Fatigue	Exposure Case Probability	Exposure Multiplier	Exposure (weld-years)
p		**0.25**	**0.0625**	**0.08972**	**2898**
x Base		0.08			
p	**0.25**	**0.5**	**0.125**	**0.02243**	**724**
x Base	1.12	0.02			
p		**0.25**	**0.0625**	**0.011215**	**362**
x Base		0.01			
p		**0.25**	**0.125**	**0.08**	**2584**
x Base		0.08			
p	**0.5**	**0.5**	**0.25**	**0.02**	**646**
x Base	1.0	0.02			
p		**0.25**	**0.125**	**0.01**	**323**
x Base		0.01			
p		**0.25**	**0.0625**	**0.059813**	**1932**
x Base		0.08			
p	**0.25**	**0.5**	**0.125**	**0.014953**	**483**
x Base	0.75	0.02			
p		**0.25**	**0.0625**	**0.007477**	**241**
x Base		0.01			

Figure 2.2 Quantitative Verification & Recalculation of Event Tree Model to Represent Uncertainty in Hot Leg Weld Exposures for Thermal Fatigue from

It was unclear during the recalculation of Fleming and Lydell's work why the probabilities of 0.25 for the low and high estimates and 0.5 for the "best" estimate values were chosen. Through a set of questions sent to Karl Fleming and Bengt Lydell, it was found that engineering judgement was used for this aspect of the STPNOC risk-informed project. In addition, it was determined that the weld counts and failure mechanism susceptibilities probability distributions were based on supporting data such as the quantification of the number of welds at each of the U.S. PWRs.

The next step in the failure rate development required a Bayesian update of prior distributions for the failure rates for each failure mechanism using the number of failures found in service experience with the exposures. Bayesian analysis is a statistical method that combines prior beliefs of unknown values of interest and concrete observed information regarding the values to infer about their true values. Bayes' theorem states that for two events A and B:

$$\Pr(A \mid B) = \frac{\Pr(B \mid A)\Pr(A)}{\Pr(B)} \tag{2.4}$$

where: Pr(A|B) is the updated posterior probability that event A occurs, considering the new evidence; the occurrence of event B, Pr(A) is the prior probability that event A occurs, before knowledge of the occurrence of event B is known; and Pr(B|A) is the likelihood that event B will occur, if event A occurs. Therefore, the theorem states that one's state of knowledge about the occurrence of event A is updated per Bayes' formula upon the availability of new information regarding the occurrence of event B.

The prior distributions were developed for the failure rate development in the Electric Power Research Institute (EPRI) risk-informed in-service inspection program. Fleming and Lydell provided the prior distributions for SCC, D&C, and TF from EPRI TR-111880. These three failure mechanisms were provided to recreate the results for the hot leg example. However, as part of the critical review of this work, more information was required to recreated the rest of the results provided in Fleming and Lydell's report. To find the prior distribution for V-F, a few details came into question. In Table 2-3 of the EPRI report, the D&C failure mechanism was listed as having a lognormal distribution with a mean of 1.24E-06 and a RF=100. Fleming and Lydell's STPNOC report listed the D&C failure mechanism with a mean of 2.75E-06 and a RF=100. Following an email with Karl Fleming regarding this question, this answer was provided:

> *"We simply made an adjustment to address insights from more than 15 years of service experience that was analyzed since TR 111880 was published. STP was based on PIPExp data whereas TR-111880 was based on data collected in SKI 96:20 which had many data classification issues and was found to under-report D&C. The large range factor (100) means that the results are not very sensitive to this change. One additional thought is that service experience does show aging effects – every time we revisit this data we see upward trends. See Chart below [Figure 2.3] from the attached summary of PIPExp data."*

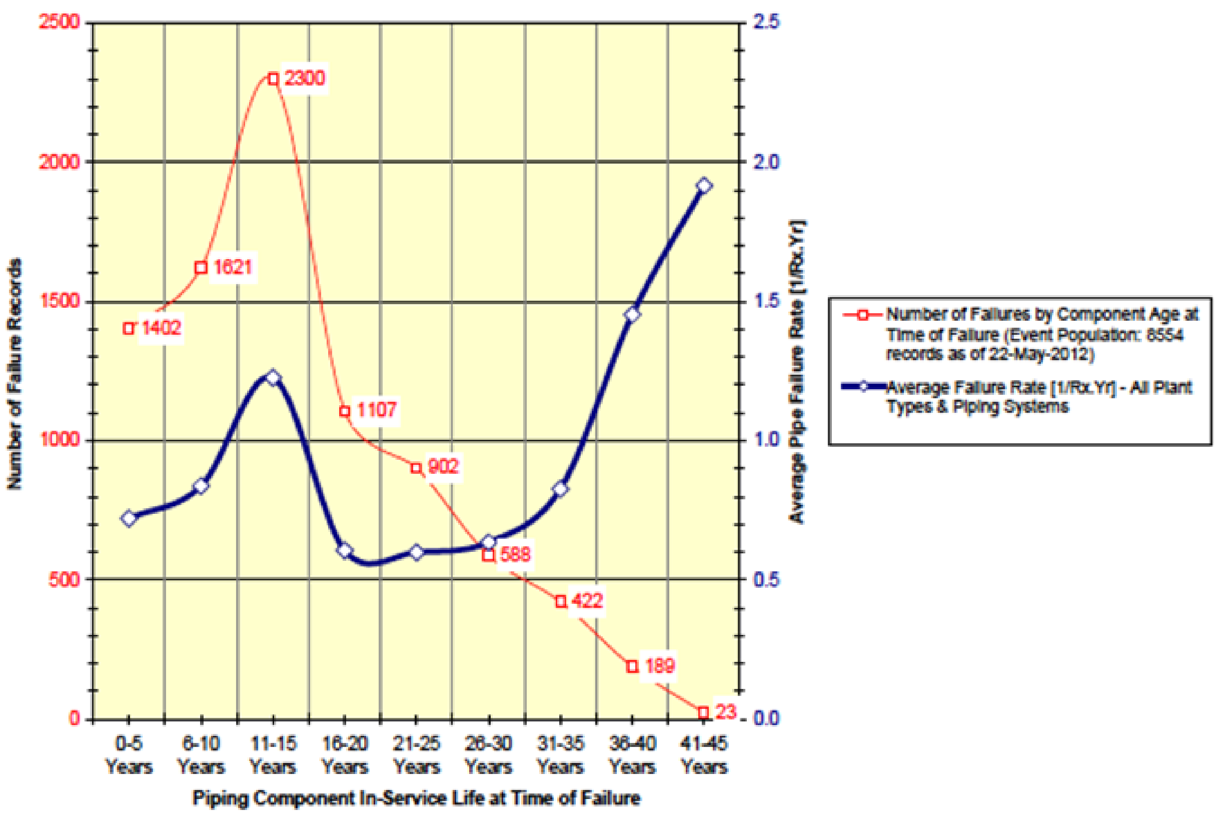

Figure 2.3 Summary of PIPExp Data Demonstrating Aging Effects of NPPs Provided by Karl Fleming[14]

To recreate failure rates for calculation cases 6A, 6B, and 8A-8D, a V-F prior distribution was required (Table 2.1). Additionally, Fleming noted that V-F failures are unconditional failures and that RI-ISI evaluation does not have any criteria for deciding when V-F applies, so it needs to be applied wherever the weld category specifies its application. After reviewing EPRI report TR-11016[13], the interpretation was that this unconditional failure means that some failure mechanisms such as V-F do not show a transient life. Once a crack initiates, failures occur quickly. There is no failure that can result in rupture. There is only the probability of pipe rupture, so conditional rupture probability is equal to unity for the V-F failure mechanism. Thus, the V-F prior distribution has units of failures per system-year.

Table 2.1 Updated Prior Distribution Table for Weld Failure Rates

Damage Mechanism	**Prior Distribution**			
	Distribution Type	**Failure Rate per Weld-Yr**		**Range Factor**
		Mean	**Median**	
Stress Corrosion Cracking	Lognormal	4.27E-05	8.48E-07	100
Design and Construction Errors	Lognormal	2.75E-06	5.46E-08	100
Thermal Fatigue	Lognormal	1.34E-05	2.66E-07	100
Additional Prior Distributions				
Vibrational Fatigue	Lognormal	1.00E-04	1.98E-06	100
Small Bore (all DMs)	Lognormal	1.70E-03	3.38E-05	30

It is interesting to note from Table 2.1 that the small bore piping prior distribution includes contributions from all the failure mechanisms. Collected data shows that this prior mechanism includes contributions from intergranular SCC, V-F, and D&C. Therefore, unlike the other calculation categories, the small bore calculation categories only deal with a combined failure mechanism contribution.

The next step in Fleming and Lydell's quantification procedure is to perform a Bayesian update for each component/failure mechanism susceptibility/population-exposure estimate combination. Fleming and Lydell update the lognormal prior distributions for each failure mechanism using a Poisson likelihood function that incorporates the number of failures for each failure mechanism and the failure mechanism-specific exposure time. For the discrete uncertainty distributions for failure mechanism-specific exposure time, a Bayesian update of the prior distribution is performed for every possible exposure value.

To quantitatively verify the Bayesian update step of Fleming and Lydell's methodology, in this thesis, the updates were performed using R-DAT Plus version 1.5.8, a reliability data collection and an analysis tool developed by Prediction Technologies[15]. The recalculation of the data for the hot leg B-F welds susceptible to SCC can be found in Figure 2.4. From Figure 2.4, by entering the median and the error factor which is also known as the range factor for any lognormal prior distribution, R-DAT Plus generates a prior distribution represented by the red distribution. Upon entering the six observed failures in 12,074 weld-years as the evidence, R-DAT Plus updates the distribution providing both an image, the blue distribution, and a list of summary statistics for the posterior distribution. The results from the R-DAT Plus Bayesian updates exactly match the results provided by Fleming and Lydell for the hot leg calculation categories.

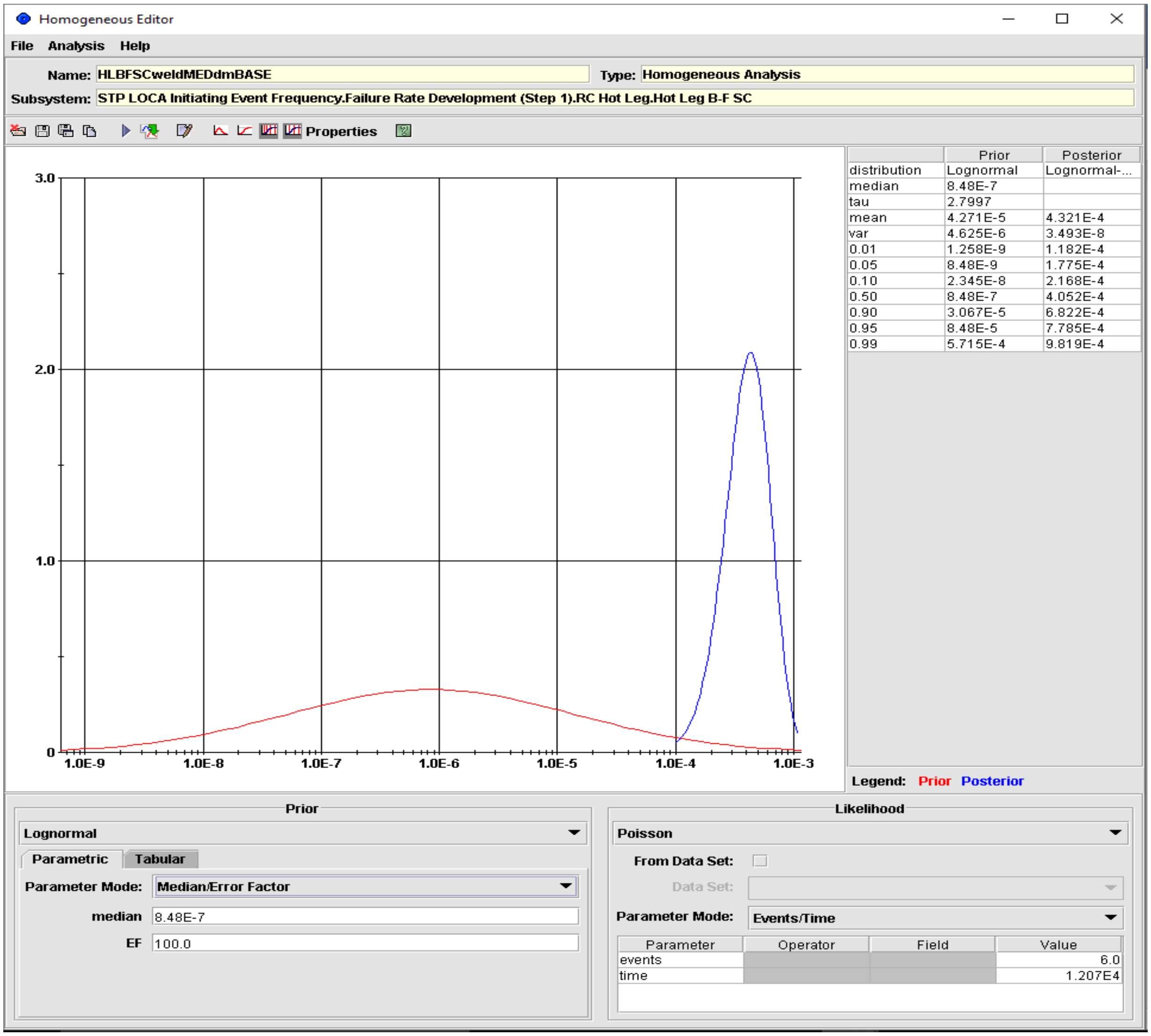

Figure 2.4 Quantitative Verification and Recalculation of Bayesian Updating Results

The final step in Fleming and Lydell's development of the total failure rates requires the development of a mixture distribution for each of the calculation cases. Fleming and Lydell develop total failure rates for each category using a Monte Carlo posterior weighting technique to develop a mixture distribution. A mixture distribution combines the values from the different weld-count and failure mechanism susceptibility fraction uncertainty distributions. The failure rate for each failure mechanism is developed by Monte Carlo sampling from a discrete distribution defined by probabilities and exposure cases. The result of each sample determines from which posterior distribution another Monte Carlo sample will be taken. This process is repeated for 100,000 trials. The resulting failure rate incorporates a probabilistically weighted contribution from each of the weld-count and failure mechanism susceptibility fraction values.

In order to quantitatively verify the total failure rates, in this thesis, the mixture distribution is put together using a Microsoft Excel Add-in, Crystal Ball version 11.1[16], developed by Oracle to run a Monte Carlo simulation which samples from a discrete distribution defined by the probabilities developed for each case, such as the one developed in Figure 2.2. The resulting distributions from the Bayesian updating performed with RDAT Plus for the SCC and D&C mechanisms matched perfectly with the data from Fleming and Lydell. These parameters were then fit to lognormal distributions. The inputs to the SCC distribution were: mean = 4.32E-04 and standard deviation = 2.04E-04. The inputs for the D&C distribution were mean = 1.02E-06 and standard deviation = 4.07E-05. These distributions were then sampled from 100,000 times adding the samples for each damage mechanism. This resulted in the parameters listed under the UIUC heading in Table 2.2

Table 2.2 Comparison of Initial Recalculation of Fleming and Lydell's Mixture Distributions

	Fleming	UIUC	% Error
Mean	4.13E-04	4.33E-04	4.84%
5%	1.79E-04	1.87E-04	4.47%
50%	3.73E-04	3.91E-04	4.83%
95%	7.82E-04	8.20E-04	4.86%

To determine the differences in the calculations, Karl Fleming was consulted. He responded with the following explanation:

> *"…. when we did the STP calculations in 2011 we used a method of fitting the Bayes' updates to lognormal distributions that is different than the method used by your graduate student- but I think his procedure [Nick O'Shea's] is more appropriate than the one we used. The method we used was to preserve the 95%tile and to fix the 50%tile of the lognormal distribution at the geometric mean of the 5%tile and 95%tile of the Bayes'*

update distribution. This created a lognormal distribution that has a slightly different mean than the mean of the Bayes' update. The new means you get from our fitting procedure is 4.11E-4 for SC (smaller than the Bayes mean) and 1.86E-6 for D&C (larger than the Bayes' mean). .....

When we moved on to Vogtle, Wolf Creek, Calvert Cliffs, and Palisades we changed our lognormal fitting procedure to preserving the mean and the range factor of the Bayes' update distribution where the range factor is calculated as the geometric mean of the 5%tile and 95%tile of the Bayes posterior distribution. Using this approach – which I believe is better than what we did for STP – the Crystal ball calculated sums from different damage mechanisms will generally match the mean point estimates."

The response from Fleming allowed for the recalculation of the parameters provided in the report by Fleming and Lydell that would not have been possible from the information originally provided. Replacing the median value of the resulting posterior distributions from the R-DAT Plus Bayesian updates with the square root of the 95%*5% is not explained or justified in the report. However, it appears that Fleming and Lydell recognized this and changed their methodology for the future applications of the methodology.

One of the questions posed to Karl Fleming and Bengt Lydell during the review of their methodology regarded their selection of 100,000 Monte Carlo simulations. Their response indicated that they ran an informal convergence study to make sure that 100,000 simulations was sufficient for the calculations in their report. Based on this response, 100,000 Monte Carlo simulations was also used in the recalculation of their results. The results from the recalculation using the methodology explained in Fleming's email can be found in Table 2.3.

Table 2.3 Comparison of Mixture Distribution Recalculations for Hot Leg Calculation Cases

Recalculation of Total Failure Rates for Hot Leg Weld Calculation Cases								
Calculation Case	**Weld Type**	**DM**	**Failure Rate Distribution (failures per weld-year)**					
			Mean	**5%tile**	**50%tile**	**95%tile**	**RF**	
1A	B-F	SC+D&C	4.13E-04	1.78E-04	3.73E-04	7.81E-04	2.1	
1B	B-J	D&C	1.39E-06	5.10E-10	4.12E-08	3.25E-06	79.8	
1C		TF+D&C	1.26E-05	1.81E-08	5.85E-07	2.85E-05	39.7	
Total Failure Rates for Hot Leg Weld Calculation Cases (copied from Fleming and Lydell report)								
Calculation Case	**Weld Type**	**DM**	**Failure Rate Distribution (failures per weld-year)**					
			Mean	**5%tile**	**50%tile**	**95%tile**	**RF**	
1A	B-F	SC+D&C	4.13E-04	1.79E-04	3.73E-04	7.82E-04	2.1	
1B	B-J	D&C	1.44E-06	5.27E-10	4.12E-08	3.19E-06	77.8	
1C		TF+D&C	1.07E-05	1.79E-08	5.79E-07	2.83E-05	39.8	
Percent Differences Between Recalculated Values and Published Results by Fleming and Lydell								
1A	B-F	SC+D&C	-0.08	-0.67	-0.02	-0.10	-0.18	
1B	B-J	D&C	-3.22	-3.16	0.09	1.99	2.63	
1C		TF+D&C	17.57	0.89	1.10	0.60	-0.24	

Calculation case 1A in Table 2.3 shows results that agree with the results published by Fleming and Lydell. This indicates that the methodology described by Fleming was correctly implemented in Crystal Ball for the recalculation of the mixture distributions. However, for calculation cases 1B and 1C there is less agreement. The most notable case is the mean value for calculation case 1C, which shows an over 17% difference between the value published by Fleming and Lydell and the value that was calculated using Crystal Ball from the approach described by Karl Fleming. The variation in the mean for case 1C is particularly confusing, because the remaining parameters for the distribution are very close together.

During the attempted recalculation of the results published by Fleming and Lydell in support of the STPNOC project, many questions arose concerning various details of the report.

The communication with Karl Fleming regarding these questions can be found in Table A.1 in Appendix A. Some of the issues were never closed. Therefore, when further information is provided, these communications can be updated for future publications.

2.1.2 CRITICAL REVIEW & QUANTITATIVE VERIFICATION OF CONDITIONAL RUPTURE PROBABILITY DEVELOPMENT

This section discusses the recalculation and critical review of the conditional rupture probability (CRP) development in the location-specific estimation of LOCA frequencies performed by Fleming and Lydell for the STPNOC risk-informed GSI-191 project. The surrogate failure rates developed by Fleming and Lydell represented the rate at which a precursor event occurred, such as a crack or a leak. A precursor event does not include any type of rupture event that would lead to the occurrence of a LOCA. Fleming and Lydell's approach assumes that for a LOCA to occur, a precursor failure event must occur. Once a precursor failure event occurs, there is a probability that the component will rupture completely. This probability is called the conditional rupture probability (CRP). The approach Fleming and Lydell used to develop the CRPs contains the following steps:

1. Utilize expert reference LOCA distributions and multiplier distributions from NUREG-1829
2. Determine 40-year LOCA distributions for each of the NUREG-1829 experts and find the geometric mean of all the experts' distributions
3. Calculate LOCA frequency distribution from Lydell's base case analysis in NUREG-1829
4. Develop target LOCA frequency distributions
5. Calculate CRP prior distributions for each calculation case category

6. Perform Bayesian updates of the CRP prior distributions with failure and rupture evidence from service data

The expert elicitation results in NUREG-1829 capture the current state of knowledge among experts from two schools of thought: statistical analysis of service data and probabilistic fracture mechanics. One of the NUREG-1829 experts, Bengt Lydell, co-author of the approach developed by Fleming and Lydell, created a "base case analysis" for informing the elicitation. Lydell's base case analysis implements an approach like the approach used by Fleming and Lydell. This approach develops a set of LOCA frequencies for the RCS hot leg, surge line, and high pressure safety injection system line. Four independent estimates were provided for each applicable LOCA break size category (see Table 1.1) for each of the three component categories. Two of the estimates were based on statistical analysis of service experience while the other two estimates were based on probabilistic fracture mechanics analysis. In addition to Lydell's base case analysis, nine NUREG-1829 experts provided estimations of LOCA frequencies for a range of components[17].

Fleming and Lydell use information from NUREG-1829 to convert the information provided as LOCA frequencies vs. LOCA category to CRPs vs. break size. This step required establishing the target LOCA frequencies for key components and then deriving the equivalent CRP probability model that, when multiplied by the failure rate model, produced the same target LOCA frequencies. This approach was applied to the RCS hot leg, cold leg, surge line, and high pressure injection line, while using the following equation:

$$F(LOCA_j) = \sum_l m_l \lambda_l P(R_j \mid F) \tag{2.5}$$

where: $F(LOCA_j)$ is the unconditional LOCA frequency for break size category j; m_l is the number of pipe welds of type l in each component category; λ_l is the failure rate for component category l within the selected component in Lydell's base case analysis from Appendix D of NUREG-1829; and $P(R_j|F)$ is the CRP in LOCA category j given a precursor failure in the selected component. Combining Equation (2.5) with the failure rates developed in Lydell's base case analysis allows Fleming and Lydell to derive uncertainty distributions for the CRPs in each LOCA category.

The failure rate development began with eight component categories which covered the 775 weld locations in the Class 1 piping at STPNOC. However, for the CRP estimation Fleming and Lydell only created four categories: the hot leg, cold leg, surge line, and high pressure injection system. The four CRP categories were selected due to the information available in NUREG-1829 and because these four categories provide a unique model for all the large pipe sizes (≥12"). These four models are used to develop prior CRP distributions. Fleming and Lydell determined that the smaller pipe sizes did not require further detail. The prior CRP distributions are then updated with the number of precursor failures and ruptures for each failure rate case.

Nine NUREG-1829 experts provided LOCA frequency inputs at the component level including the hot leg, cold leg, surge line, and high pressure injection line components. The first of the LOCA frequencies provided by the experts was for the existing fleet of nuclear power plants, which had an average age of 25 years at the time of the elicitation. The experts provided multipliers for normalizing these LOCA frequencies to plant ages of 40 years and 60 years. It is through these multipliers that the experts in NUREG-1829 incorporated the effects of aging components on LOCA frequencies. The experts implicitly incorporated the aging effects. Chapter 4 of this thesis explains a methodology for the explicit incorporation of temporal variation of LOCA frequencies.

Fleming and Lydell's study took the estimations for LOCA frequencies at 25 years and used the NUREG-1829 multipliers to create estimations of LOCA frequencies for 40 years. Creating the 40-year estimations of LOCA frequencies from the experts' inputs was a simple process as both the 25-year estimations of LOCA frequencies and the 40-year multipliers were provided as lognormal distributions. The product of two lognormal distributions is also a lognormal distribution. Therefore, the parameters of the 40-year estimations of LOCA frequencies from the NUREG-1829 experts were calculated using the following formulas:

$$median_{40YLF} = median_{Base} * median_{40YM} \tag{2.6}$$

$$RF_{40YLF} = e^{1.645\sigma_{40YLF}} \tag{2.7}$$

$$\sigma_{40YLF} = \sqrt{\left(\frac{\ln\left(RF_{Base}\right)}{1.645}\right)^2 + \left(\frac{\ln\left(RF_{40YM}\right)}{1.645}\right)^2} \tag{2.8}$$

where: $median_{40YLF}$ is the median of the lognormal distribution for the 40-year LOCA frequency, evaluated for each combination of expert and LOCA frequency; $median_{Base}$ is the median of the lognormal distribution for the base LOCA frequency; $median_{40YM}$ is the median of the lognormal distribution for the 40-year multiplier provided by each expert for each LOCA category; RF_{40YLF} is the range factor of the lognormal distribution for the 40-year LOCA frequency, equal to the square root of the 95th percentile divided by the 5th percentile of the lognormal distribution; σ_{40YLF} is the logarithmic standard deviation for the lognormal distribution for the 40-year LOCA frequency; RF_{Base} is the range factor of the lognormal distribution for the base LOCA frequency provided by each expert for each LOCA category; and RF_{40YM} is the range factor of the lognormal distribution for the 40-year multiplier provided by each expert for each LOCA category.

In order to do the quantitative verification, using Equations (2.6)-(2.8), the 40-year LOCA frequency distributions for each expert and LOCA component break size category were recreated. The results were an exact match to the ones published for the hot leg by Fleming and Lydell. Fleming and Lydell's report for STPNOC includes the information for the 9 experts from NUREG-1829 for only the hot leg. However, to recreate the 40-year LOCA Frequency distributions for the cold leg, surge line, and HPI line categories, the information needed to be pulled out of the NUREG-1829 supporting information[18]. Using the same structure as Fleming and Lydell used, the cold leg, surge line, and HPI line information was added to the hot leg information and the resulting 40-year LOCA frequency distributions can be found in Appendix A, Table A.2.

The next step is to aggregate the expert LOCA frequency distributions into a composite distribution. Fleming and Lydell preserved the median value and the range factor for the experts' 40-year LOCA frequency distributions. The geometric mean of the median values and the range factors were calculated for each LOCA break size category for the hot leg, cold leg, surge line, and HPI line categories. Once the median and the range factors were calculated, the remaining lognormal distribution parameters were calculated. The results of the recalculation can be found in Table 2.4.

Table 2.4 Recalculation of Aggregated NUREG-1829 Expert LOCA Frequency Distribution

Component	LOCA Cat.	Break Size (Inches)	Geometric Mean Distribution Parameters Events per Reactor-Calendar Year				
			Mean	5%tile	50%tile	95%tile	RF
Hot Leg	1	≥ 0.5	4.08E-07	9.32E-09	1.21E-07	1.57E-06	13.0
	2	≥ 1.5	1.28E-07	2.25E-09	3.34E-08	4.95E-07	14.8
	3	≥ 3	6.51E-08	1.01E-09	1.59E-08	2.52E-07	15.8
	4	≥ 6.75	2.59E-08	2.49E-10	4.96E-09	9.88E-08	19.9
	5	≥ 14	1.50E-08	6.70E-11	1.90E-09	5.37E-08	28.3
	6	≥ 31.5	3.16E-09	4.84E-12	2.18E-10	9.78E-09	45.0
Cold Leg	1	≥ 0.5	1.47E-07	3.27E-09	4.30E-08	5.66E-07	13.2
	2	≥ 1.5	5.20E-08	9.07E-10	1.35E-08	2.01E-07	14.9
	3	≥ 3	2.19E-08	3.33E-10	5.31E-09	8.48E-08	16.0
	4	≥ 6.75	7.85E-09	7.41E-11	1.49E-09	2.99E-08	20.1
	5	≥ 14	4.53E-09	1.94E-11	5.60E-10	1.62E-08	28.9
	6	≥ 31.5	1.10E-09	1.56E-12	7.23E-11	3.36E-09	46.4
Surge Line	1	≥ 0.5	3.60E-07	1.33E-08	1.34E-07	1.35E-06	10.1
	2	≥ 1.5	1.26E-07	3.46E-09	4.09E-08	4.83E-07	11.8
	3	≥ 3	6.45E-08	1.29E-09	1.79E-08	2.49E-07	13.9
	4	≥ 6.75	1.92E-08	2.47E-10	4.28E-09	7.41E-08	17.3
	5	≥ 14	2.72E-09	4.22E-11	6.66E-10	1.05E-08	15.8
HPI Line	1	≥ 0.5	1.27E-05	6.40E-07	5.45E-06	4.65E-05	8.5
	2	≥ 1.5	4.58E-06	1.51E-07	1.62E-06	1.74E-05	10.7
	3	≥ 3	7.21E-07	1.53E-08	2.06E-07	2.78E-06	13.5
	4	≥ 6.75	1.29E-07	1.41E-09	2.64E-08	4.95E-07	18.8
	5	≥ 14	1.12E-08	1.03E-09	6.20E-09	3.73E-08	6.0
	5 (KF,BL)	≥ 14	3.04E-08	3.30E-10	6.20E-09	1.16E-07	18.8
% Difference			-170.65%	68.01%	0.00%	-212.59%	-212.59%

The recreated values match Fleming and Lydell's published numbers exactly with the exception of LOCA category 5 for the HPI Line. The result from Fleming and Lydell has been added to the bottom of Table 2.4 for ease of comparison. Clearly, the recreated median value exactly matches the published number in Fleming and Lydell's report. However, the mean, 5%, 95% and range factor values are very far apart. Since the 5%, 95%, and mean values are calculated from the median and range factor values, it appears that only the RF is varied. To determine the cause of this major variation in the results, the authors asked Karl Fleming and Bengt Lydell for some insight, and their answer is the following:

> *"They were adjusted to be the same as the RF for the maximum RF for the previous breaks sizes calculated. The justification is to prevent the range factors determined from the mixture distribution to have an illogical trend in RF vs. decreasing frequency – based on what we believe is a reasonable engineering judgment."*

While this statement from Karl Fleming does not specifically relate to Table 2.4, it is assumed that the range factor for Case 5 of the HPI line was increased by Fleming and Lydell to match the range factor calculated for Case 4 to prevent "an illogical trend" in the range factors. This means that as experts estimated LOCA frequencies for higher component break size categories, the range factor should stay the same or increase because the range factor is a measure of the broadness of the distribution, or the uncertainty associated with the true value. As the frequencies being estimated are decreasing, the uncertainty in the values should not decrease. However, the range factor for Case 5 of the surge line category was not increased despite being smaller than the range factor calculated for Case 4 of the surge line. Therefore, this research has determined that the methodology being applied by Fleming and Lydell for the STPNOC project should be corrected to maintain consistency in all places. Whether it is decided to adjust the range factors to prevent "an illogical trend" or to keep the range factors the same as the expert elicitation process produced, the process should be consistent.

After the experts' LOCA frequency distributions are aggregated, the next step is to develop the CRP distributions from Lydell's NUREG-1829 Appendix D base case analysis. Using the same files Lydell used for NUREG-1829, they fit a lognormal distribution to the estimates of failure rates that Lydell derived. A lognormal distribution for the CRP was assumed for each LOCA break size category. Fleming and Lydell created CRP distributions that when multiplied by Lydell's failure rate distributions closely approximated the LOCA frequency distributions created by Lydell for NUREG-1829.

The next step in the recalculation of the conditional rupture probability distributions is to take the geometric mean values from the NUREG-1829 experts and to develop a mixture distribution between with the LOCA frequency distribution developed from Lydell's base case analysis. To run the quantitative verification, in this thesis, using the Microsoft Excel add-in, Crystal Ball, the mixture distributions were created. Both the geometric mean of the NUREG-1829 experts and Lydell's base case LOCA frequency distributions were given an equal 0.5 probability in the development of the mixture distribution. Table 2.5 demonstrates the calculated results using 100,000 Monte Carlo simulations.

Table 2.6 provides the percent differences between the calculated values and the values provided by Fleming and Lydell. The differences between the calculated values are all rather small, which this research attributes to sampling variation.

Table 2.5 Recreated Values for Mixture Distribution of Geometric Mean and Lydell Base Case for LOCA Frequency Distributions

Component	LOCA Cat.	Break Size (in.)	Target LOCA Frequency Distribution Parameters Events per Reactor-Calendar Year				
			Mean	5%tile	50%tile	95%tile	RF
Hot Leg	1	≥ .5	5.10E-07	5.48E-09	1.05E-07	1.85E-06	18.4
	2	≥ 1.5	8.22E-08	4.10E-10	1.47E-08	3.28E-07	28.3
	3	≥ 3	4.06E-08	1.62E-10	6.36E-09	1.61E-07	31.5
	4	≥ 6.75	1.63E-08	5.74E-11	2.11E-09	6.06E-08	32.5
	5	≥ 14	8.53E-09	2.05E-11	7.59E-10	2.90E-08	37.6
	6	≥ 31.5	2.19E-09	5.20E-12	1.79E-10	6.55E-09	35.5
Cold Leg	1	≥ .5	2.21E-07	2.42E-09	4.33E-08	7.94E-07	18.1
	2	≥ 1.5	3.63E-08	2.03E-10	6.55E-09	1.42E-07	26.5
	3	≥ 3	1.51E-08	8.22E-11	2.62E-09	5.98E-08	27.0
	4	≥ 6.75	5.36E-09	2.62E-11	8.00E-10	2.08E-08	28.2
	5	≥ 14	2.71E-09	9.07E-12	2.91E-10	9.76E-09	32.8
	6	≥ 31.5	8.02E-10	2.04E-12	7.37E-11	2.55E-09	35.4
Surge Line	1	≥ .5	2.35E-07	3.59E-09	6.58E-08	9.37E-07	16.2
	2	≥ 1.5	6.69E-08	2.72E-10	1.03E-08	2.77E-07	31.9
	3	≥ 3	3.46E-08	1.06E-10	4.06E-09	1.43E-07	36.8
	4	≥ 6.75	1.04E-08	3.55E-11	1.14E-09	4.01E-08	33.6
	5	≥ 14	1.61E-09	1.36E-11	2.87E-10	6.23E-09	21.4
HPI Line	1	≥ .5	1.40E-05	3.85E-07	4.75E-06	5.21E-05	11.6
	2	≥ 1.5	3.43E-06	5.57E-08	9.72E-07	1.35E-05	15.5
	3	≥ 3	8.28E-07	1.41E-08	2.13E-07	3.16E-06	15.0
	4	≥ 6.75	1.29E-07	1.41E-09	2.64E-08	4.95E-07	18.8
	5	≥ 14	3.04E-08	3.30E-10	6.20E-09	1.16E-07	18.8

Note: Categories 4,5 of HPI are simply the GM of the experts from NUREG-1829, as Lydell did not produce results for these categories

Table 2.6 Calculated Percent Differences Between Recreated Mixture Distribution Values and Fleming and Lydell's Published Values

Component	LOCA Cat.	Break Size (in.)	Target LOCA Frequency Distribution Parameters Events per Reactor-Calendar Year				
			Mean	5%tile	50%tile	95%tile	RF
Hot Leg	1	≥ .5	0.67%	1.68%	-0.18%	0.98%	-0.20%
	2	≥ 1.5	-0.06%	-4.32%	-1.51%	-0.72%	1.99%
	3	≥ 3	-1.09%	-3.29%	-1.77%	0.44%	1.78%
	4	≥ 6.75	4.10%	1.52%	1.19%	-0.20%	-0.92%
	5	≥ 14	-1.80%	-1.98%	-0.62%	-1.18%	0.52%
	6	≥ 31.5	3.75%	3.76%	-0.12%	-1.20%	-2.48%
Cold Leg	1	≥ .5	-3.17%	2.43%	0.25%	-1.79%	-2.06%
	2	≥ 1.5	-2.03%	-3.09%	-1.16%	-0.59%	1.50%
	3	≥ 3	-1.43%	1.66%	0.18%	1.02%	-0.49%
	4	≥ 6.75	-0.31%	-2.40%	-1.59%	2.62%	2.62%
	5	≥ 14	-0.23%	1.15%	-0.94%	3.31%	0.93%
	6	≥ 31.5	-0.09%	-0.37%	1.35%	-3.24%	-1.21%
Surge Line	1	≥ .5	0.23%	1.03%	-0.26%	0.23%	-0.22%
	2	≥ 1.5	-1.31%	-0.17%	-0.81%	-2.10%	-1.11%
	3	≥ 3	3.94%	0.91%	0.61%	3.92%	1.63%
	4	≥ 6.75	-0.53%	0.78%	0.02%	-1.24%	-1.12%
	5	≥ 14	-0.03%	0.98%	1.02%	0.94%	-0.12%
HPI Line	1	≥ .5	0.57%	-0.87%	0.32%	-0.89%	0.36%
	2	≥ 1.5	-2.16%	1.20%	-0.62%	-1.81%	-1.61%
	3	≥ 3	2.04%	-0.33%	0.98%	1.75%	0.71%
	4	≥ 6.75	0.09%	-0.33%	-0.11%	-0.03%	-0.18%
	5	≥ 14	0.33%	-0.12%	-0.05%	0.43%	0.00%

The target LOCA frequencies are then developed with Equations (2.6)-(2.8) and the failure rates developed from Lydell's base case analysis from NUREG-1829 Appendix D. The results from the recalculation are shown in Table 2.7. The percent differences between the calculated value and the results provided by Fleming and Lydell can be found in Table 2.8.

The results shown in Table 2.7 match the results provided by Fleming and Lydell for most calculation cases. However, some of the calculation cases for higher LOCA categories such as the 5D case for surge line are significantly different than the published results. After discussing this point with Karl Fleming, it was discovered that the range factors for some categories were adjusted:

> *"They were adjusted to be the same as the RF for the maximum RF for the previous breaks sizes calculated. The justification is to prevent the range factors determined from the mixture distribution to have an illogical trend in RF vs. decreasing frequency – based on what we believe is a reasonable engineering judgment."*

When the range factors were adjusted to match the results published by Fleming and Lydell, the recreated parameters are all in agreement with the values published by Fleming and Lydell.

Table 2.7 Recalculation of Conditional Rupture Probability Prior Distributions

Component	LOCA Category	Break Size (in.)	Conditional Rupture Probability Distribution Parameters				
			Mean	5th Percentile	Median	95th Percentile	Range Factor [1]
Hot Leg	1	≥ .5	1.47E-03	1.84E-04	9.13E-04	4.52E-03	5.0
	2	≥ 1.5	3.33E-04	1.35E-05	1.30E-04	1.24E-03	9.6
	3	≥ 3	1.66E-04	5.01E-06	5.63E-05	6.32E-04	11.2
	4	≥ 6.75	5.78E-05	1.49E-06	1.82E-05	2.22E-04	12.2
	5	≥ 14	2.51E-05	4.55E-07	6.64E-06	9.71E-05	14.6
	6	≥ 31.5	5.68E-06	1.10E-07	1.56E-06	2.19E-05	14.1
	6D[2]	44.5	3.06E-06	6.13E-08	8.52E-07	1.18E-05	13.9
Cold Leg	1	≥ .5	1.21E-03	1.50E-04	7.49E-04	3.74E-03	5.0
	2	≥ 1.5	2.75E-04	1.31E-05	1.15E-04	1.01E-03	8.8
	3	≥ 3	1.14E-04	4.89E-06	4.54E-05	4.21E-04	9.3
	4	≥ 6.75	3.59E-05	1.49E-06	1.41E-05	1.34E-04	9.5
	5	≥ 14	1.60E-05	4.23E-07	5.10E-06	6.14E-05	12.1
	6	≥ 31.5	4.49E-06	9.15E-08	1.26E-06	1.74E-05	13.8
	6D[2]	44.5	2.68E-06	4.86E-08	7.11E-07	1.04E-05	14.6
Surge Line	1	≥ .5	2.07E-02	2.44E-03	1.26E-02	6.48E-02	5.2
	2	≥ 1.5	7.23E-03	1.40E-04	1.98E-03	2.80E-02	14.1
	3	≥ 3	3.26E-03	4.70E-05	7.70E-04	1.26E-02	16.4
	4	≥ 6.75	8.47E-04	1.44E-05	2.17E-04	3.28E-03	15.1
	5	≥ 14	1.20E-04	6.76E-06	5.41E-05	4.33E-04	8.0
	5D[3]	19.8	4.90E-05	4.91E-06	2.80E-05	1.60E-04	5.7
HPI Line	1	≥ .5	1.08E-02	5.88E-03	1.02E-02	1.76E-02	1.7
	2	≥ 1.5	2.99E-03	5.28E-04	2.10E-03	8.38E-03	4.0
	3	≥ 3	6.06E-04	1.30E-04	4.54E-04	1.59E-03	3.5
	4	≥ 6.75	9.70E-05	1.03E-05	5.68E-05	3.12E-04	5.5
	5	≥ 14	2.28E-05	2.43E-06	1.33E-05	7.32E-05	5.5

Notes:

[1] Range Factor = SQRT(95%tile/5%tile).

[2] 6D corresponds to a double-ended break of a 31.5" pipe.

[3] 5D corresponds to a double-ended break of a 14" pipe.

[4] Range factors adjusted upwards to ensure no RF decrease with decreasing LOCA frequency.

Table 2.8 Calculated Percent Differences Between Recreated Conditional Rupture Probability Distributions and STPNOC Results Published by Fleming and Lydell

Component	LOCA Category	Break Size (in.)	Conditional Rupture Probability Distribution Parameters				
			Mean	5th Percentile	Median	95th Percentile	Range Factor[1]
Hot Leg	1	≥ .5	0.35%	0.21%	0.33%	0.47%	1.06%
	2	≥ 1.5	0.62%	0.11%	0.44%	0.99%	-0.14%
	3	≥ 3	0.45%	0.04%	0.29%	0.57%	0.23%
	4	≥ 6.75	0.68%	-0.09%	0.41%	0.85%	0.07%
	5	≥ 14	0.81%	0.11%	0.35%	0.63%	0.11%
	6	≥ 31.5	-2.81%	4.14%	0.42%	-2.89%	-3.42%
	6D[2]	44.5	-4.23%	5.34%	0.37%	-4.47%	-4.79%
Cold Leg	1	≥ .5	0.70%	-0.19%	0.09%	0.65%	0.02%
	2	≥ 1.5	0.27%	-0.05%	-0.08%	0.84%	0.88%
	3	≥ 3	0.56%	-0.57%	0.02%	0.83%	0.89%
	4	≥ 6.75	0.27%	-0.30%	-0.07%	0.49%	-0.15%
	5	≥ 14	0.70%	-0.53%	0.10%	0.68%	0.44%
	6	≥ 31.5	0.26%	-0.25%	0.00%	0.32%	0.54%
	6D[2]	44.5	0.55%	-0.38%	0.08%	0.84%	0.11%
Surge Line	1	≥ .5	-0.68%	0.82%	-0.23%	-0.80%	-0.91%
	2	≥ 1.5	-0.12%	0.25%	0.05%	-0.14%	0.10%
	3	≥ 3	-0.62%	0.47%	-0.06%	-0.84%	-0.21%
	4	≥ 6.75	-8.28%	8.94%	0.07%	-8.16%	-7.93%
	5	≥ 14	-47.71%	105.53%	-0.01%	-51.38%	-51.22%
	5D[3]	19.8	-58.82%	188.96%	0.00%	-65.30%	-65.24%
HPI Line	1	≥ .5	-0.42%	1.83%	-0.27%	-2.16%	-3.82%
	2	≥ 1.5	-0.20%	0.15%	0.15%	-0.10%	-0.37%
	3	≥ 3	-5.98%	14.73%	0.17%	-12.26%	-12.50%
	4	≥ 6.75	0.36%	0.36%	0.13%	0.26%	-0.14%
	5	≥ 14	0.40%	-0.10%	0.25%	0.31%	-0.14%

Next step of the methodology uses the target distributions of LOCA frequencies and the failure rate distributions developed by Lydell for the base case analysis in Appendix D of

NUREG-1829 to derive CRP distributions. The target distributions, Lydell's failure rate distributions, and the CRP distributions are lognormal distributions; therefore, the CRP distributions can be derived by dividing the lognormal target distributions of LOCA frequencies by the lognormal failure rate distributions using the same methodology behind Equations (2.6)-(2.8). The conditional rupture probabilities developed from the target distributions of LOCA frequencies and Lydell's base case analysis distributions of failure rates are then used as prior distributions which are then updated with service experience. The evidence for each Bayesian update is the number of service experience precursor failures and zero experienced LOCAs for each system. Since there were no occurrences of LOCAs in the service experience, the Bayesian update of the prior distributions resulted in posterior CRP distributions that demonstrated a small decrease in rupture probabilities.

To run quantitative verification on this stage of the results, using R-DAT Plus, each distribution was updated with zero ruptures and the number of precursor failures associated with each calculation case. The values recreated for this research are shown in Table 2.9. The calculated percent difference for each of the parameters of the updated CRP distributions can be found in Table 2.10.

Table 2.9 Recreated Conditional Rupture Probability Posterior Distributions

Component	Bayes' Update Evidence	LOCA Category	Break Size (in.)	Conditional Rupture Probability Distribution Parameters				
				Mean	5%tile	Median	95%tile	RF[1]
Hot Leg	0 Ruptures/ 6 Failures; Hot Leg CRP Model	1	≥ .5	1.43E-03	1.85E-04	9.04E-04	4.39E-03	4.9
		2	≥ 1.5	3.28E-04	1.34E-05	1.29E-04	1.23E-03	9.6
		3	≥ 3	1.64E-04	5.01E-06	5.60E-05	6.25E-04	11.2
		4	≥ 6.75	5.74E-05	1.48E-06	1.81E-05	2.20E-04	12.2
		5	≥ 14	2.49E-05	4.53E-07	6.62E-06	9.66E-05	14.6
		6	≥ 31.5	5.85E-06	1.06E-07	1.55E-06	2.26E-05	14.6
		6D[2]	44.5	3.20E-06	5.82E-08	8.49E-07	1.24E-05	14.6
Hot Leg at SG Inlet	0 Ruptures/ 19 Failures; Hot Leg CRP Model	1	≥ .5	1.39E-03	1.84E-04	8.91E-04	4.25E-03	4.8
		2	≥ 1.5	3.22E-04	1.34E-05	1.28E-04	1.20E-03	9.5
		3	≥ 3	1.61E-04	5.00E-06	5.58E-05	6.18E-04	11.1
		4	≥ 6.75	5.70E-05	1.48E-06	1.81E-05	2.19E-04	12.2
		5	≥ 14	2.48E-05	4.53E-07	6.61E-06	9.63E-05	14.6
		6	≥ 31.5	5.84E-06	1.06E-07	1.55E-06	2.26E-05	14.6
		6D[2]	44.5	3.20E-06	5.82E-08	8.49E-07	1.24E-05	14.6
Cold Leg	0 Ruptures/ 3 Failures; Cold Leg CRP Model	1	≥ .5	1.20E-03	1.49E-04	7.46E-04	3.71E-03	5.0
		2	≥ 1.5	2.72E-04	1.32E-05	1.15E-04	9.97E-04	8.7
		3	≥ 3	1.13E-04	4.93E-06	4.54E-05	4.17E-04	9.2
		4	≥ 6.75	3.60E-05	1.48E-06	1.41E-05	1.34E-04	9.5
		5	≥ 14	1.59E-05	4.24E-07	5.09E-06	6.11E-05	12.0
		6	≥ 31.5	4.47E-06	9.20E-08	1.26E-06	1.73E-05	13.7
		6D[2]	44.5	2.68E-06	4.86E-08	7.10E-07	1.04E-05	14.6
Surge Line	0 Ruptures/ 3 Failures; Surge Line CRP Model	1	≥ .5	1.89E-02	2.36E-03	1.20E-02	5.81E-02	5.0
		2	≥ 1.5	6.09E-03	1.38E-04	1.91E-03	2.46E-02	13.3
		3	≥ 3	2.92E-03	4.66E-05	7.56E-04	1.18E-02	15.9
		4	≥ 6.75	8.86E-04	1.32E-05	2.16E-04	3.49E-03	16.2
		5	≥ 14	2.27E-04	3.30E-06	5.40E-05	8.83E-04	16.4
		5D[3]	19.8	1.18E-04	1.71E-06	2.80E-05	4.58E-04	16.4
CVCS Line	0 Ruptures/ 14 Failures; HPI CRP Model	1	≥ .5	1.07E-02	5.59E-03	1.00E-02	1.79E-02	1.8
		2	≥ 1.5	2.88E-03	5.17E-04	2.05E-03	7.97E-03	3.9
		3	≥ 3	6.40E-04	1.13E-04	4.50E-04	1.79E-03	4.0
		4	≥ 6.75	9.68E-05	1.03E-05	5.66E-05	3.11E-04	5.5

Table 2.9 (Cont.)

		5	≥ 14	2.27E-05	2.42E-06	1.33E-05	7.31E-05	5.5
Safety Injection Recirculation (SIR) Lines	0 Ruptures/ 14 Failures; HPI CRP Model	1	≥ .5	1.07E-02	5.59E-03	1.00E-02	1.79E-02	1.8
		2	≥ 1.5	2.88E-03	5.17E-04	2.05E-03	7.97E-03	3.9
		3	≥ 3	6.40E-04	1.13E-04	4.50E-04	1.79E-03	4.0
		4	≥ 6.75	9.68E-05	1.03E-05	5.66E-05	3.11E-04	5.5
		5	≥ 14	2.27E-05	2.42E-06	1.33E-05	7.31E-05	5.5
Pressurizer Lines	0 Ruptures/ 12 Failures; HPI CRP Model	1	≥ .5	1.07E-02	5.60E-03	1.00E-02	1.80E-02	1.8
		2	≥ 1.5	2.89E-03	5.18E-04	2.05E-03	8.03E-03	3.9
		3	≥ 3	6.41E-04	1.13E-04	4.51E-04	1.79E-03	4.0
		4	≥ 6.75	9.68E-05	1.03E-05	5.66E-05	3.11E-04	5.5
		5	≥ 14	2.27E-05	2.42E-06	1.33E-05	7.31E-05	5.5
Small Bore	0 Ruptures/ 79 Failures; HPI CRP Model	1	≥ .5	9.78E-03	5.26E-03	9.25E-03	1.61E-02	1.8
		2	≥ 1.5	2.48E-03	4.87E-04	1.85E-03	6.59E-03	3.7
		3	≥ 3	6.15E-04	1.11E-04	4.40E-04	1.70E-03	3.9

Notes:

[1] Range Factor = SQRT(95%tile/5%tile).

[2] 6D corresponds to a double-ended break of a 31.5" pipe.

[3] 5D corresponds to a double-ended break of a 16" pipe.

Table 2.10 Calculated Percent Differences Between Updated Conditional Rupture Probability Distributions and STPNOC Results Published by Fleming and Lydell

Component	Bayes' Update Evidence	LOCA Category	Break Size (in.)	Conditional Rupture Probability Distribution Parameters				
				Mean	5%tile	Median	95%tile	RF[1]
Hot Leg	0 Ruptures/ 6 Failures; Hot Leg CRP Model	1	≥ .5	0.14%	0.00%	-0.03%	-0.05%	-0.61%
		2	≥ 1.5	0.12%	0.15%	-0.31%	-0.24%	-0.40%
		3	≥ 3	-0.12%	-0.10%	0.02%	0.00%	-0.23%
		4	≥ 6.75	-0.09%	0.20%	-0.06%	0.18%	-0.07%
		5	≥ 14	0.16%	0.09%	-0.03%	-0.05%	-0.05%
		6	≥ 31.5	-0.03%	0.19%	0.00%	0.09%	-0.04%
		6D[2]	44.5	0.13%	-0.09%	0.00%	-0.08%	-0.02%
Hot Leg at SG Inlet	0 Ruptures/ 19 Failures; Hot Leg CRP Model	1	≥ .5	0.29%	-0.22%	-0.06%	-0.07%	0.20%
		2	≥ 1.5	-0.16%	-0.15%	-0.08%	0.33%	-0.15%
		3	≥ 3	0.25%	-0.04%	0.05%	0.00%	0.18%
		4	≥ 6.75	-0.04%	0.14%	-0.17%	0.18%	-0.27%
		5	≥ 14	5.70%	5.66%	5.65%	5.74%	-0.15%
		6	≥ 31.5	0.03%	0.19%	0.00%	0.04%	-0.06%
		6D[2]	44.5	0.06%	-0.09%	-0.01%	-0.08%	-0.02%
Cold Leg	0 Ruptures/ 3 Failures; Cold Leg CRP Model	1	≥ .5	0.00%	0.27%	-0.03%	0.11%	-0.28%
		2	≥ 1.5	0.04%	0.08%	-0.09%	0.02%	-0.13%
		3	≥ 3	-0.35%	0.08%	-0.04%	0.02%	-0.06%
		4	≥ 6.75	-0.14%	0.27%	0.00%	-0.07%	-0.01%
		5	≥ 14	0.19%	0.05%	0.00%	-0.07%	-0.02%
		6	≥ 31.5	-0.04%	-0.03%	0.00%	-0.23%	-0.01%
		6D[2]	44.5	0.00%	0.06%	0.00%	-0.29%	0.02%
Surge Line	0 Ruptures/ 3 Failures; Surge Line CRP Model	1	≥ .5	0.00%	-0.08%	0.00%	0.00%	-0.72%
		2	≥ 1.5	-0.08%	0.22%	0.00%	0.00%	0.28%
		3	≥ 3	-0.14%	-0.02%	0.03%	0.00%	0.09%
		4	≥ 6.75	-0.06%	0.00%	-0.05%	-0.14%	0.30%
		5	≥ 14	0.09%	-0.09%	0.06%	-0.06%	-0.24%
		5D[3]	19.8	0.17%	-0.18%	-0.07%	-0.02%	-0.13%
CVCS Line	0 Ruptures/ 14 Failures; HPI CRP Model	1	≥ .5	0.00%	-0.07%	0.00%	0.00%	-0.55%
		2	≥ 1.5	-0.17%	0.08%	-0.20%	-0.01%	0.63%
		3	≥ 3	0.03%	-0.09%	0.09%	0.06%	-0.43%
		4	≥ 6.75	-0.04%	0.00%	0.05%	-0.03%	-0.11%

Table 2.10 (Cont.)

		5	≥ 14	0.18%	-0.08%	0.00%	0.00%	-0.03%
Safety Injection Recirculation (SIR) Lines	0 Ruptures/ 14 Failures; HPI CRP Model	1	≥ .5	0.00%	-0.07%	0.00%	0.00%	-0.55%
		2	≥ 1.5	-0.17%	0.08%	-0.20%	-0.01%	0.63%
		3	≥ 3	0.03%	-0.09%	0.09%	0.06%	-0.43%
		4	≥ 6.75	-0.04%	0.00%	0.05%	-0.03%	-0.11%
		5	≥ 14	0.18%	-0.08%	0.00%	0.00%	-0.03%
Pressurizer Lines	0 Ruptures/ 12 Failures; HPI CRP Model	1	≥ .5	0.00%	-0.05%	0.00%	0.00%	-0.37%
		2	≥ 1.5	0.03%	0.08%	0.20%	-0.05%	0.89%
		3	≥ 3	0.02%	-0.09%	-0.04%	0.22%	-0.34%
		4	≥ 6.75	0.00%	0.00%	0.07%	0.00%	-0.09%
		5	≥ 14	0.18%	-0.08%	0.00%	0.01%	-0.02%
Small Bore	0 Ruptures/ 79 Failures; HPI CRP Model	1	≥ .5	19.14%	-52.23%	309.20%	-44.67%	-51.38%
		2	≥ 1.5	48.38%	-86.47%	800.98%	-49.34%	-54.04%
		3	≥ 3	34.60%	-89.09%	695.12%	-54.27%	-52.32%

Notes:

[1] Range Factor = SQRT(95%tile/5%tile).

[2] 6D corresponds to a double-ended break of a 31.5" pipe.

[3] 5D corresponds to a double-ended break of a 16" pipe.

The results in Table 2.9 and Table 2.10 show that for almost all the parameters, the recreated values are in complete agreement with the reported values in Fleming and Lydell's report. However, there are four cases that do not show this same level of agreement. The hot leg at steam generator inlet category 5 case appears to use a median value that is roughly 5% larger than the recreated values. Also, it appears that the median and range factors for the small bore calculation cases have all been adjusted significantly. The 5%tile values reported by Fleming and Lydell for the small bore cases all have values that are larger than the values reported for the median values. This may have been a simple error in reporting the values in the spreadsheet; however, even if the 5%tile and median values were swapped, there is still a very large discrepancy between the reported values and the ones recreated in this research. This issue was included in the email conversations with Karl Fleming regarding the recalculation of the conditional rupture probability distributions. Table A.3 in Appendix A provides an overview of the email communications with Karl Fleming.

2.1.3 CRITICAL REVIEW & QUANTITATIVE VERIFICATION OF LOCATION- AND BREAK SIZE-SPECIFIC ESTIMATIONS OF LOCA FREQUENCIES

The final step of the methodology to develop location- and break size-specific estimations of LOCA frequencies requires the multiplication of the lognormal CRP distributions with the lognormal failure rate distributions. To develop LOCA frequency distributions for break sizes that were not included in the development of the previous results, a linear interpolation or extrapolation technique was used on a log frequency versus log break size curve.

Table 2.11 shows the resulting values from the recalculation process. Most of the LOCA frequency distribution parameters could be recreated with agreement to the values provided by Fleming and Lydell, as can be seen in Table 2.12 which provides the percent differences between the values calculated in Table 2.11 and the values reported by Fleming and Lydell. However, there are calculation cases that have some discrepancies that could never be reconciled. These cases have been highlighted in yellow. The most concerning discrepancies are calculation cases 6A, 6B, 7N, and 7O in which all or most of the parameters could not be recreated using the same procedure that enabled the rest of the values to be recreated with agreement. These items were communicated with Karl Fleming to be considered for the update and advancement of the work for nuclear power plants. The discussion is shown in Table A.4 in Appendix A.

Table 2.11 Recalculation of the Final LOCA Frequency Distributions for the STPNOC Project

Weld Case[Note 1,2]	Failure Mode		Weld Failure Rate Distribution Parameters Per weld-calendar-year				
			Mean	5%tile	Median	95%tile	RF[Note 4]
Hot Leg Case 1A B-F Welds Subject to PWSCC+D&C	Break Size (in.)	FR[Note 3]	4.14E-04	1.79E-04	3.74E-04	7.82E-04	2.1
		0.5	5.95E-07	5.84E-08	3.37E-07	1.95E-06	5.8
		1.5	1.37E-07	4.44E-09	4.80E-08	5.19E-07	10.8
		2.0	1.02E-07	2.97E-09	3.40E-08	3.90E-07	11.5
		3.0	6.82E-08	1.67E-09	2.09E-08	2.62E-07	12.5
		4.0	4.70E-08	1.09E-09	1.41E-08	1.81E-07	12.9
		6.0	2.79E-08	5.99E-10	8.03E-09	1.08E-07	13.4
		6.8	2.37E-08	4.97E-10	6.75E-09	9.17E-08	13.6
		14.0	1.03E-08	1.53E-10	2.47E-09	4.00E-08	16.1
		20.0	5.46E-09	8.09E-11	1.31E-09	2.11E-08	16.2
		29.0	2.81E-09	4.16E-11	6.72E-10	1.08E-08	16.1
		31.5	2.42E-09	3.59E-11	5.79E-10	9.35E-09	16.1
		41.0	1.53E-09	2.27E-11	3.66E-10	5.92E-09	16.1
Hot Leg Case 1C B-J Welds Subject to TF+D&C	Break Size (in.)	FR	8.74E-06	1.79E-08	7.12E-07	2.83E-05	39.8
		0.5	1.26E-08	1.16E-11	6.41E-10	3.54E-08	55.3
		1.5	2.89E-09	1.21E-12	9.14E-11	6.89E-09	75.4
		2.0	2.16E-09	8.31E-13	6.47E-11	5.04E-09	77.9
		3.0	1.44E-09	4.86E-13	3.98E-11	3.26E-09	81.9
		4.0	9.91E-10	3.22E-13	2.68E-11	2.23E-09	83.2
		6.0	5.88E-10	1.79E-13	1.53E-11	1.30E-09	85.2
		6.8	5.01E-10	1.50E-13	1.28E-11	1.10E-09	85.8
		14.0	2.18E-10	4.94E-14	4.71E-12	4.48E-10	95.2
		20.0	1.15E-10	2.61E-14	2.49E-12	2.37E-10	95.2
		29.0	5.92E-11	1.34E-14	1.28E-12	1.22E-10	95.2

Table 2.11 (Cont.)

		31.5	5.11E-11	1.16E-14	1.10E-12	1.05E-10	95.2
		41.0	3.23E-11	7.32E-15	6.97E-13	6.64E-11	95.2
Hot Leg Case 1B B-J Welds Subject to D&C	Break Size (in.)	FR	1.36E-06	5.27E-10	4.10E-08	3.19E-06	77.8
		0.5	1.96E-09	3.59E-13	3.70E-11	3.81E-09	103.0
		1.5	4.50E-10	3.89E-14	5.26E-12	7.12E-10	135.2
		2.0	3.36E-10	2.68E-14	3.73E-12	5.19E-10	139.1
		3.0	2.24E-10	1.58E-14	2.29E-12	3.34E-10	145.4
		4.0	1.54E-10	1.05E-14	1.54E-12	2.27E-10	147.4
		6.0	9.17E-11	5.84E-15	8.80E-13	1.32E-10	150.6
		6.8	7.81E-11	4.88E-15	7.40E-13	1.12E-10	151.6
		14.0	3.40E-11	1.63E-15	2.71E-13	4.51E-11	166.2
		20.0	1.80E-11	8.61E-16	1.43E-13	2.38E-11	166.2
		29.0	9.23E-12	4.43E-16	7.36E-14	1.22E-11	166.2
		31.5	7.96E-12	3.82E-16	6.35E-14	1.05E-11	166.2
		41.0	5.04E-12	2.42E-16	4.02E-14	6.67E-12	166.2
Hot Leg SG Inlet Case 2 B-F Weld Subject to PWSCC+D&C	Break Size (in.)	FR	1.42E-03	9.22E-04	1.38E-03	2.06E-03	1.5
		0.5	1.98E-06	2.41E-07	1.22E-06	6.16E-06	5.1
		1.5	4.60E-07	1.77E-08	1.75E-07	1.72E-06	9.9
		2.0	3.44E-07	1.18E-08	1.24E-07	1.30E-06	10.5
		3.0	2.30E-07	6.67E-09	7.66E-08	8.80E-07	11.5
		4.0	1.60E-07	4.34E-09	5.15E-08	6.12E-07	11.9
		6.0	9.51E-08	2.38E-09	2.95E-08	3.66E-07	12.4
		6.8	8.13E-08	1.97E-09	2.48E-08	3.13E-07	12.6
		14.0	3.35E-08	5.72E-10	8.62E-09	1.30E-07	15.1
		20.0	1.81E-08	3.10E-10	4.66E-09	7.01E-08	15.0
		29.0	9.57E-09	1.63E-10	2.46E-09	3.70E-08	15.1
		31.5	8.30E-09	1.42E-10	2.13E-09	3.21E-08	15.1
		41.0	5.28E-09	9.00E-11	1.36E-09	2.04E-08	15.1
Cold Leg Cases 3A and 3B B-F Weld Subject to PWSCC+D&C	Break Size (in.)	FR	1.17E-04	2.72E-05	8.96E-05	2.95E-04	3.3
		0.5	1.40E-07	8.98E-09	6.66E-08	4.94E-07	7.4
		1.5	3.18E-08	8.68E-10	1.03E-08	1.22E-07	11.8
		2.0	2.20E-08	5.79E-10	6.99E-09	8.44E-08	12.1
		3.0	1.31E-08	3.27E-10	4.06E-09	5.05E-08	12.4
		4.0	8.76E-09	2.14E-10	2.68E-09	3.37E-08	12.6
		6.0	4.95E-09	1.17E-10	1.49E-09	1.91E-08	12.7
		6.8	4.19E-09	9.87E-11	1.26E-09	1.61E-08	12.8
		14.0	1.86E-09	2.89E-11	4.56E-10	7.18E-09	15.8
		20.0	1.06E-09	1.49E-11	2.47E-10	4.10E-09	16.6

Table 2.11 (Cont.)

		27.5	6.45E-10	8.20E-12	1.43E-10	2.49E-09	17.4
		31.5	5.22E-10	6.36E-12	1.13E-10	2.01E-09	17.8
		38.9	3.82E-10	4.32E-12	7.96E-11	1.47E-09	18.4
		44.5	3.13E-10	3.38E-12	6.37E-11	1.20E-09	18.8
Cold Leg Cases 3C and 3D B-J Weld Subject to D&C	Break Size (in.)	FR	7.06E-07	5.03E-10	3.08E-08	1.89E-06	61.3
		0.5	8.47E-10	2.76E-13	2.29E-11	1.90E-09	83.0
		1.5	1.92E-10	3.38E-14	3.54E-12	3.70E-10	104.6
		2.0	1.33E-10	2.28E-14	2.41E-12	2.54E-10	105.7
		3.0	7.95E-11	1.30E-14	1.40E-12	1.50E-10	107.3
		4.0	5.30E-11	8.55E-15	9.23E-13	9.97E-11	107.9
		6.0	3.00E-11	4.73E-15	5.15E-13	5.60E-11	108.8
		6.8	2.54E-11	3.98E-15	4.34E-13	4.73E-11	109.0
		14.0	1.12E-11	1.28E-15	1.57E-13	1.92E-11	122.5
		20.0	6.43E-12	6.73E-16	8.50E-14	1.07E-11	126.3
		27.5	3.91E-12	3.78E-16	4.91E-14	6.38E-12	129.8
		31.5	3.16E-12	2.96E-16	3.89E-14	5.11E-12	131.3
		38.9	2.31E-12	2.04E-16	2.74E-14	3.68E-12	134.2
		44.5	1.89E-12	1.61E-16	2.19E-14	2.98E-12	135.9
Surge Line Case 4A B-F Weld Subject to PWSCC+TF+D&C	Break Size (in.)	FR	5.15E-04	1.26E-04	4.02E-04	1.28E-03	3.2
		0.5	9.73E-06	6.47E-07	4.70E-06	3.42E-05	7.3
		1.5	3.27E-06	4.34E-08	7.40E-07	1.26E-05	17.0
		2.0	2.41E-06	2.77E-08	5.07E-07	9.27E-06	18.3
		3.0	1.57E-06	1.48E-08	2.98E-07	5.98E-06	20.1
		4.0	1.02E-06	9.48E-09	1.92E-07	3.88E-06	20.2
		6.0	5.55E-07	5.05E-09	1.03E-07	2.11E-06	20.4
		6.8	4.65E-07	4.21E-09	8.62E-08	1.77E-06	20.5
		14.0	1.18E-07	1.05E-09	2.17E-08	4.48E-07	20.7
		16.0	9.14E-08	8.17E-10	1.68E-08	3.47E-07	20.6
		19.8	6.12E-08	5.44E-10	1.12E-08	2.32E-07	20.7
		22.6	4.75E-08	4.24E-10	8.75E-09	1.80E-07	20.6
Surge Line Case 4B and 4D B-J Weld Subject to TF+D&C	Break Size (in.)	FR	3.95E-06	1.53E-08	4.63E-07	1.40E-05	30.2
		0.5	7.50E-08	1.25E-10	5.42E-09	2.35E-07	43.4
		1.5	2.52E-08	1.18E-11	8.53E-10	6.16E-08	72.3
		2.0	1.86E-08	7.72E-12	5.84E-10	4.43E-08	75.7
		3.0	1.21E-08	4.25E-12	3.43E-10	2.77E-08	80.7
		4.0	7.86E-09	2.73E-12	2.21E-10	1.79E-08	81.1
		6.0	4.28E-09	1.46E-12	1.19E-10	9.71E-09	81.7
		6.8	3.58E-09	1.21E-12	9.93E-11	8.13E-09	81.8

Table 2.11 (Cont.)

		14.0	9.09E-10	3.04E-13	2.50E-11	2.06E-09	82.3
		16.0	7.04E-10	2.36E-13	1.94E-11	1.59E-09	82.2
		19.8	4.71E-10	1.57E-13	1.30E-11	1.07E-09	82.3
		22.6	3.66E-10	1.23E-13	1.01E-11	8.28E-10	82.2
Surge Line Case 4C BC Weld Subject to TF+D&C	Break Size (in.)	FR	6.63E-06	1.80E-08	6.35E-07	2.24E-05	35.3
		0.5	1.25E-07	1.49E-10	7.44E-09	3.71E-07	49.9
		1.5	4.21E-08	1.43E-11	1.17E-09	9.57E-08	81.8
		2.0	3.11E-08	9.37E-12	8.02E-10	6.86E-08	85.6
		3.0	2.02E-08	5.17E-12	4.71E-10	4.29E-08	91.0
		4.0	1.31E-08	3.32E-12	3.03E-10	2.77E-08	91.5
		6.0	7.15E-09	1.77E-12	1.63E-10	1.50E-08	92.1
		6.8	5.99E-09	1.48E-12	1.36E-10	1.26E-08	92.3
		14.0	1.52E-09	3.70E-13	3.43E-11	3.18E-09	92.8
		16.0	1.18E-09	2.87E-13	2.66E-11	2.47E-09	92.6
		19.8	7.88E-10	1.92E-13	1.78E-11	1.65E-09	92.8
		22.6	6.12E-10	1.49E-13	1.38E-11	1.28E-09	92.7
Pressurizer Cases 5A,5B, and 5J B-J Welds Subject to TF+D&C	Break Size (in.)	FR	4.32E-06	1.63E-07	1.62E-06	1.61E-05	10
		0.50	4.62E-08	1.51E-09	1.63E-08	1.75E-07	10.8
		0.75	2.77E-08	7.69E-10	9.03E-09	1.06E-07	11.7
		1.00	1.97E-08	4.68E-10	5.95E-09	7.57E-08	12.7
		1.50	1.24E-08	2.28E-10	3.30E-09	4.79E-08	14.5
		2.00	6.66E-09	1.21E-10	1.76E-09	2.58E-08	14.6
		3.00	2.77E-09	4.96E-11	7.29E-10	1.07E-08	14.7
		4.24	1.23E-09	1.91E-11	3.01E-10	4.75E-09	15.8
		5.66	6.27E-10	8.54E-12	1.44E-10	2.42E-09	16.8
		6.00	5.48E-10	7.26E-12	1.24E-10	2.11E-09	17.1
		6.75	4.18E-10	5.22E-12	9.17E-11	1.61E-09	17.5
		8.49	2.65E-10	3.32E-12	5.82E-11	1.02E-09	17.5
Pressurizer Cases 5C, 5D, 5E, and 5I B-J Weld Subject to D&C	Break Size (in.)	FR	1.61E-06	7.31E-08	6.58E-07	5.93E-06	9
		0.50	1.72E-08	6.80E-10	6.61E-09	6.43E-08	9.7
		0.75	1.03E-08	3.45E-10	3.67E-09	3.91E-08	10.6
		1.00	7.32E-09	2.09E-10	2.42E-09	2.80E-08	11.6
		1.50	4.61E-09	1.01E-10	1.34E-09	1.78E-08	13.3
		2.00	2.48E-09	5.37E-11	7.17E-10	9.58E-09	13.4
		3.00	1.03E-09	2.20E-11	2.96E-10	3.98E-09	13.4
		4.24	4.57E-10	8.46E-12	1.22E-10	1.77E-09	14.5
		5.66	2.34E-10	3.78E-12	5.84E-11	9.03E-10	15.5
		6.00	2.04E-10	3.21E-12	5.04E-11	7.89E-10	15.7

Table 2.11 (Cont.)

		6.75	1.56E-10	2.31E-12	3.73E-11	6.01E-10	16.1
		8.49	9.86E-11	1.47E-12	2.36E-11	3.81E-10	16.1
Pressurizer Case 5G B-F Weld Subject to PWSCC+D&C	Break Size (in.)	FR	4.67E-04	2.56E-04	4.43E-04	7.68E-04	1.7
		0.50	5.00E-06	2.02E-06	4.45E-06	9.83E-06	2.2
		0.75	3.00E-06	8.89E-07	2.47E-06	6.87E-06	2.8
		1.00	2.13E-06	4.89E-07	1.63E-06	5.43E-06	3.3
		1.50	1.34E-06	2.10E-07	9.04E-07	3.90E-06	4.3
		2.00	7.21E-07	1.11E-07	4.83E-07	2.11E-06	4.4
		3.00	3.00E-07	4.52E-08	1.99E-07	8.80E-07	4.4
		4.24	1.33E-07	1.65E-08	8.24E-08	4.12E-07	5.0
		5.66	6.79E-08	7.06E-09	3.94E-08	2.19E-07	5.6
		6.00	5.93E-08	5.95E-09	3.39E-08	1.93E-07	5.7
		6.75	4.52E-08	4.21E-09	2.51E-08	1.50E-07	6.0
		8.49	2.87E-08	2.67E-09	1.59E-08	9.48E-08	6.0
Pressurizer Case 5F B-F Weld Subject to PWSCC+TF+D&C	Break Size (in.)	FR	4.74E-04	2.59E-04	4.50E-04	7.83E-04	1.7
		0.50	5.08E-06	2.05E-06	4.52E-06	9.98E-06	2.2
		0.75	3.05E-06	9.03E-07	2.51E-06	6.98E-06	2.8
		1.00	2.16E-06	4.96E-07	1.65E-06	5.51E-06	3.3
		1.50	1.36E-06	2.13E-07	9.18E-07	3.96E-06	4.3
		2.00	7.33E-07	1.12E-07	4.90E-07	2.14E-06	4.4
		3.00	3.04E-07	4.59E-08	2.03E-07	8.94E-07	4.4
		4.24	1.35E-07	1.67E-08	8.37E-08	4.18E-07	5.0
		5.66	6.90E-08	7.17E-09	4.00E-08	2.23E-07	5.6
		6.00	6.03E-08	6.05E-09	3.44E-08	1.96E-07	5.7
		6.75	4.59E-08	4.27E-09	2.55E-08	1.52E-07	6.0
		8.49	2.91E-08	2.71E-09	1.62E-08	9.63E-08	6.0
Pressurizer Case 5H B-F Weld Subject to D&C (Weld Overlay)	Break Size (in.)	FR	1.63E-06	5.29E-10	4.40E-08	3.66E-06	83.2
		0.50	1.74E-08	5.11E-12	4.42E-10	3.82E-08	86.5
		0.75	1.05E-08	2.71E-12	2.45E-10	2.22E-08	90.6
		1.00	7.43E-09	1.71E-12	1.62E-10	1.53E-08	94.8
		1.50	4.68E-09	8.79E-13	8.97E-11	9.16E-09	102.1
		2.00	2.52E-09	4.67E-13	4.79E-11	4.91E-09	102.5
		3.00	1.05E-09	1.92E-13	1.98E-11	2.04E-09	102.9
		4.24	4.64E-10	7.62E-14	8.17E-12	8.76E-10	107.2
		5.66	2.37E-10	3.51E-14	3.91E-12	4.35E-10	111.4
		6.00	2.07E-10	3.00E-14	3.37E-12	3.78E-10	112.3
		6.75	1.58E-10	2.18E-14	2.49E-12	2.85E-10	114.3
		8.49	1.00E-10	1.38E-14	1.58E-12	1.80E-10	114.2

Table 2.11 (Cont.)

Small Bore Cases 6A and 6B B-J Welds Subject to VF+TF+D&C	Break Size (in.)	FR	1.26E-04	7.03E-05	1.19E-04	2.02E-04	1.7
		0.50	1.38E-06	2.42E-07	9.66E-07	3.85E-06	4.0
		0.75	8.89E-07	1.02E-07	5.35E-07	2.81E-06	5.3
		1.00	6.65E-07	5.48E-08	3.52E-07	2.25E-06	6.4
		1.41	4.80E-07	2.61E-08	2.13E-07	1.74E-06	8.2
		1.50	4.54E-07	2.29E-08	1.95E-07	1.66E-06	8.5
		1.99	2.72E-07	1.34E-08	1.15E-07	9.94E-07	8.6
		2.00	2.69E-07	1.33E-08	1.14E-07	9.85E-07	8.6
		2.83	1.40E-06	7.05E-09	1.89E-07	5.09E-06	26.9
SIR Case 7C B-J Welds Subject to SC+TF+D&C	Break Size (in.)	FR	2.90E-04	3.06E-05	1.69E-04	9.37E-04	5.5
		0.5	3.09E-06	2.80E-07	1.69E-06	1.03E-05	6.1
		0.8	1.85E-06	1.39E-07	9.41E-07	6.38E-06	6.8
		1.0	1.31E-06	8.25E-08	6.20E-07	4.65E-06	7.5
		1.5	8.31E-07	3.87E-08	3.44E-07	3.06E-06	8.9
		2.0	4.46E-07	2.06E-08	1.84E-07	1.64E-06	8.9
		2.8	2.10E-07	9.64E-09	8.65E-08	7.75E-07	9.0
		4.0	9.44E-08	3.78E-09	3.65E-08	3.53E-07	9.7
		4.2	8.24E-08	3.21E-09	3.15E-08	3.09E-07	9.8
		5.7	4.21E-08	1.42E-09	1.50E-08	1.59E-07	10.6
		6.0	3.68E-08	1.20E-09	1.30E-08	1.40E-07	10.8
		6.8	2.80E-08	8.61E-10	9.58E-09	1.07E-07	11.1
		7.2	2.47E-08	7.57E-10	8.43E-09	9.39E-08	11.1
		8.5	1.78E-08	5.46E-10	6.08E-09	6.77E-08	11.1
		10.0	1.29E-08	3.94E-10	4.39E-09	4.89E-08	11.1
		11.3	1.01E-08	3.09E-10	3.44E-09	3.83E-08	11.1
		14.1	6.46E-09	1.98E-10	2.21E-09	2.46E-08	11.1
		17.0	4.50E-09	1.38E-10	1.54E-09	1.71E-08	11.1
SIR Case 7A 7B B-J Welds Subject to TF+D&C	Break Size (in.)	FR	2.61E-04	2.17E-05	1.38E-04	8.81E-04	6.4
		0.5	2.78E-06	1.98E-07	1.38E-06	9.68E-06	7.0
		0.8	1.67E-06	9.88E-08	7.68E-07	5.97E-06	7.8
		1.0	1.19E-06	5.92E-08	5.06E-07	4.33E-06	8.6
		1.5	7.50E-07	2.80E-08	2.81E-07	2.82E-06	10.0
		2.0	4.02E-07	1.49E-08	1.50E-07	1.51E-06	10.1
		2.8	1.90E-07	6.99E-09	7.06E-08	7.13E-07	10.1
		4.0	8.52E-08	2.75E-09	2.98E-08	3.23E-07	10.8
		4.2	7.44E-08	2.33E-09	2.57E-08	2.83E-07	11.0
		5.7	3.80E-08	1.04E-09	1.23E-08	1.46E-07	11.9
		6.0	3.32E-08	8.78E-10	1.06E-08	1.27E-07	12.0

Table 2.11 (Cont.)

		6.8	2.53E-08	6.30E-10	7.83E-09	9.72E-08	12.4
		7.2	2.23E-08	5.54E-10	6.88E-09	8.55E-08	12.4
		8.5	1.60E-08	3.99E-10	4.96E-09	6.17E-08	12.4
		10.0	1.16E-08	2.89E-10	3.59E-09	4.46E-08	12.4
		11.3	9.08E-09	2.26E-10	2.81E-09	3.49E-08	12.4
		14.1	5.83E-09	1.45E-10	1.80E-09	2.24E-08	12.4
		17.0	4.06E-09	1.01E-10	1.26E-09	1.56E-08	12.4
SIR Case 7D ACC Case 7M B-J Welds Subject to SC+D&C	Break Size (in.)	FR	3.34E-05	1.24E-06	1.24E-05	1.25E-04	10.1
		0.5	3.56E-07	1.15E-08	1.25E-07	1.35E-06	10.9
		0.8	2.14E-07	5.84E-09	6.92E-08	8.19E-07	11.8
		1.0	1.52E-07	3.55E-09	4.56E-08	5.84E-07	12.8
		1.5	9.60E-08	1.72E-09	2.53E-08	3.71E-07	14.7
		2.0	5.15E-08	9.19E-10	1.35E-08	1.99E-07	14.7
		2.8	2.43E-08	4.30E-10	6.36E-09	9.39E-08	14.8
		4.0	1.09E-08	1.71E-10	2.68E-09	4.22E-08	15.7
		4.2	9.52E-09	1.45E-10	2.31E-09	3.68E-08	15.9
		5.7	4.86E-09	6.51E-11	1.11E-09	1.88E-08	17.0
		6.0	4.25E-09	5.54E-11	9.52E-10	1.64E-08	17.2
		6.8	3.24E-09	3.99E-11	7.05E-10	1.25E-08	17.7
		7.2	2.85E-09	3.51E-11	6.20E-10	1.10E-08	17.7
		8.5	2.05E-09	2.53E-11	4.47E-10	7.90E-09	17.7
		10.0	1.48E-09	1.83E-11	3.23E-10	5.71E-09	17.7
		11.3	1.16E-09	1.43E-11	2.53E-10	4.47E-09	17.7
		14.1	7.46E-10	9.18E-12	1.62E-10	2.87E-09	17.7
		17.0	5.19E-10	6.39E-12	1.13E-10	2.00E-09	17.7
SIR Cases 7E-7L B-J Welds Subject to D&C	Break Size (in.)	FR	1.07E-06	5.61E-08	4.67E-07	3.89E-06	8.3
		0.5	1.14E-08	5.20E-10	4.67E-09	4.20E-08	9.0
		0.8	6.83E-09	2.63E-10	2.59E-09	2.56E-08	9.9
		1.0	4.85E-09	1.59E-10	1.71E-09	1.84E-08	10.7
		1.5	3.07E-09	7.64E-11	9.49E-10	1.18E-08	12.4
		2.0	1.65E-09	4.07E-11	5.08E-10	6.32E-09	12.5
		2.8	7.76E-10	1.91E-11	2.39E-10	2.98E-09	12.5
		4.0	3.48E-10	7.54E-12	1.01E-10	1.34E-09	13.3
		4.2	3.04E-10	6.41E-12	8.68E-11	1.17E-09	13.5
		5.7	1.55E-10	2.86E-12	4.15E-11	6.01E-10	14.5
		6.0	1.36E-10	2.43E-12	3.57E-11	5.25E-10	14.7
		6.8	1.03E-10	1.75E-12	2.64E-11	4.00E-10	15.1
		7.2	9.10E-11	1.54E-12	2.33E-11	3.52E-10	15.1
		8.5	6.56E-11	1.11E-12	1.68E-11	2.54E-10	15.1

Table 2.11 (Cont.)

		10.0	4.74E-11	8.01E-13	1.21E-11	1.83E-10	15.1
		11.3	3.71E-11	6.27E-13	9.49E-12	1.44E-10	15.1
		14.1	2.38E-11	4.02E-13	6.09E-12	9.22E-11	15.1
		17.0	1.66E-11	2.80E-13	4.24E-12	6.42E-11	15.1
ACC Case 7N B-J Welds Subject to TF+D&C	Break Size (in.)	FR	4.87E-06	1.42E-08	4.86E-07	1.66E-05	34.2
		0.5	5.19E-08	1.35E-10	4.86E-09	1.74E-07	35.9
		0.8	3.11E-08	7.09E-11	2.70E-09	1.03E-07	38.0
		1.0	2.21E-08	4.42E-11	1.78E-09	7.13E-08	40.2
		1.5	1.40E-08	2.23E-11	9.86E-10	4.35E-08	44.1
		2.0	7.50E-09	1.19E-11	5.28E-10	2.33E-08	44.2
		2.8	3.54E-09	5.59E-12	2.48E-10	1.10E-08	44.4
		4.0	1.59E-09	2.26E-12	1.05E-10	4.85E-09	46.3
		4.2	1.39E-09	1.93E-12	9.02E-11	4.22E-09	46.8
		5.7	7.08E-10	8.80E-13	4.31E-11	2.11E-09	49.0
		6.0	6.19E-10	7.50E-13	3.71E-11	1.84E-09	49.5
		6.8	4.71E-10	5.44E-13	2.75E-11	1.39E-09	50.5
		7.2	4.15E-10	4.79E-13	2.42E-11	1.22E-09	50.5
		8.5	2.99E-10	3.45E-13	1.74E-11	8.80E-10	50.5
		10.0	2.16E-10	2.49E-13	1.26E-11	6.36E-10	50.5
		11.3	1.69E-10	1.95E-13	9.86E-12	4.98E-10	50.5
		14.1	1.09E-10	1.25E-13	6.33E-12	3.20E-10	50.5
		17.0	7.56E-11	8.73E-14	4.41E-12	2.23E-10	50.5
ACC Case 7O B-J Welds Subject to D&C	Break Size (in.)	FR	5.87E-07	4.61E-10	2.72E-08	1.60E-06	59
		0.5	6.25E-09	4.42E-12	2.72E-10	1.67E-08	61.5
		0.8	3.75E-09	2.33E-12	1.51E-10	9.76E-09	64.7
		1.0	2.66E-09	1.46E-12	9.94E-11	6.74E-09	67.9
		1.5	1.68E-09	7.48E-13	5.52E-11	4.07E-09	73.7
		2.0	9.03E-10	3.99E-13	2.95E-11	2.18E-09	73.9
		2.8	4.26E-10	1.87E-13	1.39E-11	1.03E-09	74.1
		4.0	1.91E-10	7.61E-14	5.86E-12	4.51E-10	77.0
		4.2	1.67E-10	6.50E-14	5.04E-12	3.91E-10	77.6
		5.7	8.53E-11	2.98E-14	2.41E-12	1.95E-10	80.9
		6.0	7.45E-11	2.55E-14	2.08E-12	1.69E-10	81.6
		6.8	5.68E-11	1.85E-14	1.54E-12	1.28E-10	83.0
		7.2	4.99E-11	1.63E-14	1.35E-12	1.12E-10	83.0
		8.5	3.60E-11	1.17E-14	9.75E-13	8.10E-11	83.0
		10.0	2.60E-11	8.48E-15	7.04E-13	5.85E-11	83.0
		11.3	2.04E-11	6.64E-15	5.52E-13	4.58E-11	83.0
		14.1	1.31E-11	4.27E-15	3.54E-13	2.94E-11	83.0

Table 2.11 (Cont.)

		17.0	9.11E-12	2.97E-15	2.47E-13	2.05E-11	83.0
CVCS Case 8A and 8B B-J Weld Subject to VF+TF+D&C	Break Size (in.)	FR	4.03E-06	2.43E-07	1.86E-06	1.43E-05	7.7
		0.50	4.29E-08	2.23E-09	1.86E-08	1.56E-07	8.4
		0.75	2.57E-08	1.12E-09	1.04E-08	9.53E-08	9.2
		1.00	1.82E-08	6.78E-10	6.82E-09	6.86E-08	10.1
		1.50	1.15E-08	3.24E-10	3.78E-09	4.42E-08	11.7
		2.00	6.20E-09	1.73E-10	2.02E-09	2.37E-08	11.7
		3.00	2.58E-09	7.13E-11	8.38E-10	9.86E-09	11.8
		4.00	1.31E-09	3.20E-11	4.02E-10	5.05E-09	12.6
		5.66	5.85E-10	1.21E-11	1.65E-10	2.26E-09	13.7
CVCS Cases 8C, 8D, and 8F B-J Weld Subject to VF+D&C	Break Size (in.)	FR	1.75E-06	1.37E-07	9.07E-07	6.01E-06	6.6
		0.50	1.87E-08	1.26E-09	9.08E-09	6.54E-08	7.2
		0.75	1.12E-08	6.30E-10	5.04E-09	4.03E-08	8.0
		1.00	7.94E-09	3.78E-10	3.32E-09	2.92E-08	8.8
		1.50	5.03E-09	1.79E-10	1.84E-09	1.89E-08	10.3
		2.00	2.70E-09	9.55E-11	9.85E-10	1.02E-08	10.3
		3.00	1.12E-09	3.94E-11	4.08E-10	4.23E-09	10.4
		4.00	5.71E-10	1.76E-11	1.96E-10	2.17E-09	11.1
		5.66	2.55E-10	6.64E-12	8.06E-11	9.77E-10	12.1
CVCS Case 8E BC Welds Subject to TF+D&C	Break Size (in.)	FR	7.50E-06	3.03E-07	2.91E-06	2.80E-05	9.6
		0.50	7.98E-08	2.82E-09	2.91E-08	3.01E-07	10.3
		0.75	4.79E-08	1.43E-09	1.62E-08	1.83E-07	11.3
		1.00	3.40E-08	8.70E-10	1.07E-08	1.30E-07	12.2
		1.50	2.15E-08	4.21E-10	5.91E-09	8.31E-08	14.1
		2.00	1.15E-08	2.24E-10	3.16E-09	4.46E-08	14.1
		3.00	4.80E-09	9.25E-11	1.31E-09	1.85E-08	14.2
		4.00	2.44E-09	4.17E-11	6.28E-10	9.45E-09	15.1
		5.66	1.09E-09	1.59E-11	2.59E-10	4.21E-09	16.3

Notes:

1. Two or more cases are listed together when they only differ by pipe size, see Tables 5-1 through 5-4 to see the different pipe sizes and DEGB sizes for those combined in this table.

2. PWSCC = primary water stress corrosion cracking; SC = stress corrosion cracking; TF = thermal fatigue; D&C = design and construction defects

3. FR = total failure rate including any failure resulting in weld repair or replacement

4. RF = range factor = SQRT(95%tile/5%tile)

Table 2.12 Percent differences between the LOCA frequency distributions recalculated in this thesis and the values reported by Fleming and Lydell

Weld Case[Note 1,2]	Failure Mode		Weld Failure Rate Distribution Parameters Per weld-calendar-year				
			Mean	5%tile	Median	95%tile	RF[Note 4]
Hot Leg Case 1A B-F Welds Subject to PWSCC+D&C	Break Size (in.)	FR[Note 3]	0.29%	0.00%	0.04%	0.00%	0.00%
		0.5	0.56%	-0.57%	0.05%	0.92%	1.35%
		1.5	0.63%	-0.36%	0.28%	0.61%	0.08%
		2.0	0.16%	-0.03%	0.09%	0.27%	0.54%
		3.0	0.52%	0.14%	0.17%	0.42%	0.15%
		4.0	0.11%	0.33%	-0.26%	-0.08%	0.47%
		6.0	-0.07%	-0.21%	-0.04%	-0.36%	0.04%
		6.8	0.17%	-0.17%	-0.13%	0.08%	-0.15%
		14.0	0.41%	0.18%	0.20%	0.16%	0.30%
		20.0	0.19%	-0.13%	-0.27%	0.00%	0.31%
		29.0	0.23%	-0.04%	-0.07%	0.42%	0.31%
		31.5	0.00%	-0.11%	0.01%	0.12%	0.30%
		41.0	15.98%	15.20%	15.59%	15.55%	0.15%
Hot Leg Case 1C B-J Welds Subject to TF+D&C	Break Size (in.)	FR	0.11%	0.00%	-0.04%	0.00%	0.00%
		0.5	0.48%	-0.79%	-0.09%	0.41%	0.29%
		1.5	0.62%	-0.66%	-0.03%	0.28%	0.26%
		2.0	0.26%	-0.11%	0.05%	0.05%	0.12%
		3.0	0.56%	-0.14%	0.07%	0.35%	0.23%
		4.0	0.07%	-0.10%	-0.17%	-0.22%	0.08%
		6.0	-0.13%	-0.43%	-0.20%	0.08%	0.12%
		6.8	-0.02%	-0.26%	-0.44%	0.22%	0.05%
		14.0	0.10%	-0.11%	-0.04%	0.07%	0.12%
		20.0	0.19%	-0.38%	-0.18%	-0.35%	0.13%
		29.0	0.03%	-0.63%	-0.20%	-0.29%	0.13%
		31.5	-0.08%	-0.27%	0.15%	-0.10%	0.12%
		41.0	0.32%	-0.12%	0.01%	0.10%	0.12%
Hot Leg Case 1B B-J Welds Subject to D&C	Break Size (in.)	FR	0.19%	0.00%	0.00%	0.00%	0.00%
		0.5	0.43%	-0.11%	0.14%	0.19%	0.14%
		1.5	0.27%	-0.15%	0.07%	0.21%	0.13%
		2.0	0.02%	0.03%	-0.02%	0.15%	0.01%
		3.0	0.10%	-0.13%	0.19%	0.18%	0.07%
		4.0	-0.35%	-0.42%	0.08%	0.08%	-0.07%
		6.0	-0.20%	-0.14%	-0.15%	-0.40%	-0.01%
		6.8	-0.26%	-0.20%	-0.16%	0.14%	0.00%

Table 2.12 (Cont.)

Hot Leg Case 1B B-J Welds Subject to D&C	Break Size (in.)	14.0	0.07%	0.10%	0.09%	-0.03%	0.02%
		20.0	-0.20%	-0.09%	0.12%	0.01%	0.02%
		29.0	-0.08%	-0.07%	-0.15%	0.28%	0.02%
		31.5	-0.12%	-0.06%	-0.06%	-0.48%	0.02%
		41.0	0.13%	0.24%	0.14%	0.07%	0.01%
Hot Leg SG Inlet Case 2 B-F Weld Subject to PWSCC+D&C	Break Size (in.)	FR	0.05%	0.00%	0.60%	0.00%	0.00%
		0.5	-0.02%	0.06%	-0.11%	-0.01%	-0.90%
		1.5	0.14%	-0.33%	-0.14%	0.08%	0.51%
		2.0	-0.23%	0.35%	0.09%	0.05%	-0.18%
		3.0	-0.27%	0.17%	0.01%	-0.15%	-0.15%
		4.0	-0.21%	-0.14%	-0.12%	-0.07%	-0.29%
		6.0	-0.09%	-0.10%	-0.06%	-0.13%	-0.01%
		6.8	0.11%	-0.59%	-0.36%	0.24%	0.04%
		14.0	0.07%	-0.11%	0.07%	0.53%	0.35%
		20.0	0.14%	0.02%	0.05%	0.01%	0.25%
		29.0	-0.01%	-0.36%	-0.02%	0.04%	0.34%
		31.5	0.00%	-0.20%	-0.32%	0.02%	0.35%
		41.0	0.70%	0.28%	0.37%	0.55%	0.42%
Cold Leg Cases 3A and 3B B-F Weld Subject to PWSCC+D&C	Break Size (in.)	FR	-0.36%	0.00%	-0.14%	0.00%	0.00%
		0.5	-0.08%	-0.58%	-0.30%	0.01%	0.25%
		1.5	0.18%	-0.41%	-0.23%	-0.33%	0.28%
		2.0	-0.02%	-0.30%	-0.14%	-0.04%	-0.26%
		3.0	0.25%	-0.37%	-0.21%	-0.04%	0.23%
		4.0	-0.37%	-0.64%	-0.65%	-0.34%	0.46%
		6.0	-0.80%	-1.45%	-0.99%	-0.74%	0.37%
		6.8	-0.04%	-0.34%	0.12%	0.18%	-0.12%
		14.0	-0.15%	-0.18%	-0.02%	0.01%	0.32%
		20.0	0.20%	-0.26%	-0.06%	0.01%	0.06%
		27.5	0.22%	-0.17%	-0.18%	0.25%	0.10%
		31.5	0.12%	-0.10%	0.01%	0.34%	0.33%
		38.9	0.36%	-0.16%	0.06%	0.51%	0.13%
		44.5	-0.05%	-0.17%	-0.03%	-0.13%	0.10%
Cold Leg Cases 3C and 3D B-J Weld Subject to D&C	Break Size (in.)	FR	0.08%	0.00%	0.11%	0.00%	0.00%
		0.5	0.08%	-0.33%	0.11%	0.19%	0.04%
		1.5	0.11%	0.09%	-0.08%	0.22%	0.05%
		2.0	0.10%	-0.11%	-0.16%	0.09%	-0.04%
		3.0	0.11%	0.19%	-0.14%	0.04%	0.03%
		4.0	-0.36%	-0.41%	-0.40%	-0.34%	0.03%
		6.0	-0.79%	-1.07%	-0.85%	-0.89%	0.11%

Table 2.12 (Cont.)

Cold Leg Cases 3C and 3D B-J Weld Subject to D&C	Break Size (in.)	6.8	-0.19%	0.10%	0.05%	0.05%	-0.01%
		14.0	0.37%	0.12%	-0.04%	0.09%	-0.04%
		20.0	0.14%	0.14%	0.20%	0.28%	0.06%
		27.5	0.17%	0.13%	0.27%	0.29%	0.01%
		31.5	0.23%	0.08%	0.25%	0.15%	0.01%
		38.9	0.19%	0.14%	0.06%	0.25%	0.07%
		44.5	0.19%	0.18%	0.09%	0.31%	0.01%
Surge Line Case 4A B-F Weld Subject to PWSCC+TF+D&C	Break Size (in.)	FR	-0.62%	-0.79%	-0.59%	-0.78%	-0.40%
		0.5	-0.22%	-1.21%	-0.58%	-0.07%	0.94%
		1.5	-0.92%	-0.63%	-0.81%	-0.72%	-0.35%
		2.0	-0.65%	-0.90%	-0.75%	-0.54%	-0.12%
		3.0	-0.62%	-0.43%	-0.73%	-0.54%	-0.14%
		4.0	-0.95%	-0.71%	-0.61%	-0.49%	0.15%
		6.0	-0.54%	-0.77%	-0.77%	-0.53%	0.16%
		6.8	-0.63%	-0.79%	-0.58%	-0.77%	-0.04%
		14.0	0.00%	-0.98%	-0.56%	-0.50%	0.27%
		16.0	-0.56%	-0.65%	-0.41%	-0.61%	0.04%
		19.8	-0.37%	-0.71%	-0.54%	-0.37%	0.27%
		22.6	-0.39%	-0.18%	-0.38%	-0.36%	0.09%
Surge Line Case 4B and 4D B-J Weld Subject to TF+D&C	Break Size (in.)	FR	0.00%	0.00%	0.18%	0.00%	0.16%
		0.5	0.75%	-0.08%	0.17%	0.49%	0.44%
		1.5	-0.04%	0.00%	0.20%	0.04%	-0.05%
		2.0	0.54%	0.11%	0.25%	0.36%	0.17%
		3.0	0.81%	0.32%	0.35%	0.33%	-0.02%
		4.0	0.51%	0.19%	0.49%	0.18%	0.15%
		6.0	0.37%	0.43%	-0.05%	0.45%	0.09%
		6.8	0.36%	0.32%	0.34%	0.36%	0.04%
		14.0	0.67%	0.21%	0.33%	0.28%	0.22%
		16.0	0.30%	0.47%	0.50%	0.23%	-0.05%
		19.8	0.49%	0.26%	0.40%	0.54%	0.10%
		22.6	0.57%	0.54%	0.80%	0.66%	-0.02%
Surge Line Case 4C BC Weld Subject to TF+D&C	Break Size (in.)	FR	2.85%	2.27%	2.42%	2.75%	0.22%
		0.5	3.61%	2.08%	2.42%	3.04%	0.59%
		1.5	2.51%	2.21%	2.63%	2.52%	0.07%
		2.0	3.01%	2.09%	2.41%	2.71%	0.31%
		3.0	2.71%	2.25%	2.58%	2.77%	0.23%
		4.0	2.71%	2.32%	2.47%	2.77%	0.31%
		6.0	3.05%	2.42%	2.63%	2.93%	0.32%
		6.8	2.97%	1.86%	2.47%	3.08%	0.30%

Table 2.12 (Cont.)

		14.0	3.44%	2.07%	2.62%	2.90%	0.39%
		16.0	2.40%	2.25%	2.36%	2.71%	0.24%
		19.8	3.04%	1.90%	2.72%	3.03%	0.39%
		22.6	3.25%	2.24%	2.44%	3.34%	0.27%
Pressurizer Cases 5A,5B, and 5J B-J Welds Subject to TF+D&C	Break Size (in.)	FR	0.36%	0.00%	0.00%	0.00%	0.00%
		0.50	0.62%	-0.61%	0.40%	0.64%	0.62%
		0.75	0.39%	-0.34%	0.13%	0.97%	0.33%
		1.00	0.32%	-0.28%	0.17%	0.52%	0.17%
		1.50	-0.05%	0.32%	0.12%	-0.14%	0.06%
		2.00	0.37%	-0.22%	0.24%	0.31%	0.09%
		3.00	0.67%	-0.46%	-0.06%	0.08%	0.67%
		4.24	-5.55%	-18.83%	-12.52%	-5.81%	8.05%
		5.66	0.22%	-0.42%	-0.13%	0.03%	0.19%
		6.00	0.22%	-0.66%	-0.09%	0.18%	0.36%
		6.75	0.46%	-0.29%	0.09%	0.56%	0.28%
		8.49	0.35%	-0.43%	-0.08%	0.00%	0.23%
Pressurizer Cases 5C, 5D, 5E, and 5I B-J Weld Subject to D&C	Break Size (in.)	FR	-0.20%	0.00%	-0.09%	0.00%	0.00%
		0.50	-0.03%	-0.02%	0.15%	0.11%	0.24%
		0.75	0.16%	-0.01%	0.02%	-0.10%	0.39%
		1.00	-0.12%	0.01%	-0.08%	-0.08%	-0.26%
		1.50	-0.55%	0.28%	0.21%	-0.55%	-0.32%
		2.00	-0.34%	-0.03%	-0.27%	-0.14%	-0.33%
		3.00	0.07%	-0.28%	0.04%	-0.03%	0.27%
		4.24	-6.13%	-18.65%	-12.64%	-5.96%	7.88%
		5.66	-0.17%	-0.23%	-0.26%	-0.28%	-0.28%
		6.00	-0.44%	-0.23%	-0.29%	-0.23%	-0.17%
		6.75	-0.26%	-0.02%	-0.10%	-0.12%	0.22%
		8.49	-0.27%	-0.30%	-0.27%	-0.22%	0.17%
Pressurizer Case 5G B-F Weld Subject to PWSCC+D&C	Break Size (in.)	FR	-0.41%	0.00%	0.09%	0.00%	0.00%
		0.50	-0.23%	0.83%	0.04%	-0.73%	0.34%
		0.75	-0.36%	0.92%	0.08%	-0.82%	-0.70%
		1.00	-0.08%	0.79%	-0.09%	-0.81%	-2.01%
		1.50	-0.63%	1.38%	-0.07%	-1.59%	-2.06%
		2.00	-0.36%	0.55%	-0.03%	-0.56%	-0.78%
		3.00	-0.12%	0.21%	-0.29%	-0.47%	0.28%
		4.24	-6.41%	-22.62%	-12.66%	-1.53%	13.58%
		5.66	-0.57%	0.49%	-0.09%	-0.75%	-0.50%
		6.00	-0.45%	0.05%	-0.26%	-0.42%	-0.06%
		6.75	-0.37%	0.46%	-0.02%	-0.25%	-0.63%

Table 2.12 (Cont.)

		8.49	-0.44%	0.45%	0.11%	-0.71%	-0.71%
Pressurizer Case 5F B-F Weld Subject to PWSCC+TF+D&C	Break Size (in.)	FR	-0.55%	0.00%	0.07%	0.00%	0.00%
		0.50	-0.26%	1.39%	0.03%	-1.18%	0.34%
		0.75	-0.46%	1.23%	0.03%	-1.12%	-0.70%
		1.00	-0.39%	0.91%	0.24%	-0.89%	-2.01%
		1.50	-1.27%	1.49%	-0.06%	-1.79%	-2.06%
		2.00	-0.46%	1.20%	-0.12%	-0.88%	-0.78%
		3.00	-0.22%	0.44%	-0.23%	-0.60%	0.28%
		4.24	-6.27%	-22.50%	-12.68%	-1.64%	13.58%
		5.66	-0.62%	0.63%	-0.05%	-0.99%	-0.50%
		6.00	-0.56%	0.26%	-0.17%	-0.91%	-0.06%
		6.75	-0.35%	0.59%	-0.05%	-0.68%	-0.63%
		8.49	-0.61%	0.51%	-0.21%	-0.82%	-0.71%
Pressurizer Case 5H B-F Weld Subject to D&C (Weld Overlay)	Break Size (in.)	FR	0.03%	0.00%	0.00%	0.00%	0.00%
		0.50	0.28%	-0.06%	0.18%	0.30%	0.12%
		0.75	-0.30%	-0.12%	0.13%	0.15%	0.04%
		1.00	0.12%	-0.26%	-0.24%	0.08%	0.06%
		1.50	-0.37%	0.22%	-0.07%	-0.30%	-0.19%
		2.00	-0.08%	-0.13%	-0.17%	-0.15%	0.03%
		3.00	0.57%	-0.33%	-0.05%	-0.21%	0.17%
		4.24	-6.10%	-16.32%	-12.68%	-8.90%	4.30%
		5.66	0.02%	-0.13%	-0.09%	-0.16%	0.03%
		6.00	0.05%	-0.48%	-0.44%	-0.25%	0.13%
		6.75	-0.07%	-0.02%	0.02%	0.20%	0.06%
		8.49	0.09%	-0.52%	-0.03%	-0.31%	0.03%
Small Bore Cases 6A and 6B B-J Welds Subject to VF+TF+D&C	Break Size (in.)	FR	-0.37%	0.00%	0.14%	0.00%	0.00%
		0.50	12.83%	-52.31%	-12.15%	62.65%	81.31%
		0.75	23.88%	-54.35%	-10.86%	74.55%	94.60%
		1.00	33.05%	-55.42%	-10.10%	81.73%	100.34%
		1.41	45.55%	-55.95%	-8.62%	89.47%	109.00%
		1.50	47.42%	-56.39%	-9.09%	90.14%	107.64%
		1.99	55.33%	-53.32%	-3.84%	98.78%	105.07%
		2.00	55.71%	-53.27%	-3.93%	98.57%	105.12%
		2.83	1517.77%	-48.18%	223.68%	1926.71%	524.79%
SIR Case 7C B-J Welds Subject to SC+TF+D&C	Break Size (in.)	FR	-0.44%	0.00%	0.19%	0.00%	0.00%
		0.5	-0.48%	0.58%	0.23%	-0.38%	-0.69%
		0.8	-0.44%	0.46%	0.06%	-0.45%	-0.23%
		1.0	-0.49%	0.59%	0.10%	-0.55%	-1.16%

Table 2.12 (Cont.)

SIR Case 7C B-J Welds Subject to SC+TF+D&C	Break Size (in.)	1.5	-1.38%	0.52%	0.02%	-0.37%	-0.11%
		2.0	-0.46%	0.57%	0.00%	-0.49%	-0.84%
		2.8	13.08%	14.13%	13.46%	12.83%	-0.39%
		4.0	-0.38%	0.52%	0.01%	3.71%	-0.42%
		4.2	-0.21%	0.53%	0.17%	-0.48%	-0.93%
		5.7	-0.42%	0.54%	-0.45%	-0.37%	0.04%
		6.0	-0.54%	0.14%	-0.38%	-0.32%	-0.22%
		6.8	-0.22%	0.42%	-0.07%	-0.25%	-0.57%
		7.2	-0.53%	0.41%	0.01%	-0.43%	-0.57%
		8.5	-0.64%	0.33%	-0.19%	-0.59%	-0.56%
		10.0	-0.38%	0.35%	0.05%	-0.37%	-0.56%
		11.3	-1.32%	-0.37%	-0.58%	-1.00%	-0.56%
		14.1	-2.40%	-1.37%	-1.86%	-2.40%	-0.55%
		17.0	-0.48%	0.74%	-0.18%	-0.45%	-0.55%
SIR Case 7A 7B B-J Welds Subject to TF+D&C	Break Size (in.)	FR	0.15%	0.00%	0.19%	0.00%	0.00%
		0.5	0.12%	-0.66%	0.22%	0.38%	-0.05%
		0.8	0.04%	-0.41%	0.00%	0.34%	0.95%
		1.0	0.43%	-0.40%	-0.01%	0.39%	0.61%
		1.5	0.27%	-0.28%	-0.02%	0.24%	0.26%
		2.0	0.33%	-0.45%	0.16%	0.11%	0.62%
		2.8	13.63%	13.23%	13.50%	13.79%	0.06%
		4.0	0.24%	-0.43%	0.03%	0.42%	0.44%
		4.2	0.36%	-0.28%	-0.06%	0.60%	0.06%
		5.7	0.27%	-0.45%	-0.20%	0.37%	-0.11%
		6.0	0.31%	-0.76%	-0.24%	0.25%	0.34%
		6.8	0.38%	-0.34%	-0.06%	0.34%	0.20%
		7.2	0.25%	-0.34%	-0.08%	0.28%	0.20%
		8.5	0.28%	-0.38%	-0.13%	0.12%	0.20%
		10.0	-0.05%	-0.47%	-0.10%	0.37%	0.21%
		11.3	-0.32%	-0.86%	-0.75%	-0.28%	0.21%
		14.1	-1.70%	-1.96%	-2.01%	-1.73%	0.21%
		17.0	0.20%	0.01%	-0.38%	-0.01%	0.22%
SIR Case 7D ACC Case 7M B-J Welds Subject to SC+D&C	Break Size (in.)	FR	0.44%	0.00%	0.40%	0.00%	0.00%
		0.5	0.62%	-0.24%	-1.94%	0.88%	0.51%
		0.8	0.84%	-0.14%	0.22%	0.69%	0.32%
		1.0	0.43%	-0.19%	0.34%	0.70%	0.16%
		1.5	0.61%	0.21%	0.38%	0.61%	0.52%
		2.0	0.56%	-0.01%	0.21%	0.58%	0.15%
		2.8	14.01%	13.51%	13.72%	14.13%	0.52%

Table 2.12 (Cont.)

SIR Case 7D ACC Case 7M B-J Welds Subject to SC+D&C	Break Size (in.)	4.0	0.95%	-0.07%	0.15%	0.61%	0.04%
		4.2	0.70%	0.27%	0.55%	0.79%	0.04%
		5.7	0.47%	-0.26%	0.48%	0.30%	0.41%
		6.0	0.44%	-0.43%	0.02%	0.47%	0.58%
		6.8	0.53%	-0.11%	0.23%	0.47%	0.45%
		7.2	0.63%	-0.11%	0.31%	0.55%	0.45%
		8.5	0.65%	-0.09%	0.21%	0.53%	0.46%
		10.0	0.93%	-0.19%	0.29%	0.52%	0.46%
		11.3	0.17%	-0.66%	-0.43%	-0.18%	0.46%
		14.1	-1.33%	-2.01%	-1.61%	-1.35%	0.47%
		17.0	0.64%	0.03%	0.02%	0.43%	0.47%
SIR Cases 7E-7L B-J Welds Subject to D&C	Break Size (in.)	FR	-0.11%	0.00%	0.03%	0.00%	0.00%
		0.5	-0.16%	0.48%	0.06%	-0.35%	-0.24%
		0.8	-0.13%	0.42%	0.19%	-0.04%	-0.38%
		1.0	-0.08%	0.67%	-0.04%	-0.16%	-0.50%
		1.5	-0.10%	0.43%	0.12%	-0.10%	-0.65%
		2.0	-0.29%	0.34%	0.12%	-0.24%	-0.32%
		2.8	13.28%	14.18%	13.59%	13.03%	-0.72%
		4.0	-0.17%	0.32%	-0.28%	-0.41%	-0.38%
		4.2	0.03%	0.53%	0.20%	0.35%	-0.51%
		5.7	-0.39%	0.07%	-0.07%	-0.34%	-0.06%
		6.0	-0.17%	0.03%	-0.20%	-0.35%	-0.01%
		6.8	-0.54%	0.41%	0.15%	-0.22%	-0.44%
		7.2	-0.22%	0.46%	0.26%	-0.28%	-0.44%
		8.5	-0.29%	-0.17%	-0.18%	-0.47%	-0.43%
		10.0	-0.19%	0.33%	0.14%	-0.33%	-0.43%
		11.3	-0.72%	-0.31%	-0.52%	-0.94%	-0.43%
		14.1	-2.31%	-1.59%	-1.90%	-2.12%	-0.43%
		17.0	-0.04%	0.43%	0.02%	-0.17%	-0.42%
ACC Case 7N B-J Welds Subject to TF+D&C	Break Size (in.)	FR	0.00%	0.00%	0.11%	0.00%	0.00%
		0.5	0.12%	0.30%	0.14%	0.11%	-0.09%
		0.8	0.09%	0.32%	0.25%	0.53%	-0.20%
		1.0	-0.08%	0.32%	0.37%	0.06%	-0.11%
		1.5	-0.18%	0.21%	0.25%	0.11%	-0.13%
		2.0	0.09%	0.21%	0.11%	0.17%	-0.14%
		2.8	13.33%	13.83%	13.72%	13.60%	-0.10%
		4.0	-4.94%	-14.10%	-10.54%	-6.74%	4.35%
		4.2	95.43%	119.44%	109.25%	99.85%	-4.58%
		5.7	14.39%	17.13%	15.87%	14.78%	-1.02%

Table 2.12 (Cont.)

ACC Case 7N B-J Welds Subject to TF+D&C	Break Size (in.)	6.0	31.35%	38.20%	35.52%	32.18%	-2.02%
		6.8	13.85%	13.87%	14.02%	13.71%	-0.03%
		7.2	91.97%	92.30%	91.86%	92.20%	-0.03%
		8.5	169.34%	169.70%	170.22%	169.92%	-0.03%
		10.0	185.75%	186.71%	186.22%	186.41%	-0.02%
		11.3	-100.00%	-100.00%	-100.00%	-100.00%	47.63%
		14.1	-99.79%	-99.91%	-99.87%	-99.82%	40.64%
		17.0	-99.76%	-99.88%	-99.84%	-99.78%	32.52%
ACC Case 7O B-J Welds Subject to D&C	Break Size (in.)	FR	-0.25%	0.00%	-0.15%	0.00%	0.00%
		0.5	-0.22%	-0.04%	-0.12%	0.03%	-0.02%
		0.8	-0.03%	0.08%	-0.10%	-0.11%	-0.01%
		1.0	-0.02%	0.31%	-0.02%	-0.10%	-0.06%
		1.5	-0.41%	0.05%	-0.03%	-0.02%	-0.09%
		2.0	-0.13%	0.11%	0.04%	0.01%	-0.03%
		2.8	13.25%	13.50%	13.67%	13.34%	-0.07%
		4.0	-5.35%	-14.03%	-11.95%	-7.48%	3.71%
		4.2	95.18%	117.50%	108.47%	100.70%	-4.11%
		5.7	14.16%	16.48%	15.92%	14.68%	-0.79%
		6.0	30.94%	37.66%	34.88%	32.35%	-1.85%
		6.8	13.53%	13.58%	13.86%	13.95%	-0.08%
		7.2	91.34%	91.83%	91.81%	91.61%	-0.08%
		8.5	168.70%	169.93%	170.07%	169.84%	-0.08%
		10.0	185.28%	185.66%	185.21%	185.34%	-0.08%
		11.3	-100.00%	-100.00%	-100.00%	-100.00%	40.74%
		14.1	-99.79%	-99.90%	-99.87%	-99.82%	35.02%
		17.0	-99.76%	-99.87%	-99.84%	-99.79%	28.34%
CVCS Case 8A and 8B B-J Weld Subject to VF+TF+D&C	Break Size (in.)	FR	0.15%	0.00%	-0.32%	0.00%	0.00%
		0.50	0.17%	-0.33%	-0.28%	0.48%	0.63%
		0.75	0.10%	-0.48%	-0.48%	0.18%	0.04%
		1.00	0.26%	-0.46%	-0.19%	0.08%	0.57%
		1.50	0.41%	-0.54%	-0.16%	0.14%	0.61%
		2.00	2.74%	-3.40%	-0.28%	3.05%	3.60%
		3.00	6.45%	-7.41%	-0.31%	7.39%	7.89%
		4.00	4.15%	-5.34%	-0.28%	4.94%	5.55%
		5.66	1.44%	-2.31%	-0.31%	1.38%	1.95%
CVCS Cases 8C, 8D, and 8F B-J Weld Subject to VF+D&C	Break Size (in.)	FR	-0.44%	0.00%	-0.18%	0.00%	0.00%
		0.50	-0.22%	-0.02%	-0.15%	-0.46%	0.07%
		0.75	-0.03%	0.04%	-0.23%	-0.30%	-0.07%
		1.00	-0.35%	-0.08%	-0.35%	-0.50%	-0.16%

Table 2.12 (Cont.)

CVCS Cases 8C, 8D, and 8F B-J Weld Subject to VF+D&C	Break Size (in.)	1.50	-0.28%	0.06%	-0.44%	-0.30%	-0.16%
		2.00	2.14%	-3.24%	-0.26%	2.70%	3.18%
		3.00	5.78%	-7.37%	-0.46%	7.10%	7.99%
		4.00	4.04%	-5.34%	-0.19%	4.50%	4.82%
		5.66	1.09%	-2.37%	-0.67%	1.09%	1.97%
CVCS Case 8E BC Welds Subject to TF+D&C	Break Size (in.)	FR	-0.05%	0.00%	0.09%	0.00%	0.00%
		0.50	0.04%	0.34%	0.12%	0.03%	0.33%
		0.75	0.01%	0.17%	-0.17%	-0.21%	-0.08%
		1.00	-0.07%	0.19%	0.49%	0.36%	-0.42%
		1.50	0.01%	0.14%	0.04%	0.02%	-0.30%
		2.00	3.00%	-2.45%	0.10%	2.76%	2.91%
		3.00	6.36%	-6.34%	0.00%	6.58%	6.44%
		4.00	4.43%	-4.54%	-0.17%	4.45%	4.54%
		5.66	0.92%	-1.97%	-0.55%	1.21%	1.77%
Notes:							
1. Two or more cases are listed together when they only differ by pipe size, see Tables 5-1 through 5-4 to see the different pipe sizes and DEGB sizes for those combined in this table.							
2. PWSCC = primary water stress corrosion cracking; SC = stress corrosion cracking; TF = thermal fatigue; D&C = design and construction defects							
3. FR = total failure rate including any failure resulting in weld repair or replacement							
4. RF = range factor = SQRT(95%tile/5%tile)							

2.2 KEY GAPS IDENTIFIED IN THE EXISTING LOCATION-SPECIFIC LOCA FREQUENCY ESTIMATION METHODOLOGY

After thorough review of Fleming and Lydell's work, this research has identified five outstanding gaps and , therefore, the following ways are suggested to advance the estimations of LOCA frequencies:

1. Include contributions from non-piping components
2. Develop a methodology to explicitly incorporate the underlying physics of failure models of the failure mechanisms
3. Incorporate an explicit time dependence for the LOCA frequencies
4. Develop a method that explicitly considers maintenance programs and accounts for changes to maintenance programs

5. Develop plant specific failure mechanism contributions

The first advancement suggested for this research concerns the incorporation of non-piping components. Fleming and Lydell's work considered LOCAs initiated at or near the location of pipe and nozzle welds. This means that contributions from non-piping components were not considered in the estimation of LOCA frequencies. This was identified as a key gap, because the most recent NRC-sponsored approach for the estimation of LOCA frequencies, NUREG-1829, did include non-piping component contributions. Therefore, the significance of the assumption of LOCAs occurring at only pipe and nozzle welds should be further examined. Chapter 3 of this thesis develops a qualitative analysis to examine the significance of the contributions of non-piping components to the estimations of LOCA frequencies.

The second advancement pursued for this research concerns the explicit incorporation of the underlying physics of failure models of the failure mechanisms. An explicit incorporation of the failure models would enable the estimations of LOCA frequencies to be guided by scientific knowledge of how failure mechanisms work instead of being almost entirely data driven. This is important, because data can be misleading. Additionally, the data that is available is sparse and only accounts for the failure mechanisms and maintenance programs of the past. Using past data to predict the future can also be misleading.

Incorporation of physical failure models can be used to develop an explicit time dependence for LOCA frequencies. Instead of relying on multiplier distributions to mask the temporal dependence of LOCA frequencies, explicitly incorporated failure models can provide a more detailed insight into how the LOCA frequencies change over a reactor's lifetime. This can also enable the incorporation of maintenance program information that currently is only implicitly included in the past failure data. Changes in maintenance programs can have a significant effect on LOCA frequencies. Finally, plant specific information can be used as an input into the failure mechanism models. This would allow for a plant's uniqueness to be taken into consideration and enable the estimations of LOCA frequencies for each plant. Chapter 4 develops a new spatio-temporal probabilistic methodology that provides more explicit incorporation of physical failure mechanisms associated with location and time into estimations of LOCA frequencies to address the gaps 2-5.

REFERENCES

1. Kee, E., Z. Mohaghegh, R. Kazemi, S.A. Reihani, B. Letellier, and R. Grantom. *Risk-Informed Decision Making: Application in Nuclear Power Plant Design & Operation*. in *American Nuclear Society Winter Meeting and Technology Expo*. 2013. Washington D.C.: American Nuclear Society.
2. Fleming, K., B. Lydell, and D. Chrun. *Development of LOCA Initiating Event Frequencies for South Texas Project GSI-191*, 2011.
3. Lydell, B.O.Y., *Pipexp-2011: Monthly summary of database content (status as of 31-july-2011)*, S.-P. Inc., Editor. 2011: Vail AZ.
4. Mikschl, T. and K. Fleming. *Piping System Failure Rates and Rupture Frequencies for Use In Risk Informed In-Service Inspection Applications*, TR-111880-NP, 2000.
5. Electric Power Research Institute. *Revised Risk-Informed In-Service Inspection Procedure*, TR 112657 Revision B-A, 1999.
6. Andresen, P., F. Ford, K. Gott, R. Jones, P. Scott, T. Shoji, R. Staehle, and R. Tapping. *Expert Panel Report on Proactive Materials Degradation Assessment*, Report, 2007.
7. OECD Nuclear Energy Agency. *Technical Basis for Commendable Practices on Ageing Management - SCC and Cable Ageing Project (SCAP)*, 2011.
8. Scott, P. *Primary Water Stress Corrosion Cracking of Nickel-base Alloys*, 2010.
9. OECD Nuclear Energy Agency. *Proc. Specialists Meeting on Experienc ewith Thermal Fatigue in LWR Piping Caused by Mixing and Stratification*, 1998.
10. Fleming, K. and B. Lydell, *Database Developent and Uncertainty Treatment for Estimating Pipe Failure Rates and Rupture Frequencies.* Reliability Engineering & System Safety, 2004. **86**: p. 227-246.

11. Fleming, K. and B. Lydell. *Pipe Rupture Frequencies for Internal Flooding PRAs*, 1013141, 2006.

12. Fleming, K. and B. Lydell. *Pipe Rupture Frequencies for Internal Flooding PRAs*, 1021086, 2010.

13. Fleming K. et al. *Piping System Reliability and Failure Rate Estimation Models for Use in Risk-Informed In-Service Inspection Applications*, TR-110161, 19998.

14. Fleming, K., *Email communication between Karl Fleming and Seyed A. Reihani*, S.A. Reihani, Editor. 2014.

15. Prediction Technologies. *R-DAT*. 2015; Available from: http://www.prediction-technologies.com/rdat.html.

16. Oracle. *Oracle Crystal Ball*. 2016; Available from: http://www.oracle.com/us/products/applications/crystalball/overview/index.html.

17. Tregoning, R., L. Abramson, and P. Scott. *NUREG-1829 Raw Data*, Report, 2008.

18. U.S. Nuclear Regulatory Commission. *PWR Piping Raw Data*,

CHAPTER 3 : QUALITATIVE EVALUATION OF THE SIGNIFICANCE OF NON-PIPING COMPONENT CONTRIBUTIONS FOR LOCA FREQUENCIES

This chapter relates to Step #3 in the roadmap of the research presented in Figure 3.1. It focuses on evidence-seeking and expert elicitation to investigate the significance of incorporating contributions from non-piping components in the estimations of LOCA frequencies for the STPNOC risk-informed GSI-191 project, which was first presented in [1]. Chapter 1 introduced the STPNOC risk-informed Generic Safety Issue 191 project[2]. The STPNOC project is an example of a risk-informed regulatory project which requires estimations of location-specific LOCA frequencies. In support of the STPNOC project, Fleming and Lydell[3] developed location-specific estimations of LOCA frequencies. Chapter 2 provides a critical review of the Fleming and Lydell method and identifies the key gaps. Step #3 in Figure 3.1 shows that the next step in the research progression is to examine the significance of one of the key gaps identified, i.e., the lack of incorporation of non-piping RCS components into the estimation of LOCA frequencies. Fleming and Lydell's work assumes that LOCAs initiate at or near the location of pipe and nozzle welds. This chapter reports on the results of investigating the significance of the non-piping RCS component contributions to LOCA frequencies for nuclear power plants (NPPs).

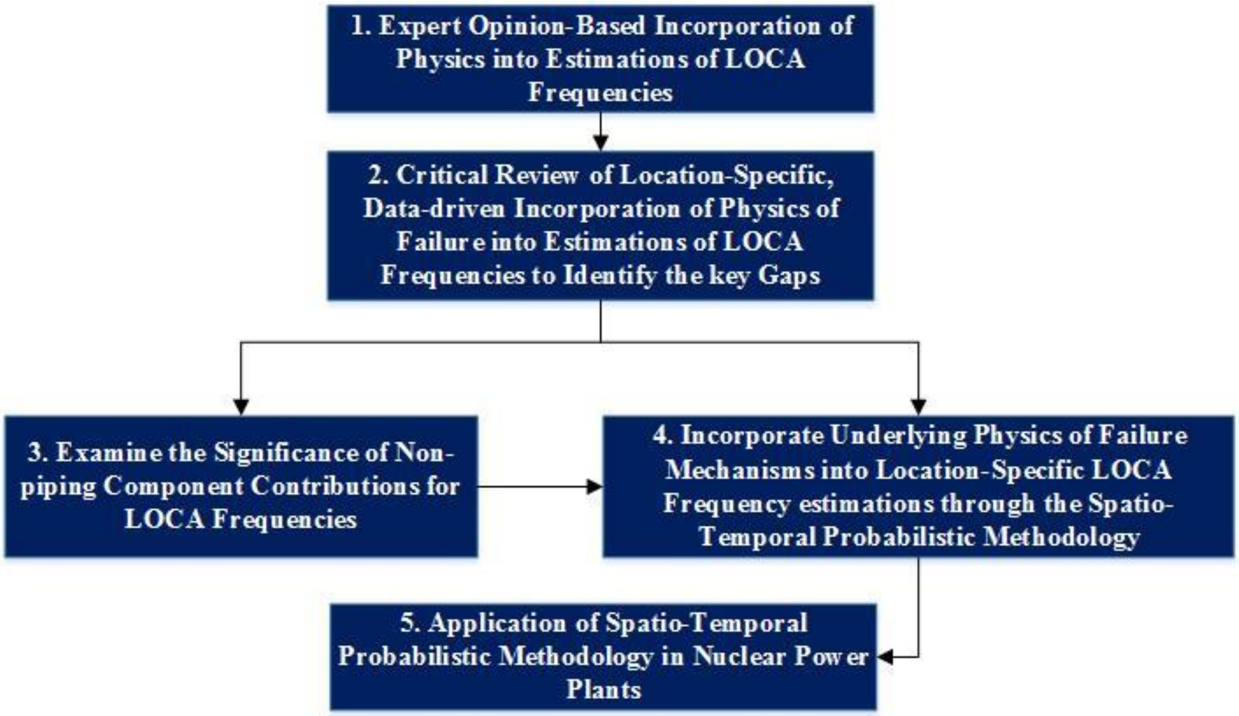

Figure 3.1 Roadmap of the Research

3.1 NON-PIPING COMPONENT IMPACT FOR GENERIC SAFETY ISSUE 191

The primary function of the reactor coolant system (RCS) in NPPs is to transfer heat from the fuel to the steam generators. The RCS consists of the reactor vessel, the steam generators, the reactor coolant pumps, the pressurizer, and the piping that connects each of the major non-piping components[4]. A depiction of an RCS for a U.S. PWR can be found in Figure 3.2. Breaks in the RCS can lead to the escape of large quantities of primary coolant. If this coolant exceeds the capabilities of the reactor to replace the coolant, a LOCA can occur. Therefore, to understand the risk associated with the operation of NPPs, it is important to understand the probability or the frequency of such a break occurring. NRC has, therefore, sponsored multiple reports that support the estimation of LOCA frequencies[5-8]. These reports have investigated the frequency at which RCS piping could break and the potential there is to produce a LOCA.

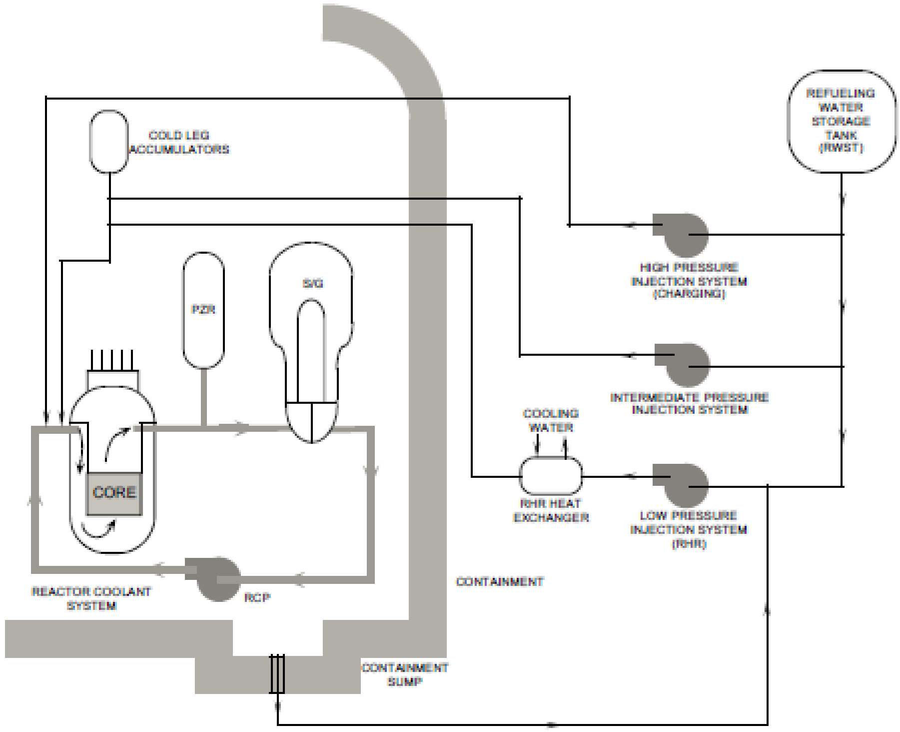

Figure 3.2 PWR Reactor Coolant System, Emergency Core Cooling System, and Sump Depiction from [4]

Many risk-informed regulatory decision-making applications, such as the STPNOC risk-informed pilot project to resolve GSI-191[9], need estimations of LOCA frequencies as a critical input. As explained in Section 1.4.2 in Chapter 1, the initiating event frequencies for the risk-informed resolution of GSI-191 need to be location-specific. The NRC-sponsored estimations of LOCA frequencies provided cumulative frequencies as a function of component break size that included the contributions from all potential LOCA locations, but did not provide the individual contribution for each of the locations. Since two breaks of equivalent size in different locations may have significantly different likelihoods of occurrence and effects on GSI-191 related phenomena (e.g., quantity of debris generated, transport fractions, in-vessel flow paths, etc.), the cumulative frequencies needed to be distributed to each of the potential break locations.

In support of the STPNOC project, Fleming and Lydell[3] utilized service data from 4,000 reactor-years of PWR service experience to estimate location-specific LOCA frequencies. Fleming and Lydell's works did not consider non-piping passive components, and mentioned that the most important degradation mechanisms, such as thermal fatigue (TF) and stress corrosion cracking (SCC) occur at or near welds. However, the expert elicitation process documented in NUREG-1829 revealed that despite a dearth of precursor data available for the non-piping components compared with piping components, panelists believe non-piping components provide significant contributions for Category 1 and 2 LOCA frequencies. According to the experts documented in NUREG-1829, assessment of non-piping component failure frequencies and their impact on estimations of LOCA frequencies are more difficult than for piping components as there are multiple aspects to consider including the different operating requirements, designs, materials, and inspection considerations for each non-piping component[8]. Non-piping component related information has been extracted from NUREG-1829 and can be found in Appendix B. Despite the information regarding the potential for non-piping components provided by the experts of NUREG-1829, Fleming and Lydell chose not to consider non-piping components and to consider only the pipe and nozzle welds for three main reasons:

1. Apart from leaks from valves and seals, piping system failures occur almost exclusively at or near welds.
2. Since primary reactor coolant system (RCS) pressure boundary welds are distributed relatively evenly around the piping systems, these welds provide a representative set of pipe failure locations for both pipe and non-pipe failures.
3. The most important degradation mechanisms, such as thermal fatigue (TF) and stress corrosion cracking (SCC) occur at or near welds due to the localized metallurgical changes from elevated temperature service, including increased residual stress distributions across the heat-affected zones[10-13].

Step #3 in the roadmap of this research, presented in Figure 3.1, focuses on investigating further evidence to help support or refute the necessity for including non-piping component contributions into the estimations of LOCA frequencies associated with GSI-191. This chapter reports the results of this investigation consisting of two steps:

1. Evidence Seeking: utilized the references developed by academia, industry, regulatory, and national laboratory
2. Evidence Screening: conducted by experts in academia and industry

A flowchart of the investigation procedure can be seen in Figure 3.3. Section 3.2 provides a description of the "evidence-seeking" process in Figure 3.2. Section 3.3 explains the "evidence screening" process in Figure 3.2. The evidence seeking and evidence screening processes were based on the following two criteria:

A. *LOCA Relevancy*: the potential for the failure of each component or sub-component to result in a LOCA
B. *Debris Generation Relevancy:* the potential for the failure of a component or sub-component to generate debris that could travel to the containment floor, and ultimately to the sump strainer of the emergency core cooling system

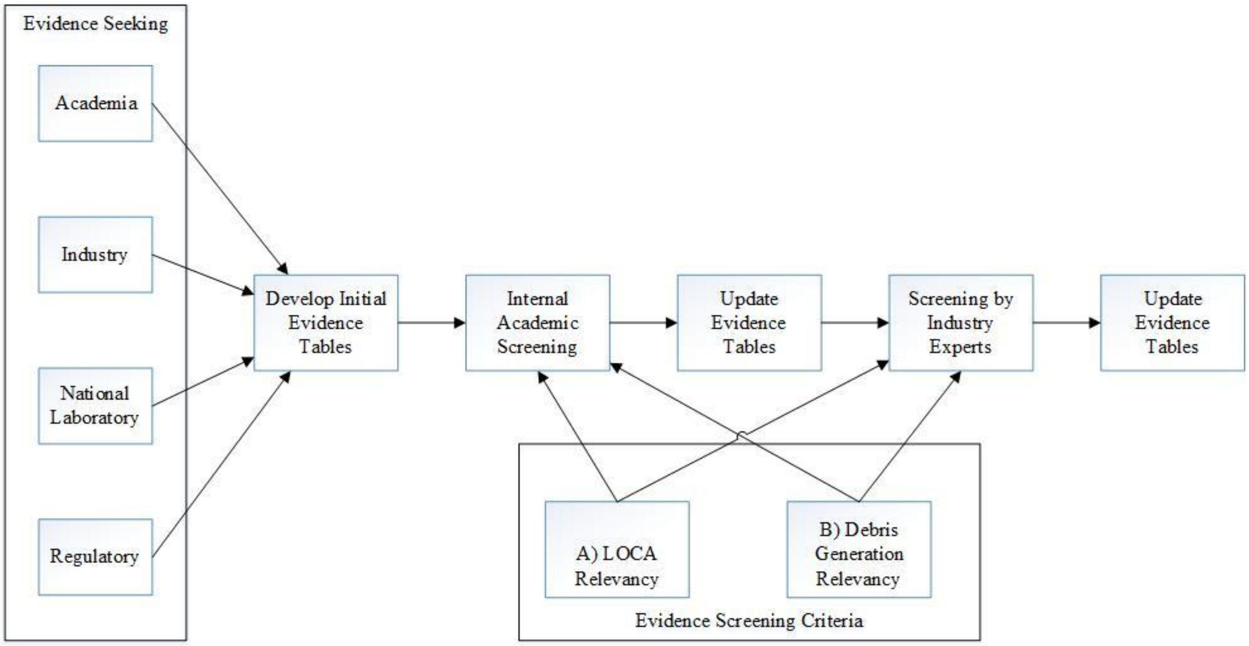

Figure 3.3 Investigation Procedure for Importance of Passive Non-Piping RCS Components for the Estimations of LOCA Frequencies Associated with GSI-191

3.2 EVIDENCE-SEEKING PROCESS FOR NON-PIPING COMPONENTS

To determine the significance of non-piping components for estimations of LOCA frequencies and GSI-191, evidence-seeking research was performed. Due to the rare nature of LOCA phenomena, this evidence-seeking research required extensive literature review and included approximately 500 academic, industry, national laboratory, and regulatory publications.[1] Due to the extensive nature of the evidence-seeking process, it was necessary to develop specific criteria (criteria A and B in Figure 3.3) by which to judge whether the literature provided relevant evidence for the research.

[1] The evidence-seeking process was conducted with help from undergraduate research intern, John Simmons

Evidence regarding the importance of non-piping RCS components or sub-components for GSI-191 phenomena is classified into six groups based on the functionality of each component or sub-component. The six categories include:

- Reactor coolant pump (RCP)
- Pressurizer
- Steam generator
- Reactor vessel
- ECCS
- Chemical volume and control system (CVCS)

The collected evidence is limited to the period from 1975 to 2014 to reduce irrelevancies due to design changes.

The following sub-sections (3.2.1 to 3.2.6) provide selected evidence to highlight the scope and multi-dimensional nature of evidence seeking research. A few examples of the accumulated evidence are included in each sub-section to provide an understanding of the information within the evidence tables as well as to highlight the range of the information. The complete evidence tables for this investigation are provided in Appendix B of this thesis.

3.2.1 REACTOR COOLANT PUMP

In the reactor coolant pump (RCP) category, 16 sub-component categories were initially identified as satisfying the evidence seeking criteria. These sub-component categories are:

- turning vane bolts/cap screws
- pump shaft
- pump closure
- pump body/casing
- flange
- flywheel
- framing and support
- thermal barrier
- seals

- suction deflector bolting
- motor exterior
- oil collection system tank[2]
- motor stator coolers
- heat exchanger components
- motor lube oil coolers[2]
- valves[2]

These sub-component categories were developed based on similarities in function and/or location within a typical RCP.

The RCP evidence search included 121 academic, industry, national laboratory, and regulatory publications related to reactor coolant pumps spanning the period from 1980-2014. Relevant information was brought into the evidence tables (see Appendix B) in the form of quotations, names of tables within the documents, or descriptive information from 51 of these publications, including:

- 14 regulatory publications
- 9 national laboratory publications
- 26 industry publications
- 2 news articles from Nuclear Street News and South Jersey Times

For the RCP category, no information of high relevancy to the evidence-seeking criteria was found from the academic sector. Examples of the collected evidence include:

LOCA Relevancy:

[2] Component in Reactor Coolant Pump Motor Oil Collection Sub-System

- Industry: In 2000, the Application for Renewed Operating License of Turkey Point Units 3&4 from the Florida Power and Light Co. stated, "*Mechanical closure bolting associated with the reactor coolant pump components is made of low alloy steel bolting material and is subject to aggressive chemical attack*."[14]
- National Laboratory: An Idaho National Laboratory document from 1989[15] found, "*Visual inspection of closure studs at other PWR plants has revealed that the studs in all pump designs are susceptible to boric acid corrosion*." The document later states, "*Leakage of borated water across LWR primary coolant pump case-to-cover gaskets can cause corrosion of the pump closure studs and corrosion of carbon steel pump body base metal*."
- Regulatory: Information Notice No. 90-68 from the NRC in 1994[16] states, "*On September 2, 1993, the licensee for Millstone Unit 3 was inspecting the reactor's lower core support plate before reloading fuel. The licensee discovered pieces of a locking cup for the Westinghouse model 93A-1 reactor coolant pump turning vane cap screws. The cap screws connect the flanged interfaces of the turning vane and thermal barrier*."
- News: A 2014 news article from the South Jersey Times[17] reports, "*Sheehan said one of the main concerns was having the bolt heads damage or stop the impeller at the bottom of the pump which spins and draws the water into the pump in then sends it into the reactor vessel. Also, Sheehan said, there could be the possibility of the impeller, moving at such a high rate of speed, striking and disintegrating a bolt head and sending tiny pieces of metal circulating throughout the cooling system and possibly causing damage*."

Debris Generation Relevancy:

- Industry: The Electric Power Research Institute, in 1988[18] reported, "*The RC pump main flange showed the greatest capacity for producing large leak rates owing to the large diameter of the sealing surface and smaller number of studs per arc length*."
- Regulatory: Information Notice No. 90-68 from the NRC in 1994[16] states, "*The licensee subsequently removed four turning vane cap screws for inspection. A visual and liquid penetrant inspection at the juncture of the head and body of the cap screws revealed cracks in two cap screws. One cap screw had no cracks. The head of the fourth cap screw was almost completely severed. The cap screws are made of alloy A286 stainless steel, designated by the American Society for Testing and Materials as A453 grade 660. The cap screw or cap screw head may deform, loosen, fracture, or fail the locking cup restraints. Cap screw failures could present a safety hazard because failed parts could enter the reactor coolant system and cause damage to vital components*."
- News: A 2014 news article from the Nuclear Street News Team[19] reported, "*Inspections during a refueling outage at unit 2 of PSEG's Salem nuclear plant revealed bolt fragments at the bottom of the reactor pressure vessel. Quoting spokesmen from the plant and the Nuclear Regulatory Commission, the South Jersey Times reported that as many as 17 bolt heads have been found beneath fuel assemblies and at the bottom of a reactor coolant pump. The bolts came from RCP turning vanes and may have been affected by stress corrosion cracking*."

- National Laboratory: An Idaho National Laboratory document from 1989[15] explained, *"Failure of pump internals, for example, shafts and bearings, will not compromise the integrity of the pressure boundary, but the broken pieces may be carried over to the reactor vessel and damage the vessel internals, fuel rods, and other core components."*

3.2.2 PRESSURIZER

In the pressurizer category, 13 sub-component categories were identified, including:

- thermal/heater sleeve
- manway bolts/studs
- instrument nozzles
- walls/vessel shell
- valve bonnet bolts
- bolted relief valve
- spray head
- support skirt and the immediate surrounding insulation
- seismic lugs
- power-operated relief valve (PORV)
- spray line nozzle
- surge line nozzle
- surge line

These categories were developed based on similarities in function and/or location within a pressurizer.

The pressurizer evidence search covered 82 academic, industry, national laboratory, and regulatory publications related to pressurizers that spanned 30 years (from 1981-2011). Relevant information was brought into the evidence tables in the form of quotations, names of tables within the documents, or descriptive information from 30 of these publications, including:

- 3 academic publications

- 8 regulatory publications
- 7 national laboratory publications
- 12 industry publications

A complete set of collected evidence is available in Appendix B. Examples of the collected evidence include:

LOCA Relevancy:

- Industry*:* In 1992, Dominion Engineering released [20], which stated, "*In May 1989, approximately 20 of 120 heater sleeves were found to be leaking in the Calvert Cliffs Unit 2 pressurizer*."
- National Laboratory: In 2008, Brookhaven National Laboratory and the Korea Atomic Energy Research Institute released [21], which reports, "*Since the late 1980's, approximately 50 Alloy 600 pressurizer heater sleeves at Combustion Engineering-designed (CE- designed) facilities in the United States have shown evidence of RCPB leakage which has been attributed to PWSCC*."
- Regulatory: In 2008, the NUREG-1829[8] Appendix B states, "*Heater sleeves fail due to PWSCC, but as a result of their size, multiple failures are required in order to result in a LOCA*."

Debris Generation Relevancy:

- National Laboratory: In 1989, Idaho National Laboratory, in [22], stated, "*Failure of heater sleeve welds has the potential of becoming a serious problem because it is* *possible that these sleeves could blow out and result in an unisolable small-break LOCA*”

- Regulatory: In 2008, NUREG-1829[10] Appendix L reported, “*Again, for the Category 2 LOCAs, the major contributors are the CRDMs and the pressurizer heater sleeves.”*
- Industry: In 1981, Burns and Roe Inc. released [23], which explained, *“The potential for large amounts of insulation debris reaching the sump from inside the shield wall exist. Two partial floors exist within the shield wall at E. 605’-4” and El. 609’-1”. Although these floors will capture much of the insulation, some could pass through the gap between the two floors to reach the sump. Any insulation below the floor at El. 606’-0” and El. 605’-4” will reach the basement floor. In the region surrounding the sump, there exists several pipes above the sump. The largest of these pipes is a 10-inch residual heat removal pipe. A pipe break could dislodge the insulation from these pipes and the insulation could land on the sump.”*
- Academia: In 2011, the Korea Institute of Nuclear Safety released [24], which stated, *“In the US, Trojan plant reported unexpectedly large piping displacements due to thermal stratification, which resulted in crushed insulation.”*

3.2.3 STEAM GENERATOR

In the steam generator category, 7 sub-component categories were identified, including:

- steam generator tubes
- primary manway cover
- bolts
- studs
- nozzles
- tubesheet

- support bolts
- embedded anchor studs
- primary divider plate
- steam generator shell

These categories were developed based on similarities in function and/or location within a steam generator.

The steam generator evidence search examined 104 academic, industry, national laboratory, and regulatory publications related to steam generators and spanned the years 1975 through 2014. Relevant information was brought into the evidence tables in the form of quotations, names of tables within the documents, or descriptive information from 41 of these publications, including:

- 3 academic publications
- 15 regulatory publications
- 7 national laboratory publications
- 16 industry publications

A complete set of collected evidence is available in Appendix B. Examples of the collected evidence include:

LOCA Relevancy:

- National Laboratory: In 1998, Idaho National Laboratory published Rates of Initiating Events at U.S. Nuclear Power Plants 1987-1995[7], which reported, "*This study identified three steam generator tube rupture (SGTR) events. The SGTR frequency estimate based on the three SGTR events is 7.0E-3 per critical year. Based* *on the current PWR population, this frequency correlates to about one event every two calendar years. The last SGTR identified in the 1987–1995 experience occurred at Palo Verde 2 in 1993*."

- Regulatory: In 2013, the NRC released the Summary of Event and Plant Conditions (as of May 16, 2013) regarding SONGS steam generator tube degradation[25], which states, "*SONGS unit 3 experienced a leak on Jan. 31, 2012 from tube wear at retainer bars, 74 tubes had indications of potential failure*"
- Academia: In 2011, the University of Maryland published a journal paper[26], A Probabilistic Physics-of-Failure Approach to Prediction of Steam Generator Tube Rupture Frequency, which states, "…*there were ten SGTR occurrences in the United States between 1975 and 2000. For example, on July 15, 1987, an SGTR event occurred at the North Anna Unit 1 PWR, shortly after the unit reached 100% power. The cause of the tube rupture was determined to be high cycle fatigue*."

Debris Generation Relevancy:

- Industry: In Stress Corrosion Cracking of a Kori 1 Retired Steam Generator Tube, [27], a 2007 report from the Korean Atomic Energy Research Institute, it was found that pitting may cause penetration through a wall leading to loss of primary coolant water.
- National Laboratory: In a 1996 document, Steam Generator Tube Failures[28], from the Idaho National Laboratory, it was reported, *"Although the damaged tubes on the tube bundle periphery were plugged as a result of eddy-current inspection indications*

and/or small leaks, the debris, in conjunction with the hydraulic and pressure loadings, continued to damage the plugged tubes and eventually caused the tubes to collapse and in some cases to become completely severed near the top of the tubesheet."

- Regulatory: In 2008, NUREG-1829 Appendix H[8] stated, "*From 1990 to 2002 there were 15 reports of steam generator tube leaks. There is a total of 929 reactor calendar years represented in this period, so the mean leak frequency over this period is 1.6x10-3 per calendar year*.", "*Therefore, the frequency of steam generator tube Category 1 ruptures (with resultant leak rates greater than 100 gpm [380 lpm]) was 4/1,133 calendar years, or 3.5x 103 per calendar year. NUREG/CR-5750 [4.1] conducted a similar assessment of SGTRs, and estimated a frequency of 7x 10-3 per calendar year*"

3.2.4 REACTOR VESSEL

In the reactor vessel category, 20 sub-component categories were identified, including:

- lower support structure
- core barrel
- upper grid
- plenum cover
- lower grid
- fuel
- flow distributor
- vent valve
- core support shield
- core barrel and its support
- shield and shroud
- baffle and former
- control rod guide tube
- upper/lower internals
- upper guide structure support barrel
- control element assembly shroud

- control element drive mechanism
- rod cluster control assembly guide tube
- RV closure upper/lower head

These categories were developed based on similarities in function and/or location within a reactor vessel

The reactor vessel evidence search reviewed 59 academic, industry, national laboratory, and regulatory publications related to reactor vessels and spanned the years from 1988-2012. Relevant information was brought into the evidence tables in the form of quotations, names of tables within the documents, or descriptive information from 26 of these publications, including:

- 1 academic publication
- 1 regulatory publication
- 1 national laboratory publication
- 23 industry publications

A complete set of collected evidence is available in Appendix B. Examples of the collected evidence include:

LOCA Relevancy:

- <u>Industry</u>: In 2002, the First Energy Nuclear Operating Company released the "Root Cause Analysis report: Significant Degradation of the Reactor Pressure Vessel Head"[29] which stated, "*Circumferential cracking in CRDM nozzles were identified at Oconee 2 and 3, and axial cracking in the J-groove weld in CRDM nozzles were identified at Oconee 1 and ANO 1 (i.e., B&W plants)*."

- National Laboratory: In 2002, a Brookhaven National Laboratory ASME conference paper[30] reported that said, "… *identified flow-induced vibration as a cause for wear (i.e., thinning) of the thimble tubes ...*"
- Regulatory: In 1988, the NRC released Generic Letter No. 88-05, "Boric Acid Corrosion of Carbon Steel Reactor Pressure Boundary Components in PWR Plants"[31] which stated, "*At Turkey Point Unit 4, leakage of reactor coolant from the lower instrument tube seal on one of the incore instrument tubes resulted in corrosion of various components on the reactor vessel head including three reactor vessel bolts. The maximum depth of corrosion was 0.25 inches*."
- Academia: In 2011, the Universidad Politecnica de Madrid, released, "Accident Management Actions in an Upper-head Small-break Loss-of-Coolant Accident with high-pressure Safety Injection Failed"[32] which stated, "*In 2002, the discovery of thinning of the vessel head wall at the Davis Besse nuclear power plant reactor indicated the possibility of an SBLOCA in the upper head of the reactor vessel as a result of circumferential cracking of a control rod drive mechanism penetration nozzle*…"

Debris Generation Relevancy:

- Industry: In 2007, Entergy Nuclear Operations' License renewal for Indian Point nuclear generating units 2 and 3, appendix A[33] stated, "*Flux thimble tubes are subject to loss of material at certain locations in the reactor vessel where flow-*

induced fretting causes wear at discontinuities in the path from the reactor vessel instrument nozzle to the fuel assembly instrument guide tube."

- Regulatory*:* In 1988, the NRC released Generic Letter No. 88-05, "Boric Acid Corrosion of Carbon Steel Reactor Pressure Boundary Components in PWR Plants"[31] which stated, "*At San Onofre Unit 2, boric acid solution corroded nearly through the bolts holding the valve packing follow plate in the shutdown cooling system isolation valve. During an attempt to operate the valve, the bolts failed and the valve packing follow plate became dislodged causing leakage of approximately 18,000 gallons of reactor coolant into the containment*."

3.2.5 EMERGENCY CORE COOLING SYSTEM

In the ECCS category, 22 sub-component categories were identified, including:

- CSS heat exchanger (shell)
- tanks
- bolting and bearings
- valves and valve bodies
- tubing
- strainers
- suction
- grating
- sump
- seals
- nozzles
- orifices
- thermowell
- filters
- heater housing
- oil cooler shell and channel head
- spray system
- flex hose
- high pressure injection system
- structural coating
- pump casings
- pumps

- heat exchanger (channel heads and coils)
- heat exchanger (tubes and tube sheets/ shields)

These categories were developed based on similarities in function and/or location within an ECCS.

The ECCS evidence search covered 131 academic, industry, national laboratory, and regulatory publications related to ECCSs spanning the years from 1986-2010. Relevant information was brought into the evidence tables in the form of quotations, names of tables within the documents, or descriptive information from 20 of these publications, including:

- 10 regulatory publications
- 10 industry publications

An example is shown below to provide an understanding of the information included within the evidence tables. A complete set of collected evidence is available in Appendix B.

There was no LOCA-Relevancy information identified, because the ECCS does not operate until there is already an issue with insufficient cooling.

Debris Generation Relevancy:

- Regulatory*:* In the 1998 report, “Potential for Degradation for the Emergency Core Cooling System and the Containment Spray System after a Loss-of-Coolant-Accident because of Construction and Protective Coating Deficiencies and Foreign Material in Containment (Generic Letter No. 98-04)” released by the NRC [34], it states that, "*September 18, 1992: During Technical Specification in-service inspection testing of the A containment spray pump the pump was declared inoperable. A foam rubber plug was blocking pump suction. Plug removed and pump tested satisfactorily. One train of Unit 2 residual heat removal, safety injection, and containment spray systems inoperable for entire operating cycle. Plug was part of a cleanliness barrier*."

3.2.6 CHEMICAL VOLUME AND CONTROL SYSTEM

In the CVCS category, 14 sub-component categories were identified, including:

- valves and bodies
- housings
- thermowell
- gauges and indicators
- vessels
- accumulators
- reservoirs
- pumps and cases
- bolting and fasteners
- filters and strainers
- tanks
- orifices and elements
- piping
- hoses
- fittings
- heat exchanger (channel heads and covers)
- heat exchanger (shell)
- heat exchanger (tubes and tubesheets)

These categories were developed based on similarities in function and/or location within a CVCS.

The CVCS evidence search reviewed 29 academic, industry, national laboratory, and regulatory publications related to steam generators spanning the years from 2001-2010. Relevant information was brought into the evidence tables in the form of quotations, names of tables within the documents, or descriptive information from 10 industry license renewal applications.

The CVCS is not directly part of the primary reactor pressure boundary and, therefore, is not a concern for LOCA. However, some of the CVCS components are connected to the RCS pressurized systems, so they do have a potential for debris generation that could play a role in the GSI-191 scenario.

The only information currently found regarding the CVCS relates to the potential failure modes of components within the CVCS. It is theorized in this research that failures in the CVCS could create debris that could be transported to the RCS and thus become a contributor to a GSI-191 issue.

3.3 EXPERT SCREENING OF NON-PIPING COMPONENT INFORMATION

After the initial evidence aggregation, the evidence tables underwent an internal academic review by Professor Zahra Mohaghegh and Dr. Seyed A. Reihani. The evidence was evaluated with respect to the two criteria presented in Figure 3.3 (i.e., *LOCA Relevancy* and *Debris Generation Relevancy*). The reviewers were sent copies of the evidence tables and asked to provide any relevant information they may personally have in relation to the two evidence-seeking criteria. The resulting qualitative feedback helped eliminate some of the sub-components identified in Subsections 3.2.1 – 3.2.6 that did not meet the evaluation criteria.

Upon completion of the internal academic review, the evidence tables were sent for external review to three nuclear industry experts. The nuclear industry experts were selected due to their many years of experience working with PRAs involving LOCA frequencies. These experts provided their opinions regarding each component and sub-component based on the information collected from the evidence seeking process of the investigative procedure in addition to their professional experiences. In the screening provided by experts, some contributors were identified as ‘indirect’ contributors to LOCA. These were internal components such as turning vanes, thermal barrier, and suction deflector, or sub-components such as flywheels, framing, etc. that can add stress, for example, to pressure boundary components, but their failure would not directly cause the occurrence of a LOCA.

Subsections 3.3.1. – 3.3.6. report the results of the expert screening for each of the six categories: RCP, pressurizer, steam generator, reactor vessel, ECCS, and CVCS. In each category of components, two sets of examples of review comments are included in the subsections to demonstrate the type of information provided by the experts. The remaining comments can be found in Appendix B. The first set of examples of comments provided in each subsection are on the “agreement” expressed by the expert regarding the importance and the potential contribution of the sub-component to debris generation and the GSI-191 issue. This has benefitted this research and helped identify the sub-component as a potential non-piping concern for GSI-191. The second set of examples of comments relate to “disagreement” expressed by the experts regarding the importance and the potential contribution of the sub-component to debris generation and the GSI-191 issue and has helped this research eliminate subcomponents regarding potential concerns for GSI-191 from further consideration.

The review comments from the academic and industry experts have assisted in the identification process of the potential importance of non-piping components for GSI-191. The items identified in each category are not based on any ranking. They only show items identified as being potential contributors to the GSI-191 project.

3.3.1 REACTOR COOLANT PUMP

After receiving the academic and industry reviews from the experts, the following 6 RCP sub-component categories were identified as having the potential to make a significant contribution for non-piping components:

- Pump shaft
- Pump closure (studs, bolts, main flange, and nuts)
- Pump body/casing
- Flywheel
- Framing and support
- Thermal barrier

Examples of the review comments include:

- <u>Pump closure</u> (studs, bolts, main flange, and nuts): "*Potential for large LOCA here. Probably the most important issue for reactor coolant pump (because seal package failure has been experienced).*"
- <u>Turning vane bolts and cap screws</u>: "*Not an issue for the GSI-191, because the bolt fragments are too heavy. If the flow through the reactor pressure vessel isn't strong enough to push the fragments out, then in the case of a LOCA, the flow on the containment floor will not push the fragments to help clog the sump strainer.*"

3.3.2 PRESSURIZER

After receiving the academic and industry reviews from the experts, the following 5 pressurizer sub-component categories have been identified as potentially important non-piping components for the GSI-191 project:

- Spray head
- Manway bolts/studs
- Thermal/heater sleeves
- Power-operated relief valves (some plants)
- Walls/vessel shell.

Examples of the review comments include:

- Spray head: "*This is interesting because it is talking about the vessel walls. We should look into this and find out what the exposure may be. The pressurizer has a large volume of liquid in it and there would be a very large break potential (much bigger than a pipe)*."
- Instrument nozzles: "*Instrument nozzles addressed in bottom-up approach. PWSCC susceptibility exists only for B&W and CE plants. Current fleet has implemented mitigation.*"

3.3.3 STEAM GENERATOR

After receiving the academic and industry reviews from the experts, the following 2 steam generator sub-component categories have been identified as potentially important non-piping components for the GSI-191 project:

- Primary manway cover, bolts, and studs
- Support bolts and embedded anchor studs.

Examples of the review comments include:

- Support bolts, embedded anchor studs: "*Steam generator supports failures could result in greater load on the connected piping. So this is something to consider*."
- Primary divider plate: "*This is not a GSI-191 concern because it is internal to the primary system*."

3.3.4 REACTOR VESSEL

After receiving the academic and industry reviews from the experts, the following 8 reactor vessel sub-component categories have been identified as potentially important non-piping components for the GSI-191 project:

- Reactor vessel flange
- Instrument tubes
- Control rod drive mechanisms and housings
- Thimble tubes
- Thermal shield
- Nozzle safe ends
- Closure heads (torus, dome and cladding)
- Nozzles.

Examples of the review comments include:

- Control rod drive mechanism housings: "*CRDM housing failures, especially the drive shaft housing could result in debris generation*."
- Reactor vessel internals: "*Internal components would not cause debris generation*."

3.3.5 EMERGENCY CORE COOLING SYSTEM

After receiving the academic and industry reviews from the experts, the following 3 ECCS sub-component categories have been identified as potentially important non-piping components for the GSI-191 project:

- Strainers, suction grating
- Sump, thermowell
- High pressure injection system.

Examples of the review comments include:

- <u>Strainers, suction, grating, and sump</u>: "*If the ECCS suction strainers are weakened by corrosion or have additional buildup of corrosion prior to the need for recirculation, they could fail mechanically (allowing excess debris bypass to the core) or collapse and prevent pumping*."
- <u>Seals</u>: "*ECCS equipment requiring seals would not result in debris generation that would cause sump blockage*."

3.3.6 CHEMICAL VOLUME AND CONTROL SYSTEM

After receiving the academic and industry reviews from the experts, no CVCS sub-component categories were identified as potentially important non-piping components for the GSI-191 project. The consensus of the reviewers for the CVCS category has shown to be that

> "*Some CVCS equipment and piping is connected to RCS pressurized systems. This equipment could create debris*." However, "*CVCS is another system located out of RCS pressure boundary between the first and second valves. The potential for debris generation could be an issue, but they are isolable-LOCA*."

Therefore, since there was not any evidence of the potential for an unisolable-LOCA to occur from a subcomponent in the CVCS category, this category was eliminated from the investigative research.

3.4 CONCLUSION OF INVESTIGATIVE RESEARCH

Non-piping components are a major part of the RCS in NPPs. Like all things, non-piping components have the potential to break. The investigative research presented in this chapter explored the significance of the potential for non-piping component breaks to contribute to GSI-191. This research consisted of two steps. The first step of the investigation required an extensive evidence-seeking process, which spanned over 500 academic, industry, national laboratory and regulatory publications, to gather as much information as possible regarding the potential contributions of non-piping RCS components in PWRs to GSI-191. This initial evidence was then screened by academic and industry experts. The expert-screening process identified many components that should be eliminated from the investigative process. However, after the expert-screening, 24 subcomponent categories were identified as having potentially significant GSI-191 contributions.

The 24 subcomponent categories identified by this investigative process indicates that estimations of LOCA frequencies for risk-informed decision-making applications such as GSI-191 should not focus exclusively on the RCS piping components, because there is a potential for impact from the non-piping components. However, the investigative procedure could not determine “how significant” the exclusion of non-piping components could be on the results of risk-informed analyses.

A quantitative methodology is needed to determine the “level of impact” of the inclusion/exclusion of non-piping components on the estimations of LOCA frequencies for risk-informed applications. Chapter 4 develops a quantitative methodology which could be used to quantitatively compare the LOCA frequencies associated with non-piping components with the ones for the piping components. The spatio-temporal probabilistic methodology developed in Chapter 4 explicitly incorporates the underlying physical failure mechanisms into location-specific LOCA frequency estimations through the integration of the Markov modeling technique with Probabilistic Physics of Failure models to develop LOCA frequencies for specific RCS locations and age. In addition, a case study is provided in Chapter 5 of this thesis to implement the Spatio-Temporal Probabilistic methodology to compare the effects of material selection on the rupture probability of steam generator tubes.

REFERENCES

1. O'Shea, N., Z. Mohaghegh, S.A. Reihani, E. Kee, K. Fleming, and B. Lydell. *Analyzing Non-Piping Location-Specifc LOCA Frequency For Risk-Informed Resolution of Generic Safety Issue 191*. in *International Topical Meeting on Probabilistic Safety Assessment and Analysis*. 2015. Sun Valley, ID, USA: American Nuclear Society.
2. Mohaghegh, Z., E. Kee, S.A. Reihani, R. Kazemi, D. Johnson, R. Grantom, K. Fleming, T. Sande, B. Letellier, G. Zigler, D. Morton, J. Tejada, K. Howe, J. Leavitt, Y. Hassan, R. Vaghetto, S. Lee, and S. Blossom. *Risk-Informed Resolution of Generic Safety Issue 191*. in *International Topical Meeting on Probabilistic Safety Assessment and Analysis*. 2013. LaGrange Park, IL, USA: American Nuclear Society.
3. Fleming, K., B. Lydell, and D. Chrun. *Development of LOCA Initiating Event Frequencies for South Texas Project GSI-191*, 2011.
4. NRC Technical Training Center, *Reactor Concepts Manual: Pressurized Water Reactor (PWR) Systems*.
5. U.S. Nuclear Regulatory Commission. *Reactor Safety Study: An Assessment of Accident Risks in U.S. Commercial Nuclear Power Plants*, WASH-1400 (NUREG 75/014), 1975.
6. Nuclear Regulatory Commission. *Severe Accident Risks: An Assessment for Five U.S. Nuclear Power Plants (NUREG-1150)*, 1990.
7. Poloski, J.P. and D.G. Marksberry, *Rates of Initiating Events at US Nuclear Power Plants: 1987-1995 (NUREG/CR-5750).* Washington, DC: US Nuclear Regulatory Commission, 1998. **12**.
8. Tregoning, R., L. Abramson, and P. Scott. *Estimating Loss-of-Coolant Accident (LOCA) Frequencies Through the Elicitation Process*, NUREG-1829, 2008.

9. Kee, E., Z. Mohaghegh, R. Kazemi, S.A. Reihani, B. Letellier, and R. Grantom. *Risk-Informed Decision Making: Application in Nuclear Power Plant Design & Operation*. in *American Nuclear Society Winter Meeting and Technology Expo*. 2013. Washington D.C.: American Nuclear Society.

10. Lundin, C., *Dissimilar Metal Welds- Transition Joints Literature Review.* Welding Journal, 1982. **63**(2): p. 58-s - 63-s.

11. Roberts, D., R. Ryder, and R. Viswanathan, *Performance of Dissimilar Welds in Service.* Journal of Pressure Vessel Technology, 1985. **107**.

12. Benson, M., D. Rudland, and A. Csontos. *Weld Residual Stress Finite Element Analysis Validation: Part 1 - Data Development Effort (NUREG-2162)*, 2014.

13. Electric Power Research Institute. *Materials Reliability Program: Primary System Piping Butt Weld Instpection and Evaluation Guideline (MRP-139, Revision 1)*, 1015009, 2008.

14. Florida, P. and C. Light. *Application for Renewed Operating Licenses Turkey Point Units 3 & 4*, Report, 2000.

15. Shah, V.N., A.S. Amar, M.H. Bakr, B.F. Beaudoin, B.J. Buescher, D.A. Conley, F.R. Drahos, J.B. Gardner, R.W. Garner, B.J. Kirkwood, L.C. Meyer, W.L. Server, V.N. Shah, E.A. Siegel, U.P. Sinha, and A.G. Ware. *Residual life assessment of major light water reactor components: Overview*, Report, 1989.

16. Grimes, B., *Information Notice No. 90-68: Supplement 1: Stress Corrosion Cracking of Reactor Coolant Pump Bolts*. 1994, U.S. Nuclear Regulatory Commission: Washington, D.C.

17. Gallo Jr, B., *Broken Bolt Pieces Found in Pump, Reactor Vessel Delay Salem 2 Nuclear Plant Restart*. 2014.

18. Nickell, R. *Degradation and Failure of Bolting in Nuclear Power Plants*, Report, 1988.

19. Nuclear Street News, T., *Loose Bolt Fragments Extend Salem Nuclear Plant Outage*. 2014.

20. Nestell, J.E. *Safety evaluation for pressurizer heater sleeve cracking*, Report, 1992.

21. Nie, J., J.I. Braverman, C.H. Hofmayer, Y.S. Choun, M.K. Kim, and I.K. Choi, *Identification and assessment of recent aging-related degradation occurrences in US nuclear power plants.* BNL Report-81741-2008, KAERI/RR-2931/2008, Brookhaven National Laboratory, 2008.

22. Amar, A., M. Bakr, B. Beaudoin, B. Buescher, D. Conley, F. Drahos, J. Gardner, R. Garner, B. Kirkwood, L. Meyer, W. Server, V. Shah, E. Siegel, U. Sinha, and A. Ware. *Residual Life Assessment of Major Light Water Reactor Components - Overview*, NUREG/CR-4731, V02, ERR, 1989.

23. Kolbe, R. *Survey of Insulation Used in Nuclear Power Plants and Potential for Debris Generation Draft*, Report, 1981.

24. Kang, D., M. Jhung, and S. Chang, *Fluid–structure interaction analysis for pressurizer surge line subjected to thermal stratification*, in *Nuclear Engineering and Design*. 2011. p. 257 - 269.

25. Nuclear Regulatory Commission. *"Summary of Event and Plant Conditions (as of May 16, 2013)" in SONGS Steam Generator Tube Degradation*, Report, 2013.

26. Chatterjee, K. and M. Modarres, *A Probabilistic Physics-of-Failure Approach to Prediction of Steam Generator Tube Rupture Frequency*, in *Nuclear Science and Engineering*. 2012. p. 136 - 150.

27. Kim, H.P., S.S. Hwang, D.J. Kim, J.S. Kim, Y.S. Lim, and M.K. Joung, *Stress corrosion cracking of a Kori 1 retired steam generator tube.* EUROPEAN FEDERATION OF CORROSION PUBLICATIONS, 2007. **51**: p. 306.

28. MacDonald, P., V. Shah, L. Ward, and P. Ellison. *Steam Generator Tube Failures(NUREG/CR-6365)*, 1996.

29. Loehlin, S.A. *Root Cause Analysis Report: Significant Degradation of the Reactor Pressure Vessel Head*, Report, 2002.

30. Subudhi, M., R. Morante, and A.D. Lee. *Aging Management of Reactor Coolant System Mechanical Components in Pressurized Water Reactors for License Renewal*. 2002. American Society of Mechanical Engineers.

31. Miraglia, F., *Boric Acid Corrosion of Carbon Steel Reactor Pressure Boundary Components in PWR Plants (Generic Letter No. 88-05)*. 1988, U.S. Nuclear Regulatory Commission: Washington, D.C. 20555.

32. Queral, C., J. González-Cadelo, G. Jimenez, and E. Villalba. *Accident Management Actions in a Upper-Head Small-Break Loss-of-Coolant Accident with High-Pressure Safety Injection Failed*, Report, 2011.

33. Entergy Nuclear Operations, I. *Indian Point Nuclear Generating Unit 2 and 3 - License Renewal Application Appendix A*, Report, 2007.

34. Roe, J.W., *Potential for Degradation of the Emergency Core Cooling System and the Containment Spray System after a Loss-of-Coolant-Accident Because of Construction and Protective Coating Deficiencies and Foreign Material in Containment (GENERIC LETTER NO. 98-04)*. 1998.

CHAPTER 4 : SPATIO-TEMPORAL PROBABILISTIC METHODOLOGY FOR ESTIMATIONS OF LOSS-OF-COOLANT ACCIDENT (LOCA) FREQUENCIES

This chapter relates to Step #4 in the roadmap of the research presented in Figure 4.1. Chapter 1 introduces the risk-informed GSI-191 project [1] and the current state of estimations of LOCA frequencies. Chapter 2 provides a critical review of the location-specific, data-driven incorporation of physical failure mechanisms into the estimation of LOCA frequencies developed by Fleming and Lydell [1]. Chapter 2 also identifies key gaps in the Fleming and Lydell's methodology including (a) the lack of inclusion of non-piping components in the estimations of LOCA frequencies and (b) the lack of explicit incorporation of physics of failure. Chapter 3 qualitatively examines the significance of including the contributions of non-piping components into the estimations of LOCA frequencies. However, the qualitative investigative procedure in Chapter 3 cannot specify "how significantly" the exclusion of non-piping components could affect the results of risk-informed analyses. Step #4 in Figure 4.1, which is the focus of this chapter, relates to the development of the Spatio-Temporal Probabilistic methodology for LOCA frequency estimations. The Spatio-Temporal Probabilistic methodology can be used to quantitatively compare non-piping and piping components with respect to LOCA frequencies.

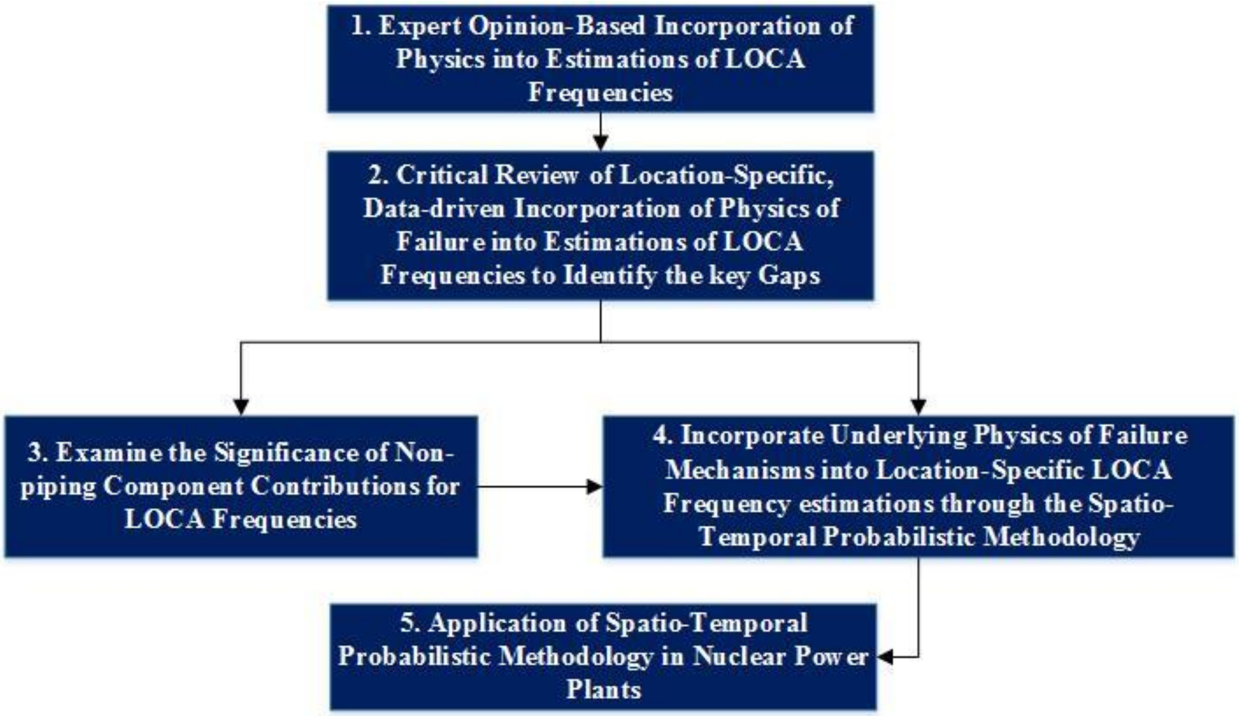

Figure 4.1 Roadmap of the Research

The Spatio-Temporal Probabilistic methodology, which is an integration of the Markov modeling technique with the Probabilistic Physics of Failure (PPoF) models, provides the possibility for *explicitly* including the effects of location-specific causal factors, such as operating conditions (e.g., temperature, pressure, pH), maintenance quality, and material properties (e.g., yield strength and corrosion resistance) on the probability of LOCA occurrence. This methodology is beneficial, not only for estimation of location-specific LOCA frequencies, but also for incorporation of spatio-temporal physics of failure into Probabilistic Risk Assessment (PRA); therefore, it helps advance risk estimation and risk prevention. The *explicit* incorporation of failure mechanisms helps more accurately estimate the likelihood of LOCA occurrences, dealing with limited historical data. Additionally, the *explicit* incorporation of the causal factors enables the use of sensitivity analyses, which allow the causal factors to be ranked in order of their risk significance. Ranking of causal factors helps optimize maintenance practices by indicating the most resource-efficient methods to reduce risks.

Section 4.1 and its sub-sections explain the foundations and the logical tasks of the Spatio-Temporal Probabilistic methodology. To show the feasibility of this new methodology, a case study is demonstrated in Chapter 5.

4.1 THE FOUNDATIONS AND LOGICAL TASKS OF THE SPATIO-TEMPORAL PROBABILISTIC METHODOLOGY

A Loss-of-Coolant Accident (LOCA) can occur when a Reactor Coolant System (RCS) experiences a break that is large enough so that the high-pressure coolant flowing through the RCS can escape confinement at a rate greater than the reactor coolant makeup systems can replace the coolant[2]. Because NPPs are under a periodic maintenance, the underlying mechanisms that affect the state of degradation of a component in the RCS fall into two categories: (1) degradation and (2) repair. Degradation mechanisms, also known as failure mechanisms, move components into a "more degraded state". The definition of "more degraded state" is application specific, and usually describes some ability of a component, such as its resistance to an applied load. For RCS components, exposure to degradation mechanisms can result in a decrease of a component's ability to contain high-pressure coolant. Eventually, degradation of a component reaches a threshold where the component is no longer capable of withstanding the coolant pressure, and a LOCA may occur. While degradation mechanisms move a component to more degraded states, repair mechanisms can restore a component's ability, thus moving a component into a less degraded state. NPPs have periodic maintenance programs to assist with prevention of LOCA occurrence. The maintenance programs enable degradation of RCS components to be detected and repaired, counter-acting the effects of the degradation mechanisms, and bringing a component back to a less degraded state. Therefore, it is important that LOCA frequency estimation models consider both degradation and repair phenomena. The proposed Spatio-Temporal Probabilistic methodology integrates the following two types of modeling:

(1) The Markov modeling technique (the left side of Figure 4.2) to depict the renewal processes of components' repair due to periodic maintenance after degradations.
(2) Probabilistic Physics of failure (PPoF) models (the right side of Figure 4.2) to explicitly incorporate the failure mechanisms, associated with the location and age of components, into the estimation of LOCA frequencies. PPoF models integrate the underlying mechanisms related to degradation into the Markov modeling technique and, subsequently, into LOCA frequency estimations.

To capture the back-and-forth and periodic nature of the degradation and repair mechanisms, the Markov modeling technique that is a technique for renewal process modeling [3-6] is selected. Appendix C provides a review for renewal process modeling. The Markov modeling technique uses discrete states to represent a component's level of degradation as a function of both degradation and repair mechanisms. One of the underlying assumptions of the Markov modeling technique is "perfect repair", i.e., the repair mechanisms would return the component or system to an "as good as new" state. Future research can use more advanced renewal process techniques (See Appendix C) to relax this assumption in the Spatio-Temporal Probabilistic methodology.

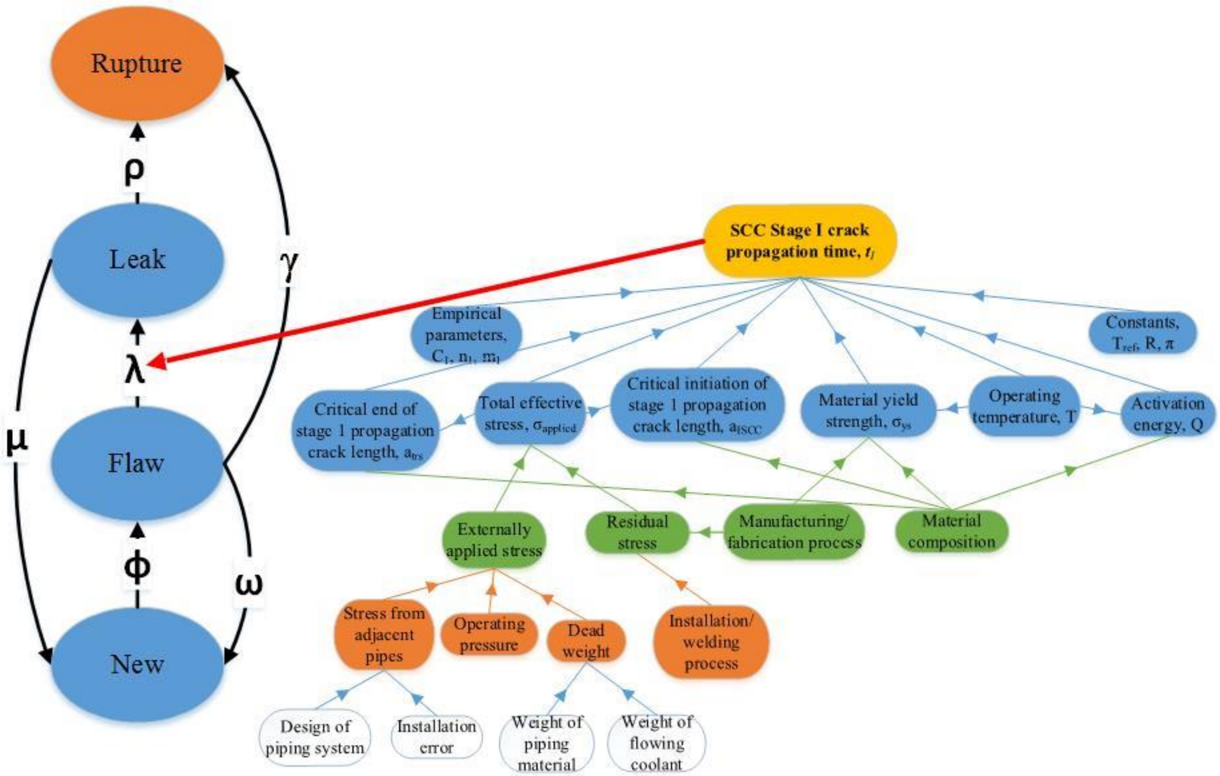

Figure 4.2 Integration of the Markov Modeling Technique with Probabilistic Physics of Failure Models in the Spatio-Temporal Probabilistic Methodology for Location-Specific LOCA Frequency Estimations

The left side of Figure 4.2 demonstrates the Markov model and its four states for crack propagation failure and repair mechanisms developed in this research. The four ovals in the figure represent the Markov states of degradation including: New, Flaw, Leak, and Rupture. In most of Markov models developed in this area of research, e.g., Fleming [7-10], the "transition rates" among the states (i.e., degradation transition rates: ϕ, λ, ρ , γ in Figure 4.2 and repair transition rates: ω, μ in Figure 4.2) are developed using solely data-driven approaches and utilizing service data. For example, Fleming develops a Markov model for piping system reliability that incorporates statistical estimates for the transition rates from Electric Power Research Institute (EPRI) studies performed for thermal fatigue[11] and water hammer events[12]. Other multi-state physics-based models have been also developed in recent years for applications, such as the exploration of aging degradation of passive components[13, 14], to predict long-term failure rates of passive components[15-17], passive component degradation for the RELAP 7 reactor simulation environment[18], and SCC of dissimilar metal in RELAP 7[19]. These multi-state physics-based models have implemented a data-driven approach by fitting uncertainty distributions to available data to quantify the probability of transitions between states. While these approaches try to explicitly incorporate the progression of damage through the Markov model development, the transition rates themselves are developed through a solely data-driven approach. The main problems with the Markov models with the solely data-driven transition rates are (1) inaccuracy due to insufficient data and (2) the lack of "explicit" connections with location-specific physics of failure mechanisms associated with transition rates.

The rate of change in degradation of a component varies at each location. For example, some locations in the RCS may not be inspected as frequently as other locations. Therefore, the probability that the maintenance program will identify the component degradation and repair the component is much lower for an infrequently inspected location than it would be for a more frequently inspected location. Additionally, some failure mechanisms may degrade a component very quickly at one location due to the operating conditions such as temperature or humidity. However, that same failure mechanism may have a much lower rate of degradation at another location due to a change in operating conditions or material properties. Some locations may not experience that same failure mechanism at all because of the component being made from a different material. Therefore, to explicitly incorporate this spatial variation of the effects of the underlying failure mechanisms into LOCA frequency estimations, it is necessary to integrate the transition rates in the Markov modeling technique with the associated location-specific physics of failure mechanisms.

Vinod et al. [56] combine the Markov modeling technique with a stress-strength model of erosion corrosion (E-C) for the piping components of Pressurized Heavy Water Reactors (PHWR), using an analytical model to estimate corrosion rates. Vinod et al. define a limit state function (LSF) to determine the probability that the stress applied to the piping component will exceed the strength of the piping component. The "failure probability" in the Vinod et al. methodology is the probability that the crack size in the component exceeds the maximum allowable crack size of the Markov state before transitioning to another Markov state. Although Vinod et al.'s approach utilizes a physical failure mechanism model for erosion-corrosion to depict the underlying physical failure mechanism of transition rates in the Markov model more explicitly than solely data-driven approaches, due to some unrealistic assumptions, their approach does not adequately provide explicit incorporation of physical factors associated with locations. For example, the progression of erosion-corrosion damage propagation, like stress corrosion cracking, changes with the size of the crack. As the damage progresses, the damage rate of the mechanism changes. Vinod et al.'s approach lumps the failure rate into a distribution and treats the failure mechanism the same through each stage of crack progression. Therefore, the variations in the failure probability, based on the underlying spatio-temporal physics, are masked by the average rate distribution.

To develop more explicit connection between the Markov model and the spatio-temporal physical failure mechanisms, this research proposes the Spatio-Temporal Probabilistic methodology that integrates the Markov modeling technique with Probabilistic Physic of Failure (PPoF) models (i.e., the causal model in the right side of Figure 4.2). The physics of failure models directly incorporate the operating conditions (e.g., temperature and pressure) and environmental factors (e.g., load) into the estimation of "time-to-failure," by incorporating the scientific knowledge of failure mechanisms (e.g., SCC). Bayesian regression analysis is used to fit the physics of failure models to the available service experience information. Probabilistic Physics-of-Failure (PPoF) models [20] combine scientific knowledge of failure mechanisms with uncertainty in the operating conditions and environmental factors to predict the time-to-failure of a component. Modarres [21, 22] developed probabilistic relationships for common failure mechanisms using Bayesian updating to incorporate test or field data as evidence to find distributions for the time-to-failure parameters. This allows for the epistemic uncertainties of deterministic physics-based models to be determined. The models are turned into probabilistic forms and able to be used in current Probabilistic Risk Assessment (PRA) frameworks.

One of the main challenges of PPoF models relates to their quantifications. Since these models are based on curve-fitting to specific conditions, they are not generic and their accuracy and scope rely heavily on the availability of historical or experimental data. Mohaghegh et al. [23] proposed combination of causal modeling techniques (e.g., Bayesian Belief Network) and Finite Element methods for quantification of PPoF models, more specifically, where two failure mechanisms interact. The scope of the research in this thesis focuses on single failure mechanism and future work can expand the Spatio-Temporal Probabilistic methodology to include the interactions of two failure mechanisms. To overcome the quantification difficulties of PPoF models, this research proposes the Data-Theoretic approach, first presented in [24], that is explained in Section 4.1.2.1 as a part of Task #2.1 in the Spatio-Temporal Probabilistic methodology.

The Spatio-Temporal probabilistic methodology, developed in this research for LOCA frequency estimations, has four key tasks that are listed here and explained in the following sub-sections. These tasks are also implemented in a case study explained in Chapter 5.

- Task #1: Defining Markov States of Degradation
- Task #2: Modeling and Quantification of the Transition Rates of Degradation
    - Task # 2.1: Developing and quantifying physics of failure causal models
    - Task #2.2: Propagating uncertainties in the physics of failure causal models to develop Probabilistic Physics of failure (PPoF) models
    - Task #2.3: Calculating transition rates of degradation based on the output of Probabilistic Physics of failure (PPoF) models
    - Task # 2.4: Bayesian integration of the estimated transition rate from PPoF models (from step 3) and the ones from solely data-oriented approaches (e.g., Fleming [7-10])
- Task #3: Modeling and Quantification of the Transition Rates of Repair
- Task #4: Developing the Time-dependent Distributions of State Probabilities

Although the tasks are explained mainly based on the Stress Corrosion Cracking mechanism (SCC), which is a dominant mechanism associated with LOCA in NPPs, the Spatio-Temporal Probabilistic methodology can be applied for any other failure mechanisms (e.g., wear, creep) and for other industry applications than NPPs (e.g., oil and gas).

4.1.1 TASK #1: DEFINING MARKOV STATES OF DEGRADATION

The first step in the development of the Markov model is to define a set of discrete, mutually exclusive, and collectively exhaustive states that completely model the possible states of degradation to which the component of concern can belong. The modeler has the freedom to select the number of states of degradation utilized in the model. An assumption utilized in the application of a Markov model is that the modeled component can transition from one state to any other state (depending on the underlying mechanisms) independently of the components past states. Therefore, the system has no memory of a component's past existence, only the components current state. For defining the states in the Markov model, the modeler should consider the following three criteria:

1. The desired output information from the Markov model
2. How state thresholds align with the underlying mechanisms
3. The computational cost of the model

The first criterion that the modeler should consider is the desired output information from the Markov model. For example, if the modeler would like to find the probability that a component will leak, then the modeler should include a "Leak" state in the model. A component may be defined as belonging to a "leak" state if the component has a crack that penetrates 100% through the thickness of the component. Therefore, when the model is solved for the time-dependent probability that the component is in each state, the probability that the component will leak will be directly output from the solution to the model.

Markov states are defined by characteristic thresholds. The second criterion for development of the states in the Markov model is how the threshold criteria of each state aligns with the underlying PoF models. For example, some failure mechanisms only begin propagating after a specific threshold criterion has been met. Aligning the threshold criterion of the failure mechanism with the threshold criterion of the Markov states can make quantification of the model much simpler. However, if the failure mechanism threshold criterion occurs at the middle of a degradation state, the development of the transitions between states can become much more complex, especially after a layer of uncertainty is added for the input parameters. The development of the "Flaw" state in the case study in Chapter 5 provides an example of the state of degradation that is defined in a way to align with a failure mechanism, in this case, Stress-Corrosion Cracking (SCC).

In some cases, the choice of the characteristic threshold for defining a Markov state may be accompanied with uncertainty. For example, the modeler may want to find the probability that a component will rupture within a given mission time. However, the modeler may not be certain as to what value to use as the characteristic threshold of the “rupture” state. In this case, the suggestion is to quantify the Markov model using the range of possible characteristic threshold values. The resulting distribution of output values would represent the model uncertainty for the characteristic threshold. Investigating the model uncertainty enables the modeler to see the significance of assuming a specific characteristic value.

The third criterion that should be considered for degradation state development is the computational cost required for solving the model. Obtaining time-dependent state probabilities from a Markov model requires the analyst to solve a series of coupled differential equations, which represent the rate of change of a component belonging to a given state at a given time. The complexity of such a solution depends on the number of states and the number of paths through which a component can transition from one state to another. Further information regarding Markov model solutions is provided in Section 4.1.4.

As an example, the left side of Figure 4.2 demonstrates the Markov model with four states: New, Flaw, Leak, and Rupture. The choice of four states in this model relates to the case study that is demonstrated in Chapter 5.

4.1.2 TASK #2: MODELING AND QUANTIFICATION OF TRANSITION RATES OF DEGREDATION

A component can transition from one state to another at any time, depending on the underlying failure and repair mechanisms that are appropriate for each state. Once a component transitions to another state, it has no memory of how it reached a given state. Transition rates represent the paths through which a component can transition from one state to another. The numerical value of a transition rate represents the rate of change in the probability that the modeled component occupies a given state. Transition rates of degradation represent the pathways that a component moves along as it transitions into a more degraded state. In the Markov model in the left side of Figure 4.2, the transition rates of degradation are represented by ϕ, λ, ρ, and γ, which represent the pathways of transition from the "New" state to the "Flaw state, "Flaw" to "Leak", "Leak" to "Rupture", and "Flaw" to "Rupture", respectively.

As mentioned at the beginning of Section 4.1, in most of Markov models developed in this area of research, e.g., Fleming [7-10], the transition rates are developed using solely data-driven approaches and utilizing service data. For example, to calculate the transition rate for λ and ρ, Fleming assumes the component to be a weld in a Combustion Engineering (CE) PWR RCS subject to thermal fatigue and design and construction errors. Fleming then utilizes leak and rupture frequencies developed by Mikschl and Fleming[11] using NPP service data. For the calculation of ϕ, Fleming assumes that the thermal fatigue damage mechanism will create 3 flaws in a component for every leak or rupture that is observed. Therefore, the leak and rupture frequencies are added together and multiplied by a factor of 3. In order to calculate γ, Fleming assumes that the conditional frequencies of rupture are equal to the frequency of severe water hammer events, which is developed by Stone and Webster Engineering Corporation[12]. This data-oriented approach enables the modeler to bring historical experience into the Markov models, however, their main challenges are (1) inaccuracy due to insufficient data and (2) the lack of “explicit” connections with location-specific physics of failure mechanisms associated with transition rates.

In the proposed Spatio-Temporal Probabilistic methodology, the Markov modeling technique is integrated with PPoF models. The transition rates of degradation provide the *explicit* pathway for connecting the PPoF models to the Markov model. For example, in Figure 4.2, a SCC physics of failure causal model is shown on the right-hand side of the image. This causal model can be used to develop the rate that the probability of a component being in the “Flaw” state decreases due to transitions into the “Leak” state from SCC. The transition rates are also the *explicit* pathway for incorporation of spatio-temporal factors, as the physics of failure causal factors (e.g., coolant temperature or material composition, stress) depend on the specific location of the component and on the age of the component. The following sub-tasks are proposed to model and quantify transition rates of degradation in the Spatio-Temporal Probabilistic methodology:

- TASK #2.1: Developing and quantifying physics of failure causal models based on the identified failure mechanisms to find the “transition time between two states” as a function of underlying physical causal factor. This research proposes a Data-Theoretic approach to overcome the challenges of quantification of these casual models. Section 4.1.2.1 explain this approach.
- TASK #2.2: Propagating uncertainties in the physics of failure causal models to make the Probabilistic Physic of Failure (PPoF) models and to develop a probabilistic estimation of “transition time between two states”. This step is explained in Section 4.1.2.2.

- TASK #2.3: Calculating transition rates of degradation based on the output of PPoF models, i.e., the estimated probabilistic "transition time between two states". This step is explained in Section 4.1.2.3.
- TASK #2.4: Bayesian integration of the estimated transition rate from PPoF (from step 3) and the transition rate from solely data-oriented approaches (e.g., Fleming [7-10]) to combine different sources of information, i.e., information from historical data and from physics-based simulations. This step is out of the scope of this research and will be elaborated in future research.

4.1.2.1 TASK #2.1: DEVELOPING AND QUANTIFYING PHYSICS OF FAILURE CAUSAL MODELS

This section explains the development of physics of failure casual models (the right side of Figure 4.2). The target node of the causal model is the "transition time between two states", which refers to the yellow node at the top of the casual model of Figure 4.2. Development of physic of failure casual models using a theory-based approach requires quantification and validation of the models through experimentation and simulation. The challenge of this approach is that the quantification and validation of large-scale models with many factors becomes expensive and time consuming. On the other hand, the use of a solely data-oriented approach can create potentially misleading results due to the lack of guidance from an underlying theory. It also requires extensive data, not always available, for every possible failure, e.g., LOCAs. To overcome the quantification challenge of these multi-level causal models, this research proposes the Data-Theoretic methodology which integrates theory-based and data-oriented techniques by utilizing a comprehensive underlying theory to guide the data analysis. The underlying theory supports the completeness of contextual factors and the accuracy of their causal relationships. It also helps avoid the potential for being misled by results from a solely data-informed analysis. The proposed Data-Theoretic methodology (in the context of PoF and PRA research) is originally published in [24] and is under development in a parallel research

[25] for the context of socio-technical risk analysis, sponsored by the National Science Foundation.

The proposed Data-Theoretic methodology (in the context of physics of failure and PRA research) is broken down into four steps:

a. Determine causal factors and relationships and develop physics of failure causal models of underlying damage mechanisms
b. Extract historical data and update the generic causal model
c. Scientifically reduce physical factors in the network
d. Quantify and validate important factors and causal paths

Step a: *Determine causal factors and relationships and develop physic of failure causal models of underlying damage mechanisms:*

The first step of Data-theoretic methodology is to establish the underlying theory associated with the physical failure mechanisms of the system. Theory development often requires a thorough review of published literature from academia, industry, and regulatory regarding the failure mechanisms. Causal factors, sub-factors, and pathways are determined based on the literature review and the knowledge of the system (i.e., expert opinion). Each causal factor and sub-factor is represented by a node in the causal model. This process is repeated for each underlying failure mechanism. These causal models are then connected by their common factors, or common nodes. An example of a causal model is developed for stress corrosion cracking (SCC) presented in the right side of Figure 4.2. The first-round quantification of the causal model in the Data-Theoretic approach is based on generic equations and information available in the literature that would lead to development of DT-base causal model.

Step b: *Extract historical data and update the generic causal model:*

The DT-base casual model, developed in Step 1, will would be updated by the historical data to quantify the missing links and/or update the generic casual model with the available historical data. The data are often buried in a wide variety of documentation and a large volume of unstructured or excess information. Therefore, this Data-Theoretic approach proposes the application of advanced data analytic techniques (i.e., text mining) to extract and interpret information from historical documentation such as: Root Cause Analysis (RCA) reports, Corrective Action Program (CAP) entries, Licensee Event Reports (LER), and LOCA databases. The extracted information is used to determine frequencies of occurrence for each causal node in the theoretical model (developed in Step a). The frequency of each node is then converted to probability that enables the use of predictive modeling techniques, such as Bayesian Belief Networks (BBNs), to develop the initial causal network.

Step c: *Scientifically reduce physical factors in the network:*

The cost of validating every causal link due to time and resource constraints, would make a theory-based approach impractical. The Data-Theoretic method scientifically narrows the scope of the factors, making the modeling of large or complex systems practical without the loss of critical information. To avoid this loss, sensitivity analysis is proposed to perform on the initial causal network to determine which factors have the most significant impact on the target node (e.g., time-to-failure). The factors are ranked by their significance to failure and the factors requiring more detailed quantification are determined.

Step d*: Quantify and validate important factors and causal paths:*

Step c scientifically narrows the scope of the factors so that time and resources are focused on the quantification of the most important factors. These factors are quantified using available classical theory-based techniques, such as controlled experimentations and finite element simulations. The important factor quantification information is stored, updated, and operationalized in an updated physics of failure causal model.

The four steps of the Data-Theoretic methodology help manage the quantification of multi-level causal model (e.g., the one presented on the right side of Figure 4.2.) and to reduce the scope of the casual network in a scientific way without missing the critical risk factors. However, in this thesis, the scope of the causal model is reduced (from the beginning) in a way that only the first level of the causal model in Figure 4.2 (i.e., the blue casual factors in Figure 4.2) is covered. Therefore, this research mainly focuses on step "a" of the Data-theoretic approach explained above. Other steps are the focus of future research.

The first step of the Data-Theoretic methodology is to establish a physics of failure theory that provides the foundation for the causal models and guides the data analytics in Step 2. After a review of academic, industry, and regulatory publications, the underlying failure mechanisms of the system need to be determined. High-level qualitative causal models are then developed to depict causal pathways that lead to a failure in the system. To demonstrate the causal modeling development, Figure 4.3 shows a high-level causal model depicting the causal progression of a LOCA for a PWR RCS. Fleming and Lydell identified four main categories of failure mechanisms for a PWR RCS: fatigue, flow-assisted degradation, stress corrosion cracking (SCC), and other corrosion mechanisms[1]. These failure mechanisms are represented as green nodes in Figure 4.3. It should be noted that, for simplicity, the repair (maintenance) paths are not included in this figure but it is covered in the Markov model of Figure 4.2.

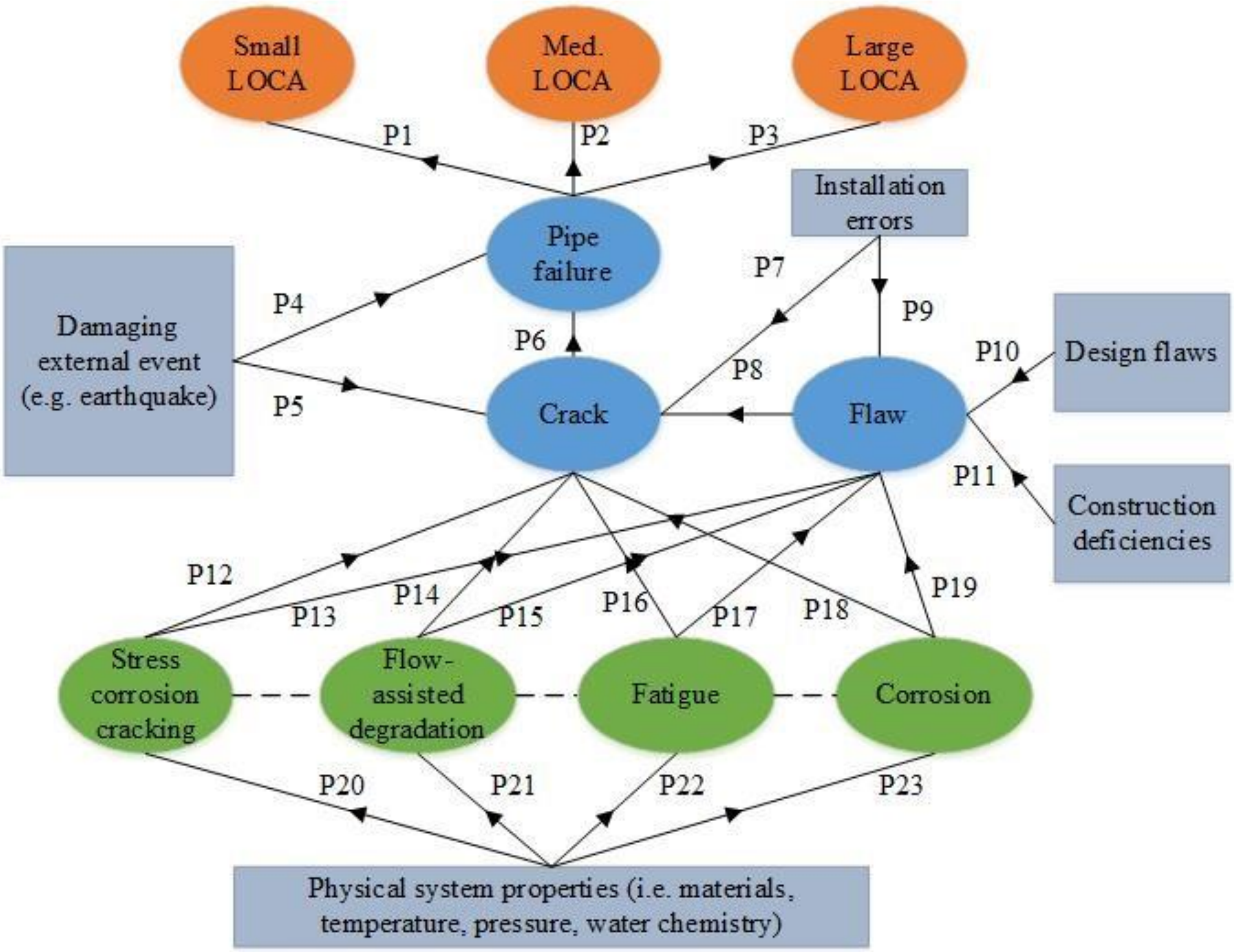

Figure 4.3 High Level Causal Model for RCS Failures Leading to a LOCA in a PWR

The causal pathways are represented by the black arrows in Figure 4.3. Each causal pathway is labeled with P_i (i.e., P1, P2, …, P23), which represents the degree of influence of the causal factor on the effect (e.g., the influence of each failure mechanism on the flaw/crack progression). The causal pathways in Figure 4.3. demonstrate that the failure mechanisms can lead to the nucleation of flaws in the components of a RCS. These flaws, for this research, are undetectable by conventional non-destructive examination (NDE) methods. Other events, such as design flaws, construction deficiencies, and installation errors may also lead to the nucleation of flaws in RCS components.

Once flaws have nucleated in a RCS component, the damage mechanisms drive the propagation and coalescence of these flaws, which leads to the formation of cracks large enough to be detected by conventional NDE methods. External events (e.g., seismic, flood, installation errors) may cause physical degradation, resulting in cracking of RCS components. Once developed, a crack may propagate until the piping component fails, resulting in a loss of primary coolant. The reactor coolant makeup system is designed to supply the RCS with additional coolant to mitigate the loss of coolant. A LOCA occurs once the loss of coolant rate exceeds the capabilities of the reactor coolant makeup system.

Figure 4.3 shows that the failure mechanisms have a causal relationship with the system properties (e.g., pressure, temperature, material properties, etc.). For example, to occur, SCC requires three factors: material susceptibility, corrosive environment, and a constant tensile stress[26]. Without all three of these factors, SCC will not occur. Once the high-level causal model of the underlying failure mechanisms is established, a more detailed causal model needs to be developed for each of the failure mechanisms. To facilitate communication, the rest of casual modeling development is explained based on the Stress Corrosion Cracking mechanism (SCC), which is a dominant mechanism associated with LOCA in NPPs. However, the Spatio-Temporal Probabilistic methodology and the physics of failure causal models can be applied for any other failure mechanisms (e.g., wear, creep).

A more detailed causal model for SCC is presented in the right side of Figure 4.2. A two-stage process SCC model proposed by Wu [3] is used for the development of SCC causal model in this thesis. The SCC models, developed by Wu[27], are shown in Equations (4.1)- (4.5).

$$CPR = \begin{Bmatrix} CPR_I & \text{for } K < K_{trs} \\ CPR_I(1-x) + CPR_{II}(x) & \text{for } K \le K < K_{tre} \\ CPR_{II} & \text{for } K \ge K_{tre} \end{Bmatrix} \tag{4.1}$$

$$CPR_I = C_I \cdot \exp\left[\frac{Q}{R}\left(\frac{1}{T} - \frac{1}{T_{ref}}\right)\right] \cdot \left[\sigma_{ys}\right]^{m_I} \cdot \left[K - K_{th}\right]^{n_I} \tag{4.2}$$

$$CPR_{II} = C_{II} \cdot \exp\left[\frac{Q}{R}\left(\frac{1}{T} - \frac{1}{T_{ref}}\right)\right] \cdot \left[pH\right]^{\beta_{II}} \cdot \left[\sigma_{ys}\right]^{m_{II}} \cdot \left[K - K_{th}\right]^{n_{II}} \tag{4.3}$$

$$K = \sigma_{applied} \cdot \sqrt{\pi \cdot a} \tag{4.4}$$

$$x = \frac{K - K_{trs}}{K_{tre} - K_{trs}} \tag{4.5}$$

where: *CPR*- linearly combined crack propagation rate, CPR_I- crack propagation rate for Stage I crack propagation, CPR_{II}- crack propagation rate for Stage II crack propagation, *K*- stress intensity factor (SIF), defined by Equation (4.4) where $\sigma_{applied}$ – total effective stress on the material, and *a*- depth of crack, K_{trs}- approximate SIF at the beginning of the Stage I to Stage II transition, K_{tre}- approximate SIF at the end of the Stage I to Stage II transition, *x* - transition ratio defined by Equation(4.5), *Q*- activation energy (130 kJ/mol for alloy 600[28, 29]), *R*- universal gas constant (8.314E-3 kJ/mol-K), *T*- operating temperature, T_{ref}- reference temperature (588 K), *pH*- pH of the bulk environment, σ_{ys} – material yield strength, K_{th}- threshold SIF (9MPa√m), and C_I, C_{II}, m_I, m_{II}, n_I, n_{II}, β_{II} are empirical model parameters used to fit the SCC propagation model to data. A summary of the model parameters can be found in Table 4.1.

Table 4.1 Parameters of SCC Two-stage Model Developed by Wu[27]

CPR	linearly combined crack propagation rate (m/s)
CPR_I	crack propagation rate for Stage I crack propagation (m/s)
CPR_{II}	crack propagation rate for Stage II crack propagation (m/s)
K	stress intensity factor (SIF) (MPa√m)
K_{trs}	approximate SIF at beginning of Stage I to Stage II transition (MPa√m)
K_{tre}	approximate SIF at end of Stage I to Stage II transition (MPa√m)
x	transition ratio
Q	activation energy for SCC (130 kJ/mol for alloy 600)
R	universal gas constant (8.314E-3 kJ/mol-K)
T	operating temperature (K)
T_{ref}	reference temperature (588K)
pH	pH of the bulk environment
σ_{ys}	material yield strength (MPa)
K_{th}	threshold SIF (9MPa√m)
C,n,m,β	empirical model parameters
$\sigma_{applied}$	total effective stress on the component (MPa)
a	crack depth (m)

As mentioned above, the target node of the SCC causal model is the "transition time between two states", which refers to the yellow node at the top of the casual model of Figure 4.2. Therefore, for building this SCC causal model, it is required to isolate the time it takes to transition between Markov states via SCC. For the sake of explaining the casual model in Figure 4.2, the propagation time for stage I SCC crack propagation is isolated. CPR_I is a time rate, so Equation (4.2) needs to be integrated so that the propagation time for stage I can be solved for explicitly. To isolate crack length, *a*, Equation (4.4) is substituted into Equation (4.2). a_{th} is defined as the length of the crack the instant it initiates. The integral will be invalid at the instant the crack propagation begins, since $a=a_{th}=0$ at that instant, causing division by zero. Therefore, the integration interval for the crack length will be from a_{th}^+, the crack length immediately after propagation begins, to a_{trs}, the critical crack length when $K=K_{trs}$. Similarly, the time interval of integration will be from $t=0^+$ to $t=t_I$, where t_I is the time it takes a crack to propagate from crack initiation ($t=0^+$) to the threshold at which the transition between Markov states occurs.

Despite attempting to separate this differential equation, it still cannot be integrated analytically. This is due to the dependence of σ_{ys} on the crack length, a. The magnitude of this dependence is not in a quantifiable equation format; therefore, the dependence cannot be analytically manipulated to analytically integrate the differential equation. A numerical method, such as finite difference, is, therefore, required to numerically solve the integral. However, the results of the integral are represented in Equation (4.6).

$$t_I = \frac{fn\left(\sigma_{applied}, a_{trs}, a_{th}, n_I\right)}{C_I \cdot \exp\left[\frac{Q}{R}\left(\frac{1}{T} - \frac{1}{T_{ref}}\right)\right] \cdot \left[\sigma_{ys}\right]^{m_I}} \tag{4.6}$$

The resulting numerator will be a function of $\sigma_{applied}$, a_{trs}, a_{th}, n_I. Now that t_I has been approximately solved, using a placeholder for the function in the numerator, it is clear to identify the "primary-level" causal factors (i.e., the blue factors in the casual model of Figure 4.2) that affect the time it takes for a crack to propagate under stage I SCC. This helps the development of the causal factors for SCC stage I crack propagation time in Figure 4.2. In this casual model, the yellow node at the top of the model is the target node, t_I, which is the unknown of interest. The blue nodes immediately leading to the target node are the "primary-level" causal factors, which have a direct effect on the target node. The relationship between the "primary-level" causal factors and the target node can be explicitly seen in the result of the integration of the equation for CPR_I, Equation (4.6).

The green-colored nodes in the casual model of Figure 4.2 represent the "secondary-level" causal factors. The "secondary-level" causal factors have a direct effect on the "primary-level" causal factors. The figure shows that the externally applied stress and the residual stress nodes have an immediate causal relationship to the total effective stress node. This relationship is simply the contribution of all external stresses applied to a component in addition to all the internal, or residual stresses applied to each component. Figure 4.2 also shows that the material composition node has a direct causal relationship to the activation energy node, the material strength node, and the critical crack length at the end of the stage I propagation node. All three of these "primary-level" nodes are inherently dependent on the material composition, as different compositions have varying material properties. Activation energy and material strength are inherently material properties. The critical crack length node at the end of the SCC stage I crack propagation is also material dependent, because different materials are able to handle varying amounts of stress due to their different tensile strengths[30]. The manufacturing/ fabrication process node has a causal relationship to material strength and residual stress nodes. This results from the microstructural changes in the material during fabrication[31].

The orange and white nodes in the casual model of Figure 4.2 represent the "root" causal factors. The installation/ welding process node affects the residual stresses inside a component, because flaws can form in the microstructure of the material due to the heating applied during welding[31]. The weight of the coolant flowing through a component, as well as the weight of the component itself, result in a force, and ultimately stress, on the component due to gravity. Pipes connected to other pipes or components in the RCS also need to be supported. Often, adjacent pipes will be supported by a component in the RCS, which results in additional stress on the component. Finally, the operating pressure of the coolant flowing through the component exerts a pressure force on the component, as the component must contain the internal pressure[30].

The Data-Theoretic methodology is required to quantify all levels of this causal model and that is the scope of future research; however, in this research the focus is only on the casual relationships between the primary-level factors (the blue factors in the casual model of Figure 4.2) and the target node (the transition time estimated from equation (4.6)). Equation (4.6) cannot be solved analytically. Therefore, to isolate the SCC propagation time required to transition between Markov states, a SCC propagation simulation technique is required to numerically estimate the time. The structure of this simulation combined with uncertainty propagation is explained in the next section (Section 4.1.2.2).

4.1.2.2 TASK #2.2: PROPAGATING UNCERTAINTIES IN PHYSICS OF FAILURE CAUSAL MODELS

After the development of the physics of failure causal models, the next step is to propagate the uncertainties to generate the Probabilistic Physic of Failure (PPoF) models and to develop a probabilistic estimation of "transition time between two states". This section explains this process in the scope of primary-level causal factors (i.e. blue factors in the causal model of Figure 4.2) of SCC model.

To numerically solve equation (4.6), a simulation process is developed along with sampling to take care of uncertainties. Using Monte Carlo sampling, the uncertainty in the model parameters can be incorporated. Sampling from the input distributions allows for the incorporation of all the possible values in each of the distributions to be incorporated into the results. Therefore, the output distribution of failure or state transition times includes the total uncertainty in the quantity of concern. The results of the simulations can be used in Section 4.1.2.3 to quantify the transition rates between the Markov states. The SCC propagation simulation procedure has the following main steps:

1. Sample from the SCC model parameter uncertainty distributions.
2. Sample from the initial crack length distribution, sample from the aspect ratio uncertainty distribution, and calculate the initial crack depth.
3. Check initial conditions against threshold criteria for the Flaw, Leak, and Rupture states. If the sample is found to be in the New, Leak, or Rupture states, reject the sample and repeat the second step. This step serves as a method of truncating the initial crack distribution to only allow samples that are initially in the Flaw state, as transitions of components that were initially in the Flaw state are the concern of the simulation.
4. Iteratively integrate the crack length and crack depth until one of three possible outcomes occurs: transition into the Leak state, transition into the Rupture state, or maximum time limit is reached. The maximum time limit for the simulation is set as 60 years, which represents an extended lifetime for an NPP.
5. If the sample transitions into the Rupture state, the time of transition from the Flaw to the Rupture state is recorded and the next sample is simulated. If the sample transitions from the Flaw state to the Leak state, the time of transition is also recorded. However, the simulation continues from the Leak state with a new time counter to simulate when the sample transitions from the Leak to the Rupture state. The SCC propagation model is still used along with the aspect ratio to propagate the crack length, but the crack depth is held constant once the Leak state has been reached. Crack depth is held constant since once a SCC crack propagates 100% through the thickness of the component, the depth cannot continue to increase. If the sample transitions from the Leak to the Rupture state, the time of the transition from entering the Leak state until transitioning into the Rupture state is recorded.

Chapter 5 demonstrates how this process is developed in a MATLAB code to estimate the transitions rates of degradation in the case study.

4.1.2.3 TASK #2.3: CALCULATING TRANSITION RATES OF DEGRADATION BASED ON THE OUTPUT OF PROBABILISTIC PHYSICS OF FAILURE MODELS

This section focuses on the calculation of the transition rates ϕ, λ, ρ, and γ, based on the result of probabilistic simulation from Section 4.1.2.2, which is the probabilistic estimation of "transition time between two states". Using the simulation explained in the previous section and sampling, the probability that a component in the Flaw state will transition to the Leak state is calculated by dividing the number of transitions from the Flaw state to the Leak state by the total number of samples. The probability that a component in the Flaw state will transition directly to the Rupture state is calculated by dividing the number of transitions from the Flaw to the Rupture state by the total number of samples. To have a reliable number of samples for this estimation, a "convergence study" is required. A discussion regarding the convergence of the results for the case study is provided in Chapter 5.

The transition rates for a Markov model are rates of probability transition. This means the rate at which the probability that a component is in each state is changing or "flowing" into another state. Therefore, the time it takes for each sample to transition from the Flaw state to either the Leak or Rupture state is stored. The mean of the time-from-flaw-to-leak data (MTFL) is calculated. Then to find the rate at which probability transitions from the Flaw to the Leak state, the inverse of the MTFL is multiplied by the probability that a component transitions from the Flaw state to the Leak state, as shown in Equation (4.7). For the same reason, to find the rate at which probability transitions from the Flaw to the Rupture state, the inverse of the mean of the time-from-flaw-to-rupture (MTFR) is multiplied by the probability that a component transitions from the Flaw state to the Rupture state, as shown in Equation (4.8).

Using the simulation explained in Section 4.1.2.2 and sampling, the probability that a component will transition from the Leak state to the Rupture state is calculated by dividing the total number of transitions from the Leak to the Rupture state by the total number of transitions from the Flaw to the Leak state. For each sample that transitioned from the Flaw state to the Leak state, a separate time counter is implemented in the simulation process. Therefore, for each sample that transitioned from the Leak to the Rupture state, a time-from-Leak-to-Rupture is recorded. The mean of the time-from-Leak-to-Rupture (MTLR) is calculated. To find the rate at which probability transitions from the Leak state to the Rupture state, the inverse of the MTLR is then multiplied by the probability that a component in the Leak state transitions into the Rupture state, as shown in Equation (4.9).

$$\lambda = \left(\frac{\#\ \text{Transitions}\ (Flaw \rightarrow Leak)}{\text{Total}\ \#\ \text{Samples}} \right) * \left(\frac{1}{MTFL} \right) \tag{4.7}$$

$$\gamma = \left(\frac{\#\ \text{Transitions}\ (Flaw \rightarrow Rupture)}{\text{Total}\ \#\ \text{Samples}} \right) * \left(\frac{1}{MTFR} \right) \tag{4.8}$$

$$\rho = \left(\frac{\#\ \text{Transitions}\ (Leak \rightarrow Rupture)}{\text{Total}\ \#\ \text{Transitions}\ (Flaw \rightarrow Leak)} \right) * \left(\frac{1}{MTLR} \right) \tag{4.9}$$

The same method is used for estimation of transition rate from New to flaw that is explained in Chapter 5 where the New states is clarified. Chapter 5 further explains the implementations of these equations in the context of the case study.

4.1.3 MODELING AND QUANTIFICATION OF THE TRANSITION RATES OF REPAIR

Transition rates of repair represent the possible pathways by which a component can move to a less degraded state. In Figure 4.2, the transition rates of repair are represented by ω and μ, which represent the pathways of transition from the "Flaw" state to the "New" state and the "Leak" state to the "New" state respectively. The quantification of the transition rates of repair provides the explicit pathway for including the effects of the maintenance mechanisms. Like the causal model development for degradation mechanisms, causal models should be developed for the maintenance mechanisms. These causal models could include the probability that a component will be inspected. For some components in certain states of degradation, inspection may never occur. For example, a component that is in the "Flaw" state may never be inspected. Therefore, such a component would not be repaired from the "Flaw" state to the "New" state. In other words, for the model in Figure 4.2, ω=0. Additionally, the causal models could include the probability that degradation would be detected if the component was inspected. Probability of detection could depend on many causal factors such as the training of the maintenance team or the quality of the inspection tools. These causal models of the maintenance mechanisms should be spatio-temporal to account for the variation that may occur in the probability of repair based on a component's location or age. Interested readers may refer to Mohaghegh-Ahmadabadi[32] for more information regarding the development of a maintenance model. Additionally, readers may refer to Pence et al.[25] for more information regarding modeling of the quality of training within organizations. In the scope of this research, solely data-driven approaches are used for transition rates of repair. Future research is required to use model-based approaches for transition rates of repair.

4.1.4 DEVELOPING THE TIME-DEPENDENT DISTRIBUTIONS OF STATE PROBABILITIES

For each Markov state of degradation, a differential equation which represents the rate of change of the probability that a component is in each state at any given time can be set-up. The resulting series of coupled differential equations can be solved to find the time-dependent distribution of the state probabilities. When solving a Markov model, it is common to assume that the transition rates are constant values. Using this assumption, Equations (4-10) -(4-14) are developed for the Markov model shown in Figure 4.2.

$$\frac{dNew(t)}{dt} = (\omega \cdot Flaw(t)) + (\mu \cdot Leak(t)) - (\varphi \cdot New(t)) \tag{4-10}$$

$$\frac{dFlaw(t)}{dt} = (\varphi \cdot New(t)) - (\omega \cdot Flaw(t)) - (\gamma \cdot Flaw(t)) - (\lambda \cdot Flaw(t)) \tag{4-11}$$

$$\frac{dLeak(t)}{dt} = (\lambda \cdot Flaw(t)) - (\mu \cdot Leak(t)) - (\rho \cdot Leak(t)) \tag{4-12}$$

$$\frac{dRupture(t)}{dt} = (\rho \cdot Leak(t)) + (\gamma \cdot Flaw(t)) \tag{4-13}$$

$$New(t) + Flaw(t) + Leak(t) + Rupture(t) = 1 \tag{4-14}$$

where: New(t), Flaw(t), Leak(t), and Rupture(t) represent the probability that a component is in each state at a given time, t, and ω, μ, ϕ, γ, λ, and ρ represent the transition rates from Figure 4.2. These differential equations can be written in vector form as:

$$\frac{d\mathbf{X}}{dt} = \mathbf{AX} \tag{4-15}$$

where:

$$\mathbf{X}(t) = \begin{pmatrix} New(t) \\ Flaw(t) \\ Leak(t) \\ Rupture(t) \end{pmatrix} \tag{4-16}$$

$$\mathbf{A} = \begin{pmatrix} -\phi & \omega & \mu & 0 \\ \phi & -(\omega+\gamma+\lambda) & 0 & 0 \\ 0 & \lambda & -(\mu+\rho) & 0 \\ 0 & \gamma & \rho & 0 \end{pmatrix} \tag{4-17}$$

Since the Markov states of degradation are mutually exclusive, the summation of the probabilities of each state at any given time must be equal to 1, as shown by the condition in Equation (4-14). The diagonal elements of the matrix **A** represent the change in probability that is leaving each state. The final diagonal element of matrix **A** is equal to zero, because this research assumes that the Rupture state cannot be repaired. Therefore, there are no transitions out of the Rupture state and it becomes a probability sink. Each column of matrix **A** adds to zero. This is because probability is conserved. As the probability flows out of one state (represented by the negative elements), it must flow into another Markov state (represented by the positive matrix elements). The quantification results for the time-dependent distribution of state probabilities for the case study can be found in Chapter 5.

REFERENCES

1. Fleming, K., B. Lydell, and D. Chrun. *Development of LOCA Initiating Event Frequencies for South Texas Project GSI-191*, 2011.

2. Tregoning, R., L. Abramson, and P. Scott. *Estimating Loss-of-Coolant Accident (LOCA) Frequencies Through the Elicitation Process*, NUREG-1829, 2008.

3. Kijima, M. and U. Sumita, *A Useful Generalization of Renewal Theory: Counting Processes Governed by Non-Negative Markovian Increments.* Journal of Applied Probability, 1986. **23**(1): p. 71-88.

4. Kijima, M., H. Morimura, and Y. Suzuki, *Periodical Replacement Problem Without Assuming Minimal Repair.* European Journal of Operational Research, 1988. **37**: p. 194-203.

5. Kijima, M., *Some Results for Repairable Systems with General Repair.* Journal of Applied Probability, 1989. **26**(1): p. 89-102.

6. Modarres, M., M. Kaminskiy, and V. Krivtsov, *System Reliability Analysis*, in *Reliability Engineering and Risk Analysis: A Practical Guide*. 2010, CRC Press: Boca Raton, FL. p. 153.

7. Fleming, K.N., *Markov models for evaluating risk-informed in-service inspection strategies for nuclear power plant piping systems.* Reliability Engineering & System Safety, 2004. **83**(1): p. 27-45.

8. Gosselin, S. and K. Fleming. *Evaluation of pipe failure potential via degradation mechanism assessment*. in *International Conference on Nuclear Engineering*. 1997. Nice, France.

9. Fleming, K., S. Gosselin, and J. Mitman. *Application of markov models and service data to evaluate the influence of inspection on pipe rupture frequencies*. in *Pressure Vessels Piping Conference*. 1999. Boston, MA: ASME.

10. Fleming, K. and J. Mitman. *Quantitative assessment of a risk informed inspection strategy for BWR weld overlays*. in *International Conference on Nuclear Engineering*. 2000. Baltimore, MD.

11. Mikschl, T. and K. Fleming. *Piping System Failure Rates and Rupture Frequencies for Use In Risk Informed In-Service Inspection Applications*, TR-111880-NP, 2000.

12. Stone and Webster Engineering Corporation. *Water Hammer Prevention, Mitigation, and Accommodation - volume 1: Plant Water Hammer Experience*, EPRI NP-6766, 1992.

13. Unwin, S., P. Lowry, R. Layton, P. Heasler, and M. Toloczko. *Multi-State Physics Models of Aging Passive Components in Probabilistic Risk Assessment*. in *International Topical Meeting on Probabilistic Safety Assessment and Analysis*. 2008. LaGrange Park, IL: American Nuclear Society.

14. Unwin, S., P. Lowry, and M. Toyooka. *Component Degradation Susceptibilities as the Bases for Modeling Reactor Aging Risk*. in *ASME 2010 Pressure Vessels & Piping Division / K-PVP Conference*. 2010. Bellevue, Washington: ASME.

15. Unwin, S., P. Lowry, and M. Toyooka, *Reliability models of Aging Passive Components Informed by Materials Degradation Metrics to Support Long-Term Reactor Operations.* Nuclear Science and Engineering, 2012. **171**: p. 69-77.

16. Unwin, S., P. Lowry, M. Toyooka, and B. Ford. *Degradation Susceptibility Metrics as the Bases for Bayesian Models of Aging Passive Components and Long-term Reactor*

Risk. in *ASME 2011 Pressure Vessels & Piping Division Conference*. 2011. Baltimore, Maryland: ASME.

17. Unwin, S., P. Lowry, and M. Toyooka. *A Methodology Supporting the Risk-Informed Management of Materials Degradation*. in *American Nuclear Society Winter Meeting and Nuclear Technology Expo*. 2011. LaGrange Park, IL: American Nuclear Society.
18. Unwin, S., R. Layton, K. Johnson, and P. Lowry, *Physics-Based Multi-State Models of Passive Component Degradation for the R7 Reactor Simulation Environment.* 11th International Probabilistic Safety Assessment and Management Conference and the Annual European Safety and Reliability Conference 2012, 2012. **3**: p. 1761-1770.
19. Unwin, S., K. Johnson, R. Layton, P. Lowry, S. Sanborn, and M. Toloczko. *Physics-Based Stress Corosion Cracking Component Reliability Model cast in an R7-Compatible Cumulative Damage Framework*, PNNL-20596, 2011.
20. Modarres, M., *Risk Analysis in Engineering: Techniques, Tools, and Trends*. 2006, Boca Rator, FL: Taylor & Francis Group, LLC.
21. Chookah, M., M. Nuhi, and M. Modarres. *Assessment of the Integrity of Oil Pipelines Subject to Corrosion Fatigue and Pitting Corrosion*. in *3rd International Conference on Integrity, Reliability and Failure*. 2009. Porto, Portugal.
22. Chatterjee, K. and M. Modarres, *A Probabilistic Physics-of-Failure Approach to Prediction of Steam Generator Tube Rupture Frequency*, in *Nuclear Science and Engineering*. 2012. p. 136 - 150.
23. Mohaghegh, Z., M. Modarres, and A. Christou. *Physics-Based Common Cause Failure Modeling in Probabilistic Risk Analysis: A Mechanistic Perspective*. in *ASME Power Conference*. 2011. Denver, Colorado, USA: ASME.

24. O’Shea, N., J. Pence, Z. Mohaghegh, and E. Kee. *Physics of Failure, Predictive Modeling & Data Analytics for LOCA Frequency*. in *Annual Reliability andd Maintainability Symposium*. 2015. Palm Harbor, FL, USA: IEEE.

25. Pence, J., Z. Mohaghegh, C. Ostroff, V. Dang, E. Kee, R. Hubenak, and M. Billings. *Quantifying Organizational Factors in Human Reliability Analysis Using the Big Data-Theoretic Algorithm*. in *International Topical Meeting on Probabilistic Safety Assessment and Analysis*. 2015. Sun Valley, ID, USA: American Nuclear Society.

26. Davis, J., *Corrosion - Understanding the Basics*. 2000, Materials Park, Ohio, USA: ASM International.

27. Wu, G., *A Probabilistic-Mechanistic Approach to Modeling Stress Corrosion Cracking Propagation in Alloy 600 Components with Applications, Master of Science,* from the *Mechanical Engineering, 2007.* University of Maryland, College Park.

28. Hicking, J., A. McIlree, and R. Pathania. *Crack Growth Rates for Evaluating Primary Water Stress Corrosion Cracking (PWSCC) of Thick-Wall Alloy 600 Material (MRP-55),* ML023010510, 2002.

29. Scott, P. and P. Combrade. *On the Mechanism of Stress Corrosion Crack Initiation and Growth in Alloy 600 Exposed to PWR Water*. in *International Conference on Environmental Degradation of Materials in Nuclear Systems*. 2003.

30. Ashby, M. and D. Jones, *Engineering Materials 1: An Introduction to Properties, Applications and Design*. Vol. 3. 2005, Burlington, MA: Butterworth-Heinemann.

31. Ashby, M. and D. Jones, *Engineering Materials 2: An Introduction to Microstructures, Processing and Design*. Vol. Third. 2005, Burlington, MA: Butterworth-Heinemann.

32. Mohaghegh-Ahmadabadi, Z., *On the Theoretical Foundations and Principles of Organizational Safety Risk Analysis*, *Doctor of Philosophy*, from the *Department of Mechanical Engineering*, *2007.* University of Maryland, College Park.

CHAPTER 5 : APPLICATION OF SPATIO-TEMPORAL PROBABILISTIC METHODOLOGY FOR STRESS CORROSION CRACKING IN PWR STEAM GENERATOR TUBES

This chapter relates to Step #5 in the roadmap of the research presented in Figure 5.1. It focuses on the implementation of the Spatio-Temporal Probabilistic methodology that is introduced in Chapter 4. The case study in this chapter compares the time-dependent rupture probabilities, due to Stress Corrosion Cracking (SCC), for the expansion-transition region of a steam generator tube fabricated from alloy 690 and stainless steel (SS).

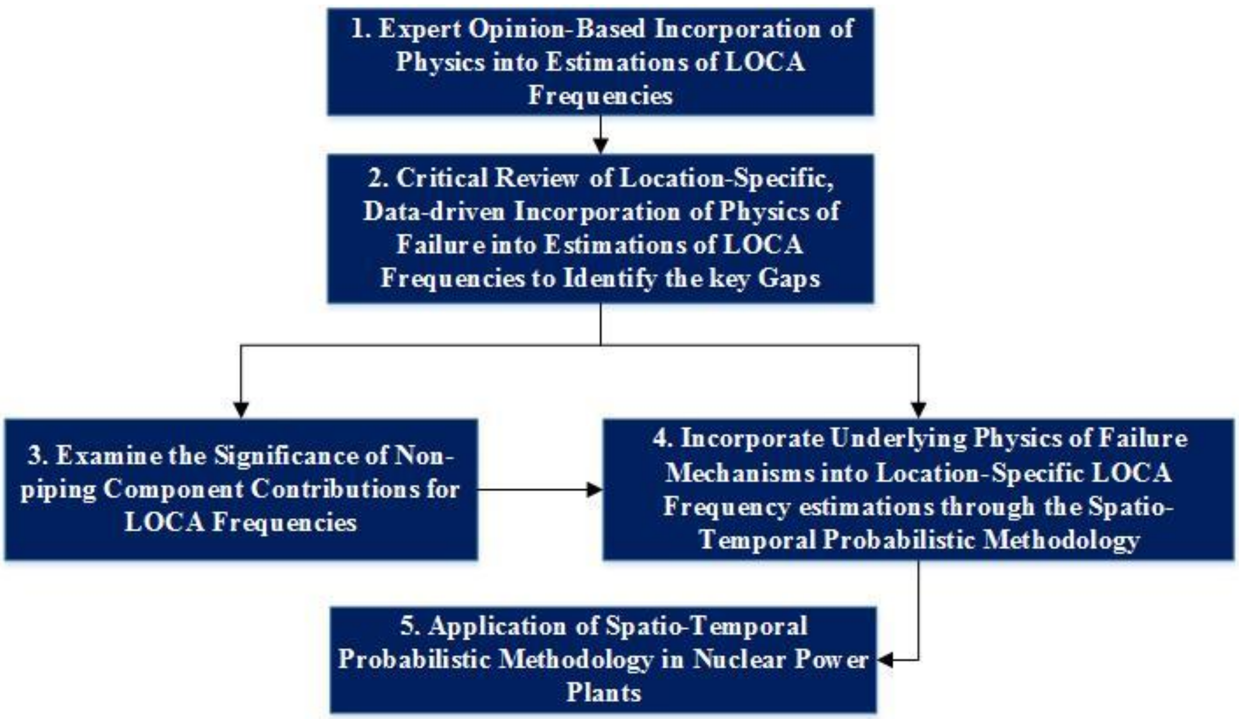

Figure 5.1 Roadmap of the Research

SCC was selected for the case study of this research, because it has been identified as a dominant failure mechanism in the RCSs of NPPs [1, 2]. Tregoning et al. determined that steam generator tube ruptures (with resultant leak rates greater than 100 gallons per minute) occurred at a frequency of 3.5E-03 per calendar year, which provides a significant contribution to the estimation of LOCA frequencies, since it only takes one SGTR to result in a Category 1 LOCA[1]. Therefore, the steam generator tubes were investigated for this case study. Additionally, Wu identified that the expansion transition region of every steam generator tube is affected by SCC[3]. This case study will compare two expansion transition steam generator tubes, with one fabricated from alloy 690 and the other fabricated from SS. While the only difference for this case study is the selection of material, it is important to note that this methodology could be applied to compare any component fabricated from any material, at any location, experiencing any set of operating conditions, that experiences underlying degradation and repair mechanisms.

The following sections demonstrates the case study, implementing the four key tasks of the Spatio-Temporal Probabilistic methodology, listed as follows:

- <u>Task #1:</u> Defining Markov States of Degradation
- <u>Task #2:</u> Modeling and Quantification of the Transition Rates of Degradation
- <u>Task #3:</u> Modeling and Quantification of the Transition Rates of Repair
- <u>Task #4:</u> Developing the Time-dependent Distributions of State Probabilities

Although the tasks in this case study are explained based on the Stress Corrosion Cracking mechanism (SCC), which is a dominant mechanism associated with LOCA in NPPs, the Spatio-Temporal Probabilistic methodology can be applied for any other failure mechanisms (e.g., wear, creep) and for other industry applications than NPPs (e.g., oil and gas).

5.1 TASK #1: DEFINING MARKOV STATES OF DEGRADATION IN THE CASE STUDY

As explained in Section 4.1.1., the first task in the Markov modeling approach is to define a set of discrete states to depict the states of degradation. A four state Markov model (presented in the left side of Figure 5.2) has been selected for modeling a component exposed to SCC. The four states are New, Flaw, Leak, and Rupture, listed in order of increasing degradation.

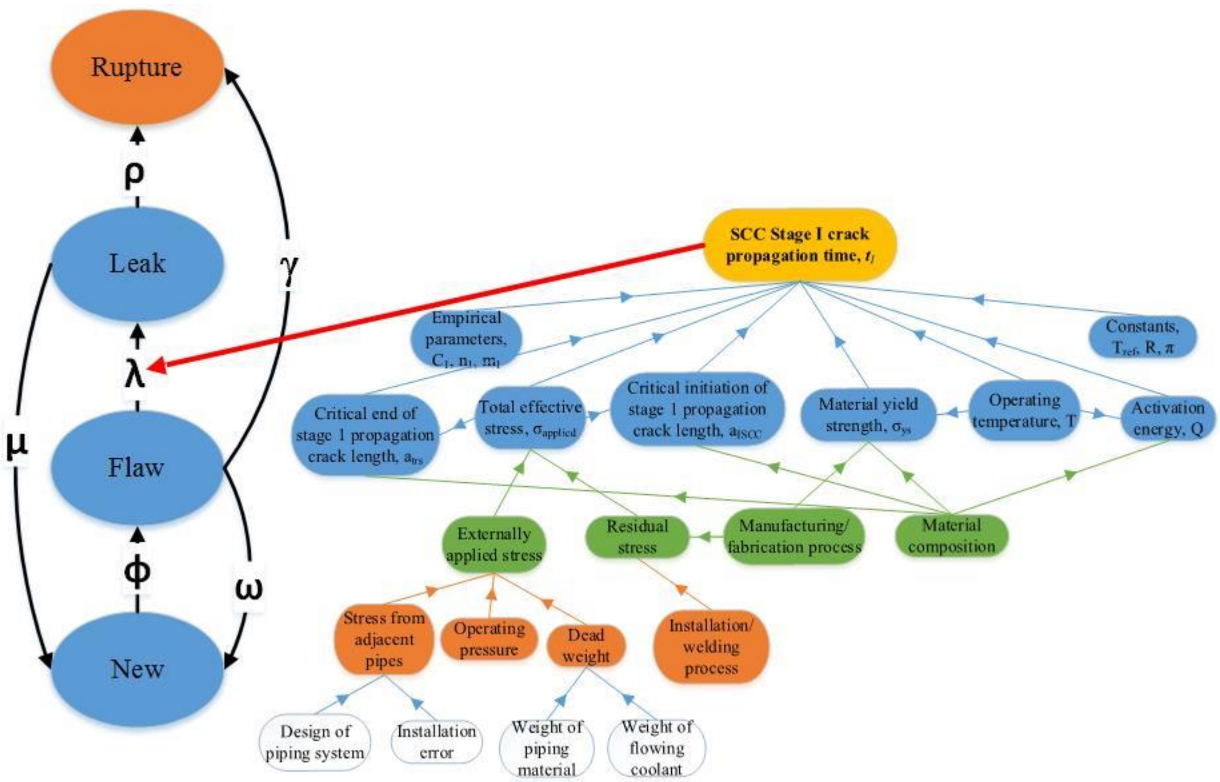

Figure 5.2 Integration of the Markov Modeling Technique with Probabilistic Physics of Failure Models in the Spatio-Temporal Probabilistic Methodology for Location-Specific LOCA Frequency Estimations

5.1.1 DEFINING RUPTURE STATES FOR ALLOY 690 & STAINLESS STEEL

The primary concern for this case study is to estimate the probability that a component will burst, and enable enough coolant to escape from the RCS to cause a LOCA to occur.

Therefore, the final state of the Markov model is defined as the Rupture state. The characteristic threshold of the Rupture state is the occurrence of the burst phenomenon. The burst phenomenon occurs when the internal pressure of the primary coolant exceeds the capability of the component to withstand the coolant pressure. The pressure at which the component cannot withstand the internal coolant pressure is the burst pressure. As a component is degraded by a failure mechanism such as SCC, the burst pressure decreases. There are models for quantifying burst pressures available in literature. For the alloy 690 steam generator tubes, two models for axial crack growth were selected. This research focuses exclusively on axial crack growth and does not cover the potential for circumferential crack growth. The American Society of Mechanical Engineers (ASME) has developed equations for the burst pressure of tubes as a function of axial crack sizes in steam generator tube walls, as shown in Equation (5.1)[4].

$$\Delta p = \left(\frac{t}{R}\right)\left(\frac{3S_m}{SF}\right)\left(\frac{\frac{t}{a}-1}{\frac{t}{a}-\frac{1}{m_1}}\right) \tag{5.1}$$

where: Δp is the pressure differential across the tube, *R* is the tube radius, *t* is the tube thickness, *SF* is the safety factor (taken to be equal to 1 in this analysis), *a* is the depth of corrosion of the largest corrosion defect in the component, S_m is the flow stress defined by Equation (5.2), and m_1 is defined by Equation (5.3).

$$S_m = \frac{1}{2}\left(S_y + S_u\right) \tag{5.2}$$

where: S_y is the yield strength of the component and S_u is the ultimate tensile stress of the component.

$$m_1 = \sqrt{1 + 1.61\frac{L^2}{4Rt}} \tag{5.3}$$

where: R is the tube radius, t is the component thickness, and L is the length of the corrosion defect. Another analytical model for burst pressure of steam generator tubes that contain a single dominant crack was provided in NUREG-6575[5], as shown by Equations (5.4)-(5.7)

$$P_b = S_m Log\left(1+\frac{t}{R}\right) \tag{5.4}$$

where: P_b is the failure pressure for defect-free straight tubing, S_m is the flow stress as defined in Equation (5.2), t is the thickness of the component, and R is the radius of the component.

$$P_{cr} = \frac{P_b}{m_2} \tag{5.5}$$

where: P_{cr} is the pressure necessary to cause unstable ductile failure of tubing with a through-wall axial crack and m_2 is defined by Equation (5.6).

$$m_2 = 0.614 + 0.481\frac{1.82c}{\sqrt{R_m t}} + 0.386\exp\left(-1.25\frac{1.82c}{\sqrt{R_m t}}\right) \tag{5.6}$$

where: c is the half of the axial crack length, t is the thickness of the component, and R_m the mean radius of the tube, defined by Equation (5.7).

$$R_m = R + \left(\frac{t}{2}\right) \tag{5.7}$$

where: R is the radius of the component and t is the thickness of the component. A conservative assumption was made to use both rupture pressure models as characteristic thresholds for the Rupture state of the alloy 690 steam generator tube. Therefore, if the pressure inside the component exceeded the burst pressure of either model, the component was considered to have experienced a burst phenomenon and to have moved into the Rupture state.

In the Markov model developed by Vinod[6], two burst pressure models were selected from the oil and gas piping industry: the Modified B31G[7], as shown in Equations (5.8)-(5.11) and the Shell-92 model[8], as shown in Equations (5.12) and (5.13).

$$P_{fB31G} = \frac{2\left(S_y + 68.95\right)t}{D}\left(\frac{1 - 0.85\frac{a}{t}}{1 - 0.85\frac{a}{t}M^{-1}}\right) \tag{5.8}$$

where: P_{fB31G} is the maximum pressure a component can hold before rupturing using the B31G model, S_y is the yield strength of the component, t is the thickness of the component, a is the depth of the corrosion defect, D is the outside diameter of the component as defined in Equation (5.9), and M is defined in Equation (5.10).

$$D = 2 * (R + t) \tag{5.9}$$

where: D is the outside diameter of the component, R is the inner diameter of the component, and t is the thickness of the component.

$$\begin{aligned} &\text{If G} \leq 50\text{: M} = \sqrt{1 + 0.6275\text{G} - 0.003375G^2} \\ &\text{If G} > 50\text{: M} = 0.032\text{G} + 3.3 \end{aligned} \tag{5.10}$$

where: G is defined by Equation (5.11).

$$G = \frac{c^4}{Dt} \tag{5.11}$$

where: c is half of the axial crack length, D is the outside diameter of the pipe as defined in Equation (5.9), and t is the thickness of the component.

$$P_{f92} = \frac{1.8S_y t}{D}\left(\frac{1 - \frac{a}{t}}{1 - \frac{a}{t}M^{-1}}\right) \tag{5.12}$$

where: P_{f92} is the maximum pressure a component can withhold before rupturing using the Shell-92 model, S_y is the ultimate tensile strength of the material, t is the thickness of the material, D is the outside diameter of the material as defined in Equation (5.9), a is the depth of the corrosion defect, and M is defined in Equation (5.13).

$$M = \sqrt{1 + 0.805\frac{L^2}{Dt}} \tag{5.13}$$

where: L is the axial length of the corrosion defect, D is the outside diameter of the material as defined in Equation (5.10), and t is the thickness of the material. Vinod's two burst pressure models were adopted in this research for modeling the stainless steel (SS) component burst pressures. Again, a conservative approach was applied for modeling the burst pressure for SS components by utilizing both burst models simultaneously. Therefore, if the operating pressure inside the SS component exceeded the burst pressure calculated by either the B31G or Shell-92 model, the component was considered to have experienced a burst phenomenon and to have moved into the Rupture state.

5.1.2 DEFINING LEAK STATES FOR ALLOY 690 & STAINLESS STEEL

The Leak state is the second most-degraded state in the Markov model. A component is defined as belonging in the Leak state when it has a corrosion defect with a depth equal to the thickness of the component, which may be referred to as a 100% through-wall crack. This means that the coolant flowing inside the component has an unimpeded path to escape from the component. Therefore, any component that has a 100% through-wall crack, but has not experienced a burst phenomenon is defined as being in the Leak state.

For alloy 690 components, the Leak state can be reached when a corrosion crack depth in the component propagates 100% through the thickness of the component wall. Additionally, when the internal pressure of the coolant exceeds the capability of a small “ligament” of remaining component material, a ligament burst phenomenon occurs. A “ligament” of component material occurs when a partially-through (not 100% through-wall) crack causes only a small portion of the material to remain. This small “ligament” of material has a reduced capability to withstand the pressure of the internal coolant. Once the internal pressure of the coolant exceeds the capability of the ligament to hold the coolant, the ligament will rapidly fail, forming a 100% through-wall crack. The pressure at which this rapid failure of the ligament will occur is called the ligament pressure. This research selected a model for ligament pressure provided in NUREG-6575, as shown in Equation (5.14)[5].

$$P_{sc} = \frac{P_b}{\dfrac{1-\left(1+0.9\left(\dfrac{a}{t}\right)^2\left(1-\dfrac{1}{m_2}\right)\right)\dfrac{a}{m_2 t}}{1-\dfrac{a}{t}}} \tag{5.14}$$

where: P_{sc} the pressure required to fail the remaining ligament of a component that has a part-way through wall axial crack, P_b is the failure pressure for defect-free tubing, a is the depth of the corrosion defect, t is the component thickness, and m_2 is defined by Equation (5.6). If the internal coolant pressure exceeds the remaining ligament pressure of a component, but does not exceed the burst pressure of the component, the ligament section will fail rapidly without the component bursting. Therefore, the component will move into the Leak state. A ligament pressure model was not selected for SS components, because the SCC model development for SS in NUREG-6986[9] did not indicate that such behavior also occurred in SS materials. Therefore, SS components only transition into the Leak state when the crack depth propagates 100% through-wall.

5.1.3 DEFINING FLAW STATES FOR ALLOY 690 & STAINLESS STEEL

The Flaw state is the second least-degraded state in the four state Markov model developed for this case study. As explained in Section 4.1.1, Markov states should be defined in a way to be aligned with the associated mechanisms acting on the component. SCC does not begin propagating in a material immediately upon the birth of a defect. SCC begins propagation in a component once an initial crack is formed from a defect in the component. There are many ways that a defect can form in a material such as construction deficiencies, external damage, or failure mechanisms. Pitting is often the precursor to SCC due to its combination of local stress concentration and solution chemistry[10, 11]. When pitting is the precursor to SCC, the fundamental steps in the overall process of crack development include: pit initiation, pit growth, transition from pit to crack, and then crack growth[12]. This research adopts the criterion developed by Kondo[13], which says that a pit transitions to crack once the SCC growth rate exceeds the pit growth rate, representing a threshold driving force. Therefore, the threshold criteria for the Flaw state are dependent on the selection of both SCC propagation models and pit growth rate models. Details on SCC propagation and pit growth models will be further explored in Section 5.2.3.

5.1.4 DEFINING NEW STATES FOR ALLOY 690 & STAINLESS STEEL

The least degraded state in the Markov model developed for this case study is the New state. A component is defined to be in the New state if it does not have any defects that satisfy the threshold criteria to enter the Flaw state. A component may not be in perfect condition (i.e., may have pits or defects), but if none of the pits or defects have become cracks, SCC will not propagate, and the component will be in the New state. A summary of all the parameters in the models of the criteria used for the development of the Markov states of degradation for the case study can be found in Table 5.1.

Table 5.1 Summary of Model Parameters Used to Define the States in the Markov Model of the Case Study

Δp	pressure differential across the tube
R	tube inner radius
t	tube thickness
SF	safety factor
a	depth of corrosion
S_m	flow stress
S_y	yield strength of component
S_u	ultimate tensile stress of component
L	axial length of corrosion defect
P_b	failure pressure for defect-free straight tubing
P_{cr}	pressure necessary to cause unstable ductile failure of tubing with a through-wall axial crack
c	half of the axial crack length
R_m	mean radius of the tube
P_{sc}	pressure required to fail the remaining ligament of a component that has a part-way through wall axial crack
P_{fB31G}	maximum pressure a component can hold before rupturing using the B31G model
D	outside diameter of a component
P_{f92}	maximum pressure a component can withstand before rupturing using the Shell-92 model

5.2 TASK #2: MODELING AND QUANTIFICATION OF TRANSITION RATES OF DEGRADATION FOR ALLOY 690 & STAINLESS STEEL

The transition rates of a Markov model represent the possible pathways by which a component can move from one state to another. These pathways are dictated by the underlying mechanisms acting on the component. Numerically, the transition rates represent the rate of change in the probability that a component occupies a Markov state at a given time. As explained in Section 4.1.2 in Chapter 4, the transition rates of degradation are the explicit pathway for incorporation of the underlying physical failure mechanisms into the Markov model. This section explains the development of transition rates of degradation for the case study, i.e., ϕ, λ, ρ, and γ , which represent the pathways of transition from the "New" state to the "Flaw state, "Flaw" to "Leak", "Leak" to "Rupture", and "Flaw" to "Rupture", respectively in the Markov model in Figure 5.2.

In Section 4.1.2 in Chapter 4, the following sub-tasks are listed for modeling and quantifying transition rates of degradation in the Spatio-Temporal Probabilistic methodology:

- TASK #2.1: Developing and quantifying physics of failure causal models based on the identified failure mechanisms to find the "transition time between two states" as a function of underlying physical causal factor.
- TASK #2.2: Propagating uncertainties in the physics of failure causal models to make the Probabilistic Physic of Failure (PPoF) models and to develop a probabilistic estimation of "transition time between two states".
- TASK #2.3: Calculating transition rates of degradation based on the output of PPoF models, i.e., the estimated probabilistic "transition time between two states".
- TASK #2.4: Bayesian integration of the estimated transition rate from PPoF (from step 3) and the transition rate from solely data-oriented approaches (e.g., Fleming [14-17]) to combine different sources of information, i.e., information from historical data and from physics-based simulations. This step is out of the scope of this research and will be elaborated in future research.

Section 5.2.1 relates to Task 2.1 and the quantification of SCC physics of failure model for Alloy 690 and Stainless Steel. Section 5.2.2 relates to implementation of Task 2.2 and Task 2.3 for estimation of ϕ for the cases of Alloy 690 and Stainless Steel. Section 5.2.3 relates to implementation of Task 2.2 and Task 2.3 for estimations of λ, ρ, and γ for the cases of Alloy 690 and Stainless Steel.

5.2.1 DEVELOPMENT OF STRESS CORROSION CRACKING PROPAGATION EQUATIONS FOR ALLOY 690 & STAINLESS STEEL

As a part of Task #2.1 of the methodology explained in Chapter 4, the Data-Theoretic approach is proposed to manage the quantification of multi-level causal model (e.g., the one presented in Figure 5.2.) and to reduce the scope of the casual network in a scientific way without missing the critical risk factors. However, in this case study, the scope of the causal model is reduced (from the beginning) in a way that only the first level of the causal model in Figure 5.2 (i.e., the blue casual factors in Figure 5.2) is covered. Therefore, this research mainly focuses on implementation of step 1 of the Data-theoretic approach that includes the development and quantification of SCC physics of failure casual model for Alloy 690 and SS. In this research, a two-stage process SCC model proposed by Wu [3] is utilized to develop physics of failure casual model and is quantified by Bayesian regression analysis. Wu's model is developed for alloy 600 and, therefore, the parameters of the model need to be updated for Alloy 690 and SS.

WinBUGS[18], a statistical software that uses Bayesian regression analysis techniques with Markov chain Monte Carlo sampling methods, is used to numerically develop a joint posterior distribution of the parameters[19]. The posterior distribution for the SCC model parameters of the model developed by Wu [3], is as follows:

$$\pi(\theta \mid E) = \frac{L(E \mid \theta)\pi_0(\theta)}{\int L(E \mid \theta)\pi_0(\theta)d\theta} \tag{5.15}$$

where: $\pi(\theta|E)$ is the posterior distribution given the data point E, $L(E|\theta)$ is the likelihood function for regression, and π_0 is the prior distribution for the model parameters, where:

$$\theta = \left[C, n, m, b, s\right] \tag{5.16}$$

$$E = \left[CPR_i, K_i, pH_i, T_i, \sigma_{ys_i}\right] \tag{5.17}$$

Bayesian regression analysis assumes that the likelihood function is used to describe the distribution of model error. Model error is the difference between the data, or evidence, and the best fitted model. Model error is a random variable that can be described by the likelihood function. Wu utilizes an additive error model[20], meaning the difference between each of the values calculated by the best fitted model and the data, or evidence, is assumed to be normally distributed with a mean value of zero. The normally distributed likelihood function used by Wu is defined by:

$$L(E \mid \theta) = \prod_{i=1}^{N} \frac{1}{s\sqrt{2\pi}} e^{-\frac{1}{2}\left(\frac{CPR_{\exp}[i]-CPR_{calc}[i,\theta]}{s}\right)^2} \tag{5.18}$$

where: N is the total number of data points, s is the standard deviation of the error, $CPR_{exp}[i]$ is the i-th experimental data value for crack propagation rate, and $CPR_{calc}[i,\theta]$ is the i-th calculated value for crack propagation rate given the parameter set θ. The posterior joint distribution was then integrated to find the marginal distributions for each empirical model parameter. The marginal distributions for each empirical model parameter capture the uncertainty associated with the true value of each empirical model parameter.

For running the case study of this thesis, General Electric Global Research experimental data[21] is used for SCC growth rates in alloy 690 specimens to update the SCC propagation model developed by Wu. After examination of the data, two important changes were made to the SCC model for alloy 690. The first change was to condense the two-stage model into a one stage model. Wu wanted to fit a three stage SCC propagation curve to available experimental data. However, Wu realized that the third stage happens very rapidly, so he did not model the third stage. The two-stage model developed by Wu represents the first two stages of the SCC propagation curve. For the first stage, Wu shows that a power law model without a dependency on pH is a sufficient fit to the data. This means that for the first stage of the model, Wu determines that the chemical effects are negligible. However, for the second stage of Wu's model, all the parameters were required to fit the model to the data, including pH. When fitting the base SCC model, developed by Wu, to the General Electric Global Research experimental data, it was determined that all dependencies, including chemical dependencies, needed to be incorporated. This determination was made because no transition in the experimental data could be seen such as the one identified by Wu, where the chemical effects transition from being negligible to necessary. The alloy 690 crack propagation data for CPR vs. SIF has been plotted in Figure 5.3 to demonstrate the clustered nature of the data. It is from this plot that it was decided to condense Wu's two-stage model into a one-stage model for this research.

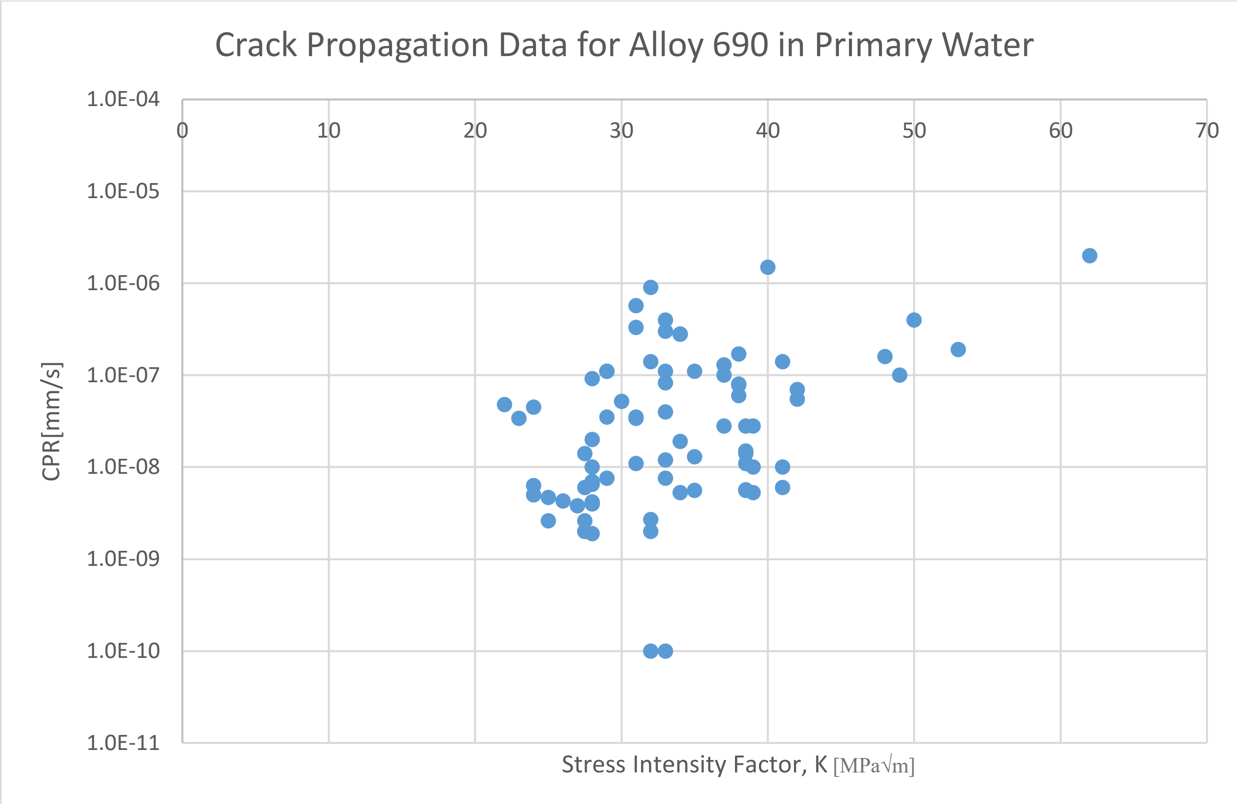

Figure 5.3 Alloy 690 Crack Propagation Data (CPR vs. SIF)

The second important change to Wu's model was to replace the pH dependency with a Hydrogen content (H_2, cc/kg) dependency. This change was made because quantifying pH at higher temperatures is challenging since true chemical elements are not known at those temperatures. This means that hydrogen concentrations cannot be easily quantified. Therefore, hydrogen concentrations were directly included into the model. The resulting alloy 690 SCC propagation model is shown in Equation (5.19). One important parameter in the CPR_{690} model is K_{th690}, which represents necessary stress concentration required for SCC to begin propagating in a component fabricated from alloy 690 material. K_{th600} was developed by Scott[22] for SCC propagation in steam generators made of alloy 600 material. Scott determined the required stress intensity factor for SCC to be $9MPa\sqrt{m}$ to propagate in alloy 600 material. After analyzing the available experimental SCC data for alloy 690, it was determined that the data did not provide sufficient evidence to choose a different value for K_{th690}. Therefore, $K_{th690} = 9MPa\sqrt{m}$ was selected.

$$CPR_{690} = C_{690} \cdot \exp\left[\frac{Q}{R}\left(\frac{1}{T} - \frac{1}{T_{ref}}\right)\right] \cdot \left[\sigma_{ys}\right]^{m_{690}} \cdot \left[K - K_{th690}\right]^{n_{690}} \cdot \left[H_2\right]^{\beta_{690}} \tag{5.19}$$

For the SS SCC propagation model, SS SCC CPR experimental data developed by Terachi et al.[23] was used to update the model developed by Wu. Again, after examination of the experimental data, two important changes were made to the SCC propagation model developed by Wu. The first change was to condense the two-stage model down to one stage, as there was no indication from the experimental data that a two-stage model was appropriate for SCC propagation in SS. This time, the Stage I model from Wu's work was selected, because no pH dependency could be derived from the available experimental data. The resulting SS SCC propagation model can be found in Equation (5.20). Like the case for the CPR_{690} model, a value for K_{thSS} needed to be determined and $K_{thSS}=10MPa\sqrt{m}$ was selected, which was determined from analysis of the experimental data from Terachi et al.[23]. It is likely that the reason for this determination stems from the experimental procedure implemented by Terachi et al., where each specimen was pre-cracked until the stress intensity factor reached $10MPa\sqrt{m}$. Therefore, it is recommended that further research be performed to explore the true value of the threshold stress intensity factor for SCC propagation in stainless steel materials.

$$CPR_{SS} = C_{SS} \cdot \exp\left[\frac{Q}{R}\left(\frac{1}{T} - \frac{1}{T_{ref}}\right)\right] \cdot \left[\sigma_{ys}\right]^{m_{SS}} \cdot \left[K - K_{thSS}\right]^{n_{SS}} \tag{5.20}$$

The empirical model parameters in the alloy 690 and SS SCC propagation models, C_{690}, m_{690}, n_{690}, β_{690}, C_{SS}, m_{SS}, and n_{SS}, were quantified with Bayesian regression analysis, using

OpenBUGS[24], an open source version of the Bayesian inference Using Gibbs Sampling (BUGS) package. Non-informative uniform prior distributions were used for the model parameters in the Bayesian regression analysis to ensure the posterior distribution was developed from the experimental data with very little contribution from the prior distributions. These prior distributions can be found in Table 5.2.

Table 5.2 Non-informative Uniform Prior Distributions

Parameter	Lower Bound	Upper Bound
C690	0	5.00E-10
m690	0	10
n690	0	10
b690	0	10
CSS	0	5.00E-10
mSS	0	10
nSS	0	10

The lower bounds for all parameters was defined as zero because increases in stress, yield strength, and hydrogen content all showed an increase in the SCC propagation rate. The upper bounds were determined to be sufficiently large, so as not to introduce any information into the calculations. The Bayesian regression analysis was performed in OpenBUGS for 100,000 trials. The trace capability of the program allowed for the mean value of each parameter to be traced as a function of the number of trials. Once the simulation reach roughly 50,000 trials, the distributions remained essentially flat. Therefore, it was deemed that 100,000 trials were sufficient for convergence of the results. The resulting posterior joint distributions are represented by marginal distributions for each of the model parameters in the SCC propagation model. These marginal distributions can be found in Table 5.3. As one can see from Table 5.3, none of the output distributions are truncated at the selected upper bounds, which supports the theory that our upper bounds were sufficiently large.

Table 5.3 SCC Propagation Empirical Model Parameters

Parameter	Mean	Std. Dev.	2.50%	Median	97.50%
C_{690}	3.8E-13	1.0E-10	9.2E-18	9.7E-15	3.0E-12
m_{690}	0.2151	0.00999	0.00517	0.1423	0.8419
n_{690}	3.22	0.02817	2.054	3.212	4.381
β_{690}	0.8252	0.5977	0.03553	0.7103	2.092
C_{SS}	9.5E-18	1.0E-10	1.1E-21	2.9E-19	5.5E-17
m_{SS}	2.547	0.4411	1.756	2.532	3.43
n_{SS}	1.052	0.4335	0.3383	0.9984	1.989

5.2.2 ESTIMATION OF ϕ FOR ALLOY 690 & STAINLESS STEEL

This section relates to the implementation of Task # 2.2 and Task #2.3 of the Spatio-Temporal probabilistic methodology to estimate the transition rates between New and Flaw states for the cases of Alloy 690 and Stainless Steel (SS). For this case study, when a component is in the New state, it is assumed that the only mechanism acting upon the component is the mechanism of pitting. As discussed in Section 5.1.4, pitting is often a precursor to SCC. This research adopts the pit-to-crack transition criteria developed by Kondo[13], which says that a pit will transition into a crack when the SCC propagation rate is greater than or equivalent to the pit growth rate. Therefore, to quantify the transition rate, ϕ, a pit growth model developed by Gorman et al.[25] and utilized by Turnbull et al.,[10] which has the form shown in Equation (5.21) was selected.

$$\frac{dx}{dt} = \beta \alpha^{\frac{1}{\beta}} x^{\left(1-\frac{1}{\beta}\right)} \tag{5.21}$$

where: *dx/dt*- pit growth rate, *x*- pit size, α and β- empirical pit growth model parameters. Turnbull et al. fit the pit growth rate model to experimental data for three environments: de-aerated pure water, aerated pure water, and aerated 1.5 ppm chloride. The β parameter of the pit growth model was assumed to be a constant while the α parameter was assumed to be normally distributed with a mean value of zero. Turnbull et al. truncated the normal distribution for negative α values, because negative values would be physically unrealistic. Selecting the mean value as zero implies that some α values will be very small, corresponding to pit growth rates very close to zero. This seems reasonable as pit growth can be very slow. The resulting empirical pit growth model parameters, fit to the experimental data, can be found in Table 5.4.

Table 5.4 Pit Growth Rate Model Parameters Derived from Experimental Data by Turnbull et al.[10]

Environment	β	Std. Dev. of α
De-aerated pure water	0.36	0.16
Aerated pure water	0.35	0.42
Aerated 1.5 ppm chloride	0.37	0.70
De-aerated pure water	0.5	0.01
Aerated pure water	0.5	0.04
Aerated 1.5 ppm chloride	0.5	0.08

Through analyzing the data provided by Turnbull et al., it was discovered that the physical units of the α were unclear, as the resulting pit propagation rates did not appear to coincide with the pit growth rates provided in the paper. Therefore, β=0.5 was set as a fixed value and the range of possible α values based on the pit growth rates provided in the paper was calculated. These calculations provided a new distribution for α. The α parameter was replaced by a uniform distribution, U(9.5917E-09, 2.8249E-07). With the pit growth model, an initial pit size model was required for the calculation of ϕ. Therefore, as suggested by the authors, a Weibull distribution was fit to the experimental data collected for pit growth in de-aerated pure water for 15,402 hours by Turnbull et al. This provided a surrogate initial pit size distribution to be utilized in simulations for pit-to-crack transitions. For this case study, the surrogate initial pit size distribution represents the natural imperfections that are associated with all materials. There are many reasons for which a material can have defects or imperfections. Therefore, the surrogate initial pit size distribution is meant to capture these random defects. The resulting a_1 and a_2 parameters for the fitted Weibull distribution can be found in Table 5.5.

Table 5.5 Weibull Distribution Parameters for Initial Pit Size Surrogate Distribution

Parameter	Value	Unit
a_1	8.274E+10	1/μm
a_2	2.7294	dimensionless

Using the developed models for SCC propagation and pit growth, as well as the initial pit distribution, a simulation technique was developed that would sample from the uncertainty distributions and determine the amount of time required for initial pits to transition into cracks. The pit growth simulation for determining the time of transition from New to Flaw states is depicted as a flow chart in Figure 5.4 and the full MATLAB code can be found in Appendix D.

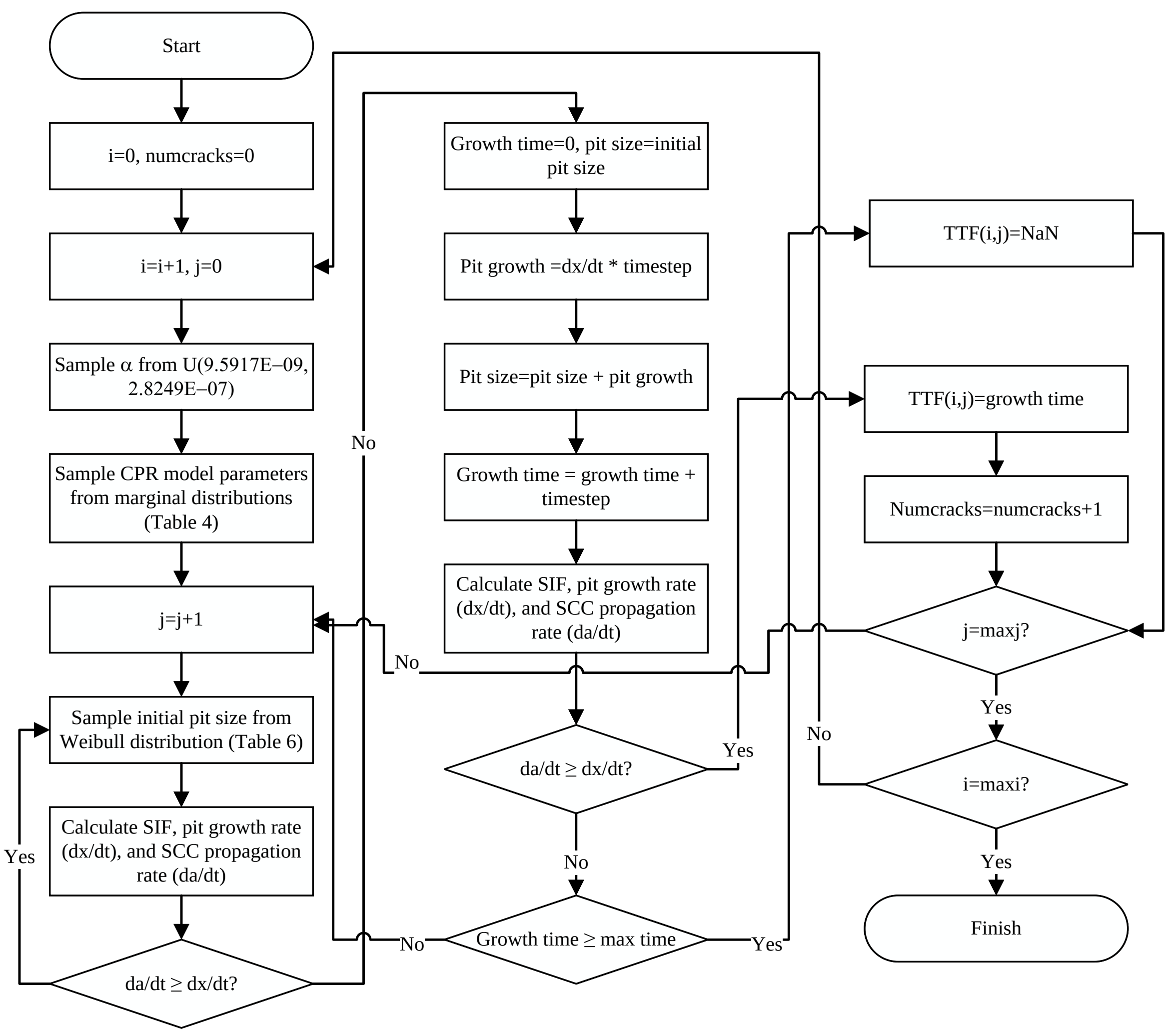

Figure 5.4 Flow Chart of Pit Growth Simulation for Modeling New to Flaw Transition with Monte Carlo Sampling Techniques

The pit growth simulation procedure has the following main steps:

1. Sample the model parameters from the SCC model marginal distributions provided in Table 5.3, and sample an α value for the pit growth model from U(9.5917E-09, 2.8249E-07).
2. Sample an initial pit size from the Weibull distribution provided in Table 5.5.
3. Check to see if the initial pit size sample is in the New state. If the calculated SCC propagation rate initially exceeds the pit growth rate, the sample is rejected because this means that the sample is already in the Flaw state. Therefore, the sample would not be physically consistent with the simulation process. In other words, we truncated the initial pit size distribution to remove any possible samples that had already moved into the Flaw state, since the purpose of this simulation is to find the probability of a sample, which starts in the New state, moving to the Flaw state. If a sample is rejected, a new sample is selected and Step 3 is repeated.
4. Iteratively integrate the pit growth until the SCC propagation rate, calculated from the models developed in Section 5.2.1 exceeds the pit growth rate. Once the SCC propagation rate exceeds the pit growth rate, the sample is considered to transition to the Flaw state. The growth time for transition from New to Flaw is stored as the time-to-Flaw. If the sample does not transition from the New state to the Flaw state within 60 years (the extended lifetime of a NPP), the sample is terminated.

To determine the probability that a pit in the New state will transition to the Flaw state, the number of samples that transition from the New state to the Flaw state is divided by the total number of samples. Using the frequentist definition of probability, this fraction will provide the probability as the number of samples approaches infinity. The transition rates for a Markov model, however, are rates of probability transition. This means the rate at which the probability that a component is in each state is changing or "flowing" into another state. Therefore, to incorporate the rate at which the samples transition from the New state to the Flaw state, the mean time-to-Flaw (MTTF) is calculated. Therefore, the probability of transition from the New state to the Flaw state is multiplied by the inverse of the MTTF to find the transition rate of probability from the New to the Flaw state. This relationship is represented in Equation (5.22).

$$\varphi = \left(\frac{\#\ \text{Transitions}\ (New \rightarrow Flaw)}{\text{Total \# Samples}} \right) * \left(\frac{1}{MTTF} \right) \tag{5.22}$$

Other research has been performed on multi-state physics models for the aging of passive components. Unwin et al. developed a multi-state physics model for SCC growth and crack propagation[26]. However, Unwin's work uses a stochastic Weibull model to calculate the crack initiation transition rate as a function of time. The time is reset after each repair. Therefore, the inhomogeneous nature of time in Unwin's work makes the model non-Markov. The work presented in this thesis uses failure mechanism models to simulate the behavior of crack initiation and progression for SCC. The transition rates are then calculated based on the simulation results. Also, this research sets the transition rates as constants and does not reset the time after each repair to the system; therefore, this research maintains the use of the Markov model.

As can be seen in Figure 5.4, the pit growth simulation consisted of two sampling loops. The outer loop sampled model parameters for the SCC propagation rate and the pit growth rate. The inner loop sampled initial pit sizes. Monte Carlo sampling technique is initially selected for the simulation of the New state to Flaw state transition phenomenon. With Monte Carlo simulation, the analyst needs to select the number of random samples while balancing computational cost with accuracy of the sampling-based estimations. For the New to Flaw transition, the sampling-based estimations of concern were the MTTF and the fraction of samples that transition from the New state to the Flaw state. A sufficient sample size for each of the performance measures is roughly estimated using Equation (5.23) from Law et al.[27]:

$$n^{*}_{r}(\varepsilon) = \min\left\{ i \geq n : \frac{t_{i-1,1-\frac{\zeta}{2}}\sqrt{S^2(n)/i}}{\left|\bar{X}(n)\right|} \leq \frac{\varepsilon}{(1+\varepsilon)} \right\} \tag{5.23}$$

where: n^{*}_{r}- approximate number of samples required to obtain a relative error of ε, $t_{i-1,1-\zeta/2}$ represents the t-distribution value with significance level ζ and i-1 degrees of freedom, and $S^2(n)$ represents the estimated sample variance. Setting ζ=ε=0.05, it was determined that an approximately sufficient sample size would require millions of samples and very long computational time. Therefore, a Latin Hypercube Sampling technique is implemented to sample from the uncertainty distributions. One of the benefits to using the Latin Hypercube Sampling technique is that it more efficiently samples from distributions than the Monte Carlo sampling method, by ensuring that samples are taken from all portions of the distribution[28-31].

With the Latin Hypercube Sampling approach, the pit growth simulations are run for 100,000, 200,000, and 400,000 samples for both alloy 690 and stainless steel using the Illinois Campus Cluster computing capabilities[32].[1] These simulations are replicated 10 times for alloy 690 and 20 times for stainless steel. The resulting mean of the sample means are presented along

[1] The Illinois Campus Cluster was run with help from undergraduate research intern, Ethan Graven

with the standard error of the mean (SEM) for each case in Table 5.6, which shows that the means do not show significant variation with increasing the number of simulations. Figure 5.5 shows how the SEM plateaus as the number of replications of the simulations increases. This indicates that the results have reached a convergence level. The resulting calculations for ϕ are presented in Table 5.7.

Table 5.6 Mean of Means and Standard Error of Mean vs. Number of Samples

Alloy 690 (10 replications)						
	100,000 samples		200,000 samples		400,000 samples	
	Mean TTF (hours)	Transitions (%)	Mean TTF (hours)	Transitions (%)	Mean TTF (hours)	Transitions (%)
Mean of means	11466.17	99.00	11555.15	99.01	11508.02	99.01
Standard Error of Mean (SEM)	29.17	0.012	23.12	0.007	16.39	0.005
Stainless Steel (20 replications)						
	100,000 samples		200,000 samples		400,000 samples	
	Mean TTF (hours)	Transitions (%)	Mean TTF (hours)	Transitions (%)	Mean TTF (hours)	Transitions (%)
Mean of means	51824.74	74.25	51797.84	74.22	51910.14	74.25
Standard Error of Mean (SEM)	87.62	0.023	44.96	0.017	40.89	0.012

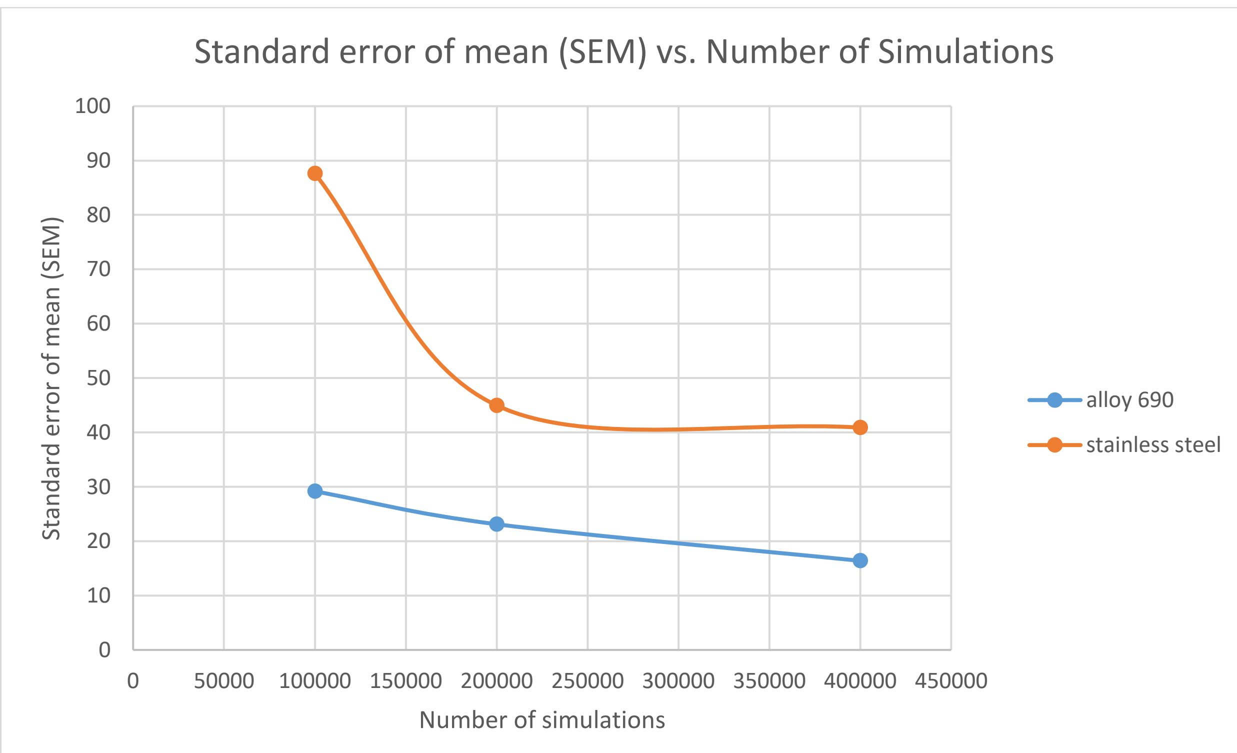

Figure 5.5 Plateau of the Standard Error of Mean vs. Number of Simulations Demonstrating Convergence

Table 5.7 Calculation of ϕ from Simulation Results of New to Flaw Transitions for Alloy 690 and SS

ϕ	Alloy 690	Stainless Steel
# Samples	400,000	400,000
Fraction of Transitions/Samples	0.99	0.74
MTTT(hours)	11,508	51,910
ϕ(1/hour)	**8.60E-05**	**1.43E-05**

5.2.3 ESTIMATION OF λ, γ, and ρ FOR ALLOY 690 & STAINLESS STEEL

This section relates to implementation of Task # 2.2 and Task # 2.3 of the Spatio-temporal Probabilistic methodology for estimations of λ, ρ, and γ for the cases of Alloy 690 and Stainless Steel. Once a component enters the Flaw state, SCC propagation occurs. The transition rates λ (Flaw to Leak), γ (Flaw to Rupture), and ρ (Leak to Flaw) represent the potential pathways by which a component can transition between Markov states. Quantification of these transition rates provides the explicit pathway for incorporation of the PoF of the SCC phenomena. For this work, the SCC propagation models are used to quantify the transition rates λ, γ, and ρ using a probabilistic physics-of-failure approach like the one used for the quantification of ϕ in Section 5.2.2. As mentioned in Chapter 4, the SCC models developed by Wu[3] (Equations 4.1 to 4.5) , are used in this research.

An initial Flaw distribution is required for the quantification of the transition rates λ, γ, and ρ. One could use a crack transition size distribution developed from the pit growth simulation used for the quantification of ϕ. However, it was decided to use a distribution of Flaw sizes from NPP service data to reduce the uncertainty accumulated in the development of the pit growth simulation for calculating ϕ. This research adopted a gamma distribution of crack lengths, which was formulated from 1994 inspection data from a Ringhals Unit 4 steam generator[33]. The parameters for the Gamma distribution are [α=3.393, β=1.395].

The SCC propagation simulation developed for the quantification of the transition rates λ, γ, and ρ require the consideration of both length and depth of cracks. Therefore, this research adopts the methodology utilized by Wu[3] and developed by Shin et al.[34], in which an aspect ratio of a crack penetration in steam generator tubes was determined to be a random variable. The uncertainty in the crack penetration aspect ratio is modeled by a uniform distribution between 0.24 and 0.35. The crack penetration aspect ratio is defined as: *a/c*, where *a* is the depth of the crack and *c* is half the length of the crack. To apply this aspect ratio, the SCC propagation simulation selects an initial crack length. The crack length is then divided by 2 to obtain the half-length, *c*. The aspect ratio is then randomly sampled from U(0.24, 0.35). The sampled aspect ratio is then multiplied by *c*, which provides the initial crack depth value, a. The SCC propagation equations shown in Equations (4.1) to (4.5) provide the rate of growth for the crack depth. Therefore, to determine the crack length growth at each time step, the aspect ratio is re-sampled. The *da/dt* value is then divided by the newly sampled aspect ratio to provide the *dc/dt* value.

Using the SCC propagation models and the initial Flaw length distribution, a simulation to sample from the uncertainty distributions associated with the model parameters and quantify the transition rates λ, γ, and ρ was developed. The structure of SCC propagation simulation is depicted in Figure 5.6 and the full MATLAB code can be found in Appendix D. As mentioned in Chapter 4, the SCC propagation simulation procedure has the following main steps:

1. Sample from the SCC model parameter uncertainty distributions (Table 5.3).

2. Sample from the initial crack length distribution, sample from the aspect ratio uncertainty distribution, and calculate the initial crack depth.
3. Check initial conditions against threshold criteria for the Flaw, Leak, and Rupture states as explained in Section 5.1. If the sample is found to be in the New, Leak, or Rupture states, reject the sample and repeat the second step. This step serves as a method of truncating the initial crack distribution to only allow samples that are initially in the Flaw state, as transitions of components that were initially in the Flaw state are the concern of the simulation.
4. Iteratively integrate the crack length and crack depth until one of three possible outcomes occurs: transition into the Leak state, transition into the Rupture state, or maximum time limit is reached. The maximum time limit for the simulation is set as 60 years, which represents an extended lifetime for an NPP.
5. If the sample transitions into the Rupture state, the time of transition from the Flaw to the Rupture state is recorded and the next sample is simulated. If the sample transitions from the Flaw state to the Leak state, the time of transition is also recorded. However, the simulation continues from the Leak state with a new time counter to simulate when the sample transitions from the Leak to the Rupture state. The SCC propagation model is still used along with the aspect ratio to propagate the crack length, but the crack depth is held constant once the Leak state has been reached. Crack depth is held constant since once a SCC crack propagates 100% through the thickness of the component, the depth cannot continue to increase. If the sample transitions from the Leak to the Rupture state, the time of the transition from entering the Leak state until transitioning into the Rupture state is recorded.

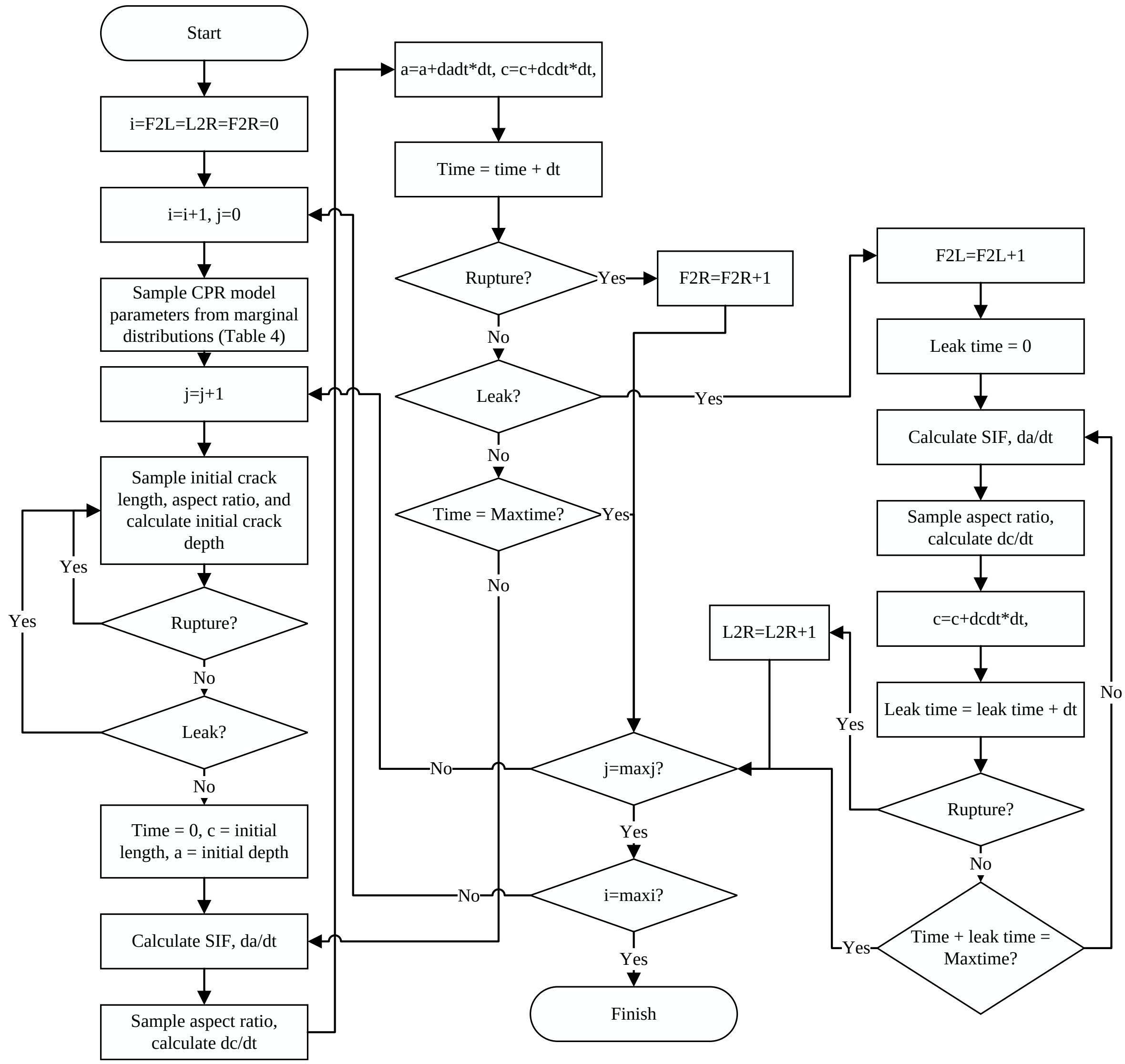

Figure 5.6 Flow Chart of SCC Propagation Simulation for Modeling with Monte Carlo Sampling

Figure 5.7 shows a figure of the simulated crack depth vs. time for 100 samples. The intercepts on the vertical axis represent the uncertainty in the initial crack depth distribution. Additionally, the plot demonstrates how the uncertainty in the input parameters of the SCC propagation simulation affects the crack growth. This ultimately results in a large variation in the time required for each sample to reach a leak or rupture state. Figure 5.8 shows a plot of the

SCC propagation rate as a function of the SIF for 100 alloy 690 samples. This plot demonstrates the uncertainty associated with the SCC propagation model parameters.

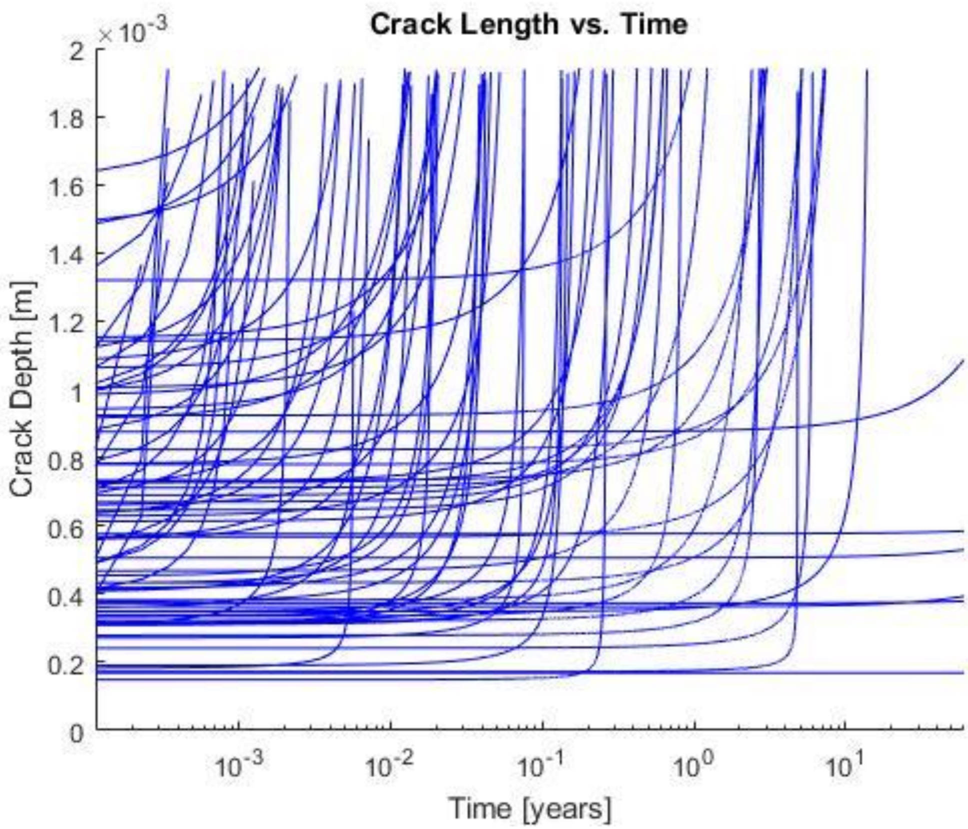

Figure 5.7 SCC Crack Depth vs. Time for 100 Alloy 690 Samples of the SCC Propagation Simulation

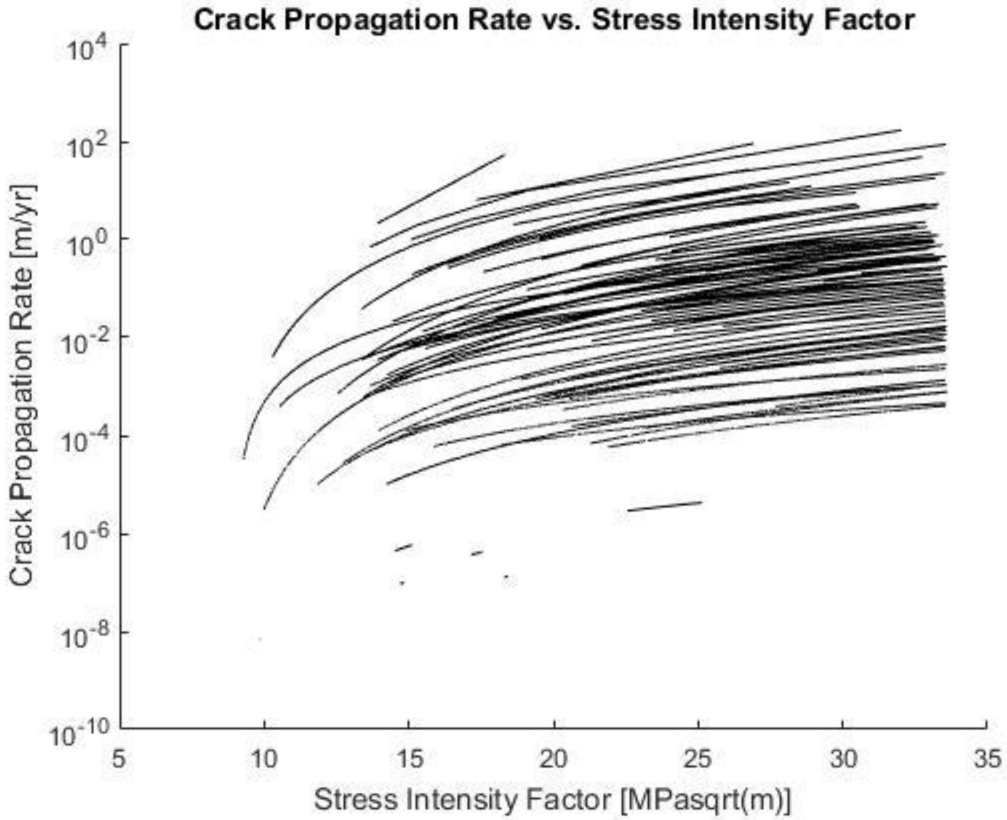

Figure 5.8 SCC Crack Propagation Rate vs. SIF for 100 Alloy 690 Samples of the SCC Propagation Simulation at T=598K, $[H_2]$=26cc/kg, and σ_{ys}=337MPa

To calculate the transition rates λ,γ, and ρ, Equations (4.7) to (4.9) are used. Once again, the Latin Hypercube Sampling approach is chosen instead of the Monte Carlo sampling approach due the high computational cost required by Monte Carlo sampling. The results for the simulations for 400,000 samples have been shown in Table 5.8.

Table 5.8 Calculation of λ, γ, and ρ from Simulation Results of Flaw to Leak, Flaw to Rupture, and Leak to Rupture Transitions for Alloy 690 and SS

λ	Alloy 690	Stainless Steel
# Samples	400,000	400,000
Fraction of Leaks/Samples	0.507	0.621
MTFL(hours)	31,895	193,439
λ(1/hour)	**1.59E-05**	**3.21E-06**
γ	Alloy 690	Stainless Steel
# Samples	400,000	400,000
Fraction of Ruptures/Samples	0.457	0.1
MTFR(hours)	31,895	193,439
γ(1/hour)	**1.43E-05**	**5.17E-07**
ρ	Alloy 690	Stainless Steel
# Leaks	400,000	400,000
Fraction of Ruptures/Leaks	0.841	0.975
MTLR(hours)	268,886	19,471
ρ(1/hour)	**3.13E-06**	**5.01E-05**

5.3 MODELING AND QUANTIFICATION OF THE TRANSITION RATES OF REPAIR IN THE CASE STUDY

Once a component is degraded enough to enter the Flaw or Leak states, there is a possibility that the degradation will be detected and repaired. These possible repairs would bring a component back into a less-degraded state. The possible repair paths are represented by ω and μ. For this case study, the Markov model does not have any repair transition rates from the Rupture state, because it is assumed that once a component ruptures, it cannot be repaired. To fix the rupture, the component must be replaced, which would then require the use of a new Markov model for the new component. Additionally, the repair rates from the Flaw and Leak states only transition to the New state, because it is assumed for this case study that all repairs are perfect. For this case study, ω (Flaw to New transition) and μ (Leak to New transition) are quantified using a solely data-informed approach, as was implemented by both Vinod[6] and Fleming[14]. For quantification of ω, the model described by Equation (5.25) is used. For quantification of μ, the model described by Equation (5.26) was used.

$$\omega = \frac{P_{IF} \cdot P_{FD}}{\left(T_{FI} + T_R\right)} \tag{5.25}$$

$$\mu = \frac{P_{IL} \cdot P_{LD}}{\left(T_{LI} + T_R\right)} \tag{5.26}$$

where: P_{IF} - probability that the component will be inspected within an inspection interval (10 years for most NPPs). This term can be 0 if a component is outside of the inspection programs or 1 if the component is inside the inspection programs. For this case study, a value of 0.25 was selected. P_{FD}- probability that the component, in the Flaw state and having degradation, will be detected. This value is assumed to be equal to 0.9 for this case study. T_{FI}- inspection interval for flaws, assumed to be 10 years. T_R- time to repair a component once it is identified to be in a degraded state. This value has been assumed to be 200 hours. P_{IL}- probability that the component will be inspected for leaks, assumed to be equal to 0.9. P_{LD}- probability that the component will be detected to be in the Leak state, assumed to be equal to 0.9. T_{LI}- inspection interval for leaks, assumed to be 10 years. The values for these repair models were selected to maintain consistency with the repair models for the Markov models developed by Vinod and Fleming and were kept the same for both alloy 690 and stainless steel. A summary of all the values for the transition rates of the Markov models developed for this case study can found in Table 5.9.

Table 5.9 Summary of Values for Transition Rates Used for Quantification of the Markov Model

Transition Rate	690 Value (1/hour)	SS Value (1/hour)
ϕ	8.60E-05	1.43E-05
λ	1.59E-05	3.21E-06
γ	1.43E-05	5.17E-07
ρ	3.13E-06	5.01E-05
ω	2.56E-06	2.56E-06
μ	9.23E-06	9.23E-06

5.4 DEVELOPING THE TIME-DEPENDENT DISTRIBUTIONS OF STATE PROBABILITIES IN THE CASE STUDY

As explained in Section 4.1.4, a differential equation can be established for each Markov state of degradation, which represents the rate in the probability that a component is in each state at a given time. The differential equations established for the Markov model of this case study can be found in Section 4.1.4 in Chapter 4. To simplify the solution to the coupled differential equations, it is assumed that the transition rates are constant over the lifetime of the component. The solution requires initial values for the four Markov states of degradation. For this case study, it is assumed that a component will begin in the New state with certainty (probability =1). Therefore, the probability that the component will begin in the Flaw, Leak, or Rupture state is zero. This initial condition is shown in Equation (5.27).

$$\begin{aligned} &New(t=0)=1 \\ &Flaw(t=0)=Leak(t=0)=Rupture(t=0)=0 \end{aligned} \tag{5.27}$$

There is no transition rate of repair leaving the Rupture state. This is due to the assumption that once a component reaches the Rupture state, it can no longer be repaired. The component must then be replaced. Therefore, the Rupture state acts as a probability sink. This means that if time increases for long enough, the probability that the component will be in the Rupture state will go to 1. Naturally, this means that the probability in the New, Flaw, and Leaks states will be zero as time increases to infinity. This steady state condition is shown in Equation (5.28).

$$\begin{aligned} &New(t\to\infty)=Flaw(t\to\infty)=Leak(t\to\infty)=0 \\ &Rupture(t\to\infty)=1 \end{aligned} \tag{5.28}$$

The coupled differential equations were solved analytically and applied the initial conditions shown in Equation (2.27). Then transition rate values from Table 5.9 were input to the solution. The resulting solution provided a time-dependent state probability distribution that showed what the probability would be that a component was in each state at a given time. In Table 5.10, the results of the state probability distributions over a 60-year period of reactor operation are given. A graphical representation for each state can be found in Figure 5.9 and Figure 5.10.

Table 5.10 Summary of Time-Dependent State Probability Distribution for Alloy 690 and Stainless Steel

Material	Time (years)	0	1	5	10	20	25	40	60
Alloy 690	N(t)	1.000	0.476	0.057	0.037	0.024	0.018	0.009	0.003
	F(t)	0.000	0.453	0.392	0.176	0.078	0.059	0.027	0.010
	L(t)	0.000	0.036	0.248	0.281	0.185	0.144	0.067	0.024
	R(t)	0.000	0.034	0.303	0.506	0.713	0.778	0.897	0.963
Stainless Steel	N(t)	1.000	0.884	0.558	0.347	0.185	0.152	0.100	0.063
	F(t)	0.000	0.115	0.406	0.547	0.548	0.507	0.374	0.241
	L(t)	0.000	0.001	0.016	0.027	0.030	0.028	0.021	0.014
	R(t)	0.000	0.000	0.020	0.080	0.236	0.313	0.505	0.683

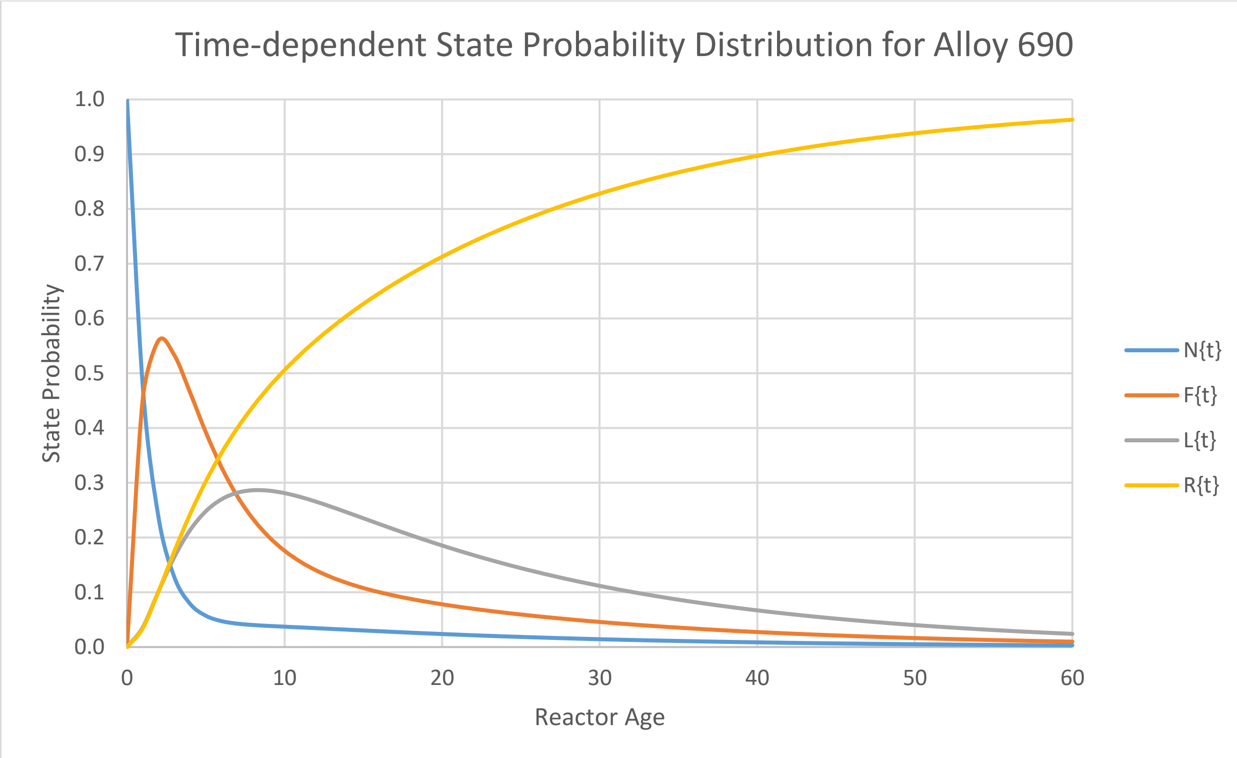

Figure 5.9 State Probability Distributions for Alloy 690 for 60 Years of Reactor Life

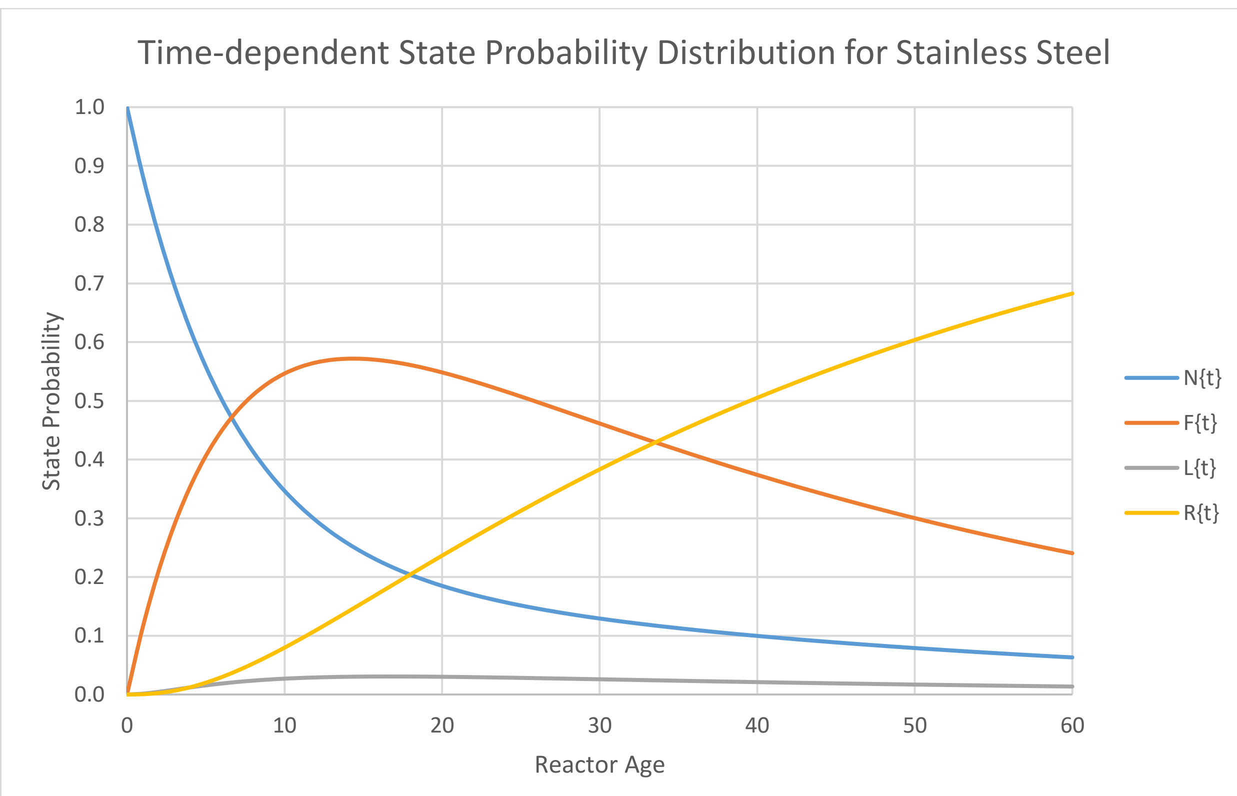

Figure 5.10 State Probability Distributions for Stainless Steel for 60 Years of Reactor Life

A few interesting comparisons can be made from the results shown in Table 5.10. The most important result is that the probability that a component made of stainless steel enters the Rupture state increases much more slowly than the probability that a component made of alloy 690 enters the Rupture state which is consistent with what was observed from the experimental data. Additionally, Figure 5.11 was created by isolating only the rupture state probability distributions and the ratio of the alloy 690 rupture state probability to the SS rupture state probability is presented in Table 5.11. The rupture state probability for alloy 690 increases much more rapidly than the rupture state distribution for stainless steel. Figure 5.12 shows the rate at which the probability that a component exists in the Rupture state changes as a function of reactor age. This figure shows that the alloy 690 component Rupture probability increases very rapidly and then decreases rapidly within the first 10 years of the reactors lifetime. The stainless steel rate increases very slowly, but does not peak until just before 20 years of reactor life. This is the result that was expected from the simulations, because stainless steel is more resistant to SCC than alloy 690. Additionally, it may appear incorrect to some readers that the Flaw state and Leak state probabilities decrease as the reactor age increases. However, this is correct. The reasoning is that as the component ages, the probability that the component undergoes a rupture event continuously increases. This research assumes that a component cannot be repaired once it has moved to the rupture state. Therefore, the rupture state acts as a probability sink. Therefore, as the reactor age increases, all the probability will eventually move into the rupture state while the probabilities of every other state will eventually decline to 0. This assumption is not perfect because a plant could just replace the ruptured component with a new component. However, this action is outside the scope of this research.

The corrosion resistance of each material was captured in the simulation process through the SCC propagation model parameters. These parameters have quite a large effect on the final time-dependent state probability distribution. Per the results of this case study, after 5 years, an alloy 690 fabricated expansion-transition region of a steam generator tube has over a 30% chance to experience a rupture phenomenon. Whereas, for a stainless steel fabricated expansion-transition region of a steam generator, the chance is only 2%. Then after 60 years, the extended lifetime of a NPP, there is a 96% chance of an alloy 690 component experiencing a rupture, but only a 68% chance of a SS component experiencing such a phenomenon. This indicates a very significant effect from material selection for the primary reactor coolant system loop. Pipe ruptures in NPPs are an infrequent event. Therefore, the probabilities of rupture output from this research are larger than expected. These probabilities will be improved as the accuracy of the physical crack propagation models are improved. However, the ability of the research

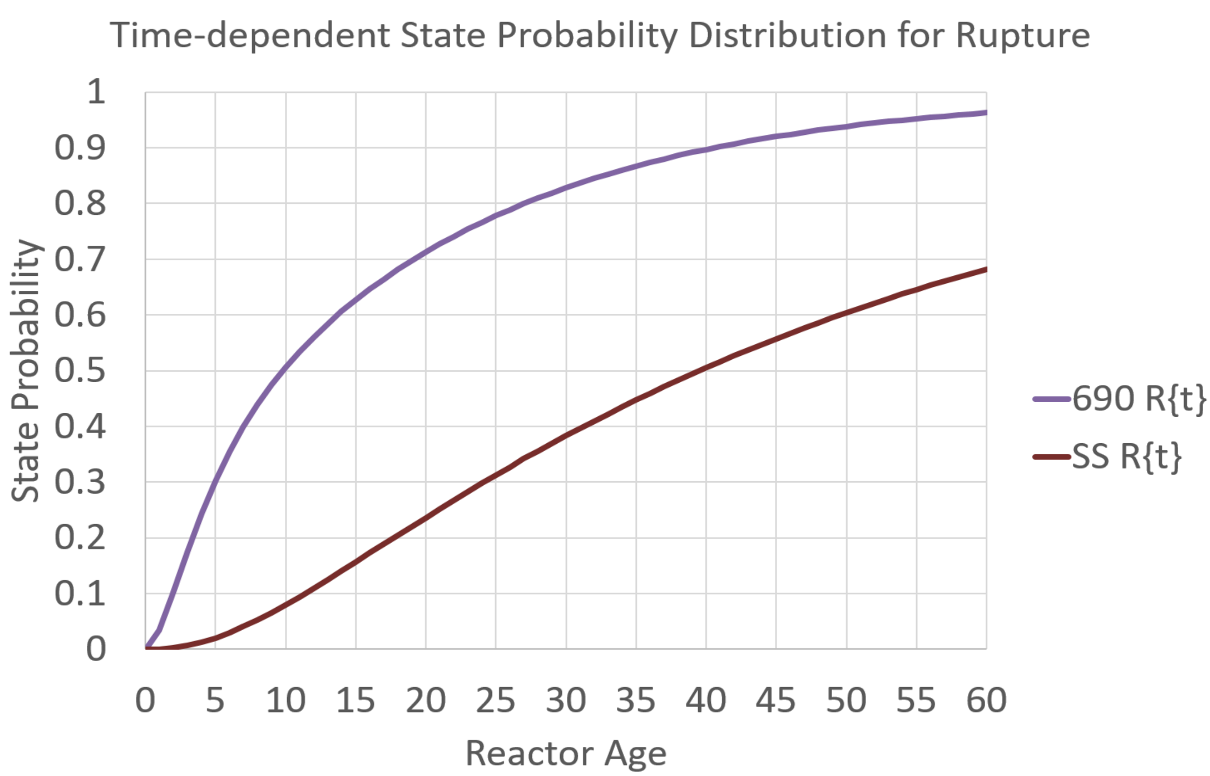

Figure 5.11 Rupture State Probability Distribution for Alloy 690 and Stainless Steel for 60 Reactor-years

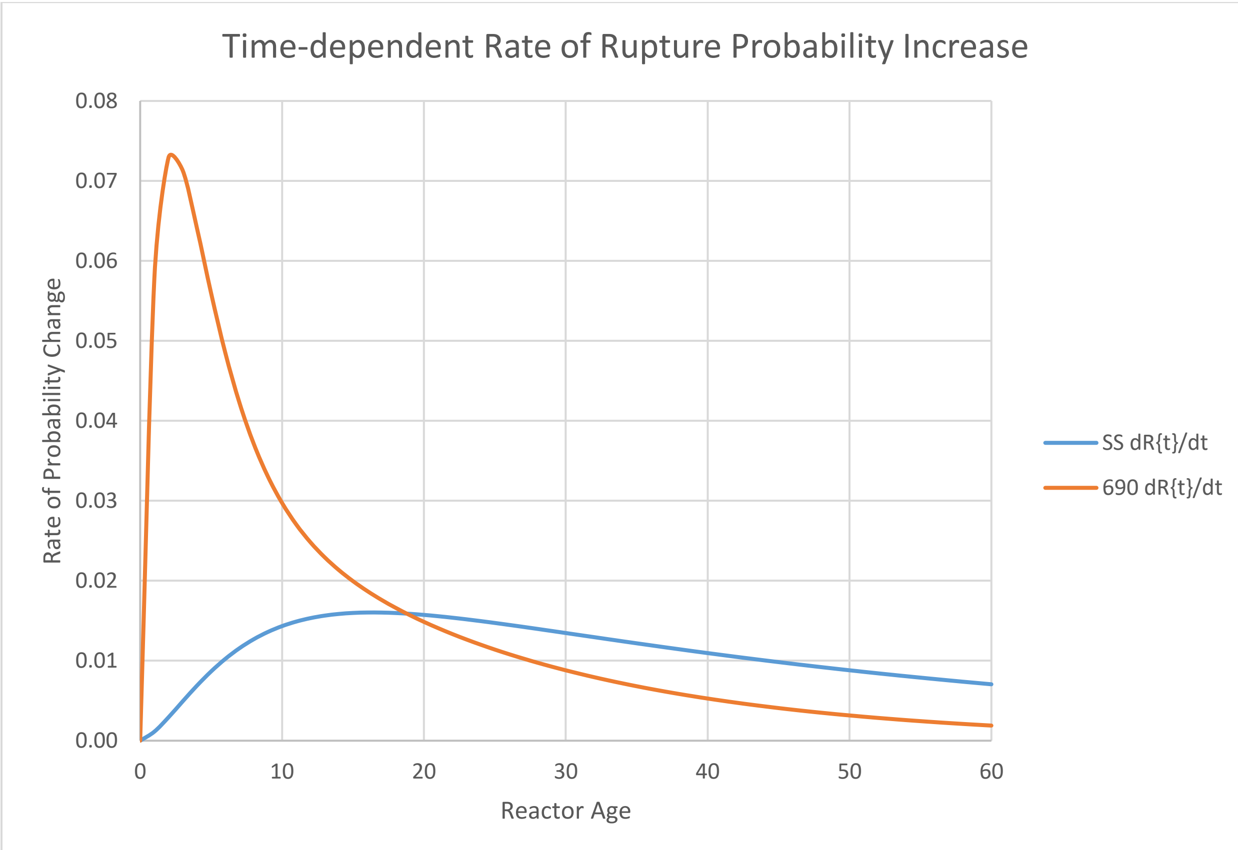

Figure 5.12 Rate of Probability Increase for Rupture State as a Function of Reactor Age

Table 5.11 State Probability Ratios for Alloy 690 and Stainless Steel

Material	Time (years)	1	5	10	20	25	40	60
Alloy 690: Stainless Steel	N(t)	0.539	0.102	0.107	0.129	0.122	0.086	0.049
	F(t)	3.958	0.966	0.322	0.142	0.117	0.073	0.041
	L(t)	25.785	15.944	10.409	6.141	5.091	3.173	1.769
	R(t)	70.530	15.041	6.341	3.014	2.487	1.776	1.411

It is recognized that there are many improvements that can be made to this study. First, the authors only selected one failure mechanism to demonstrate the application of the spatio-temporal methodology. Before application in a real-world setting, research needs to be conducted to include all the possible failure mechanisms that can act on a component. This addition is not as simple as adding the contributions from many spatio-temporal models developed for each individual failure mechanism. Failure mechanisms can interact with each other, thus causing the degradation rate to increase more quickly than suggested by a model that focuses exclusively on one failure mechanism.

Further improvement can be made for this research through repair causal models which are necessary to capture the true nature of the repair phenomena. In this model, very simple point estimates are utilized. These point estimates fail to capture the complex nature of repair phenomena. This complex nature of repair phenomena also makes the incorporation of associated uncertainties critical for the accuracy of the results. In addition, the current case study uses a Markov modeling technique as an approximation for the generalized renewal process. However, the author believes that the use of the generalized renewal process will allow for the probabilistic PoF to be included into the model more completely. Finally, the author believes that it is important for future work to perform sensitivity analyses on the outputs of the spatio-temporal methodology so that the most important factors can be identified. This identification of the critical factors will allow for the most efficient resource allocation for both improvement of accuracy of the model, as well as improvement of the overall system safety.

REFERENCES

1. Tregoning, R., L. Abramson, and P. Scott. *Estimating Loss-of-Coolant Accident (LOCA) Frequencies Through the Elicitation Process*, NUREG-1829, 2008.
2. Fleming, K., B. Lydell, and D. Chrun. *Development of LOCA Initiating Event Frequencies for South Texas Project GSI-191*, 2011.
3. Wu, G., *A Probabilistic-Mechanistic Approach to Modeling Stress Corrosion Cracking Propagation in Alloy 600 Components with Applications, Master of Science,* from the *Mechanical Engineering, 2007.* University of Maryland, College Park.
4. MacDonald, P., V. Shah, L. Ward, and P. Ellison. *Steam Generator Tube Failures*, NUREG/CR-6365, 1996.
5. Majumdar, S., W. Shack, D. Diercks, K. Mruk, J. Franklin, and L. Knoblich. *Failure Behavior of Internally Pressurized Flawed and Unflawed Steam Generator Tubing at High Temperatures - Experiments and Comparison With Model Predictions*, NUREG/CR-6575, 1998.
6. Vinod, G., S.K. Bidhar, H.S. Kushwaha, A.K. Verma, and A. Srividya, *A comprehensive framework for evaluation of piping reliability due to erosion–corrosion for risk-informed inservice inspection.* Reliability Engineering & System Safety, 2003. **82**(2): p. 187-193.
7. Ma, B., J. Shuai, J. Wang, and K. Han, *Analysis on the Latest Assessment Criteria of ASME B31G-2009 for the Remaining Strength of Corroded Pipelines.* Journal of Failue Analysis and Prevention, 2011. **11**: p. 666-671.
8. Caleyo, F., J. Gonzalez, and J. Hallen, *A Study on the Reliability Assessment Methodology for Pipelines with Active Corrosion Defects.* International Journal of Pressure Vessels and Piping, 2002. **79**: p. 77-86.

9. Khaleel, M. and F. Simonen. *Evaluations of Structural Failure Probabilities and Candidate Inservice Inspection Programs*, NUREG/CR-6986, 2009.

10. Turnbull, A., L. McCartney, and S. Zhou, *A Model to Predict the Evolution of Pitting Corrosion and the Pit-to-Crack Transition Incoporating Statistically Distributed Input Parameters.* Corrosion Science, 2006. **48**: p. 2084-2105.

11. Turnbull, A., S. Zhou, L. Orkney, and N. McCormick, *Technical Note: Visualization of Stress Corrosion Cracks Emerging from Pits.* Corrosion, 2006. **62**(7): p. 555-558.

12. Turnbull, A. and S. Zhou, *Pit to crack transition in stress corrosion cracking of a steam turbine disc steel.* Corrosion Science, 2004. **45**: p. 1239-1264.

13. Kondo, Y., *Prediction of Fatigue Crack Initiation Life Based on Pit Growth.* Corrosion Science, 1989. **45**(1): p. 7-11.

14. Fleming, K.N., *Markov models for evaluating risk-informed in-service inspection strategies for nuclear power plant piping systems.* Reliability Engineering & System Safety, 2004. **83**(1): p. 27-45.

15. Gosselin, S. and K. Fleming. *Evaluation of pipe failure potential via degradation mechanism assessment*. in *International Conference on Nuclear Engineering*. 1997. Nice, France.

16. Fleming, K., S. Gosselin, and J. Mitman. *Application of markov models and service data to evaluate the influence of inspection on pipe rupture frequencies*. in *Pressure Vessels Piping Conference*. 1999. Boston, MA: ASME.

17. Fleming, K. and J. Mitman. *Quantitative assessment of a risk informed inspection strategy for BWR weld overlays*. in *International Conference on Nuclear Engineering*. 2000. Baltimore, MD.

18. Lunn, D., D. Spiegelhalter, A. Thomas, and N. Best, *The BUGS project: Evolution, critique and future directions.* Statistics in Medicine, 2009. **28**: p. 3049-3067.

19. Cowles, M.K., *Review of WinBUGS 1.4.* The American Statistician, 2004. **58**(4): p. 330-336.

20. Mosleh, A. and G. Apostolakis, *Models for the Use of Expert Opinions*, in *Low-Probability High Consequence Risk Analysis*, R.A.W.e.a. (eds.), Editor. 1984, Springer Science + Business Media New York.

21. Electric Power Research Institute. *Materials Reliability Program: Resitance of Alloys 690, 152, and 52 to Primary Water Stress Corrosion Cracking* MRP-237, Rev. 2, 2013.

22. Scott, P., *An Analysis of Primary Water Stress Corrosion Cracking in PWR Steam Generators*, in *NEA/CSNI - UNIPEDE Specialist Meeting on Operating Experience with Steam Generators*. 1991, Framatome.

23. Terachi, T., T. Yamada, T. Miyamoto, and K. Arioka, *SCC Growth Behaviors of Austenitic Stainless Steels in Simulated PWR Primary Water.* Journal of Nuclear Materials, 2012. **426**: p. 59-70.

24. Thomas, N. *Overview of BUGS*. 2009; Available from: http://www.openbugs.net/w/FrontPage.

25. Gorman, J., R. Staehle, K. Stavropoulos, and C. Welty. *Prediction of the Performance of Tubes in Steam Generators in Pressurized Water Reactors*. in *Life Prediction of Corrodible Structures*. 1991. NACE.

26. Unwin, S., P. Lowry, R. Layton, P. Heasler, and M. Toloczko. *Multi-State Physics Models of Aging Passive Components in Probabilistic Risk Assessment*. in *International*

Topical Meeting on Probabilistic Safety Assessment and Analysis. 2008. LaGrange Park, IL: American Nuclear Society.

27. Law, A.M., *Simulation Modeling & Analysis*. Fourth ed. 2006: McGraw Hill Higher Education.

28. Helton, J.C. and F.J. Davis, *Latin hypercube sampling and the propagation of uncertainty in analyses of complex systems.* Reliability Engineering & System Safety, 2003. **81**: p. 23-69.

29. Tong, C., *Refinement strategies for stratified sampling methods.* Reliability Engineering & System Safety, 2006. **91**: p. 1257-1265.

30. Hansen, C.W., J.C. Helton, and C.J. Sallaberry, *Use of replicated Latin hypercube sampling to estimate sampling variance in uncertainty and sensitivity analysis results for the geologic disposal of radioactive waste.* Reliability Engineering & System Safety, 2012. **107**: p. 139-148.

31. Borgonovo, E., W. Castaings, and S. Tarantola, *Model emulation and moment-independent sensitivity analysis: An application to environmental modelling.* Environmental Modelling & Software, 2012. **34**: p. 105-115.

32. University of Illinois. *Illinois Campus Cluster Program*. 2016; Available from: https://campuscluster.illinois.edu/.

33. Gorman, J., P. Turner, M. Kreider, and J. Harris. *Estimating Probable Flaw Distributions in PWR Steam Generator Tubes (NUREG/CR-6521)*, 1998.

34. Shin, K., J. Park, H. Kim, and H. Chung, *Simulation of Stress Corrosion Crack Growth in Steam Generator Tubes.* Nuclear Engineering and Design, 2002. **214**: p. 91-101.

CHAPTER 6 : CONCLUDING REMARKS

The roadmap of this research is presented in Figure 6.1. The premise of the risk-informed resolution of GSI-191 is that location-specific LOCA frequencies drive the risk of GSI-191 related failure. Step #1 of the roadmap began with the most recent NRC-sponsored estimations of LOCA frequencies. These estimations are only *implicit* functions of underlying physics, space, and time. Fleming and Lydell first incorporated spatial variation into the estimations of LOCA frequencies[1]. Step #2 of this research performed a critical review and quantitative verification of the location-specific estimation of LOCA frequencies, developed by Fleming and Lydell for the STPNOC risk-informed resolution of GSI-191. The author's contributions to the improvement of the Fleming & Lydell report are detailed in Chapter 2 and the methodological gaps are identified and cover the (a) lack of inclusion of non-piping RCS components, (b) lack of explicit incorporation of underlying physics of failure that lead to the occurrence of a LOCA.

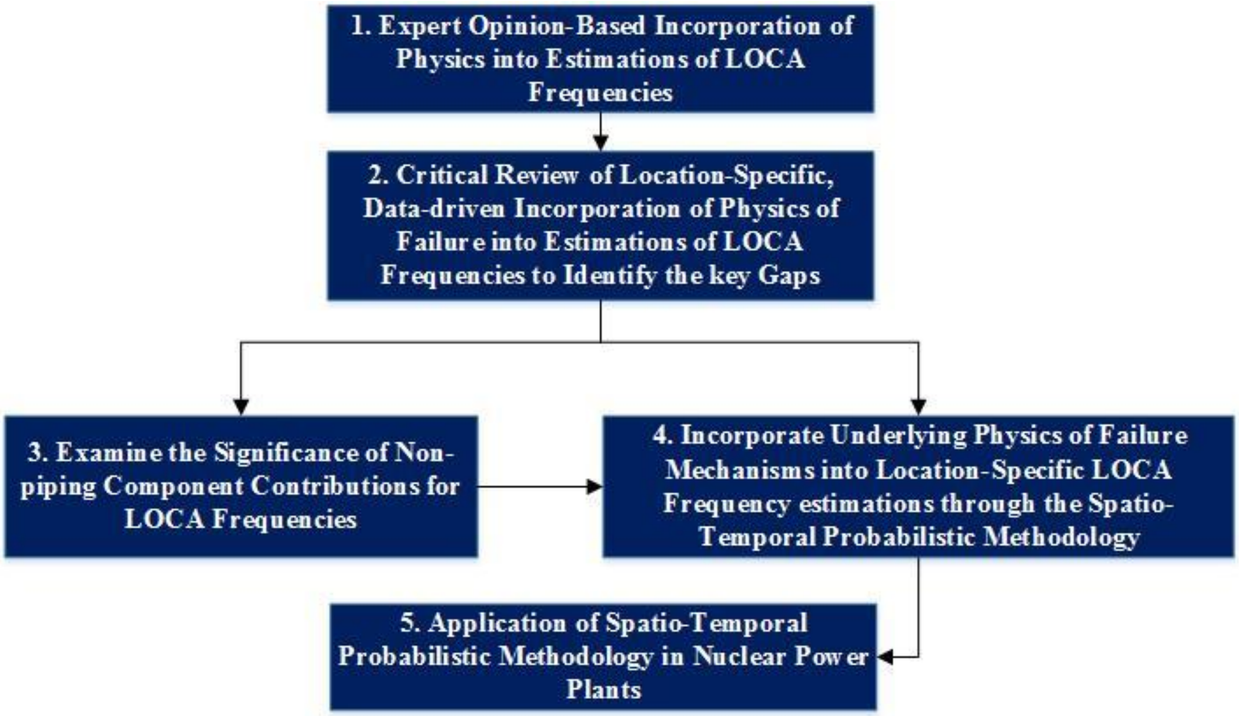

Figure 6.1 Roadmap of the Research

Step #3 of this research analyzes the criticality of one of the gaps, which is the lack of inclusion of non-piping RCS components. This research examined an evidence-seeking procedure and expert elicitation process [2] to determine the significance of the contributions of non-piping reactor coolant system (RCS) components to the estimation of LOCA frequencies. The investigative procedure performed in this research spanned over 500 academic, regulatory, national laboratory, and industry documents. The 24 subcomponent categories identified by this investigative process indicates that estimations of LOCA frequencies for risk-informed decision-making applications such as GSI-191 should not focus exclusively on the RCS piping components, because there is a potential for impact from the non-piping components. However, the investigative procedure could not determine "how significant" the exclusion of non-piping components could be on the results of risk-informed analyses.

A quantitative methodology is needed to determine the "level of impact" of the inclusion/exclusion of non-piping components on the estimations of LOCA frequencies for risk-informed applications. Therefore, Step #4 of this research focuses on the development of a quantitative methodology and on addressing the other gap in Fleming & Lydell's approach by developing the spatio-temporal probabilistic methodology [3, 4] which *explicitly* incorporates underlying physical failure mechanisms into the estimation of location-specific LOCA frequencies. In this methodology, the Markov modeling technique, which is based on the renewal process theory, is integrated with Probabilistic Physics of Failure (PPoF) models to estimate RCS LOCA frequencies as a function of location and age and with considerations of periodic degradation and repair phenomena.

In most of Markov models developed in this area of research, e.g., Fleming [5-8], the "transition rates" among the states are developed using solely data-driven approaches and utilizing service data . For example, Fleming develops a Markov model for piping system reliability that incorporates statistical estimates for the transition rates from Electric Power Research Institute (EPRI) studies performed for thermal fatigue[9] and water hammer events[10]. Other multi-state physics-based models have been also developed in recent years for applications, such as the exploration of aging degradation of passive components[11, 12], to predict long-term failure rates of passive components[13-15], passive component degradation for the RELAP 7 reactor simulation environment[16], and SCC of dissimilar metal in RELAP 7[17]. These multi-state physics-based models have implemented a data-driven approach by fitting uncertainty distributions to available data to quantify the probability of transitions between states. While these approaches try to explicitly incorporate the progression of damage through the Markov model development, the transition rates themselves are developed through a solely data-driven approach. The main problems with the Markov models with the solely data-driven transition rates are (1) inaccuracy due to insufficient data and (2) the lack of "explicit" connections with location-specific physics of failure mechanisms associated with transition rates.

The rate of change in degradation of a component varies at each location. For example, some locations in the RCS may not be inspected as frequently as other locations. Therefore, the probability that the maintenance program will identify the component degradation and repair the component is much lower for an infrequently inspected location than it would be for a more frequently inspected location. Additionally, some failure mechanisms may degrade a component very quickly at one location due to the operating conditions such as temperature or humidity. However, that same failure mechanism may have a much lower rate of degradation at another location due to a change in operating conditions or material properties. Some locations may not experience that same failure mechanism at all because of the component being made from a different material. Therefore, to explicitly incorporate this spatial variation of the effects of the underlying failure mechanisms into LOCA frequency estimations, it is necessary to integrate the transition rates in the Markov modeling technique with the associated location-specific physics of failure mechanisms.

Vinod et al. [18] combine the Markov modeling technique with a stress-strength model of erosion corrosion (E-C) for the piping components of Pressurized Heavy Water Reactors (PHWR), using an analytical model to estimate corrosion rates. Although Vinod et al.'s approach utilizes a physical failure mechanism model for erosion-corrosion to depict the underlying physical failure mechanism of transition rates in the Markov model more explicitly than solely data-driven approaches, due to some unrealistic assumptions, their approach does not adequately provide explicit incorporation of physical factors associated with locations. For example, the progression of erosion-corrosion damage propagation, like stress corrosion cracking, changes with the size of the crack. As the damage progresses, the damage rate of the mechanism changes. Vinod et al.'s approach lumps the failure rate into a distribution and treats the failure mechanism the same through each stage of crack progression. Therefore, the variations in the failure probability, based on the underlying spatio-temporal physics, are masked by the average rate distribution.

In order to develop more explicit connection between the Markov model and the spatio-temporal physical failure mechanisms, this research proposes the Spatio-Temporal Probabilistic methodology which is the first that integrates the Markov modeling technique with Probabilistic Physic of Failure (PPoF) models. This methodology has four key tasks including:

- Task #1: Defining Markov States of Degradation
- Task #2: Modeling and Quantification of the Transition Rates of Degradation
    - Task # 2.1: Developing and quantifying physics of failure causal models based on the identified failure mechanisms to find the "transition time between two states" as a function of underlying physical causal factor. This research proposes a Data-Theoretic approach [19] to overcome the challenges of quantification of these casual models.
    - Task #2.2: Propagating uncertainties in the physics of failure causal models to make the Probabilistic Physic of Failure (PPoF) models and to develop a probabilistic estimation of "transition time between two states
    - Task #2.3: Calculating transition rates of degradation based on the output of PPoF models, i.e., the estimated probabilistic "transition time between two states"
    - Task # 2.4: Bayesian integration of the estimated transition rate from PPoF models (from step 3) and the ones from solely data-oriented approaches (e.g., Fleming [5-8])
- Task #3: Modeling and Quantification of the Transition Rates of Repair
- Task #4: Developing the Time-dependent Distributions of State Probabilities

To overcome the quantification difficulties of PPoF models, this research proposes the Data-Theoretic approach as a part of Task #2.1 in the Spatio-Temporal Probabilistic methodology. The underlying theory supports the completeness of contextual factors and the accuracy of their causal relationships. It also helps avoid the potential for being misled by results from a solely data-informed analysis. The proposed Data-Theoretic methodology (in the context of PoF and PRA research) is originally published in [19] and is also under development in a parallel research [20], for the context of socio-technical risk analysis, sponsored by the National Science Foundation. The proposed Data-Theoretic methodology (in the context of physics of failure and PRA research) is broken down into four steps:

a. Determine causal factors and relationships and develop physics of failure causal models of underlying damage mechanisms
b. Extract historical data and update the generic causal model
c. Scientifically reduce physical factors in the network
d. Quantify and validate important factors and causal paths

Step #5 of the roadmap of this research (Figure 6.1) focuses on a case study for the implementation of the spatio-temporal probabilistic methodology to examine the effects of stress corrosion cracking (SCC) on the rupture probability of steam generator tubes. This case study demonstrates the comparative capabilities of the methodology by showing the variation in rupture probability based on the selection of Stainless Steel and Alloy 690 materials for the fabrication of the expansion-transition region of the steam generator tubes.

The spatio-temporal probabilistic methodology enables the effects of operating conditions, maintenance programs, and material selection to be compared with respect to their contributions to LOCA frequencies. This methodology will assist with the generation of a more efficient prevention strategy by identifying the most risk-significant causal factors. Improved prevention strategies will lead to more efficient maintenance programs allowing for a more efficient allocation of resources for improving safety and increasing system performance. These advancements will enable a more accurate estimation of LOCA frequencies, which will lead to a more accurate estimation of risk for nuclear power plants. The spatio-temporal probabilistic methodology enables ranking of the contributions to risk from each causal factor. This ranking will help advance prevention of risk by helping plants to determine the most efficient method for risk reduction.

Possible future research includes:

I. In Task #1, considering uncertainties in the thresholds of the Markov states can bring another layer of uncertainty analysis to the Spatio-temporal Probabilistic methodology. In some cases, the choice of the characteristic threshold for defining a Markov state may be accompanied with uncertainty. For example, the modeler may want to find the probability that a component will rupture within a given mission time. However, the modeler may not be certain as to what value to use as the characteristic threshold of the "rupture" state. In this case, the suggestion is to quantify the Markov model using the range of possible characteristic threshold values. The resulting distribution of output values would represent the model uncertainty for the characteristic threshold. Investigating the model uncertainty enables the modeler to see the significance of assuming a specific characteristic value.

II. In Task # 2.1. of this methodology, Data-Theoretic approach is introduced. The four steps (a, b, c, and d) of the Data-Theoretic methodology helps manage the quantification of multi-level causal model (e.g., the one presented on the right side of Figure 4.2.) and to reduce the scope of the casual network in a scientific way without missing the critical risk factors. However, in this thesis, the scope of the causal model is reduced (from the beginning) in a way that only the first level of the causal model in Figure 4.2 (i.e., the blue casual factors in Figure 4.2) is covered. Therefore, this research mainly focuses on step "a" of the Data-theoretic approach explained above. Other steps are the focus of future research.

III. In Task #2.1, this research only model single failure mechanisms. Mohaghegh et al. [21] proposed combination of causal modeling techniques (e.g., Bayesian Belief Network) and Finite Element methods for quantification of PPoF models, more specifically, where two failure mechanisms interact. Future work can expand the Spatio-Temporal Probabilistic methodology to include the interactions of two failure mechanisms.

IV. Task #2.4 has not been operationalized in this research and relates to future work.

V. For Task #3, this research only utilizes empirical estimation of transition rate of repair. Future work can be dedicated to integration of maintenance casual models. The maintenance or repair mechanisms that can be incorporated in the "degree" of repair are broad and wide ranging, but can have a significant effect on the overall quality of repair. Performance shaping factors such as fatigue, quality of training, workplace conditions, workplace culture, or weather can all play a major part in the quality of repair[20]. Incorporating these factors into the models can result in better-informed decision-makers, enabling them to more accurately make decisions to optimize costs and develop maintenance strategies. This will help decision-makers determine, not only how frequently repairs will be needed to optimize performance (and costs), but also in what ways the system can most effectively be repaired. Explicit incorporation of underlying mechanisms into GRP modeling is a long-term goal of this research.

VI. Although the tasks are explained mainly based on the Stress Corrosion Cracking mechanism (SCC), which is a dominant mechanisms associated with LOCA in NPPs, the Spatio-Temporal Probabilistic methodology can be applied for any other failure mechanisms (e.g., wear, creep) and for other industry applications than NPPs (e.g., oil and gas) .

VII. Integration of the Spatio-Temporal methodology with the Probabilistic Risk Assessment (PRA) framework is a valuable research area to be considered. The Spatio-temporal Probabilistic methodology is beneficial, not only for estimation of location-specific LOCA frequencies, but also for incorporation of spatio-temporal physics of failure into PRA; therefore, it helps advance risk estimation and risk prevention.

REFERENCES

1. Fleming, K., B. Lydell, and D. Chrun. *Development of LOCA Initiating Event Frequencies for South Texas Project GSI-191*, 2011.
2. O'Shea, N., Z. Mohaghegh, S.A. Reihani, E. Kee, K. Fleming, and B. Lydell. *Analyzing Non-Piping Location-Specific LOCA Frequency For Risk-Informed Resolution of Generic Safety Issue 191*. in *International Topical Meeting on Probabilistic Safety Assessment and Analysis*. 2015. Sun Valley, ID, USA.
3. O'Shea, N. and Z. Mohaghegh. *Spatio-Temporal Methodology for Estimating Loss-of-Coolant Accident Frequencies in the Risk-Informed Resolution of Generic Safety Issue 191*. in *American Nuclear Society Student Conference*. 2016. Madison, WI: American Nuclear Society.
4. O'Shea, N., Z. Mohaghegh, S.A. Reihani, and E. Kee, *Estimating Loss-of-coolant Accident (LOCA) Frequencies Via Spatio-Temporal Methodology,* in *13th International Conference on Probabilistic Safety Assessment and Management (PSAM 13)*. 2016: Seoul, Korea.
5. Fleming, K.N., *Markov models for evaluating risk-informed in-service inspection strategies for nuclear power plant piping systems.* Reliability Engineering & System Safety, 2004. **83**(1): p. 27-45.
6. Gosselin, S. and K. Fleming. *Evaluation of pipe failure potential via degradation mechanism assessment*. in *International Conference on Nuclear Engineering*. 1997. Nice, France.
7. Fleming, K., S. Gosselin, and J. Mitman. *Application of markov models and service data to evaluate the influence of inspection on pipe rupture frequencies*. in *Pressure Vessels Piping Conference*. 1999. Boston, MA: ASME.

8. Fleming, K. and J. Mitman. *Quantitative assessment of a risk informed inspection strategy for BWR weld overlays*. in *International Conference on Nuclear Engineering*. 2000. Baltimore, MD.

9. Mikschl, T. and K. Fleming. *Piping System Failure Rates and Rupture Frequencies for Use In Risk Informed In-Service Inspection Applications*, TR-111880-NP, 2000.

10. Stone and Webster Engineering Corporation. *Water Hammer Prevention, Mitigation, and Accommodation - volume 1: Plant Water Hammer Experience*, EPRI NP-6766, 1992.

11. Unwin, S., P. Lowry, R. Layton, P. Heasler, and M. Toloczko. *Multi-State Physics Models of Aging Passive Components in Probabilistic Risk Assessment*. in *International Topical Meeting on Probabilistic Safety Assessment and Analysis*. 2008. LaGrange Park, IL: American Nuclear Society.

12. Unwin, S., P. Lowry, and M. Toyooka. *Component Degradation Susceptibilities as the Bases for Modeling Reactor Aging Risk*. in *ASME 2010 Pressure Vessels & Piping Division / K-PVP Conference*. 2010. Bellevue, Washington: ASME.

13. Unwin, S., P. Lowry, and M. Toyooka, *Reliability models of Aging Passive Components Informed by Materials Degradation Metrics to Support Long-Term Reactor Operations.* Nuclear Science and Engineering, 2012. **171**: p. 69-77.

14. Unwin, S., P. Lowry, M. Toyooka, and B. Ford. *Degradation Susceptibility Metrics as the Bases for Bayesian Models of Aging Passive Components and Long-term Reactor Risk*. in *ASME 2011 Pressure Vessels & Piping Division Conference*. 2011. Baltimore, Maryland: ASME.

15. Unwin, S., P. Lowry, and M. Toyooka. *A Methodology Supporting the Risk-Informed Management of Materials Degradation*. in *American Nuclear Society Winter Meeting and Nuclear Technology Expo*. 2011. LaGrange Park, IL: American Nuclear Society.

16. Unwin, S., R. Layton, K. Johnson, and P. Lowry, *Physics-Based Multi-State Models of Passive Component Degradation for the R7 Reactor Simulation Environment.* 11th International Probabilistic Safety Assessment and Management Conference and the Annual European Safety and Reliability Conference 2012, 2012. **3**: p. 1761-1770.

17. Unwin, S., K. Johnson, R. Layton, P. Lowry, S. Sanborn, and M. Toloczko. *Physics-Based Stress Corosion Cracking Component Reliability Model cast in an R7-Compatible Cumulative Damage Framework*, PNNL-20596, 2011.

18. Vinod, G., S.K. Bidhar, H.S. Kushwaha, A.K. Verma, and A. Srividya, *A comprehensive framework for evaluation of piping reliability due to erosion–corrosion for risk-informed inservice inspection.* Reliability Engineering & System Safety, 2003. **82**(2): p. 187-193.

19. O'Shea, N., J. Pence, Z. Mohaghegh, and E. Kee. *Physics of Failure, Predictive Modeling and Data Analytics for LOCA Frequency*. in *Annual Reliability & Maintainability Symposium (RAMS)*. 2015. IEEE.

20. Pence, J., Z. Mohaghegh, C. Ostroff, V. Dang, E. Kee, R. Hubenak, and M. Billings. *Quantifying Organizational Factors in Human Reliability Analysis Using the Big Data-Theoretic Algorithm*. in *International Topical Meeting on Probabilistic Safety Assessment and Analysis*. 2015. Sun Valley, ID, USA: American Nuclear Society.

21. Mohaghegh, Z., M. Modarres, and A. Christou. *Physics-Based Common Cause Failure Modeling in Probabilistic Risk Analysis: A Mechanistic Perspective*. in *ASME 2011 Power Conference*. Denver, Colorado.

APPENDIX A: COMMENT RESOLUTION ON LOCATION-SPECIFIC ESTIMATION OF LOCA FREQUENCIES DEVELOPED BY FLEMING AND LYDELL

Table A.1 Communication and Comment Resolution Regarding Failure Rate Development in Fleming and Lydell's Report

UIUC Question/Issue	Karl Fleming Response
[UIUC] The failures in Table 3-3 are not specified by component case, therefore, the number of failures for the Bayesian updating cannot be determined for every case.	[KNFCS] That was not the purpose of this table. They were sorted into the correct cases in the excel spreadsheets. The excel spread sheets were not designed to be applied by non-experts. That would be a good research project for UCIC [sic] but not included in our SOW.
[UIUC] One of the goals of our current research project is to recreate the numbers throughout the report. This has largely been accomplished for most of the tables in the report. However, without a further breakdown of the failures in Table 3-3 or access to the Excel files for categories other than the Hot Leg, it is impossible to recreate every calculation case for Table 3-12. We would appreciate it if you could provide us with a breakdown of these failures into each calculation case category, or provide us access to the Excel files for the rest of the calculation cases, so we could move forward with the recreation of the report.	
This issue was not resolved.	
Pressurizer Cases (5A-5G in Table 3-12):	
[UIUC] Table 3-3 does not specify if failures listed are for B-F or B-J welds, so it is unclear in which cases these failures should be included, which is necessary in order to perform Bayesian updating	[KNFCS] See above comment. That was not the purpose of this table. We did not design the report so that all the calcs could be recreated by non-experts. We did not have sufficient budget for that. That was to be done as part of a Phase 2 project which STP decided not to fund.
[UIUC] Please see above comment under first bullet of the section titled Chapter 3 (Step 1) Failure Rate Development.	
This issue was not resolved.	
[UIUC] Table 3-11 lists B-J welds have PWSCC DM susceptibility equal to one, but Table 3-12 does not list PWSCC as a susceptible DM. Should PWSCC be included in the calculations for failure rate development?	[KNFCS] Table 3-12 uses the general label SC because we only have one prior for all the SC damage mechanisms. We did not want to suggest we have different priors for each flavor.
This issue was resolved.	
[UIUC] The Pressurizer B-J welds in Table 3-11 list damage susceptibility fractions for IGSCC, but Table 3-12 does not list SC as an applicable damage mechanism for Pressurizer B-J weld categories. Should SC be included in the calculations for the Pressurizer B-J weld categories in Table 3-12?	
This issue was not resolved.	

Table A.1 (Cont.)

[UIUC] Tables 3-11 and 3-12 do not list VF as an applicable DM for pressurizers, but Table 3-3 shows a failure by VF. Should VF be included? If not, why is this data from Table 3-3 excluded?	[KNFCS] The V-F failures in Table 3-3 were included in the failure rates for small bore pipes
[UIUC] The eighth row of Table 3-3 lists a V-F failure for system case 5, PZR-SPRAY, as a leak of a pipe between 4" and 10". If this failure was included in the failure rate calculation for small bore pipes, why was it not included in the Pressurizer category instead? Our understanding is that this VF failure was not included in the calculations for the Pressurizer cases. Please confirm whether or not our understanding is correct.	
This issue was not resolved.	
[UIUC] How does a weld overlay affect DM susceptibility fractions or prior distributions?	[KNFCS] Weld overlays eliminate the potential for PWSCC induced failures so only D&C is included for such welds.
This issue was resolved.	
Small Bore Cases (Table 3-12):	
[UIUC] Tables 3-11 and 3-12 do not show TF as applicable DM, but Table 3-3 shows 3 failures by TF. Should TF be included in the calculations? If not, why not?	[KNFCS] TF should probably be added but we did not develop conditional failure rates given susceptibility to TF for any small bore pipes. Small bore pipes were evaluated as unconditional because they were not included in the scope of the previous RI-ISI program
[UIUC] Tables 3-11 and 3-12 list IGSCC, or SC, as applicable damage mechanisms, but not TF. While, Table 5-5 includes TF, but not SC. Table 3-3 includes failure data for both. Please explain which Table represents the damage mechanisms that contribute to the calculations performed for this category?	
This issue was not resolved.	
[UIUC] Table 3-11 lists DM fractions for IGSCC, but not for PWSCC, yet Table 3-3 lists failures for SC and PWSCC separately. Should the PWSCC failures be added to the SC case, or are they already included in the SC number (SC -20, PWSCC -6)	[KNFCS] In Table 3-3 the SC failures include both IGSCC and TGSCC but in the way the failure rates were calculated all SC DMs were treated the same way. The primary reason for breaking out PWSCC is to deal with the B-F weld overlay issue otherwise it does not make any difference.
[UIUC] Please clarify when the SC prior distribution was Bayesian updated, were there 20 or 26 failures used in the updating?	
This issue was not resolved.	
SIR Cases (Table 3-12):	
[UIUC] The report does not distinguish failures between cases. Should the failures be included in the Excl accumulator or in accumulator cases?	[KNFCS] We did not intend for these table to be sufficient to recreate all the numbers. We worked this out in the preparation of the excel sheets.
This issue was not resolved.	

Table A.1 (Cont.)

[UIUC] For Cases 7E-7L and 7O, should the B-J, BC weld type be treated as if it were just a B-J weld type? The motivation of this question is that BC is not listed in Table 3-11 for DM susceptibility fractions, unless it is listed as C-F-1, which I am not sure what C-F-1 represents and it has not description.	[KNFCS] The failure rate method does not really distinguish between B-J, B-C, C-F-1. We used these terms to be consistent with the ASME classifications.
[UIUC] If the method does not distinguish between B-J, B-C, C-F-1, please explain what causes the difference between the failure rates listed in Table 3-12 cases 4B and 4C?	
This issue was not resolved.	
[UIUC] SIR w/ accumulator lines lists SC as an applicable DM, but Table 3-11 doesn't have a DM susceptibility fraction listed. Should SC be included in this case? Should the same DM fraction as SIR w/out accumulator lines be used?	[KNFCS] STP has no Category 7M welds.
[UIUC] It would be beneficial to clarify what SC damage mechanism susceptibilities were used to calculate the failure rate listed in Table 3-12?	
This issue was not resolved.	

Table A.2 Re-calculation of 40-year LOCA Frequency Distributions from NUREG-1829 Experts

Updated Table 4-3 NUREG-1829 Expert Distributions for Hot Leg LOCA Frequencies											
Expert ID	**LOCA Category**	**LOCA Frequency for System[1] (Per Reactor-Calendar Year)**				**40-Yr Multiplier[1]**				**40-Yr LOCA Frequency[1] (Per Reactor-Calendar Year)**	
		LB	**Mid**	**UB**	**RF95=UB/Mid[2]**	**LB**	**Mid**	**UB**	**RF95=UB/Mid[2]**	**Mid[3]**	**RF95[4]**
A	1 (> 100)	5.33E-08	1.60E-07	4.80E-07	3.00E+00	1.00E+00	1.00E+00	1.00E+00	1.00E+00	1.60E-07	3.00E+00
	2 (> 1,500)	5.33E-08	1.60E-07	4.80E-07	3.00E+00	1.50E-02	3.00E-01	5.85E-01	1.95E+00	4.80E-08	3.62E+00
	3 (> 5,000)	5.33E-08	1.60E-07	4.80E-07	3.00E+00	5.00E-03	1.00E-01	1.95E-01	1.95E+00	1.60E-08	3.62E+00
	4 (> 25,000)	5.33E-08	1.60E-07	4.80E-07	3.00E+00	1.50E-03	3.00E-02	5.85E-02	1.95E+00	4.80E-09	3.62E+00
	5 (> 100,000)	5.33E-08	1.60E-07	4.80E-07	3.00E+00	5.00E-04	1.00E-02	1.95E-02	1.95E+00	1.60E-09	3.62E+00
	6 (> 500,000)	5.33E-08	1.60E-07	4.80E-07	3.00E+00	1.50E-04	3.00E-03	5.85E-03	1.95E+00	4.80E-10	3.62E+00
B	1 (> 100)	3.00E-07	3.00E-07	3.00E-07	1.00E+00	1.00E-10	1.00E+00	1.00E+01	1.00E+01	3.00E-07	1.00E+01
	2 (> 1,500)	1.20E-07	1.20E-07	1.20E-07	1.00E+00	1.00E-10	1.00E+00	1.00E+01	1.00E+01	1.20E-07	1.00E+01
	3 (> 5,000)	4.80E-08	4.80E-08	4.80E-08	1.00E+00	1.00E-10	1.00E+00	1.00E+01	1.00E+01	4.80E-08	1.00E+01
	4 (> 25,000)	1.92E-08	1.92E-08	1.92E-08	1.00E+00	1.00E-10	1.00E+00	1.00E+01	1.00E+01	1.92E-08	1.00E+01
	5 (> 100,000)	7.68E-09	7.68E-09	7.68E-09	1.00E+00	1.00E-10	1.00E+00	1.00E+01	1.00E+01	7.68E-09	1.00E+01
	6 (> 500,000)	3.07E-09	3.07E-09	3.07E-09	1.00E+00	1.00E-10	1.00E+00	1.00E+01	1.00E+01	3.07E-09	1.00E+01
C	1 (> 100)	6.00E-07	6.00E-07	6.00E-07	1.00E+00	3.00E-02	1.00E+00	3.00E+01	3.00E+01	6.00E-07	3.00E+01

Table A.2 (Cont.)

	2 (> 1,500)	5.00E-08	5.00E-08	5.00E-08	1.00E+00	3.00E-02	1.00E+00	3.00E+01	3.00E+01	5.00E-08	3.00E+01
	3 (> 5,000)	2.00E-08	2.00E-08	2.00E-08	1.00E+00	3.00E-02	1.00E+00	3.00E+01	3.00E+01	2.00E-08	3.00E+01
	4 (> 25,000)	3.00E-09	3.00E-09	3.00E-09	1.00E+00	5.00E-02	1.67E+00	1.67E+02	1.00E+02	5.01E-09	1.00E+02
	5 (> 100,000)	1.00E-09	1.00E-09	1.00E-09	1.00E+00	6.00E-02	2.00E+00	2.00E+03	1.00E+03	2.00E-09	1.00E+03
	6 (> 500,000)	2.00E-10	2.00E-10	2.00E-10	1.00E+00	6.00E-02	2.00E+00	2.00E+03	1.00E+03	4.00E-10	1.00E+03
E	1 (> 100)	3.07E-07	9.22E-07	2.77E-06	3.00E+00	3.33E-04	2.83E-02	3.33E-01	1.18E+01	2.61E-08	1.49E+01
	2 (> 1,500)	3.07E-07	9.22E-07	2.77E-06	3.00E+00	3.33E-04	2.83E-02	3.33E-01	1.18E+01	2.61E-08	1.49E+01
	3 (> 5,000)	3.07E-07	9.22E-07	2.77E-06	3.00E+00	3.33E-04	2.83E-02	3.33E-01	1.18E+01	2.61E-08	1.49E+01
	4 (> 25,000)	3.67E-09	1.10E-08	3.30E-08	3.00E+00	1.00E-03	1.00E-01	1.50E+00	1.50E+01	1.10E-09	1.86E+01
	5 (> 100,000)	1.27E-09	3.80E-09	1.14E-08	3.00E+00	1.00E-04	5.00E-02	1.00E+00	2.00E+01	1.90E-10	2.43E+01
	6 (> 500,000)	4.33E-10	1.30E-09	3.90E-09	3.00E+00	1.00E-04	3.00E-02	3.00E+00	1.00E+02	3.90E-11	1.14E+02
G	1 (> 100)	5.13E-08	1.54E-07	4.62E-07	3.00E+00	1.00E-01	1.14E+00	1.00E+01	8.77E+00	1.76E-07	1.14E+01
	2 (> 1,500)	7.50E-09	2.25E-08	6.75E-08	3.00E+00	1.00E-01	1.14E+00	1.00E+01	8.77E+00	2.57E-08	1.14E+01
	3 (> 5,000)	2.78E-09	8.33E-09	2.50E-08	3.00E+00	1.00E-01	1.14E+00	1.00E+01	8.77E+00	9.50E-09	1.14E+01
	4 (> 25,000)	9.50E-10	2.85E-09	8.55E-09	3.00E+00	1.00E-01	1.14E+00	1.00E+01	8.77E+00	3.25E-09	1.14E+01
	5 (> 100,000)	1.71E-10	8.53E-10	4.27E-09	5.01E+00	1.00E-01	1.14E+00	1.00E+01	8.77E+00	9.72E-10	1.49E+01
	6 (> 500,000)	1.58E-11	1.58E-10	1.58E-09	1.00E+01	1.00E-01	1.14E+00	1.00E+01	8.77E+00	1.80E-10	2.37E+01
H	1 (> 100)	1.48E-07	4.45E-07	1.34E-06	3.01E+00	2.50E+00	2.50E+01	2.50E+02	1.00E+01	1.11E-05	1.28E+01
	2 (> 1,500)	2.03E-08	6.10E-08	1.83E-07	3.00E+00	1.00E+00	1.00E+01	1.00E+02	1.00E+01	6.10E-07	1.28E+01
	3 (> 5,000)	7.33E-09	2.20E-08	6.60E-08	3.00E+00	5.00E-01	5.00E+00	5.00E+01	1.00E+01	1.10E-07	1.28E+01
	4 (> 25,000)	2.60E-09	7.80E-09	2.34E-08	3.00E+00	5.00E-01	5.00E+00	5.00E+01	1.00E+01	3.90E-08	1.28E+01
	5 (> 100,000)	8.83E-10	2.65E-09	7.95E-09	3.00E+00	5.00E-01	5.00E+00	5.00E+01	1.00E+01	1.33E-08	1.28E+01
	6 (> 500,000)	2.93E-10	8.80E-10	2.64E-09	3.00E+00	5.00E-01	5.00E+00	5.00E+01	1.00E+01	4.40E-09	1.28E+01
I	1 (> 100)	4.00E-11	2.00E-09	1.00E-07	5.00E+01	5.00E-01	5.00E-01	5.00E-01	1.00E+00	1.00E-09	5.00E+01
	2 (> 1,500)	4.00E-11	2.00E-09	1.00E-07	5.00E+01	5.00E-01	5.00E-01	5.00E-01	1.00E+00	1.00E-09	5.00E+01
	3 (> 5,000)	4.00E-11	2.00E-09	1.00E-07	5.00E+01	5.00E-01	5.00E-01	5.00E-01	1.00E+00	1.00E-09	5.00E+01
	4 (> 25,000)	4.00E-11	2.00E-09	1.00E-07	5.00E+01	5.00E-01	5.00E-01	5.00E-01	1.00E+00	1.00E-09	5.00E+01
	5 (> 100,000)	4.00E-11	2.00E-09	1.00E-07	5.00E+01	5.00E-01	5.00E-01	5.00E-01	1.00E+00	1.00E-09	5.00E+01
	6 (> 500,000)	4.00E-11	2.00E-09	1.00E-07	5.00E+01	5.00E-01	5.00E-01	5.00E-01	1.00E+00	1.00E-09	5.00E+01
J	1 (> 100)	9.25E-12	9.80E-11	2.88E-09	2.94E+01	3.19E+01	3.19E+01	3.19E+01	1.00E+00	3.13E-09	2.94E+01
	2 (> 1,500)	5.78E-13	1.03E-11	7.61E-10	7.39E+01	5.24E+01	5.24E+01	5.24E+01	1.00E+00	5.40E-10	7.39E+01
	3 (> 5,000)	1.40E-13	3.21E-12	3.38E-10	1.05E+02	6.04E+01	6.04E+01	6.04E+01	1.00E+00	1.94E-10	1.05E+02

Table A.2 (Cont.)

	4 (> 25,000)	1.53E-14	4.82E-13	9.75E-11	2.02E+02	7.50E+01	7.50E+01	7.50E+01	1.00E+00	3.62E-11	2.02E+02
	5 (> 100,000)	2.42E-15	6.99E-14	1.93E-11	2.76E+02	9.81E+01	9.81E+01	9.81E+01	1.00E+00	6.86E-12	2.76E+02
	6 (> 500,000)	1.44E-17	6.28E-16	7.56E-13	1.20E+03	1.14E+02	1.14E+02	1.14E+02	1.00E+00	7.16E-14	1.20E+03
L	1 (> 100)	2.62E-06	9.60E-06	3.52E-05	3.67E+00	1.27E-01	1.27E-01	1.27E-01	1.00E+00	1.22E-06	3.67E+00
	2 (> 1,500)	1.58E-06	6.34E-06	2.53E-05	3.99E+00	1.27E-01	1.27E-01	1.27E-01	1.00E+00	8.05E-07	3.99E+00
	3 (> 5,000)	3.84E-07	1.92E-06	9.60E-06	5.00E+00	4.19E-01	4.19E-01	4.19E-01	1.00E+00	8.04E-07	5.00E+00
	4 (> 25,000)	1.54E-07	7.68E-07	3.84E-06	5.00E+00	1.01+00	1.01E+00	1.01E+00	1.00E+00	7.76E-07	5.00E+00
	5 (> 100,000)	6.40E-08	3.20E-07	1.60E-06	5.00E+00	2.41E+00	2.41E+00	2.41E+00	1.00E+00	7.71E-07	5.00E+00
	6 (> 500,000)	3.20E-11	3.20E-10	3.20E-09	1.00E+01	2.61E+00	2.61E+00	2.61E+00	1.00E+00	8.35E-10	1.00E+01

Notes:

[1] Data shaded in yellow are taken from NUREG-1829 expert questionnaires in Reference [14]. Data shaded in blue were calculated in this study per Notes [2] through [4].

[2] RF = Range Factor of a lognormal distribution defined by the Mid value as the median and by the UB value as the 95%tile.

[3] Median of a lognormal distribution for the 40-year LOCA frequency created by the product of two lognormal distributions: the medians of the lognormal distributions for LOCA frequency for system and the 40-year multiplier (see Equation [4.1])

[4] Range Factor of the 40-year LOCA frequency lognormal distribution (see Equation [4.2]).

Cold Leg

Expert ID	**LOCA Category**	**LOCA Frequency for System[1] (Per Reactor-Calendar Year)**				**40-Yr Multiplier[1]**				**40-Yr LOCA Frequency[1] (Per Reactor-Calendar Year)**	
		LB	**Mid**	**UB**	**RF95=UB/Mid [2]**	**LB**	**Mid**	**UB**	**RF95=UB/Mid [2]**	**Mid[3]**	**RF95[4]**
A	1 (> 100)	1.37E-08	4.10E-08	1.23E-07	3.00E+00	1.00E+00	1.00E+00	1.00E+00	1.00E+00	4.10E-08	3.00E+00
	2 (> 1,500)	1.37E-08	4.10E-08	1.23E-07	3.00E+00	1.50E-02	3.00E-01	5.85E-01	1.95E+00	1.23E-08	3.62E+00
	3 (> 5,000)	1.37E-08	4.10E-08	1.23E-07	3.00E+00	5.00E-03	1.00E-01	1.95E-01	1.95E+00	4.10E-09	3.62E+00
	4 (> 25,000)	1.37E-08	4.10E-08	1.23E-07	3.00E+00	1.50E-03	3.00E-02	5.85E-02	1.95E+00	1.23E-09	3.62E+00
	5 (> 100,000)	1.37E-08	4.10E-08	1.23E-07	3.00E+00	5.00E-04	1.00E-02	1.95E-02	1.95E+00	4.10E-10	3.62E+00
	6 (> 500,000)	1.37E-08	4.10E-08	1.23E-07	3.00E+00	1.50E-04	3.00E-03	5.85E-03	1.95E+00	1.23E-10	3.62E+00
B	1 (> 100)	3.00E-07	3.00E-07	3.00E-07	1.00E+00	2.00E-02	2.00E-01	2.00E+00	1.00E+01	6.00E-08	1.00E+01
	2 (> 1,500)	1.20E-07	1.20E-07	1.20E-07	1.00E+00	2.00E-02	2.00E-01	2.00E+00	1.00E+01	2.40E-08	1.00E+01
	3 (> 5,000)	4.80E-08	4.80E-08	4.80E-08	1.00E+00	2.00E-02	2.00E-01	2.00E+00	1.00E+01	9.60E-09	1.00E+01
	4 (> 25,000)	1.92E-08	1.92E-08	1.92E-08	1.00E+00	2.00E-02	2.00E-01	2.00E+00	1.00E+01	3.84E-09	1.00E+01
	5 (> 100,000)	7.68E-09	7.68E-09	7.68E-09	1.00E+00	2.00E-02	2.00E-01	2.00E+00	1.00E+01	1.54E-09	1.00E+01
	6 (> 500,000)	3.07E-09	3.07E-09	3.07E-09	1.00E+00	2.00E-02	2.00E-01	2.00E+00	1.00E+01	6.14E-10	1.00E+01
C	1 (> 100)	2.00E-07	2.00E-07	2.00E-07	1.00E+00	3.00E-02	1.00E+00	3.00E+01	3.00E+01	2.00E-07	3.00E+01

Table A.2 (Cont.)

	2 (> 1,500)	2.00E-08	2.00E-08	2.00E-08	1.00E+00	3.00E-02	1.00E+00	3.00E+01	3.00E+01	2.00E-08	3.00E+01
	3 (> 5,000)	7.00E-09	7.00E-09	7.00E-09	1.00E+00	3.00E-02	1.00E+00	3.00E+01	3.00E+01	7.00E-09	3.00E+01
	4 (> 25,000)	1.00E-09	1.00E-09	1.00E-09	1.00E+00	6.00E-02	2.00E+00	2.00E+02	1.00E+02	2.00E-09	1.00E+02
	5 (> 100,000)	3.00E-10	3.00E-10	3.00E-10	1.00E+00	7.00E-02	2.33E+00	2.33E+03	1.00E+03	6.99E-10	1.00E+03
	6 (> 500,000)	7.00E-11	7.00E-11	7.00E-11	1.00E+00	8.57E-02	2.86E+00	2.86E+03	1.00E+03	2.00E-10	1.00E+03
E	1 (> 100)	3.07E-07	9.22E-07	2.77E-06	3.00E+00	3.33E-04	2.83E-02	3.33E-01	1.18E+01	2.61E-08	1.49E+01
	2 (> 1,500)	3.07E-07	9.22E-07	2.77E-06	3.00E+00	3.33E-04	2.83E-02	3.33E-01	1.18E+01	2.61E-08	1.49E+01
	3 (> 5,000)	3.07E-07	9.22E-07	2.77E-06	3.00E+00	3.33E-04	2.83E-02	3.33E-01	1.18E+01	2.61E-08	1.49E+01
	4 (> 25,000)	3.67E-09	1.10E-08	3.30E-08	3.00E+00	3.33E-04	3.33E-02	5.00E-01	1.50E+01	3.66E-10	1.86E+01
	5 (> 100,000)	1.27E-09	3.80E-09	1.14E-08	3.00E+00	3.33E-05	1.67E-02	3.33E-01	1.99E+01	6.35E-11	2.42E+01
	6 (> 500,000)	4.33E-10	1.30E-09	3.90E-09	3.00E+00	3.33E-05	1.00E-02	1.00E+00	1.00E+02	1.30E-11	1.14E+02
G	1 (> 100)	5.13E-08	1.54E-07	4.62E-07	3.00E+00	1.00E-01	9.14E-01	1.00E+01	1.09E+01	1.41E-07	1.39E+01
	2 (> 1,500)	7.50E-09	2.25E-08	6.75E-08	3.00E+00	1.00E-01	9.14E-01	1.00E+01	1.09E+01	2.06E-08	1.39E+01
	3 (> 5,000)	2.78E-09	8.33E-09	2.50E-08	3.00E+00	1.00E-01	9.14E-01	1.00E+01	1.09E+01	7.61E-09	1.39E+01
	4 (> 25,000)	9.50E-10	2.85E-09	8.55E-09	3.00E+00	1.00E-01	9.14E-01	1.00E+01	1.09E+01	2.60E-09	1.39E+01
	5 (> 100,000)	1.71E-10	8.53E-10	4.27E-09	5.01E+00	1.00E-01	9.14E-01	1.00E+01	1.09E+01	7.80E-10	1.79E+01
	6 (> 500,000)	1.58E-11	1.58E-10	1.58E-09	1.00E+01	1.00E-01	9.14E-01	1.00E+01	1.09E+01	1.44E-10	2.77E+01
H	1 (> 100)	1.48E-07	4.45E-07	1.34E-06	3.01E+00	1.00E-01	1.00E+00	1.00E+01	1.00E+01	4.45E-07	1.28E+01
	2 (> 1,500)	2.03E-08	6.10E-08	1.83E-07	3.00E+00	1.00E-01	1.00E+00	1.00E+01	1.00E+01	6.10E-08	1.28E+01
	3 (> 5,000)	7.33E-09	2.20E-08	6.60E-08	3.00E+00	1.00E-02	1.00E-01	1.00E+00	1.00E+01	2.20E-09	1.28E+01
	4 (> 25,000)	2.60E-09	7.80E-09	2.34E-08	3.00E+00	1.00E-02	1.00E-01	1.00E+00	1.00E+01	7.80E-10	1.28E+01
	5 (> 100,000)	8.83E-10	2.65E-09	7.95E-09	3.00E+00	1.00E-02	1.00E-01	1.00E+00	1.00E+01	2.65E-10	1.28E+01
	6 (> 500,000)	2.93E-10	8.80E-10	2.64E-09	3.00E+00	1.00E-02	1.00E-01	1.00E+00	1.00E+01	8.80E-11	1.28E+01
I	1 (> 100)	4.00E-11	2.00E-09	1.00E-07	5.00E+01	5.00E-01	5.00E-01	5.00E-01	1.00E+00	1.00E-09	5.00E+01
	2 (> 1,500)	4.00E-11	2.00E-09	1.00E-07	5.00E+01	5.00E-01	5.00E-01	5.00E-01	1.00E+00	1.00E-09	5.00E+01
	3 (> 5,000)	4.00E-11	2.00E-09	1.00E-07	5.00E+01	5.00E-01	5.00E-01	5.00E-01	1.00E+00	1.00E-09	5.00E+01
	4 (> 25,000)	4.00E-11	2.00E-09	1.00E-07	5.00E+01	5.00E-01	5.00E-01	5.00E-01	1.00E+00	1.00E-09	5.00E+01
	5 (> 100,000)	4.00E-11	2.00E-09	1.00E-07	5.00E+01	5.00E-01	5.00E-01	5.00E-01	1.00E+00	1.00E-09	5.00E+01
	6 (> 500,000)	4.00E-11	2.00E-09	1.00E-07	5.00E+01	5.00E-01	5.00E-01	5.00E-01	1.00E+00	1.00E-09	5.00E+01
J	1 (> 100)	9.32E-12	7.58E-11	2.04E-09	2.69E+01	3.41E+01	3.41E+01	3.41E+01	1.00E+00	2.58E-09	2.69E+01
	2 (> 1,500)	5.19E-13	9.05E-12	5.69E-10	6.29E+01	5.33E+01	5.33E+01	5.33E+01	1.00E+00	4.82E-10	6.29E+01
	3 (> 5,000)	1.19E-13	2.87E-12	2.69E-10	9.37E+01	6.05E+01	6.05E+01	6.05E+01	1.00E+00	1.74E-10	9.37E+01

Table A.2 (Cont.)

	4 (> 25,000)	1.28E-14	4.51E-13	8.00E-11	1.77E+02	7.29E+01	7.29E+01	7.29E+01	1.00E+00	3.29E-11	1.77E+02
	5 (> 100,000)	2.03E-15	6.50E-14	1.82E-11	2.80E+02	9.40E+01	9.40E+01	9.40E+01	1.00E+00	6.11E-12	2.80E+02
	6 (> 500,000)	2.61E-17	1.16E-15	1.58E-12	1.36E+03	1.12E+02	1.12E+02	1.12E+02	1.00E+00	1.30E-13	1.36E+03
L	1 (> 100)	2.62E-06	9.60E-06	3.52E-05	3.67E+00	2.54E-02	2.54E-02	2.54E-02	1.00E+00	2.44E-07	3.67E+00
	2 (> 1,500)	1.58E-06	6.34E-06	2.53E-05	3.99E+00	2.54E-02	2.54E-02	2.54E-02	1.00E+00	1.61E-07	3.99E+00
	3 (> 5,000)	3.84E-07	1.92E-06	9.60E-06	5.00E+00	8.37E-02	8.37E-02	8.37E-02	1.00E+00	1.61E-07	5.00E+00
	4 (> 25,000)	1.54E-07	7.68E-07	3.84E-06	5.00E+00	2.02E-01	2.02E-01	2.02E-01	1.00E+00	1.55E-07	5.00E+00
	5 (> 100,000)	6.40E-08	3.20E-07	1.60E-06	5.00E+00	4.82E-01	4.82E-01	4.82E-01	1.00E+00	1.54E-07	5.00E+00
	6 (> 500,000)	3.20E-11	3.20E-10	3.20E-09	1.00E+01	5.22E-01	5.22E-01	5.22E-01	1.00E+00	1.67E-10	1.00E+01

Notes:

[1] Data shaded in yellow are taken from NUREG-1829 expert questionnaires in Reference [14]. Data shaded in blue were calculated in this study per Notes [2] through [4].

[2] RF = Range Factor of a lognormal distribution defined by the Mid value as the median and by the UB value as the 95%tile.

[3] Median of a lognormal distribution for the 40-year LOCA frequency created by the product of two lognormal distributions: the medians of the lognormal distributions for LOCA frequency for system and the 40-year multiplier (see Equation [4.1])

[4] Range Factor of the 40-year LOCA frequency lognormal distribution (see Equation [4.2]).

Surge Line

Expert ID	LOCA Category	LOCA Frequency for System[1] (Per Reactor-Calendar Year)				40-Yr Multiplier[1]				40-Yr LOCA Frequency[1] (Per Reactor-Calendar Year)	
		LB	Mid	UB	RF95=UB/Mid [2]	LB	Mid	UB	RF95=UB/Mid [2]	Mid[3]	RF95[4]
A	1 (> 100)	5.33E-09	1.60E-08	4.80E-08	3.00E+00	1.00E+00	1.00E+00	1.00E+00	1.00E+00	1.60E-08	3.00E+00
	2 (> 1,500)	5.33E-09	1.60E-08	4.80E-08	3.00E+00	1.50E-02	3.00E-01	5.85E-01	1.95E+00	4.80E-09	3.62E+00
	3 (> 5,000)	5.33E-09	1.60E-08	4.80E-08	3.00E+00	5.00E-03	1.00E-01	1.95E-01	1.95E+00	1.60E-09	3.62E+00
	4 (> 25,000)	5.33E-09	1.60E-08	4.80E-08	3.00E+00	1.50E-03	3.00E-02	5.85E-02	1.95E+00	4.80E-10	3.62E+00
	5 (> 100,000)	5.33E-09	1.60E-08	4.80E-08	3.00E+00	5.00E-04	1.00E-02	1.95E-02	1.95E+00	1.60E-10	3.62E+00
	6 (> 500,000)										
B	1 (> 100)	1.50E-07	1.50E-07	1.50E-07	1.00E+00	1.00E-01	1.00E+00	1.00E+01	1.00E+01	1.50E-07	1.00E+01
	2 (> 1,500)	5.10E-08	5.10E-08	5.10E-08	1.00E+00	1.00E-01	1.00E+00	1.00E+01	1.00E+01	5.10E-08	1.00E+01
	3 (> 5,000)	1.73E-08	1.73E-08	1.73E-08	1.00E+00	1.00E-01	1.00E+00	1.00E+01	1.00E+01	1.73E-08	1.00E+01
	4 (> 25,000)	5.90E-09	5.90E-09	5.90E-09	1.00E+00	1.00E-01	1.00E+00	1.00E+01	1.00E+01	5.90E-09	1.00E+01
	5 (> 100,000)	2.00E-09	2.00E-09	2.00E-09	1.00E+00	1.00E-01	1.00E+00	1.00E+01	1.00E+01	2.00E-09	1.00E+01
	6 (> 500,000)										
C	1 (> 100)	6.00E-05	6.00E-05	6.00E-05	1.00E+00	3.00E-02	1.00E+00	3.00E+01	3.00E+01	6.00E-05	3.00E+01
	2 (> 1,500)	5.00E-06	5.00E-06	5.00E-06	1.00E+00	3.00E-02	1.00E+00	3.00E+01	3.00E+01	5.00E-06	3.00E+01
	3 (> 5,000)	2.00E-06	2.00E-06	2.00E-06	1.00E+00	3.00E-02	1.00E+00	3.00E+01	3.00E+01	2.00E-06	3.00E+01

Table A.2 (Cont.)

	4 (> 25,000)	3.00E-07	3.00E-07	3.00E-07	1.00E+00	5.00E-02	1.67E+00	1.67E+02	1.00E+02	5.01E-07	1.00E+02
	5 (> 100,000)										
	6 (> 500,000)										
E	1 (> 100)	7.73E-07	2.32E-06	6.96E-06	3.00E+00	5.00E-03	1.25E-01	5.00E-01	4.00E+00	2.90E-07	5.86E+00
	2 (> 1,500)	7.73E-07	2.32E-06	6.96E-06	3.00E+00	5.00E-03	1.25E-01	5.00E-01	4.00E+00	2.90E-07	5.86E+00
	3 (> 5,000)	3.07E-07	9.22E-07	2.77E-06	3.00E+00	1.00E-03	8.50E-02	1.00E+00	1.18E+01	7.84E-08	1.49E+01
	4 (> 25,000)	3.67E-09	1.10E-08	3.30E-08	3.00E+00	3.33E-04	3.33E-02	5.00E-01	1.50E+01	3.66E-10	1.86E+01
	5 (> 100,000)										
	6 (> 500,000)										
G	1 (> 100)	3.03E-09	9.08E-09	2.72E-08	3.00E+00	1.00E-01	1.16E+00	1.00E+01	8.62E+00	1.05E-08	1.12E+01
	2 (> 1,500)	4.77E-10	1.43E-09	4.29E-09	3.00E+00	1.00E-01	1.16E+00	1.00E+01	8.62E+00	1.66E-09	1.12E+01
	3 (> 5,000)	1.67E-10	5.00E-10	1.50E-09	3.00E+00	1.00E-01	1.16E+00	1.00E+01	8.62E+00	5.80E-10	1.12E+01
	4 (> 25,000)	4.70E-11	1.41E-10	4.23E-10	3.00E+00	1.00E-01	1.16E+00	1.00E+01	8.62E+00	1.64E-10	1.12E+01
	5 (> 100,000)	4.54E-12	2.27E-11	1.14E-10	5.02E+00	1.00E-01	1.16E+00	1.00E+01	8.62E+00	2.63E-11	1.48E+01
	6 (> 500,000)										
H	1 (> 100)	2.42E-08	7.25E-08	2.18E-07	3.01E+00	1.00E+00	1.00E+01	1.00E+02	1.00E+01	7.25E-07	1.28E+01
	2 (> 1,500)	3.25E-09	9.75E-09	2.93E-08	3.01E+00	1.00E+00	1.00E+01	1.00E+02	1.00E+01	9.75E-08	1.28E+01
	3 (> 5,000)	1.15E-09	3.45E-09	1.04E-08	3.01E+00	1.00E+00	1.00E+01	1.00E+02	1.00E+01	3.45E-08	1.28E+01
	4 (> 25,000)	3.42E-10	1.03E-09	3.08E-09	2.99E+00	1.00E+00	1.00E+01	1.00E+02	1.00E+01	1.03E-08	1.28E+01
	5 (> 100,000)	9.08E-11	2.73E-10	8.18E-10	3.00E+00	2.00E+00	2.00E+01	2.00E+02	1.00E+01	5.46E-09	1.28E+01
	6 (> 500,000)										
I	1 (> 100)	2.70E-06	8.10E-06	2.43E-05	3.00E+00	1.96E-03	1.96E-02	1.96E-01	1.00E+01	1.59E-07	1.28E+01
	2 (> 1,500)	2.70E-06	8.10E-06	2.43E-05	3.00E+00	1.96E-03	1.96E-02	1.96E-01	1.00E+01	1.59E-07	1.28E+01
	3 (> 5,000)	1.77E-08	5.30E-08	1.59E-07	3.00E+00	3.00E-01	3.00E+00	3.00E+01	1.00E+01	1.59E-07	1.28E+01
	4 (> 25,000)	1.77E-08	5.30E-08	1.59E-07	3.00E+00	3.00E-01	3.00E+00	3.00E+01	1.00E+01	1.59E-07	1.28E+01
	5 (> 100,000)	2.50E-10	5.00E-09	1.00E-07	2.00E+01	3.33E-01	3.33E-01	3.33E-01	1.00E+00	1.67E-09	2.00E+01
	6 (> 500,000)										
J	1 (> 100)	6.84E-12	6.07E-11	1.82E-09	3.00E+01	3.82E+01	3.82E+01	3.82E+01	1.00E+00	2.32E-09	3.00E+01
	2 (> 1,500)	5.07E-13	6.14E-12	5.90E-10	9.61E+01	7.09E+01	7.09E+01	7.09E+01	1.00E+00	4.35E-10	9.61E+01
	3 (> 5,000)	1.20E-13	2.04E-12	2.67E-10	1.31E+02	8.42E+01	8.42E+01	8.42E+01	1.00E+00	1.72E-10	1.31E+02
	4 (> 25,000)	1.63E-14	4.45E-13	1.00E-10	2.25E+02	1.01E+02	1.01E+02	1.01E+02	1.00E+00	4.49E-11	2.25E+02
	5 (> 100,000)	2.58E-15	8.52E-14	3.04E-11	3.57E+02	1.15E+02	1.15E+02	1.15E+02	1.00E+00	9.80E-12	3.57E+02

Table A.2 (Cont.)

	6 (> 500,000)	[redacted]									
L	1 (> 100)	2.62E-06	9.60E-06	3.52E-05	3.67E+00	1.27E-02	1.27E-02	1.27E-02	1.00E+00	1.22E-07	3.67E+00
	2 (> 1,500)	1.58E-06	6.34E-06	2.53E-05	3.99E+00	1.27E-02	1.27E-02	1.27E-02	1.00E+00	8.05E-08	3.99E+00
	3 (> 5,000)	3.84E-07	1.92E-06	9.60E-06	5.00E+00	4.19E-02	4.19E-02	4.19E-02	1.00E+00	8.04E-08	5.00E+00
	4 (> 25,000)	1.54E-07	7.68E-07	3.84E-06	5.00E+00	1.01E-01	1.01E-01	1.01E-01	1.00E+00	7.76E-08	5.00E+00
	5 (> 100,000)	6.40E-08	3.20E-07	1.60E-06	5.00E+00	2.41E-01	2.41E-01	2.41E-01	1.00E+00	7.71E-08	5.00E+00
	6 (> 500,000)	[redacted]									

Notes:

[1] Data shaded in yellow are taken from NUREG-1829 expert questionnaires in Reference [14]. Data shaded in blue were calculated in this study per Notes [2] through [4].

[2] RF = Range Factor of a lognormal distribution defined by the Mid value as the median and by the UB value as the 95%tile.

[3] Median of a lognormal distribution for the 40-year LOCA frequency created by the product of two lognormal distributions: the medians of the lognormal distributions for LOCA frequency for system and the 40-year multiplier (see Equation [4.1])

[4] Range Factor of the 40-year LOCA frequency lognormal distribution (see Equation [4.2]).

HPI Line

Expert ID	LOCA Category	LOCA Frequency for System[1] (Per Reactor-Calendar Year)				40-Yr Multiplier[1]				40-Yr LOCA Frequency[1] (Per Reactor-Calendar Year)	
		LB	Mid	UB	RF95=UB/Mid [2]	LB	Mid	UB	RF95=UB/Mid [2]	Mid[3]	RF95[4]
A	1 (> 100)	8.33E-07	2.50E-06	7.50E-06	3.00E+00	1.00E+00	1.00E+00	1.00E+00	1.00E+00	2.50E-06	3.00E+00
	2 (> 1,500)	8.33E-07	2.50E-06	7.50E-06	3.00E+00	1.50E-02	3.00E-01	5.85E-01	1.95E+00	7.50E-07	3.62E+00
	3 (> 5,000)	8.33E-07	2.50E-06	7.50E-06	3.00E+00	5.00E-03	1.00E-01	1.95E-01	1.95E+00	2.50E-07	3.62E+00
	4 (> 25,000)	8.33E-07	2.50E-06	7.50E-06	3.00E+00	1.50E-03	3.00E-02	5.85E-02	1.95E+00	7.50E-08	3.62E+00
	5 (> 100,000)	8.33E-07	2.50E-06	7.50E-06	3.00E+00	5.00E-04	1.00E-02	1.95E-02	1.95E+00	2.50E-08	3.62E+00
	6 (> 500,000)	[redacted]									
B	1 (> 100)	3.00E-07	3.00E-07	3.00E-07	1.00E+00	2.00E-02	2.00E-01	2.00E+00	1.00E+01	6.00E-08	1.00E+01
	2 (> 1,500)	1.20E-07	1.20E-07	1.20E-07	1.00E+00	2.00E-02	2.00E-01	2.00E+00	1.00E+01	2.40E-08	1.00E+01
	3 (> 5,000)	4.80E-08	4.80E-08	4.80E-08	1.00E+00	2.00E-02	2.00E-01	2.00E+00	1.00E+01	9.60E-09	1.00E+01
	4 (> 25,000)	1.92E-08	1.92E-08	1.92E-08	1.00E+00	2.00E-02	2.00E-01	2.00E+00	1.00E+01	3.84E-09	1.00E+01
	5 (> 100,000)	7.68E-09	7.68E-09	7.68E-09	1.00E+00	2.00E-02	2.00E-01	2.00E+00	1.00E+01	1.54E-09	1.00E+01
	6 (> 500,000)	[redacted]									
C	1 (> 100)	1.00E-04	1.00E-04	1.00E-04	1.00E+00	1.20E-01	4.00E+00	1.20E+02	3.00E+01	4.00E-04	3.00E+01
	2 (> 1,500)	1.00E-04	1.00E-04	1.00E-04	1.00E+00	1.20E-01	4.00E+00	1.20E+02	3.00E+01	4.00E-04	3.00E+01
	3 (> 5,000)	1.00E-05	1.00E-05	1.00E-05	1.00E+00	1.20E-01	4.00E+00	1.20E+02	3.00E+01	4.00E-05	3.00E+01
	4 (> 25,000)										
	5 (> 100,000)										

Table A.2 (Cont.)

	6 (> 500,000)											
E	1 (> 100)	5.33E-06	1.60E-05	4.80E-05	3.00E+00	7.00E-02	3.30E-01	7.00E-01	2.12E+00	5.28E-06	3.79E+00
	2 (> 1,500)	7.73E-07	2.32E-06	6.96E-06	3.00E+00	1.00E-02	2.50E-01	1.00E+00	4.00E+00	5.80E-07	5.86E+00
	3 (> 5,000)	3.07E-07	9.22E-07	2.77E-06	3.00E+00	2.00E-03	1.70E-01	2.00E+00	1.18E+01	1.57E-07	1.49E+01
	4 (> 25,000)										
	5 (> 100,000)										
	6 (> 500,000)										
G	1 (> 100)	2.29E-06	6.87E-06	2.06E-05	3.00E+00	3.00E-01	5.78E-01	3.00E+00	5.19E+00	3.97E-06	7.24E+00
	2 (> 1,500)	3.83E-07	1.15E-06	3.45E-06	3.00E+00	3.00E-01	5.78E-01	3.00E+00	5.19E+00	6.65E-07	7.24E+00
	3 (> 5,000)	7.13E-08	2.14E-07	6.42E-07	3.00E+00	3.00E-01	5.78E-01	3.00E+00	5.19E+00	1.24E-07	7.24E+00
	4 (> 25,000)										
	5 (> 100,000)										
	6 (> 500,000)										
H	1 (> 100)	2.42E-08	7.25E-08	2.18E-07	3.01E+00	1.00E+00	1.00E+01	1.00E+02	1.00E+01	7.25E-07	1.28E+01
	2 (> 1,500)	3.25E-09	9.75E-09	2.93E-08	3.01E+00	1.00E+00	1.00E+01	1.00E+02	1.00E+01	9.75E-08	1.28E+01
	3 (> 5,000)	1.15E-09	3.45E-09	1.04E-08	3.01E+00	1.00E+00	1.00E+01	1.00E+02	1.00E+01	3.45E-08	1.28E+01
	4 (> 25,000)										
	5 (> 100,000)										
	6 (> 500,000)										
I	1 (> 100)	2.70E-06	8.10E-06	2.43E-05	3.00E+00	1.39E+00	2.09E+01	1.25E+02	5.98E+00	1.69E-04	8.16E+00
	2 (> 1,500)	2.70E-06	8.10E-06	2.43E-05	3.00E+00	1.39E+00	2.09E+01	1.25E+02	5.98E+00	1.69E-04	8.16E+00
	3 (> 5,000)	1.77E-08	5.30E-08	1.59E-07	3.00E+00	1.00E-01	1.00E+00	1.00E+01	1.00E+01	5.30E-08	1.28E+01
	4 (> 25,000)	1.77E-08	5.30E-08	1.59E-07	3.00E+00	1.00E-01	1.00E+00	1.00E+01	1.00E+01	5.30E-08	1.28E+01
	5 (> 100,000)										
	6 (> 500,000)										
J	1 (> 100)	1.46E-08	2.72E-07	6.82E-06	2.51E+01	2.31E+01	2.31E+01	2.31E+01	1.00E+00	6.28E-06	2.51E+01
	2 (> 1,500)	4.65E-10	1.41E-08	1.39E-06	9.86E+01	4.02E+01	4.02E+01	4.02E+01	1.00E+00	5.67E-07	9.86E+01
	3 (> 5,000)	1.10E-10	4.60E-09	7.06E-07	1.53E+02	4.29E+01	4.29E+01	4.29E+01	1.00E+00	1.97E-07	1.53E+02
	4 (> 25,000)	9.72E-12	6.77E-10	1.81E-07	2.67E+02	4.68E+01	4.68E+01	4.68E+01	1.00E+00	3.17E-08	2.67E+02
	5 (> 100,000)										
	6 (> 500,000)										
L	1 (> 100)	2.62E-06	9.60E-06	3.52E-05	3.67E+00	4.58E-01	4.58E-01	4.58E-01	1.00E+00	4.40E-06	3.67E+00

Table A.2 (Cont.)

	2 (> 1,500)	1.58E-06	6.34E-06	2.53E-05	3.99E+00	4.58E-01	4.58E-01	4.58E-01	1.00E+00	2.90E-06	3.99E+00
	3 (> 5,000)	3.84E-07	1.92E-06	9.60E-06	5.00E+00	5.25E-01	5.25E-01	5.25E-01	1.00E+00	1.01E-06	5.00E+00
	4 (> 25,000)										
	5 (> 100,000)										
	6 (> 500,000)	[redacted]									

Notes:

[1] Data shaded in yellow are taken from NUREG-1829 expert questionnaires in Reference [14]. Data shaded in blue were calculated in this study per Notes [2] through [4].

[2] RF = Range Factor of a lognormal distribution defined by the Mid value as the median and by the UB value as the 95%tile.

[3] Median of a lognormal distribution for the 40-year LOCA frequency created by the product of two lognormal distributions: the medians of the lognormal distributions for LOCA frequency for system and the 40-year multiplier (see Equation [4.1])

[4] Range Factor of the 40-year LOCA frequency lognormal distribution (see Equation [4.2]).

Table A.3 Status of Communication with Fleming and Lydell for Critical Review of CRP Development for Location-specific Estimation of LOCA Frequencies Methodology

UIUC Question/Issue	Karl Fleming Response
[UIUC] Can you clarify what is meant by selecting option 4 over option 3, "… as it exhibits a larger degree of epistemic uncertainty …" in paragraph 4 of section 4.9?	[KNFCS] This simply means that we selected the option that was a better reflection of the state of knowledge about the frequency of significant pipe ruptures, in our opinion. The CRP model is effectively a way to extrapolate data and any type of extrapolation involves uncertainty. In addition the further out you extrapolate, and in this case that means that we are extrapolating into areas of very low frequency, the uncertainty increases. We use actual data to calculate the failure rates but they are all small leaks and cracks so any attempt to predict frequency of large pipe ruptures must entail a large degree of uncertainty. When quantifying uncertainties, understating their ranges is non-conservative. So we picked the option that did a better job, in our opinion of expressing the correct degree of uncertainty.

Table A.3 (Cont.)

[UIUC] The NUREG-1829 elicitation accounts for the entire fleet of US PWR plants and therefore, is applicable to the VEGP study. However, it is unclear to us what including the base case analysis for a specific PWR design with a specific number of coolant loops, pipe sizes, and weld counts adds to the formulation of the "target" LOCA frequencies that is not captured in the expert elicitation. Also, it is not clear to us that the inclusion of the analysis for a specific PWR design is valid for the analysis of all PWRs, some of which have a different number coolant loops and welds?	[KNFCS] Your response is only addressing one aspect of the difference between Option 3 and Option 4 namely specific plant vs. fleet of plants. In our view the most important difference is the fact that Appendix D and the expert elicitation came up with LOCA frequencies using two fundamentally different methods: Appendix D used a failure rate/ CRP model that is very similar to the approach used for our report where the failure rates are estimated using the same Bayes' update procedure, service data and estimates of weld exposures, etc. The most important element that we wanted to use from Appendix D was a different CRP model than was implicit in the expert elicitation. The expert elicitation was just that. In addition, the plant specific example used in Appendix D was a Westinghouse PWR. Finally, keep in mind that the only part of the expert data that we used was for four systems: hot leg, cold leg, surge line, and HPI line. When we divided out the LOCA initiating event frequencies in converting target LOCA frequencies to CRPs, the question of different number of loops gets cancelled out. We firmly believe that using Method 4 was a better reflection of the state of knowledge than Method 3. Our independent reviewer Dr. Mosleh agreed.
[UIUC] We think that including a summary of your explanation to our questions concerning this issue, in addition to the sensitivity analysis for the selection of option 4 instead of option 3, would help the reader understand the motivation of this choice. The responses have resolved our concerns and we have no further comments.	
This issue was resolved.	
[UIUC] Why is such a heavy weight given to the Lydell base case analysis from Appendix D of NUREG-1829?	[KNFCS] We do not think it is such heavy weight. We gave the NUREGs-1829 input and Appendix D input equal weight because they come from two completely different approaches to estimating LOCA frequency and they also represent different scope of plants. The former is strictly expert opinion and the latter is the result of a LOCA frequency model quantified using data and some individual expert judgment. Also the former are for a fleet of PWR plants and the latter is for one specific PWR design. If you look at Bengt Lydell's input to the elicitation you will see it is not the same as Appendix D because of the scope of plants and systems.
This issue was resolved.	

Table A.3 (Cont.)

[UIUC] Section 4.12 investigates the inclusion of the Lydell base case analysis in the target LOCA frequency development. Is there any statistical evidence to show that the variations of the mean values are not significant in comparison with the CRP uncertainties? If a 15% shift in the mean of the CRP values is insignificant, what does this shift do to the rest of the distribution? Are the changes to the rest of the distribution also insignificant? How much would the mean of the data have to change for there to be a significant variation in the CRP distributions?	[KNFCS] The results for all the key percentiles of the cases with and without Lydell are shown in Table 4-11 so you can see this directly in the report. The conclusion was not just based on the change in the mean.
[UIUC] Excluding the Lydell's result from the GM results in a larger RF, and therefore a broader uncertainty distribution for almost every case in Table 4-11. Therefore, if an increased uncertainty better reflects the state of knowledge about the frequency of significant pipe ruptures, it seems beneficial to exclude the Lydell results from the GM. However, we also believe that resulting numbers should not drive the process, so there is no need to exclude the Lydell data from the GM.	[KNFCS] As a final remark, the main reason for including Lydell results in the first place was that he was providing his input for a broader question than he was providing in Appendix D, the LOCA frequencies for a fleet of PWRs and for the entire reactor coolant system pressure boundary rather than for specific components for a specific design in Appendix D.
This issue was resolved.	
[UIUC] Why was the data for Table 4-4 LOCA case 5 of the HPI line manipulated? It appears that the RF was increased from 6.0 to 18.8, but this adjustment was not made for the surge line, where the case 5 RF is lower than the case 4 RF.	[KNFCS] Do not understand what you mean by manipulated?
[UIUC] In Table 4-4, why was the RF for LOCA Cat. 5 of the Surge Line not increased (from 15.8 to 17.3) in order to match the RF from LOCA Cat. 4 of the Surge Line? The Table shows RF of HPI Line Cat. 5 is increased to match HPI Line Cat. 4 as a means to prevent an illogical trend in RF vs. decreasing frequency.	
This issue was not resolved.	
[UIUC] What is the justification for increasing the range factor of the data in Table 4-9. My understanding is that the RF is increased so that larger breaks, which are less frequent, do not have decreasing uncertainties. However, is there any justification for the numbers that the RFs were increased to, or are they just an expert opinion adjustment?	[KNFCS] They were adjusted to be the same as the RF for the maximum RF for the previous breaks sizes calculated. The justification is to prevent the range factors determined from the mixture distribution to have an illogical trend in RF vs. decreasing frequency – based on what we believe is a reasonable engineering judgment.
This issue was resolved.	
[UIUC] What is the justification for using the HPI priors to update CVCS, SIR, Pressurizer, and Small Bore lines?	[KNFCS] The piping designs are essentially the same – same materials and similar pipe schedules and design codes.
This issue was resolved.	

Table A.3 (Cont.)

[UIUC] The R-DAT output for Hot Leg at SG Inlet for case 5 gives values that are 5% larger for the mean, 5%, median, and 95%, than those reported. What is the reason for this? Were the numbers intentionally adjusted? If so, why?	[KNFCS] Needs further study. There was not manipulation intended.
This issue was not resolved.	
[UIUC] The R-DAT output for the Small Bore differs significantly from the values in Table 4-10. Additionally, the small bore values appear to be manipulated as the 5% listed is larger than the median values listed. What manipulation was performed to this data? Why?	[KNFCS] Needs further study. There was not manipulation intended.
This issue was not resolved.	
[UIUC] Some of the range factors for the cold leg (cases 1,3), hot leg (cases 2,5,6), surge line (case 1) appear to be varied. This could be intentional manipulation or simply a failure to replicate the data analysis. Are there Excel files available for cases other than the hot leg that the recreation results can be benchmarked against?	[KNFCS] Needs further study. There was not any manipulation intended.
This issue was not resolved.	

Table A.4 Status of Communication with Fleming and Lydell for Critical Review of Final LOCA Frequency Distributions for Location-specific Estimation of LOCA Frequencies Methodology

UIUC Question/Issue	Karl Fleming Response
[UIUC] Hot Leg case 1A, failure model of 2.0 label was skipped in the table and all of the values were shifted downward, ultimately not giving a value for failure mode of 41.0	[KNFCS] You are correct this is a typo which is corrected in the attached file. The values in Table 5-1 which was used for input to Casagrande are correct.
[UIUC] In the updated report, the value listed in Table 5-1 for case 1A, break size 41.01 is 1.53E-09, which does not match the mean value shown in Table 5-5 of 1.32E-09. We were able to successfully recreate the value listed in Table 5-1. However, the distribution (mean, 5%, median, 95%) values for the updated case in Table 5-5 are 15% lower than the values we were able to recreate. Please explain this difference.	
This issue was not resolved.	
[UIUC] The failure rates for cases 4A, 4B(&4D), and 4C do not match those from Table 3-12. It appears that the failure rates for 4B and 4C were switched, but also adjusted	[KNFCS] Yes they do not match because Table 3-12 shows the results of the monte carlo mixture distributions for the total failure rate. As explained in Section 5 near these tables we calculated the unconditional LOCA frequencies using two methods, one via Monte Carlo propagation of the Monte Carlo derived failure rates and the CRP distributions and the other using formulas for combining the product of two lognormal distributions which are used as the official results. For that step it was necessary to fit the MC failure rate distributions to Lognormal. This was done by fitting the median to the GM of the 5th and 95th percentiles and using the RF calculated using these same percentiles. You and I have discussed this earlier on several occaisions. That is why the failure rate distributions in these tables are generally not the same as those in Table 3-12. In only a few cases where the RF is small did these come out the same.

Table A.4 (Cont.)

[UIUC] We apologize for not making the question clearer. For every calculation case in Table 5-5, except for cases 4A, 4B(&4D), and 4C, the 5% and 95% values are exactly the same as those listed in Table 3-12. From these values, we were able to successfully recreate the failure rates listed in Table 5-5 with a very small amount of variation, using the method that we have discussed. However, the 5% and 95% values listed in Table 5-5 for the cases 4A, 4B(&4D), and 4C are different from the values listed in Table 3-12. Please clarify why these values are not the same as those listed in Table 3-12.	
This issue was not resolved.	
[UIUC] For case 4B, all of the 95% values were shifted. This is clear from the mean, 5%, median, and RF for each failure mode matching the report data very well, while only the 95% column is drastically different (>125% for each failure mode)	[KNFCS] Yes the data for the 95%values in Table 5-4 were copied wrong and in fact they repeat values from the 5% column. I have corrected that in the revised report..
[UIUC] Using the 5% and 95% failure rate values listed in Table 5-5 of the updated version of the report, we were able to recreate the updated values for case 4B from the updated version of the report. Thank you, we have no further comment.	
This issue was not resolved.	
[UIUC] Table 3-12 gives 5E its own failure rate, but Table 5-5 clumps 5E in with 5C, 5D, & 5H. Should the cases be separate or combined? How is the failure rate and conditional probability chosen to calculate the LOCA distributions (from which Table 3-12 cases and why?)?	[KNFCS] In tracking this down I found some weld case labeling problems in Table 3-12 and 5-5. The weld case labels in Table 3-2 and Tables 5-1 through 5-4 are correct but in the revised report I have corrected the mentioned label issues for Table 5-5 and 3-12. If you look at note [1] in Table 5-5 it is explained that when weld cases only vary by pipe size (i.e. have the same weld type and DM combinations) they are combined in this table because the only difference is which break size they are cut off at. I have modified this note to explain that the appropriate break size cutoffs are shown in Tables 5-1 through 5-4.
This issue was resolved.	
[UIUC] Table 3-12 separates cases 7D and 7M, but in Table 5-5 they are clumped together. They have the same failure rate in Table 3-12, but it is justifiable to clump them together since they are technically in different cases?	[KNFCS] The only different is the pipe size so the one with the smaller pipe size has a different DEGB size that is the only difference. This is taken care of in Tables 5-1 through 5-5. This is explained in note [1] for Table 5-5
This issue was resolved.	
[UIUC] Table 3-12 separates 8F from 8C&8D, but they are clumped together in Table 5-5. 8C&8D are affected by Vibrational fatigue, but 8F is not. Is this justifiable?	[KNFCS] Yes because we do not make the failure rates conditional on VF as a damage mechanism because VF is not evaluated in the EPRI RI-ISI. VF is only listed because some of the failures identified in the failure query involve VF.
[UIUC] The failure rate for category 8C&8D is larger than the failure rate for the 8F category. This is due to the contribution to VF that the 8F category does not include. Inclusion of the 8F weld into the 8C&8D category would increase the contributions to the total frequency of VF, by applying its failure contribution to a weld that is not affected by it. Is this done to increase the conservatism of the report?	
This issue was not resolved.	
[UIUC] Table 5-1 calculation cases 3B, 3D for break size of 43.80 use the data from Table 5-5 break size of 44.5. Should the break size in Table 5-1 be 44.5 or should there be another value calculated for 43.8?	

Table A.4 (Cont.)

[UIUC] It appears that the numbers used in Table 5-1 for the mean values for the break sizes of 43.8 for cases 3B and 3D simply use the values from the Table 5-5 break sizes of 44.5. After recalculating these values for a break size of 43.8, the results give values of 3.21E-10 (for 3B) and 1.94E-12 (for 3D), corresponding to 2.5% and 2.8% increases over the values published in Table 5-1. Is the motivation for using the values calculated for break sizes of 44.5 that these differences are considered insignificant?	
This issue was not resolved.	
[UIUC] Table 5-5 lists case 5F as its own case, but the values for case 5F in Table 5-2 correspond with case J in Table 5-5. Which is correct?	[KNFCS] See above – this is a labeling problem which I fixed in the revised report
This issue was resolved.	
[UIUC] Table 5-5 lists case 5G as its own case, but the values for case 5G in Table 5-2 correspond with case 5-F in Table 5-5. Which is correct?	[KNFCS] See above – this is a labeling problem which I fixed in the revised report
This issue was resolved.	
[UIUC] Table 5-5 lists case 5H with cases 5C, 5D, and 5E, but the values for case 5H in Table 5-2 correspond with case 5G in Table 5-5. Which is correct?	[KNFCS] See above – this is a labeling problem which I fixed in the revised report
This issue was resolved.	
[UIUC] Table 5-5 lists calculation case 5I with cases 5A and 5B, but the values in Table 5-2 would place 5I with cases 5C, 5D, 5E, and 5H. Which one is correct?	[KNFCS] See above – this is a labeling problem which I fixed in the revised report
This issue was resolved.	
[UIUC] Table 5-5 lists calculation case 5J as its own case, but the values in Table 5-2 would place 5J with cases 5A, 5B, and 5I. Which one is correct?	[KNFCS] See above – this is a labeling problem which I fixed in the revised report
This issue was resolved.	
[UIUC] The numbers for case 7N in Table 5-5 do not match the numbers for case 7N in Table 5-4, which numbers are correct?	[KNFCS] Do not understand comment. I just checked and the numbers in these two tables are identical
[UIUC] It appears this is a labeling/copying issue with the report. The numbers beginning with a break size of 5.66 do not match the values calculated in Table 5-5. Since Table 5-4 skips some of the break sizes calculated in Table 5-5, extra values are copied to Table 5-4. Ex. Table 5-4, BS of 5.66 is listed as 7.09E-10, but is listed as 6.19E-10 in Table 5-5. Another example can be seen for BS of 16.97, where 5-4 lists 7.56E-11 and 5-5 lists 3.11E-08. This same labeling/copying issue appears to have occurred for case 7O as well.	
This issue was not resolved.	

Table A.4 (Cont.)

[UIUC] There were many values that I could not replicate using strictly the data available from the report. Would you please offer any explanation or potential reasoning as to why my calculations do not replicate your own? In the attached Excel file ("STP KF ch5 LOCA Frequencies for STP GSI-191 Application (Step 3)"), under the table labeled "Table 5-5" the values that do not match the results from the report are highlighted so that they can be easily seen.	[KNFCS] As we discussed a while back when we were looking at the hot leg weld calcs the STP values were developed using randomized seeds for the monte carlo trials so even on the same computer one would get some random behavior. Then even if you are fixing the seed you may get different results on different computers depending on all kinds of things such as 32bit vs.64 bit versions of excel (I use 32bit). When you look at the standard error in the mean for the cases we ran you typically see errors in the mean due to sampling of plus or minus 5 to 10%. Given the relatively low frequency of exceeding this error magnitude in your table I would say overall your numbers are in pretty good agreement. Your thorough checking has greatly helped identify some errors in transcribing data from excel to word which I appreciate. Fortunately none identified here impact the numbers fed into CASAGRANDE but will help to clearnup the report. Your results for 6A and 6B indicated something other that MC noise so could you please send me your excel sheets for these so I can see what the source of the difference is.
[UIUC] Our discussion a while back concerning random sampling apparently does not apply for the quantification of Table 5-5 (and Tables 5-1 – 5-4), because the data from Table 5-5, as it is stated in section 5.2 of the report, is calculated using formulas for combining the product of two lognormal distributions. The input data to these calculations was taken directly from the published values in Tables 3-12 and 4-10. Therefore, there is no effect from sampling, as there was no sampling performed in these calculations. The recreation of the report values has been with a 64-bit version of Excel, so it is likely that this accounts for some of the small variations in the numbers of the report. However, it is not likely that this would result in standard errors of 5-10%. Also, there are calculation cases, such as a BS of 4.24 in the Pressurizer categories, which are significantly different from the reported values, despite all or most of the other break sizes in those categories being recreated with a high degree of accuracy. All of the data recreation was performed using the values of Tables 3-12, 4-10, and the lognormal equations. Therefore, all of the work done in Excel is contained in the file included with the questions.	
This issue was not resolved.	
[UIUC] For the first bullet point in Section 5.4, what is the statistical validation for claiming that the results are in good agreement? Table 5-6 displays the mean values, but mean values can be very misleading. What are the associated range factors?	[KNFCS] There is no statistical validation for the statement but we do not think one should be necessary. This is just a statement from reviewing the numbers and should be self explanatory.
This issue was resolved.	

APPENDIX B: COMPLETE EVIDENCE TABLES FOR INVESTIGATIVE PROCEDURE TO DETERMINE THE SIGNIFICANCE OF THE INCLUSION OF NON-PIPING COMPONENTS INTO THE ESTIMATIONS OF LOCA FREQUENCIES

PRESSURIZER

Component	Highlight	Author	GSI-191 Evidence	Expert Comments
Thermal/heater sleeve	Table 15.2 Summary of degradation processes for pressurizers [1] 1989 – 20 leaking sleeves at Calvert Cliffs 2. 1994 – Calvert cliffs 1 2 leaking sleeves. 1997 – St. Lucie 1 – 1 leaking sleeve. 2000- ANO-2 12 leaking sleeves [2] Calvert cliffs 2008, Palo Verde Unit 3 in 2004 [3] "In May 1989, approximately 20 of 120 heater sleeves were found to be leaking in the Calvert Cliffs Unit 2 pressurizer." [4]	Idaho National Lab [1] (1989) VTT technical research center of Finland [2] (2006) US NRC [3] (2012) Babcock & Wilcox [9] (1992) Dominion Engineering [4] (1992) Duke Energy Corporation [5] (2001) Idaho National Lab [6] (1990) Brookhaven National Lab [7] (2008)	"There is no reverse flow in the spray line that would allow a broken thermal sleeve to be carried into the RCS cold leg, but it is possible that a broken surge line thermal sleeve could be swept into the hot leg during an outsurge, depending on the design." "It is not likely that these thermal sleeves could become loose parts in the RCS or pressurizer." "An indication of a crack was discovered in a thermal sleeve of a Westinghouse pressurizer surge nozzle." "Failure of heater sleeve welds has the potential of becoming a serious problem because it is possible that these sleeves could blow out and result in an unisolable small-break LOCA." [1] "The staff therefore concludes that PWSCC is an applicable aging effect for the pressurizer surge and spray nozzle thermal sleeves.	The sleeves are pretty small, but they could be a SBLOCA concern. Not included in GSI-191 The thermal/ heater sleeves are welded in some reactor designs, but not in other designs. We do not believe that the thermal/ heater sleeves have been included in STP LOCA development.

	Table 3.1-1 Aging Management Review Results; “Loss of Material” [5] “Operating transients, thermal shocks, stratified flows, and flow-induced vibrations cause fatigue damage to surge and spray lines, nozzles, and thermal sleeves” [6] PWSCC cracking occurred: Millstone 2, 2/19/2002 Arkansas Nuclear 2, 7/30/2000 Palo Verde 2, 10/4/2000 Waterford 3, 10/17/2000 Braidwood Unit 1, spring 2006 “ Since the late 1980's, approximately 50 Alloy 600 pressurizer heater sleeves at Combustion Engineering-	U.S. Nuclear Regulatory Commission [10] (2003) U.S. Nuclear Regulatory Commission [11] (2008) U.S. Nuclear Regulatory Commission [8](2008)	However, neither of these sleeves are welded to the nozzles. Therefore, growth of a PWSCC-induced sleeve crack into the nozzles will not be of concern for the pressurizer surge or spray nozzles…is not an aging effect that needs to be managed during the extended periods of operation for the St. Lucie units.“[10] Table 7.10, “Additionally, in PWR plants, steam generator tubes and pressurizer heater sleeves are important contributors.”, “For LOCA Category 1, the large non-piping contribution is provided by steam generator tubes, CRDM penetrations, and pressurizer heater sleeves (Section 6.3.1).” “It was almost universally expressed that the contribution to the overall LOCA frequencies is greater for the non-piping components than for piping for the smaller category LOCAs in PWR plants. Specifically, steam generator tube, CRDM, and pressurizer heater sleeve failures are expected to be the most important Category 1 and 2 total LOCA frequency contributors.”[11]	

	designed (CE-designed) facilities in the United States have shown evidence of RCPB leakage which has been attributed to PWSCC.” [7] Table B.1.13, “Heater sleeves fail due to PWSCC, but as a result of their size, multiple failures are required in order to result in a LOCA.”, Table H.2 Summary of Non-Pipe Database by Plant Type and Piece Part [8]			
Manway bolts/studs	“… the only degradation effects that are potentially significant to pressurizer subcomponents during an extended period of operation are: fatigue of …, the	Westinghouse Electric Company LLC [14] (2000) Idaho National Lab [1] (1989)	“Pressurizer manway bolts can be and have been damaged by leaking primary coolant, which causes stress corrosion cracking. Leakage of borated coolant can also cause corrosion”[1]	Like the steam generators, these manways could cause a lot of damage if they fail. Not included in GSI-191

	manway bolts …"[14] Structural steel bolt loosened from vibration at Three Mile Island 1 2/1/2001 [7] "The upper head of the pressurizer has several potential leakage points. These include the four nozzle-to-safe end welds (Alloy 600 welds) and several bolted connections consisting of the pressurizer manway and the two sets of bolted connections for each pressurizer safety valve. The insulation is removed from the manway cover every refueling outage for the inspection of the manway bolts. " [15] Table B.1.13, "Manway failures would result by	Duke Energy Corporation [5] (2001) Brookhaven National Lab [7] (2008) Southern Nuclear Operating Company [15] (2002) U.S. Nuclear Regulatory Commission [11] (2008) U.S. Nuclear Regulatory Commission [8](2008)	Table 3.1-1 Aging Management Review Results "Loss of Material" [5] "Also, bolting failures are only expected to lead to a LOCA if multiple bolts fail due to common causes, such as improper installation and inspection, or the emergence of degradation mechanisms such as steam cutting or boric acid corrosion which affect multiple bolts." "The major PWR non-piping contributors are nozzles and component bodies for LOCA Categories 3 and 4; the manways and component bodies for Category 5; and the component bodies for Category 6."[11]	Only a potential issue given multiple bolt failure

	multiple bolt failures."[8]			
Instrument nozzles	Table 3.1-1 Aging Management Review Results; "Loss of Material" [5] "The team prepared a summary of industry experience for each of the main types of applications where PWSCC has occurred. These are reactor vessel head CRDM/CEDM nozzles (to be reported elsewhere), small diameter instrument/ vent nozzles" Table 1-1 Chronology of Key Events Relating to PWSCC of Alloy 600 Type Materials in Non-Steam Generator Tubing PWR Plant Applications:	Duke Energy Corporation [5] (2001) Electric Power Research Institute [12](2003) Korea Advanced Institute of Science and Technology [13] (2010) U.S. Nuclear Regulatory Commission [11] (2008) U.S. Nuclear Regulatory Commission [8](2008)	"Nozzle failures are a concern because system and transient stresses can be highest at these locations. Additionally, past degradation has been experienced in these locations." "The major PWR non-piping contributors are nozzles and component bodies for LOCA Categories 3 and 4; the manways and component bodies for Category 5; and the component bodies for Category 6."[11]	We have replaced CRDM and reactor vessel head with Alloy 690. We have also reduced the head temperature to reduce failure likelihoods. Also, there have been many CRDM leaks and J-Weld failures without any major problems. Instrument nozzles addressed in bottom-up approach. PWSCC susceptibility exists only for B&W and CE plants. Current fleet has implemented mitigation. Extremely low likelihood of debris formation Instrument nozzles addressed in bottom-up approach. PWSCC susceptibility exists

	1986 – leak at San Onofre Unit 3 1989 – leaks in two EDF plants (Nogent 1 and Cattenom 2) and circumferential cracks in Belleville 1 and Flamanville 2 1993- crack at St. Lucie 2 Stress relieved pressurizer instrument nozzle at ANO-1 in 1990 [12] Table H.2 Summary of Non-Pipe Database by Plant Type and Piece Part [8]			only for B&W and CE plants. Current fleet has implemented mitigation. Extremely low likelihood of debris formation
Walls/ vessel shell	Table 15.2 Summary of degradation processes for pressurizers, “The key fatigue degradation sites are calculated to have high usage factors and include the pressurizer walls near the usual steamwater interface … susceptible to	Idaho National Lab [1] (1989) Nuclear Management Company [16] (2007) Brookhaven National Lab [7] (2008) Duke Energy Corporation [5] (2001)	“The Pressurizer shell and the outside of the support skirt is insulated with Mineral Wool aluminum jacketing and wire mesh.”[16]	Similar to comment above, this is interesting for GSI-191…

	thermal aging (embrittlement) and erosion."[1] PWSCC crack 11/4/2003 Three Mile Island 1 [7] Table 3.1-1 Aging Management Review Results, "Loss of Material" [5] Table B.1.13, "The shell failure envisioned would most likely occur by boric acid wastage from the outer diameter of the B-33shell." [8]	U.S. Nuclear Regulatory Commission [8](2008)		
Valve bonnet bolts	Table H.2 Summary of Non-Pipe Database by Plant Type and Piece Part [8]	U.S. Nuclear Regulatory Commission [8](2008) U.S. Nuclear Regulatory Commission [11] (2008)	"Also, bolting failures are only expected to lead to a LOCA if multiple bolts fail due to common causes, such as improper installation and inspection, or the emergence of degradation mechanisms such as steam cutting or boric acid corrosion which affect multiple bolts."[11]	

Bolted relief valve	Table B.1.13 [8]	U.S. Nuclear Regulatory Commission [8](2008) U.S. Nuclear Regulatory Commission [11] (2008)	"Bolted relief valves could fail due to steam cutting or localized bolt corrosion resulting from boric acid leaks."[8] "Also, bolting failures are only expected to lead to a LOCA if multiple bolts fail due to common causes, such as improper installation and inspection, or the emergence of degradation mechanisms such as steam cutting or boric acid corrosion which affect multiple bolts."[11]	
Spray head	Table 15.1 Key PWR components for residual life assessment [17] Table 15.2 Summary of degradation processes for pressurizers, "The key fatigue degradation sites are calculated to have high usage factors and include the pressurizer walls near the usual steamwater interface, the spray head, and the spray and surge line	Idaho National Lab [17] (1987) Idaho National Lab [1] (1989)	Erosion, embrittlement, or fatigue. Direct contact with coolant.	This is interesting because it is talking about the vessel walls. We should look into this and find out what the exposure may be. The pressurizer has a large volume of liquid in it and there would be a very large break potential (much bigger than a pipe)

	nozzles. The cast stainless steel spray heads are also susceptible to thermal aging (embrittlement) and erosion."[1]			
Support skirt and immediately surrounding insulation	"… the only degradation effects that are potentially significant to pressurizer subcomponents during an extended period of operation are: fatigue of …, and the support skirt …"[14] Table 3.1-1 Aging Management Review Results "loss of material" [5]	Westinghouse Electric Company LLC [14] (2000) Nuclear Management Company [16] (2007) Duke Energy Corporation [5] (2001)	Coolant flows through support skirt, so failure could lead to debris entering coolant, or accumulating on containment floor. "The Pressurizer shell and the outside of the support skirt is insulated with Mineral Wool aluminum jacketing and wire mesh."[16]	Not sure about this. I didn't think the support skirt had flow through it. Not included in GSI-191 – not a pressure boundary component
Seismic lugs	Table 15.1 Key PWR components for residual life assessment [17] Table 3.3 shows seismic lug usage factor of 0.947 [1]	Idaho National Lab [17] (1987) Idaho National Lab [1] (1989) U.S. NRC [18] (2000)	"The seismic lug welds are inaccessible due to seismic lug restraints and the configuration of the Pressurizer coffin."[18]	I am not sure if seismic lugs are included in the KF analysis, although I believe that it is not. Correct – not included

	"… the only degradation effects that are potentially significant to pressurizer subcomponents … seismic support lugs…" [14]	Westinghouse Electric Company LLC [14] (2000)		
Power-operated relief valve (PORV)	"…a stuck-open PORV has the potential to overwhelm the PRT [pressure relief tank], causing burst disk rupture, debris generation, and pool formation in the containment." [19] "The thermal-hydraulic transient of a PWR during the pressurizer power-operated relief valve (PORV) stuck-open accident is characterized by the lowest break flow rate due to the highest break locations as compared to the other small break LOCA	Los Alamos National Laboratory [19] (2002) Institute of Nuclear Energy Research [20] (1998) Japan Atomic Energy Research Institute [24] (1990) Lockheed Martin Idaho Technologies Company [21] (1998) Brookhaven National Lab [7] (2008) U.S. Nuclear Regulatory Commission [22] (1995)	"…a stuck-open PORV has the potential to overwhelm the PRT [pressure relief tank], causing burst disk rupture, debris generation, and pool formation in the containment." [19]	This isn't a concern for GSI-191 (at least at STP) because the water goes to the PRT and it doesn't have insulation around it. As a historical note, a key driver for the GSI-191 issue was the July 1991 SRV rupture disc failure at the Swedish Barseback unit – see the NRC KM report for details If the contributions from active failures were to be considered, a stuck-open PORV would need to be included. Without active failure inclusion, we do not believe that

	(Kukita et al., 1990a).” [20] Table 3-1 Frequency estimates of functional impact categories: mean, percentiles, and trends, Pressurizer PORV stuck open 1.0E-3 (mean frequency per critical year) [21] “Palisades in 1993 where leakage was observed and attributed to a circumferentially-oriented PWSCC flaw in a line leading to the unit’s power operated relief valves.” [7] “On September 11, 1995, the Limerick Unit 1 plant was being operated at 100 percent power when control room personnel observed alarms and other indications that one SRV ("M") was open. Emergency	Idaho National Laboratory [23] (2007)		the PORV can contribute in a significant way to the GSI-191 issue.

	procedures were implemented. Attempts to close the valve were unsuccessful and within 2 minutes a manual reactor scram was initiated." [22] Power-Operated Relief Valve Fail to Close, 5 failures in 5054 hours/demands [23]			
Spray line nozzle	Table 15.1 Key PWR components for residual life assessment [17] Table 15.2 Summary of degradation processes for pressurizers, "The spray line head, nozzle, and thermal sleeve are susceptible to fatigue damage caused by the subcooled spray actuations associated with power changes."[1]	Idaho National Lab [17] (1987) Idaho National Lab [1] (1989) Idaho National Lab [6] (1990) Duke Energy Corporation [5] (2001) American Society of Mechanical Engineers [25] (2007)	Welded nozzle [25] "Nozzle failures are a concern because system and transient stresses can be highest at these locations. Additionally, past degradation has been experienced in these locations."[11]	The spray line might have issues. The other stuff (except the nozzle) is pretty much in the pressurizer. Covered in STP analysis, so no additional contribution

	"Operating transients, thermal shocks, stratified flows, and flow-induced vibrations cause fatigue damage to surge and spray lines, nozzles, and thermal sleeves" [6] Table 3.1-1 Aging Management Review Results; "Loss of Material" [5] Table B.1.13, Table H.2 Summary of Non-Pipe Database by Plant Type and Piece Part [8]	U.S. Nuclear Regulatory Commission [11] (2008) U.S. Nuclear Regulatory Commission [8](2008)		
Surge line nozzle	Table 15.1 Key PWR components for residual life assessment [17] Table 15.2 Summary of degradation processes for pressurizers, "The key fatigue degradation sites are	Idaho National Lab [17] (1987) Idaho National Lab [1] (1989) Idaho National Lab [6] (1990)	Welded nozzle [25] "Nozzle failures are a concern because system and transient stresses can be highest at these locations. Additionally, past degradation has been experienced in these locations."[11]	Again, the spray line is an issue, but the spray head, thermal sleeve, etc, are inside. Covered in STP analysis, so no additional contribution

	calculated to have high usage factors and include the pressurizer walls near the usual steamwater interface, the spray head, and the spray and surge line nozzles. The cast stainless steel spray heads are also susceptible to thermal aging (embrittlernent) and erosion."[1] "Operating transients, thermal shocks, stratified flows, and flow-induced vibrations cause fatigue damage to surge and spray lines, nozzles, and thermal sleeves"[6] Table 3.1-1 Aging Management Review Results; "Loss of Material" [5] Table B.1.13,	Duke Energy Corporation [5] (2001) American Society of Mechanical Engineers [25] (2007) U.S. Nuclear Regulatory Commission [11] (2008) U.S. Nuclear Regulatory Commission [8](2008)		

	Table H.2 Summary of Non-Pipe Database by Plant Type and Piece Part [8]			
Surge line	Table 15.3 Summary of degradation processes for pressurizer surge and spray lines and nozzles, “The potential failure mode (for both the surge line and spray lines) is a through-wall crack leading to leakage of the coolant.” “A break in a surge or spray line would be an unisolatable breach of the primary coolant pressure boundary and could create a severe thermal-hydraulic transient.” [1] “In the US, Trojan plant reported unexpectedly large piping displacements due to thermal	Idaho National Lab [1] (1989) Korea Institute of Nuclear Safety [26] (2011) Budapest University of Technology and Economics [28] (2008) Idaho National Lab [6] (1990) Korea Institute of Nuclear Safety [29] (2007) Burns and Roe Inc. [30] (1981) Pacific Northwest National Lab [27] (1997)	“There have been no PWR pressurizer surge or spray line failures to date.” “ There have been no known failures or cracks in the pressurizer surge and spray line piping or nozzles in any PWR. However, stratified flows and thermal striping have caused through-wall thermal fatigue cracks in the welds and stainless steel base metal of the safety injection and residual heat removal piping. In safety injection piping, the cracks were between the safety injection nozzle and the first check valve. 13, 18.19 In residual heat removal piping, the cracks were in the horizontal pipe section upstream of the first isolation valve.” [1] “The maximum equivalent stress and deflection for insurge case are almost the same as those for out-surge case, and the fatigue usage factors due to thermal stratification are relatively very low.” [26]	This is related to the spray line which can cause debris. Covered in STP analysis, so no additional contribution

	stratification, which resulted in crushed insulation"[26] "Operating transients, thermal shocks, stratified flows, and flow-induced vibrations cause fatigue damage to surge and spray lines, nozzles, and thermal sleeves"[6] Table 3.1 – CDF median of 6.38E-09 [27]	U.S. Nuclear Regulatory Commission [8] (2008)	"In the US, Trojan plant reported unexpectedly large piping displacements due to thermal stratification, which resulted in crushed insulation"[26] "The potential for large amounts of insulation debris reaching the sump from inside the shield wall exist. Two partial floors exist within the shield wall at El. 605'-4" and El. 609'-1". Although these floors will capture much of the insulation, some could pass through the gap between the two floors to reach the sump. Any insulation below the floor at El. 606'-0" and El. 605'-4" will reach the basement floor. In the region surrounding the sump, there exists several pipes above the sump. The largest of these pipes is a 10 inch residual heat removal pipe. A pipe break could dislodge the insulation from these pipes and the insulation could land on the sump. " [30] Table D.B.4 PWR-2 – Pressurizer Surge Line, "Relative to PWRs of Westinghouse design, the pipe failure database includes no records on through-wall flaws in large-diameter pressurizer surge line welds."[8]	

References

[1] A. Amar and et al. Residual life assessment of major light water reactor components -- overview. U.S. Nuclear Regulatory Commission. 1989.

[2] H. Hanninen, P. Aaltonene, A. Brederhold, U. Ehrnsten, H. Gripenberg, A. Toivonen, J. Pitkanen and I. Virkkunen, "Dissimilar metal weld joints and their performance in nuclear power plant and oil refinery conditions," Julkaisija-Utgivare, Finland, Tech. Rep. VTT Research Notes 2347, 2006.

[3] R. Borchardt, "Closure options for generic safety issue - 191, assessent of debris accumulation on pressurized water reactor sump performance," U.S. Nuclear Regulatory Commission, Tech. Rep. SECY-10-0113, August 26. 2010.

[4] J. E. Nestell, "Safety evaluation for pressurizer heater sleeve cracking," in *EPRI Workshop on PWSCC of Alloy 600 in PWRs,* 1991, pp. E41-E420.

[5] Duke Energy Corporation, "Application to renew the operating licenses of McGuire nuclear station, units 1 & 2 and catawba nuclear station, units 1 & 2," June. 2001.

[6] V. Shah, A. Ware, D. Conley and P. MacDonald, "AGING ASSESSMENT OF PWR SURGE AND SPRAY LINES AND LWR COOLANT PUMPS," in *Nuclear Engineering and Design*Anonymous 1990, pp. 329 - 342.

[7] J. Nie, J. Braverman, C. Hofmayer, Y. Choun, M. Kim and I. Choi, "Identification and assessment of recent aging-related degradation occurrences in US nuclear power plants," *BNL Report-81741-2008, KAERI/RR-2931/2008, Brookhaven National Laboratory*, 2008.

[8] R. Tregoning, L. Abramson and P. Scott, "Estimating loss-of-coolant accident (LOCA) frequencies through the elicitation process appendices A through M," U.S. Nuclear Regulatory Commission, Washington, D.C., Tech. Rep. NUREG-1829 Vol. 2, April. 2008.

[9] L. Dixon, F. Snow and K. Stuckey, "Two piece pressurizer heater sleeve,", 1992.

[10] H. Ashar and et al., "Safety evaluation report related to the license renewal of st. lucie nuclear plant, units 1 and 2," U.S. Nuclear Regulatory Commission, Tech. Rep. NUREG-1779, September. 2003.

[11] R. Tregoning, L. Abramson and P. Scott, "Estimating loss-of-coolant accident (LOCA) frequencies through the elicitation process," U.S. Nuclear Regulatory Commission, Tech. Rep. NUREG-1829, April. 2008.

[12] Dominion Engineering Inc., "Materials reliability program PWSCC of alloy 600 type materials in non-steam generator tubing applications — survey report through june 2002: Part 1: PWSCC in components other than CRDM/CEDM penetrations (MRP-87)," EPRI, Palo Alto, CA, Tech. Rep. 1007832, June. 2003.

[13] J. Hong and C. Jang, "Probabilistic fracture mechanics application for alloy 82/182 welds in PWRs," in *ASME 2010 Pressure Vessels and Piping Division/K-PVP Conference,* 2010, pp. 327-333.

[14] R. Sylvester and M. Gray, "License renewal evaluation: Aging management evaluation for pressurizers," Westinghouse Electric Company, LLC, Pittsburgh, PA, Tech. Rep. WCAP-14574-A, December. 2000.

[15] J. Beasley, "Vogtle electric generating plant - units 1 and 2 60-day response to NRC bulletin 2002-01 item 3," Southern Nuclear Operating Company, Tech. Rep. LCV-1608-C, 2002.

[16] Palisades Nuclear Plant, "Withdrawal of license amendment request to remove TSP from palisades containment," Nuclear Management Company, LLC, February 28. 2007.

[17] R. Cloud, J. Cook, M. Daye, W. Hopkins, L. House, V. Malhorta, H. Mantle, W. Mikesell, G. Odette, R. Ritchie, W. Server and V. Shah, "Residual life assessment of major light water reactor components - overview," EG&G Idaho, Inc., Idaho Falls, Idaho, Tech. Rep. NUREG/CR-4731, June. 1987.

[18] A. Mendiola, "Letter to Oliver D. Kingsley, Subject: Evaluation of the Second 10-Year Interval Inservice Inspection Program Requests for Relief for Braidwood Station, Units 1 and 2 (TAC NOS. MA7304 AND MA7305)," January 6, 2000.

[19] K. Ross, D. Rao and S. Ashbaugh. GSI-191: Thermal-hydraulic response of PWR reactor coolant system and containments to selected accident sequences. Los Alamos National Laboratory. 2002.

[20] T. Liu, C. Lee and C. Chang, "Power-operated relief valve stuck-open accident and recovery scenarios in the Institute of Nuclear Energy Research integral system test facility," *Nucl. Eng. Des.,* vol. 186, pp. 149-176, November 1, 1998.

[21] J. Poloski, D. Marksberry, C. Atwood and W. Galyean, "Rates of initiating events at U.S. nuclear power plants: 1987-1995 (DRAFT)," Lockheed Martin Idaho Technologies Company, Idaho Falls, Idaho, Tech. Rep. NUREG/CR-5750, December. 1998.

[22] D. Crutchfield, "Information notice no. 95-47: Unexpected opening of a safety/relief valve and complications involving suppression pool cooling strainer blockage," U.S. Nuclear Regulatory Commission, Tech. Rep. NRC Information Notice 95-47, October 4. 1995.

[23] S. Eide, T. Wierman and C. Gentillon, "Industry-average performance for components and initiating events at U.S. commercial nuclear power plants," Idaho National Laboratory, Tech. Rep. NUREG/CR-6928, February. 2007.

[24] Y. Kukita, K. Tasaka, H. Asaka, T. Yonomoto and H. Kumamaru, "The effects of break location on PWR small break LOCA: Experimental study at the ROSA-IV LSTF," in *Nuclear Engineering and Design*Anonymous Elsevier, 1990, pp. 255 - 262.

[25] F. Simonen, S. Gosselin, G. Wilkowski, D. Rudland and H. Xu. Calculations to benchmark probabilistic fracture mechanics computer codes. Presented at PVP2007: 2007 ASME Pressure Vessels and Piping Division Conference. 2007, .

[26] D. Kang, M. Jhung and S. Chang, "Fluid–structure interaction analysis for pressurizer surge line subjected to thermal stratification," in *Nuclear Engineering and Design*Anonymous 2011, pp. 257 - 269.

[27] T. Vo, H. Phan, B. Gore, F. Simonen and S. Doctor, "A pilot application of risk-informed methods to establish inservice inspection priorities for nuclear components at surry unit 1 nuclear power station," Pacific Northwest National Laboratory, Richland, WA, Tech. Rep. NUREG/CR-6181, February. 1997.

[28] I. Boros and A. Aszódi, "Analysis of thermal stratification in the primary circuit of a VVER-440 reactor with the CFX code," *Nucl. Eng. Des.*, vol. 238, pp. 453-459, 3, 2008.

[29] D. Kang and J. Jo, "3-D transient CFD analysis for the structural integrity assessment of a PWR pressurizer surge line subjected to thermally stratified flow," in *Transactions of the Korean Nuclear Society Autumn Meeting*, October 2007 ed.Anonymous PyeongChang, Korea: Korea Institute of Nuclear Safety, 2007, pp. 527 - 528.

[30] R. Kolbe, "Survey of insulation used in nuclear power plants and potential for debris generation draft," Burns and Roe, Inc., December. 1981.

STEAM GENERATOR

Component	Highlight	Author	GSI-191 Evidence	Expert Comments
Tubes	"Worldwide, 19 of 34 reactors in operation at the end of 1971 had experienced tube failures…" [1] Started in 1978 by 1993 12% of tubes failed to pitting and by '90 7% of tubes failed by PWSCC [2] "SONGS unit 3 experienced a leak on Jan. 31, 2012 from tube wear at retainer bars, 74 tubes had indications of potential failure**" [3]** **"**There have been 10 SGTRs (or significant leaks) in U.S. PWRs from 1975 to 2000." [4] **"**2062 cracked tubes out of 3388 tubes for French SG most affected by this degradation" [5] Table 3.1-1 Aging Management Review Results – Reactor Coolant System "Loss of Material" [6]	Bettis Labs [1] (1975) Korean Atomic Energy Research Institute [2] (2007) Tohoku University [28] (2008) U.S. NRC [3] (2014) U.S. NRC [4] (2011) EDF [5] (1992) Argonne National Lab [29] (2007) Duke Energy Corporation [6] (2001) Idaho National Lab [7] (1998) Argonne National Lab[8] (1999)	Pitting penetrates through wall leading to loss of primary coolant water [2] "Unless there is extensive circumferential cracking, SG tubes retain their integrity even if a few are locked to the TSPs by crevice deposits or corrosion products" [29] "In a corrosive environment, the erosion process may first remove a protective film from the tube, thus making the tube susceptible to more corrosion and then more erosion. In both cases, wall metal loss occurs, either directly or by accelerated corrosion of the tube surface." "Although the damaged tubes on the tube bundle periphery were plugged as a result of eddy-current inspection indications and/or small leaks, the debris, in conjunction with the hydraulic and pressure loadings, continued to	Tube failures are primary-to-secondary leaks and don't result in GSI-191 concerns. That is, the water that comes out goes in the secondary side of the steam generators.

	Table 3-1. Frequency estimates of functional impact categories: mean, percentiles, and trends. - 7.0E-3 mean frequency, “This study identified three steam generator tube rupture (SGTR) events. The SGTR frequency estimate based on the three SGTR events is 7.0E-3 per critical year. Based on the current PWR population, this frequency correlates to about one event every two calendar years. The last SGTR identified in the 1987–1995 experience occurred at Palo Verde 2 in 1993.” a 74-gpm steam generator tube leak from a tube plug at North Anna Unit 1 (LER 338/89-005) led to very small LOCA/Leak [7] “As indicated above, SCC on both the primary and secondary sides of steam generator tubes has become the principal degradation mode leading to tube plugging in the USA and worldwide. Stress corrosion	Idaho National Lab [9](1996) Chalk River Nuclear Laboratories [10] (1975) Chalk River Nuclear Laboratories [11] (1986) Politecnico de Torino [30](2011) Electric Power Research Institute [12] (1995) Siemens [13] (1993) University of Maryland College Park [14] (2011) International Atomic Energy Agency [15](1997)	damage the plugged tubes and eventually caused the tubes to collapse and in some cases to become completely severed near the top of the tubesheet."[9] “From 1990 to 2002 there were 15 reports of steam generator tube leaks. There is a total of 929 reactor calendar years represented in this period, so the mean leak frequency over this period is $1.6x10^{-3}$ per calendar year.” “Therefore, the frequency of steam generator tube Category 1 ruptures (with resultant leak rates greater than 100 gpm [380 lpm]) was 4/1,133 calendar years, or 3.5x 103 per calendar year. NUREG/CR-5750 [4. **1]** conducted a similar assessment of SGTRs, and estimated a frequency of 7x 10-3 per calendar year.” “It was almost universally expressed that the contribution to the overall LOCA frequencies is greater for the non-piping components than for piping	

	cracking can occur at numerous locations on both sides of steam generator tubes and can take on various forms and configurations." "One hundred and five steam generators in 37 PWRs around the world had been replaced by the end of 1996 because of serious tubing degradation, including 44 steam generators at 15 plants in the USA."[8] Table 18. U.S. PWR IPE results, "In a corrosive environment, the erosion process may first remove a protective film from the tube, thus making the tube susceptible to more corrosion and then more erosion. In both cases, wall metal loss occurs, either directly or by accelerated corrosion of the tube surface." [9] Table 1 – Summary of 1974 Steam Generator Tube Failures [10]	International Atomic Energy Agency [16] (1997) Pacific Northwest National Laboratory [17] (2007) U.S. Nuclear Regulatory Commission [18](2004) U.S. Nuclear Regulatory Commission [19] (1987) U.S. Nuclear Regulatory Commission [20] (1989) U.S. Nuclear Regulatory Commission [21] (2005) U.S. Nuclear Regulatory Commission [22] (2010)	for the smaller category LOCAs in PWR plants. Specifically, steam generator tube, CRDM, and pressurizer heater sleeve failures are expected to be the most important Category 1 and 2 total LOCA frequency contributors." "In addition, steam generator tubes, which were generally cited as a major small break LOCA contributor in PWRs, are susceptible to a variety of unique degradation mechanisms, including fretting and wear and denting from secondary side contamination." "The PWR plants operate at higher temperatures and several non-piping components (e.g. pressurizer, steam generator) have experienced service degradation due to PWSCC or actual rupture (e.g. steam generator tubes)."[25] "Steam generator tube rupture (Table B.1.16) can occur from a variety of	

	Table 1A Experience During 1983, Table 1B Experience During 1984[11] Table 1. Units Reporting steam generator problems worldwide “The flow-induced vibration (FIV) may result in structural damage and may compromise the integrity of the tube, due to fretting and wear and due to tube fatigue.” [12] Figure 2. Plant Status Summary of SIEMENS Steam Generators (SG) as per 31.12.1992 [13] “…there were ten SGTR occurrences in the United States between 1975 and 2000. For example, on July 15, 1987, an SGTR event occurred at the North Anna Unit 1 PWR, shortly after the unit reached 100% power. The cause of the tube rupture was determined to be high-cycle fatigue.” [14]	Brookhaven National Lab [23] (2002) Brookhaven National Lab [24] (2008) U.S. Nuclear Regulatory Commission [25] (2008) Electric Power Research Institute [26] (1997) U.S. Nuclear Regulatory Commission [27] (2008)	different mechanisms including thermal fatigue, mechanical fatigue, SCC, and general corrosion. The tubes can also be degraded by mechanical deformation (MECDEF), or denting, during installation, inspection, or cleaning. Steam generator tubes are too small to lead to a LOCA due to a single tube failure.”[27]	

	Table V. Units Reporting Steam Generator Problems, Table VI Summary of PWR Recirculating Steam Generator Tube Degradation Processes Table IX Summary of the leak rate, degradation mechanism, rupture size, rupture location, and stressor information associated with ten steam generator tube ruptures [15] Summary of CERT data for steam generator tube materials, Contributions from Czechoslovakia, Finland, Germany, India, Japan, USSR [16] “For PWR plants, the estimated frequency for steam generator tube rupture was about a factor of 10 greater, at 7 × 10-3.” “The integrity of steam generator tubes has been a significant aging issue given the various degradation			

	mechanisms that have been active at PWR plants." [17] "Circumferential cracks can occur at locations of high axial stress (e.g., small-radius U-bends and the tubesheet expansion region)."[18] Table 2.1 Key PWR components for residual life assessment – degradation sites: inside tube surfaces at U-bends and tube sheet" [19] "The primary side of some PWR steam generator tubing is susceptible to primary water stress corrosion cracking (PWSCC); Combustion Engineering and Babcock & Wilcox units are much more tolerant than most Westinghouse units." Table 8.2 Summary of degradation processes for steam generator tubes [20] Table 3.1-1 Summary of Aging Management Programs for Reactor Vessel, Internals, and Reavtor Coolant System Evaluated in			

	Chapter IV of the GALL Report[21] Table IV D1 Reactor Vessel, Internals, and Reactor Coolant System Steam Generator (Recirculating) [22] “At Shearon Harris, tube wear was detected on several tubes in row49 just above the B plate, on the cold leg side of one Model D4 SG.”[23] Table 3-2 Degradation Occurrence Records [24] “Because tube ruptures have occurred with enough regularity to be represented in the passive-system failure database, historical rupture frequencies can be estimated …” “The LER non-piping database was used to conduct this study as explained more fully in Section 3.5.2.2. From 1990 to 2002 there were 15 reports of steam generator tube leaks. There is a total of 929 reactor			

	calendar years represented in this period, so the mean leak frequency over this period is 16x10-3 per calendar year.” “Steam generator tube failure is also an expected dominant contributor based on the historically high failure rates and the decreased degradation tolerance associated with these components since the design safety factors for these tubes are less than for small bore piping.”, Table 7.18 PWR Steam Generator Tube Rupture Frequencies, Table 6.1 Major Piping and Non-Piping Contributors to the Various Size LOCA Categories [25] Table 2-1, Table 2-2, Figure 5-1 [26] “These 4 ruptures occurred at North Anna in 1987, McGuire in 1989, Palo Verde in 1993, and Indian Point in 2000.”[25]			

	Table H.2 Summary of Non-Pipe Database by Plant Type and Piece Part [27]			
Primary manway cover, bolts, studs	"5 of 20 studs failed during the March 1982 from steam generator number 2 at the Maine Yankee Atomic Power Plant"[20] "The steam generator manway closure was selected because stress corrosion cracking (SCC) was observed in studs removed from these manways in two plants."[31] Table 3.1-1 Aging Management Review Results – Reactor Coolant System "Loss of Material" [6] "The most likely reason to inspect a steam generator while at power would be in the event of a suspect manway leak or handhole inspection port leak." [32] "Some examples include common cause bolting failures resulting from maintenance that could lead to vessel head, pump or valve	Idaho National Lab [20] (1989) Electric Power Research Institute [31] (1988) Duke Energy Corporation [6] (2001) Prince's textbook [32] (2012) U.S. Nuclear Regulatory Commission [25] (2008) Technical Research Center of Finland [33] (1985) U.S. Nuclear Regulatory Commission [34] (1990) U.S. Nuclear Regulatory	"Also, bolting failures are only expected to lead to a LOCA if multiple bolts fail due to common causes, such as improper installation and inspection, or the emergence of degradation mechanisms such as steam cutting or boric acid corrosion which affect multiple bolts." "The major PWR non-piping contributors are nozzles and component bodies for LOCA Categories 3 and 4; the manways and component bodies for Category 5; and the component bodies for Category 6."[25]	This manway problem could be a GSI-191 concern because if the manway cover fails, primary water would come out at high pressure, possibly causing a lot of insulation destruction.

	bonnet, or steam generator manway failures.” [25] "The cracking has also occurred in steam generator manway studs, which were exposed to leaking borated water…" [33] Table 1-1 Summary of Degraded Threaded-Fastener Incidents Involving Reactor Coolant Pressure Boundary (RCPB) – 8 reported incidents (1977-1982) “The closures in which bolting degradation has been observed include primary side manway covers of steam generators” [31] “A common factor in six SCC events involving steam generator primary manway closure studs, which pose a potential for a LOCA, was the use of MoS2 lubricant.”[34] “On March 10, 1982, the NRC was notified by Maine Yankee Atomic Power Company and Combustion	Commission [35](1982) U.S. Nuclear Regulatory Commission [25] (2008) U.S. Nuclear Regulatory Commission [27] (2008)		

	Engineering (C-E) that during routine disassembly of a steam generator primary manway at Maine Yankee, 6 of the 20 manway closure studs, failed and another 5 were found, by ultrasonic examination using specialized techniques, to be cracked."[35] "The second difference is that some of the non-piping failure modes considered were distinct from important piping failure modes and did not lend themselves to classical modeling approaches. Some examples include common cause bolting failures resulting from maintenance that could lead to vessel head, pump or valve bonnet, or steam generator manway failures. It is for these types of failure modes that elicitation is most valuable."[25] "Steam generator failure can also occur at the manway (specifically bolt failure), the			

	steam generator shell, or the nozzles."[27] Table H.2 Summary of Non-Pipe Database by Plant Type and Piece Part [27]			
Steam generator nozzles	Table 6.1 Major Piping and Non-Piping Contributors to the Various Size LOCA Categories, "The nozzle and component body references in Table 6.1 refer to all nozzles (RPV, steam generator, and pressurizer nozzles) and/or all component bodies (RPV, steam generator, pressurizer, pumps, and valve bodies)."[25] "Steam generator failure can also occur at the manway (specifically bolt failure), the steam generator shell, or the nozzles." Table H.2 Summary of Non-Pipe Database by Plant Type and Piece Part [27] "Tensile stresses (caused by a combination of weld residual stresses and service loads) along the inner	U.S. Nuclear Regulatory Commission [25] (2008) U.S. Nuclear Regulatory Commission [27] (2008) Engineering Mechanics Corporation of Columbus [36] (2010) Sunchon National University [37] (2009) Kansai Electric Power Co. [38] (2009)	"Nozzle failures are a concern because system and transient stresses can be highest at these locations. Additionally, past degradation has been experienced in these locations." "The major PWR non-piping contributors are nozzles and component bodies for LOCA Categories 3 and 4; the manways and component bodies for Category 5; and the component bodies for Category 6."[25]	The nozzle connecting the hot leg to the steam generator is covered in KF's report. However, it is unclear if the nozzle connecting the cold leg to the steam generator is included as well.

	surface of the nozzle weld can lead to a type of corrosion termed primary-water stress corrosion cracking (PWSCC) in pressurized water reactors (PWR's), especially in the Alloy 82/182 material."[36] "Recently, it is reported that axial and circumferential PWSCCs occurred on the dissimilar welds of steam generator drain nozzle on PWR operating in South Korea."[37] Table 1 [38]			
Tubesheet	Table 3.1-1 Aging Management Review Results – Reactor Coolant System "Loss of Material" [6] Table 2 Location on 1974 Tube Failures [10] Table 1A, 1B Experience During 1983, 1984 [11] Table VI Summary of PWR Recirculating Steam Generator Tube Degradation Processes [15]	Duke Energy Corporation [6](2001) Chalk River Nuclear Laboratories [10](1975) Chalk River Nuclear Laboratories [11] (1986)	"Although the damaged tubes on the tube bundle periphery were plugged as a result of eddy-current inspection indications and/or small leaks, the debris, in conjunction with the hydraulic and pressure loadings, continued to damage the plugged tubes and eventually caused the tubes to collapse and in some cases to become completely severed near the top of the tubesheet."[9]	The tubesheet failure is similar to the tube ruptures

	"Circumferential cracks can occur at locations of high axial stress (e.g., small-radius U-bends and the tubesheet expansion region)."[18] Table 2.1 Key PWR components for residual life assessment – degradation sites: inside tube surfaces at U-bends and tube sheet" [19] Table 3.1-1 Summary of Aging Management Programs for Reactor Vessel, Internals, and Reavtor Coolant System Evaluated in Chapter IV of the GALL Report [21] "During the SG inspection in May 1997, IP2 reported the following active degradation mechanisms in the SGs: wear at the anti-vibration bars (AVBs); outside-diameter stress corrosion cracking (ODSCC) and pitting in the sludge-pile region (i.e., the area above the top of the	International Atomic Energy Agency [15] (1997) U.S. Nuclear Regulatory Commission [18] (2004) Idaho National Lab [9] (1996) U.S. Nuclear Regulatory Commission [19] (1987) U.S. Nuclear Regulatory Commission [21] (2005) Brookhaven National Lab [23] (2002) U.S. Nuclear Regulatory Commission [27] (2008)		

	tubesheet and below the first TSP); ODSCC and intergranular attack (IGA) in the crevice between the tubes and the tubesheet; and primary water stress corrosion cracking (PWSCC) at the tubesheet roll transitions and in a low row U-bend."[23] Table B.1.16 Steam Generator/Steam System Failure Scenarios [27]			
Support bolts, embedded anchor studs	Table 1-2 Summary of Degraded Threaded-Fastener Incidents Involving Components Supports – 6 reported incidents 1974-1980, 2 reported incidents 1970, 1973, "The high-strength steam generator support bolting material, in combination with high preloads, is susceptible to stress corrosion cracking because of its relatively low stress corrosion cracking (k_{ISCC}) resistance." [31] "Significant problems with anchor bolts for supports at	Electric Power Research Institute [31] (1988) Florida Power & Light Company [39] (1985) U.S. Nuclear Regulatory Commission [40] (1991) U.S Nuclear Regulatory Commission [25] (2008)	"Also, bolting failures are only expected to lead to a LOCA if multiple bolts fail due to common causes, such as improper installation and inspection, or the emergence of degradation mechanisms such as steam cutting or boric acid corrosion which affect multiple bolts."[25]	Steam generator supports failures could result in greater load on the connected piping. So this is something to consider.

	Ginna in 1970, Haddam Neck in 1973 and Surry in 1974 prompted the inclusion of consideration of support bolts in Task Action Plan A-12, "Fracture Toughness of Steam Generator and Reactor Coolant Supports."[39] “Thirteen incidents related to component support structures, such as the column support or embedded anchor bolts or studs of steam generators … were reported.” [40]			
Primary divider plate	Table 3.1-1 Aging Management Review Results – Reactor Coolant System “Loss of Material” [6] When the primary header divider design is the ‘segmented’, or ‘lap joint’ designed (plate segments bolted to each other), leakage may occur [30] Table 3.1-1 Summary of Aging Management Programs for Reactor Vessel, Internals, and Reavtor	Duke Energy Corporation[6] (2001) Politecnico de Torino [30] (2011) U.S. Nuclear Regulatory Commission [21] (2005) U.S. Nuclear Regulatory Commission [22] (2010)	“The degradation of primary header divider plates doesn’t lead to major safety impacts, but can lead to loss of thermal efficiency. Degradation permits hot reactor outlet header fluid to by-pass the tube bundle. An increase in reactor inlet header temperature has been observed.” [30] “The results of the conservative crack and fatigue life estimate analysis, using the geometry from the	This is not a GSI-191 concern because it is internal to the primary system.

	Coolant System Evaluated in Chapter IV of the GALL Report [21] Table IV D1 Reactor Vessel, Internals, and Reactor Coolant System Steam Generator (Recirculating) [22]	Electric Power Research Institute [41] (2007)	most limiting steam generator model with a nominal divider plate thickness of 2.00 inches, show that the currently observed cracks in the foreign steam generators are not capable of causing the divider plate to fail in the worst case domestic steam generator during accident or normal operating conditions." "96% (1.92 inches) of the divider plate thickness must be cracked in order for the weld to plastically fail under NOP. 93% (1.85 inches) must be cracked in order for the weld to plastically fail during an SLB. "[41]	
Steam generator shell	"Steam generator failure can also occur at the manway (specifically bolt failure), the steam generator shell, or the nozzles."[27]	U.S. Nuclear Regulatory Commission [27] (2008)		

References

[1] D. Van Rooyen, "Review of the stress corrosion cracking of Inconel 600," *Corrosion,* vol. 31, pp. 327-337, 1975.

[2] H. Kim, S. Hwang, D. Kim, J. Kim, Y. Lim and M. Joung, "Stress corrosion cracking of a Kori 1 retired steam generator tube," *EUROPEAN FEDERATION OF CORROSION PUBLICATIONS,* vol. 51, pp. 306, 2007.

[3] US NRC. "Summary of event and plant conditions (as of may 16, 2013)" in SONGS steam generator tube degradation. 2014Available: http://www.nrc.gov/info-finder/reactor/songs/songs2/event-plant-condition.html.

[4] (Thursday, March 29, 2012). *Resolution of Generic Safety Issues: Issue 188: Steam Generator Tube Leaks or Ruptures, Concurrent wiht Containment Bypass from Main Steam Line or Feedwater Line Breaches (NUREG-0933, Main Report with Supplements 1-34).* Available: http://nureg.nrc.gov/sr0933/Section%203.%20New%20Generic%20Issues/188r1.html#.

[5] P. Pitner, T. Riffard, B. Granger and B. Flesch, "Application of Probabilistic Fracture Mechanics to Optimize the Maintenance of PWR Steam Generator Tubes," *Nuclear Engineering and Design,* vol. 142, pp. 89, November 26, 1992.

[6] Duke Energy Corporation, "Application to renew the operating licenses of McGuire nuclear station, units 1 & 2 and catawba nuclear station, units 1 & 2," June. 2001.

[7] J. Poloski, D. Marksberry, C. Atwood and W. Galyean, "Rates of initiating events at U.S. nuclear power plants: 1987-1995 (DRAFT)," Lockheed Martin Idaho Technologies Company, Idaho Falls, Idaho, Tech. Rep. NUREG/CR-5750, December. 1998.

[8] D. R. Diercks, W. J. Shack and J. Muscara, "Overview of steam generator tube degradation and integrity issues," *Nucl. Eng. Des.,* vol. 194, pp. 19-30, 11, 1999.

[9] P. E. MacDonald, V. Shah, L. Ward and P. Ellison, *Steam Generator Tube Failures,* 1996.

[10] M. Hare, "Steam generator tube failures: World experience in water-cooled nuclear power reactors in 1974," Chalk River Nuclear Laboratories, Chalk River, Ontario, Tech. Rep. AECL-5242, August. 1975.

[11] O. Tatone, P. Meindl and G. Taylor, "Steam generator tube performance: Experience with water-cooled nuclear power reactors during 1983 and 1984," Chalk River Nuclear Laboratories, Chalk River, Ontario, Tech. Rep. AECL-9107, June. 1986.

[12] S. J. Green and G. Hetsroni, "PWR steam generators," *Int. J. Multiphase Flow,* vol. 21, Supplement, pp. 1-97, 12, 1995.

[13] R. Bouecke and T. Schwarz, "Siemens/KWU steam generators for reliable operation," in *Regional Meeting: Nuclear Energy in Central Europe,* Portoroz, Solvenia, 1993, pp. 436.

[14] K. Chatterjee and M. Modarres, "A probabilistic physics-of-failure approach to prediction of steam generator tube rupture frequency," in *Nuclear Science and Engineering*Anonymous 2012, pp. 136 - 150.

[15] M. Banic et al., "Assessment and management of ageing of major nuclear power plant components important to safety: Steam generators," International Atomic Energy Agency, Austria, Tech. Rep. IAEA-TECDOC-981, November. 1997.

[16] IAEA, "Coolant technology of water cooled reactors volume 2: Corrosion in the primary coolant systems of water cooled reactors," IAEA, Vienna, Austria, Tech. Rep. IAEA-TECDOC-667, September. 1992.

[17] S. Gosselin, F. Simonen, S. Pilli and B. Lydell, "Probabilities of failure and Uncertainty estimate Information for passive Components – A literature Review ," Tech. Rep. NUREG/CR-6936; PNNL-16186, 2007.

[18] B. Boger, "NRC generic letter 2004-04: Requirements for steam generator tube inspections," U.S. Nuclear Regulatory Commission, Washington, D.C., Tech. Rep. OMB Control No. 3150-0011, August 30. 2004.

[19] R. Cloud, J. Cook, M. Daye, W. Hopkins, L. House, V. Malhorta, H. Mantle, W. Mikesell, G. Odette, R. Ritchie, W. Server and V. Shah, "Residual life assessment of major light water reactor components - overview," EG&G Idaho, Inc., Idaho Falls, Idaho, Tech. Rep. NUREG/CR-4731, June. 1987.

[20] A. Amar and et al. Residual life assessment of major light water reactor components -- overview. U.S. Nuclear Regulatory Commission. 1989.

[21] Division of Regulatory Improvement Programs, "Standard review plan for review of license renewal applications for nuclear power plants," U.S. Nuclear Regulatory Commission, Washington, DC, Tech. Rep. NUREG-1800, September. 2005.

[22] B. Holian et al., "Generic aging lessons learned (GALL) report," U.S. Nuclear Regulatory Commission, Tech. Rep. NUREG-1801, December. 2010.

[23] M. Subudhi and E. Sullivan Jr., "Age-related degradation of steam generator internals based on industry responses to generic letter 97-06," in *2002 ASME Pressure Vessels and Piping Conference,* Vancouver, BC, Canada, 2002, .

[24] J. Nie, J. Braverman, C. Hofmayer, Y. Choun, M. Kim and I. Choi, "Identification and assessment of recent aging-related degradation occurrences in US nuclear power plants," *BNL Report-81741-2008, KAERI/RR-2931/2008, Brookhaven National Laboratory*, 2008.

[25] R. Tregoning, L. Abramson and P. Scott, "Estimating loss-of-coolant accident (LOCA) frequencies through the elicitation process," U.S. Nuclear Regulatory Commission, Tech. Rep. NUREG-1829, April. 2008.

[26] E. Fuller, M. Kenton, M. Epstein, R. Henry and N. Cofie, "Risks from sever accidents involving steam generator tube leaks or ruptures," Electric Power Research Institute, Tech. Rep. TR-106+194-V1, October. 1997.

[27] R. Tregoning, L. Abramson and P. Scott, "Estimating loss-of-coolant accident (LOCA) frequencies through the elicitation process appendices A through M," U.S. Nuclear Regulatory Commission, Washington, D.C., Tech. Rep. NUREG-1829 Vol. 2, April. 2008.

[28] S. Yamazaki, Z. Lu, Y. Ito, Y. Takeda and T. Shoji, "The effect of prior deformation on stress corrosion cracking growth rates of Alloy 600 materials in a simulated pressurized water reactor primary water," *Corros. Sci.*, vol. 50, pp. 835-846, 3, 2008.

[29] S. Majumdar, L. Kanza, J. Oras, J. Franklin and C. Vulyak, "Sensitivity studies of failure of steam generator tubes during main steam line break and other secondary side depressurization events," Argonne National Laboratory, Tech. Rep. NUREG/CR-6935, May. 2007.

[30] L. Bonavigo and M. De Salve, "17. Issues for Nuclear Power Plants Steam Generators," 2011.

[31] R. E. Nickell, "Degradation and failure of bolting in nuclear power plants: Volume 2: Final report," Electric Power Research Institute, United States, Tech. Rep. EPRI NP-5769, April. 1988.

[32] R. Prince, *Radiation Protection at Light Water Reactors.* Berlin; New York: Springer, 2012.

[33] H. Hanninen and I. Aho-Mantila, "Environment sensitive cracking in light water reactor pressure boundary materials," in *International Conference of Remanent Life: Life Assessment and Extension,* Brussels, 1985, .

[34] R. E. Johnson, "Resolution of generic safety issue 29: Bolting degradation or failure in nuclear power plants," United States, 1990.

[35] U.S. Nuclear Regulatory Commission, "Bulletin 82-02: Degradation of threaded fasteners in the reactor coolant pressure boundary of PWR plants," U.S. Nuclear Regulatory Commission, Washington, D.C., Tech. Rep. OMB NO. 50-0086, June 2. 1982.

[36] F.W. Brust et al., "Summary of weld residual stress analyses for dissimilar metal weld nozzles," in *ASME 2010 Pressure Vessels & Piping Division / K-PVP Conference,* Bellevue, Washington, USA, 2010, .

[37] Jong-Sung Kim et al., "PWSCC assessment of dissimilar weld on steam generator drain nozzle in PWR," in *ASME 2009 Pressure Vessels and Piping Division Conference,* Prague, Czech Republic, 2009, .

[38] Takao Nakamura et al., "Stress corrosion cracking in welds of reactor vessel nozzle at OHI-3 and of other vessel's nozzle at japan's PWR plants," in *ASME 2009 Pressure Vessels and Piping Division Conference,* Prague, Czech Republic, 2009, .

[39] D. Chaney, "Pressurized water reactor thermal shield removal and core support barrel repair in an irradiated conditon," Florida Power & Light Company, Juno Beach, Florida, 1985.

[40] Nuclear Regulatory Commission, "Resolution of generic safety issues issue 29 bolting degradation or failure in nuclear power plants (rev. 2) (NUREG-0933)," NUCLEAR REGULATORY COMMISSION, 1991.

[41] H. Cothron, "Divider plate cracking in steam generators," Electric Power Research Institute, Tech. Rep. 1014982, June. 2007.

REACTOR COOLANT PUMP

Component	Highlight	Author	GSI-191 Evidence	Expert Comments
Turning Vane Bolts/ Cap Screws	"Sheehan said one of the main concerns was having the bolt heads damage or stop the impeller at the bottom of the pump which spins and draws the water into the pump in then sends it into the reactor vessel. Also, Sheehan said, there could be the possibility of the impeller, moving at such a high rate of speed, striking and disintegrating a bolt head and sending tiny pieces of metal circulating throughout the cooling system and possibly causing damage." [1] "On September 2, 1993, the licensee for Millstone Unit 3 was inspecting the reactor lower core support plate before reloading fuel. The licensee discovered pieces of a locking cup for the Westinghouse model 93A-1 reactor coolant pump turning vane cap screws. The cap screws connect the flanged interfaces of the turning vane and thermal barrier."[2]	South Jersey Times [1] (2014) U.S. Nuclear Regulatory Commission [2] (1994) Westinghouse Electric Company [3] (2014) Electric Power Research Institute [4] (1988) Nuclear Street News Team [5] (2014)	"Inspections during a refueling outage at unit 2 of PSEG's Salem nuclear plant revealed bolt fragments at the bottom of the reactor pressure vessel. Quoting spokesmen from the plant and the Nuclear Regulatory Commission, the South Jersey Times reported that as many as 17 bolt heads have been found beneath fuel assemblies and at the bottom of a reactor coolant pump. The bolts came from RCP turning vanes and may have been affected by stress corrosion cracking." [5] "The licensee subsequently removed four turning vane cap screws for inspection. A visual and liquid penetrant inspection at the juncture of the head and body of the cap screws revealed cracks	Not an issue for the GSI-191, because the bolt fragments are too heavy. If the flow through the reactor pressure vessel isn't strong enough to push the fragments out, then in the case of a LOCA, the flow on the containment floor will not push the fragments to help clog the sump strainer.

	"Other model 93A RCPs and model 93A-1 RCPs have larger turning vane bolts of 1.5 inch diameter, and the bolted assembly uses 23 or 24 bolts. Westinghouse evaluated the RCPs with these bolts and determined that a failure could not result in a substantial safety hazard, even if left uncorrected. The basis for this is the inspection data which shows a very low incidence of bolt failure, likely due to the reduced bolt stress associated with the fastener size and load distribution."[3] (Therefore, only some plants have this issue) Surry 2 1981, incident with service water pump internals – impeller capscrew [4]		in two cap screws. One cap screw had no cracks. The head of the fourth cap screw was almost completely severed. The cap screws are made of alloy A286 stainless steel, designated by the American Society for Testing and Materials as A453 grade 660. The cap screw or cap screw head may deform, loosen, fracture, or fail the locking cup restraints. Cap screw failures could present a safety hazard because failed parts could enter the reactor coolant system and cause damage to vital components."[2] "Westinghouse determined in its evaluation that the only scenario that could potentially result in a substantial safety hazard would be if more than one RCP rotor simultaneously "looked"	

			as a result of simultaneous failures of turning vane bolts, and the turning vanes contacting the impellers. However, the possibility of multiple simultaneous locked rotors occurring is extremely unlikely. Since Westinghouse could not establish with certainty that a multiple looked rotor event could not occur, Westinghouse concluded that this deviation could potentially result in a substantial safety hazard if left uncorrected."[3]	
Pump Shaft	Fig. 7 Inspections of pump shafts [6] Table 2-4 KSB PWR Main Coolant Pumps [7] Table 3 Summary of degradation processes for LWR coolant pumps [8] "Within the last few years, several plants have found cracks in the reactor coolant pump	Siemens AG-UB KWU [6] (1989) Electric Power Research Institute [7] (1992) Idaho National Engineering Laboratory [8] (1990) REM Technologies [9] (1990)	"Failure of pump internals, for example, shafts and bearings, will not compromise the integrity of the pressure boundary, but the broken pieces may be carried over to the reactor vessel and damage the vessel internals, fuel rods, and other core components." [10]	Failure can lead to seal package damage, which can cause a lot of water to come out.

	shaft near the thermal barrier." [9] "A coolant pump shaft at Crystal River 3 completely failed in 1986. The cause of failure was determined to be a circumferential crack attributed to fatigue." [10]	Idaho National Engineering Laboratory [10] (1989)		
Pump Closure (Studs, Bolts, Main Flange, and Nuts)	"Visual inspection of closure studs at other PWR plants has revealed that the studs in all pump designs are susceptible to boric acid corrosion." "Leakage of borated water across LWR primary coolant pump case-to-cover gaskets can cause corrosion of the pump closure studs and corrosion of carbon steel pump body base metal." [10] "Boric acid corrosion in one PWR plant reduced seven reactor coolant pump studs from a nominal diameter of 90 mm (3.5 in.) to between 25 and 37 mm (1.0 and 1.5 in.)." [8] Table 1 Summary of Degraded Threaded Fasteners in Reactor Coolant Pressure Boundary [11]	Idaho National Engineering Laboratory [10] (1989) U.S. Nuclear Regulatory Commission [11] (1982) Idaho National Engineering Laboratory [8] (1990) International Atomic Energy Agency [12] (2003) Electric Power Research Institute [4] (1988)	"After complete removal of the nonmetallic insulation, further visual observations revealed three studs located side-by-side on one pump and three studs similarly located on the other pump had significant corrosion wastage in the shank area next to the lower thread section in the pump casing flange." [13] (If the coolant leakage corrodes the bolting, debris generation can flow with the coolant to the containment floor causing a GSI-191 issue) “The RC pump main flange showed the greatest capacity for	Potential for large LOCA here. Probably most important issue for reactor coolant pump (because seal package failure has been experienced).

	"PWR pump closure studs are susceptible to corrosion wastage caused by primary coolant leakage across the pump body-to-cover gaskets." [12] Table 1-1 Summary of Degraded Threaded-Fastener Incidents Involving Reactor Coolant Pressure Boundary (RCPB) Waterford 1981 incident with Reactor Coolant Pump Support Bolts (Table 1-2) Table 1-6 Incidents of Borated-Water Corrosion of Threaded Fasteners “The reactor coolant pump main closure was selected because corrosion wastage was observed in pump studs in several plants.” “The closures in which bolting degradation has been observed include primary side manway covers of steam generators and pressurizers, coolant pump main flanges, and some primary valve flanges.”[4] "On May 17, 1980, the NRC staff was informed by Omaha Public Power District (OPPD) that severe corrosion damage	U.S. Nuclear Regulatory Commission [13] (1980) U.S. Nuclear Regulatory Commission [14] (1988) Dominion Nuclear Connecticut, Inc.[15] (2004) Dominion Nuclear Connecticut, Inc. [16] (2004) Entergy Nuclear Operations, Inc. [17] (2005) Indiana Michigan Power Co. [18] (2003) Carolina Power & Light Co.[19] (2006) Southern Nuclear Operating Co., Inc. [20] (2003)	producing large leak rates owing to the large diameter of the sealing surface and smaller number of studs per arc length.”[4] "Leakage of reactor coolant across the pump casing-to-cover gasket may wet the insulation, allowing chlorides in the insulation to contaminate the coolant." [8]	

	was found on a number of closure studs in two of the four Byron Jackson reactor coolant pumps at Fort Calhoun Unit 1 (PWR)." [13] "At Fort Calhoun, the diameter of a reactor coolant pump closure bolt was reduced from 3.5 inches to 1.1 inches by boric acid corrosion." "In June 1981, the Institute for Nuclear Power Operations issued a report discussing the effect of low level leakage from the gasket of a reactor coolant pump and concluded that significant corrosion of the pump studs could occur during all modes of operation." [14] Table 3.1.2-3 Reactor Vessel, Internals, and Reactor Coolant System - Reactor Coolant - Aging Management Evaluation [15] Table 3.1.2-3 Reactor Vessel, Internals, and Reactor Coolant System - Reactor Coolant - Aging Management Evaluation [16]	Florida Power & Light Co. [21] (2000) Brookhaven National Laboratory [22] (2008) Pacific Northwest National Laboratory [23] (1995)		

	Table 3.1.2-1 Reactor Coolant System - Primary Coolant System - Summary of Aging Management Evaluation [17] Table 3.1.2-3 Class 1 Piping, Valves, and Reactor Coolant Pumps [18] Table 3.1.2-4 Reactor Vessel, Internals, and Reactor Coolant System - Summary of Aging Management Evaluation - Reactor Coolant Pump and Motor [19] Table 3.1.2-3 Reactor Coolant Systems, Reactor Coolant System and Connected Lines – Summary of Aging Management Review [20] "Mechanical closure bolting associated with the reactor coolant pump components is made of low alloy steel bolting material and is subject to aggressive chemical attack." [21]			

	“Boric acid wastage of reactor coolant pump closure flange studs” [22] Table 4.5 Aging degradation concerns and mechanisms for reactor coolant pumps [23]			
Pump Body/Casing	Table 3 Summary of degradation processes for LWR coolant pumps [8] "The most likely failure mode for a pump casting would be through wall leakage of primary coolant water." [10] Table 3.1-1 Aging Management Review Results – Reactor Coolant System [24] Table 2.1. Key PWR components for residual life assessment [25] Table 3.4-1 Applicable Aging Effects for Reactor Coolant System Components & Class 1 Component Supports [26] Table 3.2-1 Aging Effects Requiring Aging Management for Reactor Coolant System Components [27]	Idaho National Engineering Laboratory [8] (1990) Idaho National Engineering Laboratory [10] (1989) Duke Energy Carolinas, LLC [24] (2001) Idaho National Engineering Laboratory [25] (1987) Duke Energy Corp. [26] (1998) Entergy Operations, Inc. [27] (2000)	"About about 150 liters [40 gallons] of oil was collected by the oil collection system, and 150 liters [40 gallons] leaked onto the insulation and the containment floor." [31] (If oil can reach the containment floor, then whatever failed to release the oil can generate debris that can ultimately reach the containment floor and become a GSI-191 concern.) “While there is some documented evidence of degradation of such components, (e.g., [D.10]) the frequency of a through-wall defect in valve bodies and pump casings is viewed as	If casing failed it would be a problem. Oil leakage isn’t an issue, because the amount of oil would be much less than the amount of coolant water, so it would be in a small concentration. Also, the oil floats. The oil does have the potential to cause a fire. If fire occurs, it is unlikely that it would increase the chance for a LOCA, because the plant would be shutdown first. In regards to reference [31], if oil is reactive with the insulation, then that

	Table 3.1.2-3 Class 1 Piping, Valves, and Reactor Coolant Pumps [28] Table 3.1.2-3 Class 1 Piping, Valves, and Reactor Coolant Pumps [18] Table 3.1.2-3 Reactor Coolant Systems, Reactor Coolant System and Connected Lines – Summary of Aging Management Review [20] "The Reactor Coolant Pump casings and the SG Channel Heads are insulated with a stainless steel reflective insulation." [29] Table B.1.17 Pump Failure Scenarios [30] Table 4.5 Aging degradation concerns and mechanisms for reactor coolant pumps [23]	Entergy Operations, Inc. [28] (2003) Indiana Michigan Power Co. [18] (2003) Southern Nuclear Operating Co., Inc. [20] (2003) R.E. Ginna Nuclear Power Plant, LLC [29] (2002) U.S. Nuclear Regulatory Commission [31] (1994) U.S. Nuclear Regulatory Commission [30] (2008) Pacific Northwest National Laboratory [23] (1995)	being considerably lower than for welds in Class 1 systems." "Non-nuclear experience therefore provides additional justification for very low failure frequencies for components such as pump bodies, tube sheets, manways, etc. that imply large extrapolations from the limited years of nuclear plant operation."[30]	could be evidence of how insulation could break off of the RCP. Is there any evidence that oil can break off the insulation? Also, does oil pose any problems for the GSI-191 issue? Perhaps it will chemically react and form some precipitates that can help clog the sump strainer?
Flange (Bolts, Studs, Fasteners)	Table 3.1-1 Aging Management Review Results – Reactor Coolant System [24]	Duke Energy Carolinas, LLC [24] (2001)	"During the visual inspection, saturated and dripping insulation was observed at one of the Byron Jackson reactor	Main flange is a pressure boundary, so could be an issue. However, this is already included in

	Table 3-11 Reactor Coolant Pumps Flange and Seal Bolts at Risk [4] “Corrosion of flanges for primary coolant pump component cooling water connections due to external boric acid leakage” “Boric acid wastage of primary coolant pump studs” [22] Table 3.1.2-3 Class 1 Piping, Valves, and Reactor Coolant Pumps [18] Table 3.1.2-3 Reactor Coolant Systems, Reactor Coolant System and Connected Lines – Summary of Aging Management Review [20] Table 3.2-1 Aging Effects Requiring Aging Management for Reactor Coolant System Components [27] Table 3.1.2-3 Class 1 Piping, Valves, and Reactor Coolant Pumps [28]	Electric Power Research Institute [4] (1988) Brookhaven National Laboratory [22] (2008) U.S. Nuclear Regulatory Commission [33] (1980) Entergy Nuclear Operations, Inc. [17] (2005) Indiana Michigan Power Co. [18] (2003) Southern Nuclear Operating Co., Inc. [20] (2003) Entergy Operations, Inc. [27] (2000) Entergy Operations, Inc. [28] (2003) Duke Energy Corp. [26] (1998)	coolant pump flange regions." [33] "A review of plant specific operating experience related to the Boric Acid Corrosion Program and aging revealed that the following issues had been addressed: Corrosion of flanges for primary coolant pump component cooling water connections due to external boric acid leakage" [17]	the pump closure category.

	Table 3.4-1 Applicable Aging Effects for Reactor Coolant System Components & Class 1 Component Supports [26] Table 3.2-1 Reactor Coolant System - Aging Management Programs Evaluated in NUREG-1801 that are Relied on for License Renewal Table 3.2-2 Reactor Coolant System - Component Types Subject to Aging Management not Evaluated in NUREG-1801 [29] Table 3.1.2-1 Reactor Coolant System - Class 1 Piping/Components System - Summary of Aging Management Evaluation [32] Table 3.2-1 Reactor Coolant System [21] "An example of the first type is the corrosion of fasteners in the reactor coolant pressure boundary, for example, in reactor coolant pumps." [14] "However, except for the reactor coolant pump stud wastage,	R.E. Ginna Nuclear Power Plant, LLC [29] (2002) NextEra Energy Point Beach, LLC [32] (2004) Florida Power & Light Co. [21] (2000) U.S. Nuclear Regulatory Commission [14] (1988) U.S. Nuclear Regulatory Commission [11] (1982)		

	most failures have occurred in fastener sizes 2 inches and smaller."[11]			
Flywheel	"The aging effect of concern is fatigue crack initiation in the flywheel bore key way from stresses due to starting the motor." [24] "The aging effect of concern for the reactor coolant pump flywheel is fatigue crack initiation in the flywheel bore keyway." [34] “The only unique mode considers an incipient failure of a pump flywheel which could initiate collateral damage in other components or in other piping systems.” Table B.1.17 Pump Failure Scenarios [30]	Duke Energy Carolinas, LLC [24] (2001) Entergy Nuclear Operations, Inc. [17] (2005) STP Nuclear Operating Co. [34] (2010) U.S. Nuclear Regulatory Commission [30] (2008)	"A reactor coolant pump flywheel could theoretically burst because of centrifugal stresses, which could produce missiles inside containment and could also damage pump seals or other pressure boundary components." [17] “There was no appropriate passive pump failure data that was identified by the group.”[30]	This could be a problem. If one were to occur, it may bend the pump over, or possibly open a big hole in the seal package. There have not been many (or any?) flywheel issues. However, if one were to occur, the damage to the nearby components would be a major GSI-191 issue, potentially causing a LOCA as well as generating debris.
Framing and Support (Leg-Support Anchor Bolts, Embedded Anchor Studs, Driver Mounts)	"Failures of ASTM A 490 high-strength RCP leg-support anchor bolts due to stress corrosion cracking; other factors contributing to the failures were improper heat-treatment and excessive preload during original installation;" [29]	R.E. Ginna Nuclear Power Plant, LLC [29] (2002) Electric Power Research Institute [4] (1988) Omaha Public Power District [35] (2002)	“Field experience has shown that steam generator supports and their anchor bolting, and the anchor bolting of reactor coolant pumps and of reactor pressure vessels support skirts have suffered from	Support failure can increase the probability of failure due to excessive bending loads and shear as well, if support was being relaxed. Also, snubbers may have

	Table 4-1 Summary of Structural Support Bolting Failures [4] Table 3.1-3 Components in Reactor Vessel, Internals, and Reactor Coolant System not Evaluated in NUREG-1801 that rely on Ageing Management Programs in NUREG-1801 for FCS License Renewal [35] Table 3.1.2-3 Class 1 Piping, Valves, and Reactor Coolant Pumps [28] Table 3.5.2-1 Containment Buildings Structural Components and Commodities Summary of Aging Management Review [36] Table 3.5.2-24 Structures and Component Supports - NSSS Equipment Supports - Aging Management Evaluation [15] Table 3.5.2-35 Structures and Component Supports - NSSS Equipment Supports - Aging Management Evaluation [16]	Entergy Operations, Inc. [28] (2003) Entergy Nuclear Operations, Inc. [36] (2007) Dominion Nuclear Connecticut, Inc.[15] (2004) Dominion Nuclear Connecticut, Inc. [16] (2004) Indiana Michigan Power Co. [18] (2003) Carolina Power & Light Co. [19] (2006) Virginia Electric & Power Co. [37] (2001) Virginia Electric & Power Co. [38] (2001)	degradation by SCC." [4]	an effect for seismic events. Degradation and loss of material from the framing and support would lead to debris falling down onto the containment floor, thus causing a GSI-191 issue.

	Table 3.5.2-1 Containment Summary of Aging Management Evaluation [18] Table 3.5.2-1 Containments, Structures, and Component Support - Summary of Aging Management Evaluation - Containment Building [19] Table 3.5.9-1 NSSS Equipment Supports [37] Table 3.5.9-1 NSSS Equipment Supports [38]			
Thermal Barrier (Heat Exchanger, Assembly, and Housing)	Table 3.1.2-3 Class 1 Piping, Valves, and Reactor Coolant Pumps [18] Table 3.1.2-3 Reactor Coolant Systems, Reactor Coolant System and Connected Lines – Summary of Aging Management Review [20] "The integral thermal barrier heat exchangers are exposed to an internal environment of treated water and treated water primary, and an external environment of containment air and potential borated water leaks (see Tables 3.0-1 and 3.0-2)." [21]	Indiana Michigan Power Co. [18] (2003) Southern Nuclear Operating Co., Inc. [20] (2003) Florida Power & Light Co. [21] (2000) U.S. Nuclear Regulatory Commission [39] (1997)	"The safety concerns were identified and evaluated with regard to the potential consequences of (1) the formation of loose parts, generated by the thermal barrier housing, which could damage the pump seals…" [39]	Consists of pretty small pipes, so small concern.

	Table 3.2-2 Reactor Coolant System - Component Types Subject to Aging Management not Evaluated in NUREG-1801 [29]	R.E. Ginna Nuclear Power Plant, LLC [29] (2002)		
Seals	"The reactor coolant pump seal LOCA frequency of 2.5E-3 per critical year was calculated in this study, based on 2 catastrophic seal failures with leak rates greater than 300 gpm in the total U.S. operating experience (1969–1997)." [40] Table 3-11 Reactor Coolant Pumps Flange and Seal Bolts at Risk [4] Table A.3-1 Examples of Generic Safety Issues that Should/Should Not Be Specifically Addressed for License Renewal and Basis for Disposition [41] "The staff determined that RCP seal leakage could exceed 25 gpm and lead to core uncovery during an SBO in any of the PWRs and in any of the four BWRs (Millstone Unit 1, Oyster	Idaho National Laboratory [40] (1998) Electric Power Research Institute [4] (1988) U.S. Nuclear Regulatory Commission [41] (2010) U.S. Nuclear Regulatory Commission [42] (1991) U.S. Nuclear Regulatory Commission [43] (1990) U.S. Nuclear Regulatory	"The staff has determined that the accident sequences involving pump seal failures are potentially risk-significant for only a handful of plants. Therefore, this matter no longer qualifies as a GSI." [47] "The normal operational seal failure rate has since been significantly reduced through improvements in design and operation of RCP seals." [48] "This issue relates to reactor coolant pump seal failures, which challenge the makeup capacity of the emergency core cooling system in PWRs." [41]	Based on experience, no GSI-191 concerns. Primary coolant can squirt up and hit pump motor. This may lead to a small LOCA, but no debris. Also, considered by NUREG-1829 as an active failure, and thus not included in that analysis.

	Creek, Nine Mile Point Unit 1" [42] "The inability of the reactor coolant pump seals to survive loss of cooling and injection without developing significant leakage dominates the core damage frequency." [43] "On May 24, 1992, the licensee commenced a reactor shutdown from 100 percent power because of excessive leakage from the 1A2 Reactor Coolant Pump seal. The maximum leakage was approximately 23 liters per minute [6 gpm]." [44] “At Indian Point Unit 2 Nuclear Station (IP2) there have been a number of primary reactor coolant pump (RCP) shaft seal failures which have led to loss of reactor primary coolant.”[45] Table 4.5 Aging degradation concerns and mechanisms for reactor coolant pumps [23] Table 1 Calculations Used to Estimate Frequency that Sump will be Required [46]	Commission [47] (1999) U.S. Nuclear Regulatory Commission [48] (2000) Los Alamos National Laboratory [46] (2000) U.S. Nuclear Regulatory Commission [44] (1993) Brookhaven National Laboratory [45] (1987) Pacific Northwest National Laboratory [23] (1995) STP Nuclear Operating Co. [34] (2010)	"Borated water solution traveled to the shanks of all the seal housing bolts, which were constructed of low alloy steel. All of the bolts experienced some degradation, with 15 of the 16 failing VT-1 inspection for continued service." [34]	

Suction Deflector Bolting/ Diffuser Bolting	"Of the three bolts inspected to date, two had cracks of 40 percent and 100 percent of the circumference and the third bolt head sheared during removal" [49] (This shows evidence of degradation which leads to debris generation)	Calvert Cliffs Nuclear Power Plant Inc. [50] (1998) Northeast Utilities [49] (1993)	"The 1988 and 1996 failures of the RCP suction deflector bolting... A portion of the failed bolt was not recovered at the pump in each case... bolt fragments were recovered during the 1989 refueling outage." [50]	Not a problem for GSI-191.
Motor Exterior	Table 3.4-1 Applicable Aging Effects for Reactor Coolant System Components & Class 1 Component Supports - Lateral support assemblies loss of material from boric acid wastage [26] "There were a number of small oil leaks on each pump motor although there was more leakage from the `A' pump motor. The inspector observed that various equipment around the `A' reactor coolant pump was coated with a film of oil and he estimated that several gallons of oil had collected in various areas outside the oil collection system." [31]	Duke Energy Corp. [26] (1998) U.S. Nuclear Regulatory Commission [31] (1994) Pacific Gas & Electric Co. [51] (2009)		Not much of a concern for GSI-191.

	"Reactor coolant pump (RCP) motor feeder cables experienced cracking and one failed a polarization index test." [51]			
Oil Collection System Tank **	Table 3.3.2-31: Auxiliary Systems - Unit 2 Fire Protection - Aging Management Evaluation [15] Table 3.3.2-36: Auxiliary Systems - Unit 2 Fire Protection - Aging Management Evaluation [16] Table 3.1.2-4 Reactor Vessel, Internals, and Reactor Coolant System - Summary of Aging Management Evaluation - Reactor Coolant Pump and Motor [19] Table 3.3.2-19 : Auxiliary Systems, Liquid Waste and Drains – Summary of Aging Management [20] Table 3.4-14 Fire Protection [21]	Dominion Nuclear Connecticut, Inc.[15] (2004) Dominion Nuclear Connecticut, Inc. [16] (2004) Carolina Power & Light Co. [19] (2006) Southern Nuclear Operating Co., Inc. [20] (2003) Florida Power & Light Co. [21] (2000)		Not much of a concern for GSI-191. A lot of external rust can form, and the tank can overfill and spill oil on the containment floor.
Motor Stator Coolers	Table 3.1.2-3: Reactor Vessel, Internals, and Reactor Coolant System - Reactor Coolant - Aging Management Evaluation	Dominion Nuclear Connecticut, Inc. [16] (2004)		Not much of a concern for GSI-191. No interface with the reactor coolant, this

	– Loss of material due to borated water leakage [16] Table 3.1.1-1 Reactor Coolant System – borated water leakage causing loss of material [37] Table 3.1.1-1 Reactor Coolant System – borated water leakage loss of material [38]	Virginia Electric & Power Co. [37] (2001) Virginia Electric & Power Co. [38] (2001)		still could be an external debris source if not properly coated.
Heat Exchanger components	Table 3.1.2-2 Reactor Vessel, Internals, and Reactor Coolant System – Summary of Aging Management Evaluation – Reactor Coolant System [51] Table 3.1.2-4 Reactor Vessel, Internals, and Reactor Coolant System - Summary of Aging Management Evaluation - Reactor Coolant Pump and Motor [19] Table 3.3.2-8 : Auxiliary Systems, Chemical and Volume Control System – Summary of Aging Management Review [20] Table 3.3.1-1 Primary Process Systems — Chemical and Volume Control [37]	Pacific Gas & Electric Co. [51] (2009) Carolina Power & Light Co. [19] (2006) Southern Nuclear Operating Co., Inc. [20] (2003) Virginia Electric & Power Co. [37] (2001) Virginia Electric & Power Co. [38] (2001) Entergy Operations, Inc. [27] (2000)	Tables show loss of material from borated water exposure	Not much of a concern for GSI-191.

	Table 3.3.1-1 Primary Process Systems — Chemical And Volume Control [38] Table 3.2-1 Aging Effects Requiring Aging Management for Reactor Coolant System Components [27]			
Motor Lower/Upper Lube Oil Coolers**	Table 3.1.2-3: Reactor Vessel, Internals, and Reactor Coolant System - Reactor Coolant - Aging Management Evaluation [16] Table 3.1.2-3: Reactor Vessel, Internals, and Reactor Coolant System - Reactor Coolant - Aging Management Evaluation [15] Table 3.2-1 Reactor Coolant System [21] Table 3.1.1-1 Reactor Coolant System [37] Table 3.1.1-1 Reactor Coolant System [38]	Dominion Nuclear Connecticut, Inc. [16] (2004) Dominion Nuclear Connecticut, Inc.[15] (2004) Florida Power & Light Co. [21] (2000) Virginia Electric & Power Co. [37] (2001) Virginia Electric & Power Co. [38] (2001)	Loss of material from borated water leakage or containment air	Not much of a concern for GSI-191. No interface with the reactor coolant, this still could be an external debris source if not properly coated
Valves**	Table 3.3.2-19 : Auxiliary Systems, Liquid Waste and Drains – Summary of Aging Management [20]	Southern Nuclear Operating Co., Inc. [20] (2003)	Loss of material from borated water leakage	Valves are generally packed to not leak and capped. Boric acid could be a problem.

	Table 3.3.9-2 Fire Protection and Supporting Systems — Reactor Coolant [37] Table 3.4-14 Fire Protection [21]	Virginia Electric & Power Co. [37] (2001) Florida Power & Light Co.[21] (2000)		
Non-regenerative and regenerative heat exchanger				Had a problem in Japan where it was blown apart due to cyclic fatigue due to thermal cycling of coolant water. Could cause a leak outside of containment. Unsure if it is isolatable or not.

* Plant specific whether welded or non-welded

** Component in Reactor Coolant Pump Motor Oil Collection Sub-System

References

[1] (May 19, 2014). *Broken Bolt Pieces Found in Pump, Reactor Vessel Delay Salem 2 Nuclear Plant Restart*. Available: http://www.nj.com/salem/index.ssf/2014/05/broken_bolt_pieces_in_pump_reactor_vessel_delay_salem_2_reactor_restart.html.

[2] B. Grimes, "Information Notice No. 90-68: Supplement 1: Stress Corrosion Cracking of Reactor Coolant Pump Bolts," 1994.

[3] J. Gresham, "Notification of the Potential Existence of Defects Pursuant to 10CFR Part 21," 2014.

[4] R. E. Nickell, "Degradation and failure of bolting in nuclear power plants: Volume 1," United States, 1988.

[5] (May 21, 2014). *Loose Bolt Fragments Extend Salem Nuclear Plant Outage*. Available: https://nuclearstreet.com/nuclear_power_industry_news/b/nuclear_power_news/archive/2014/05/21/loose-bolt-fragments-extend-salem-nuclear-plant-outage-052102.aspx#.U__Z5_ldV8H.

[6] R. Loehberg, W. Ullrich and K. Gaffal, "Shafts of main coolant pumps - failure analysis and remedies," *Nucl. Eng. Des.*, vol. 112, pp. 243-257, 3, 1989.

[7] W. Brose, K. Chen, A. Kuo and P. Riccardella, "Evaluation of main coolant pump shaft cracking," Structural Integrity Associated, Inc., San Jose, California, 1992.

[8] V. Shah, A. Ware, D. Conley and P. MacDonald, "AGING ASSESSMENT OF PWR SURGE AND SPRAY LINES AND LWR COOLANT PUMPS," in *Nuclear Engineering and Design*Anonymous 1990, pp. 329 - 342.

[9] W. Miller and W. Brook, "Shaft Crack Detection Method,", 1990.

[10] V. N. Shah, A. S. Amar, M. H. Bakr, B. F. Beaudoin, B. J. Buescher, D. A. Conley, F. R. Drahos, J. B. Gardner, R. W. Garner, B. J. Kirkwood, L. C. Meyer, W. L. Server, V. N. Shah, E. A. Siegel, U. P. Sinha and A. G. Ware, "Residual life assessment of major light water reactor components: Overview," United States, 1989.

[11] U.S. Nuclear Regulatory Commission, "Bulletin 82-02: Degradation of threaded fasteners in the reactor coolant pressure boundary of PWR plants," U.S. Nuclear Regulatory Commission, Washington, D.C. 20555, Tech. Rep. Bulletin 82-02, June 2,1982.

[12] IAEA, "Assessment and management of ageing of major nuclear power plant components important to safety: Primary piping in PWR's," International Atomic Energy Agency, Vienna, Austria, Tech. Rep. IAEA-TECDOC-1361, July 2003.

[13] U.S. Nuclear Regulatory Commission, "Information notice no. 80-27 - degradation of reactor coolant pump studs," Washington, D.C. 20555, Tech. Rep. Information Notice No. 80-27, 1980.

[14] F. Miraglia, "Boric Acid Corrosion of Carbon Steel Reactor Pressure Boundary Components in PWR Plants (Generic Letter No. 88-05)," March, 17 1988.

[15] I. Dominion Nuclear Connecticut, "Millstone nuclear power station, units 2 - license renewal application," U.S. Nuclear Regulatory Commission, January 2004.

[16] I. Dominion Nuclear Connecticut, "Millstone nuclear power station, units 3 - license renewal application," U.S. Nuclear Regulatory Commission, January 2004.

[17] I. Entergy Nuclear Operations, "Palisades nuclear plant - application for renewed operating license," U.S. Nuclear Regulatory Commission, March 2005.

[18] Indiana Michigan Power Co., "License renewal application donald C cook nuclear plant," U.S. Nuclear Regulatory Commission, October 2003.

[19] Carolina Power & Light Co., "Harris nuclear plant license renewal application," U.S. Nuclear Regulatory Commission, November 2006.

[20] Southern Nuclear Operating Co., Inc., "Joseph M. farley license renewal application," U.S. Nuclear Regulatory Commission, September 2003.

[21] Florida Power & Light Co., "Application for renewed operating licenses turkey point units 3 & 4," U.S. Nuclear Regulatory Commission, 2000.

[22] J. Nie, J. Braverman, C. Hofmayer, Y. Choun, M. Kim and I. Choi, "Identification and assessment of recent aging-related degradation occurrences in US nuclear power plants," *BNL Report-81741-2008, KAERI/RR-2931/2008, Brookhaven National Laboratory*, 2008.

[23] W. Morgan and J. V. Livingston, "A review of information for managing aging in nuclear power plants," Pacific Northwest National Laboratory, United States, Tech. Rep. PNL-10717, 1995.

[24] L. Duke Energy Carolinas, "Application to renew the operating licenses of McGuire nuclear station, units 1 and 2 and catawba nuclear station, units 1 and 2," U.S. Nuclear Regulatory Commission, June 2001.

[25] A. Amar, U.S. Nuclear Regulatory Commission. Office of Nuclear Regulatory Research. Division of Engineering Technology, Idaho National Engineering Laboratory, EG & G Idaho, V. Shah and P. MacDonald, "Residual life assessment of major light water reactor components: Overview, volume 1," Division of Engineering; Office of Nuclear Regulatory Research; U.S. Nuclear Regulatory Commission, the University of Michigan, 1987.

[26] Duke Energy Corp., "Oconee nuclear station, units 1, 2 & 3- license renewal application volume II," U.S. Nuclear Regulatory Commission, June 1998.

[27] I. Entergy Operations, "License renewal application arkansas nuclear one - units 1," U.S. Nuclear Regulatory Commission, February 2000.

[28] I. Entergy Operations, "License renewal application arkansas nuclear one - units 2," U.S. Nuclear Regulatory Commission, October 2003.

[29] R.E. Ginna Nuclear Power Plant, LLC, "Application for renewed operating license R. E. ginna nuclear power plant," U.S. Nuclear Regulatory Commission, 2002.

[30] R. Tregoning, L. Abramson and P. Scott, "Estimating loss-of-coolant accident (LOCA) frequencies through the elicitation process appendices A through M," U.S. Nuclear Regulatory Commission, Washington, D.C., Tech. Rep. NUREG-1829, 2008.

[31] B. Grimes, "Information Notice No. 94-58: Reactor Coolant Pump Lube Oil Fire," 1994.

[32] NextEra Energy Point Beach, LLC, "Application for renewed operating licenses point beach nuclear plant units 1 & 2," U.S. Nuclear Regulatory Commission, 2004.

[33] Office of Inspection and Enforcement, "Degradation of reactor coolant pump studs," U.S. Nuclear Regulatory Commission, Washington, D.C. 20555, Tech. Rep. Information Notice No.80-27, June 1980.

[34] STP Nuclear Operating Co., "License renewal application south texas project unit 1 and unit 2," U.S. Nuclear Regulatory Commission, 2010.

[35] Omaha Public Power District, "Fort calhoun station, unit 1- license renewal application section 3," U.S. Nuclear Regulatory Commission, January 2002.

[36] I. Entergy Nuclear Operations, "License renewal application indian point nuclear generating sections 1-4," U.S. Nuclear Regulatory Commission, April 2007.

[37] Virginia Electric & Power Co., "Application for renewed operating licenses north anna power station units 1 and 2," U.S. Nuclear Regulatory Commission, 2001.

[38] Virginia Electric & Power Co., "Application for renewed operating licenses surry power station units 1 and 2," U.S. Nuclear Regulatory Commission, 2001.

[39] M. Slosson, "Information Notice No 97-31 Failures of Reactor Coolant Pump Thermal Barriers and Check Valves in Foreign Plants," 1997.

[40] J. Poloski, J. Poloski and D. MARKSBERRY, "Rates of Initiating Events at US Nuclear Power Plants: 1987-1995 (NUREG/CR-5750)," *Washington, DC: US Nuclear Regulatory Commission,* vol. 12, 1998.

[41] Office of Nuclear Reactor Regulation, "Standard review plan for review of license renewal applications for nuclear power plants - final report," U.S. Nuclear Regulatory Commission, Washington, D.C. 20555-0001, Tech. Rep. NUREG-1800, Revision 2, December 2010.

[42] J. Partlow, "GI-23, "Reactor Coolant Pump Seal Failures" and its Possible Effect on Station Blackout," 1991.

[43] Division of Systems Research, "Severe accident risks: An assessment for five U.S. nuclear power plants - final summary report," U.S. Nuclear Regulatory Commission, Washington, D.C. 20555, Tech. Rep. NUREG-1150, Volume 1, December 1990.

[44] B. Grimes, "Information Notice No. 93-61: Excessive Reactor Coolant Leakage Following a Seal Failure in a Reactor Coolant Pump or Reactor Recirculation Pump," 1993.

[45] M. Subudhi, J. H. Taylor, J. H. Clinton, C. J. Czajkowski and J. R. Weeks, "Indian point 2 reactor coolant pump seal evaluations," Brookhaven National Laboratory, Long Island, New York, Tech. Rep. NUREG/CR-4985, 1987.

[46] J. Darby, D. Rao and B. Letellier, "Technical letter report GSI-191 study: Technical approach for risk assessment of PWR sump-screen blockage," 2000.

[47] D. Powers, "Proposed resolution of generic safety issue 23 (GSI-23), "reactor coolant pump seal failure"," U.S. Nuclear Regulatory Commission, Washington, D.C. 20555-0001, October 1999.

[48] D. Matthews, "NRC regulatory issue summary 2000-02 closure of generic safety issue 23, reactor coolant pump seal failure," U.S. Nuclear Regulatory Commission, Washington, D.C. 20555-0001, February 2000.

[49] Anonymous "Priority attention required morning report - region I september 22,1993," Northeast Utilities, Waterford, Connecticut, 1993.

[50] Calvert Cliffs Nuclear Power Plant Inc., "Calvert cliffs nuclear power plant, units 1 & 2 - license renewal application volume 1," U.S. Nuclear Regulatory Commission, April 1998.

[51] Pacific Gas & Electric Co., "License renewal application diablo canyon power plant units 1 and 2," U.S. Nuclear Regulatory Commission, November 2009.

REACTOR VESSEL

Component	Highlight	Author	GSI-191 Evidence	Expert Comments
Reactor Vessel (Bolting, Studs, Nuts and Washers)	"The Inservice Inspection Program manages cracking of the… reactor vessel bolting, and supplements the Boric Acid Corrosion Prevention Program with regard to detecting loss of material at external surfaces of the reactor vessel and control element drive mechanism (CEDM) pressure boundary." [1] Table 3.4-1 Applicable Aging Effects for Reactor Coolant System Components & Class 1 Component Supports [2] Table 3.1.2-2 Reactor Coolant System - Reactor Vessel - Summary of Aging Management Evaluation [3]	Entergy Operations, Inc. [1] (2003) Duke Energy Corp. [2] (1998) Entergy Nuclear Operations, Inc. [3] (2005)		Excessive flange failures could result in debris generation
Instrument Tubes	"On the other hand, a break at the reactor vessel bottom by such as instrument-tube break allows no gas discharge until the whole vessel becomes empty of coolant." [4]	Thermohydraulic Safety Engineering Laboratory [4] (2012) U.S. Nuclear Regulatory		Instrument tube penetrations could result in bebris generation

	"At Turkey Point Unit 4, leakage of reactor coolant from the lower instrument tube seal on one of the incore instrument tubes resulted in corrosion of various components on the reactor vessel head including three reactor vessel bolts. The maximum depth of corrosion was 0.25 inches." [5] Table 3.1.1 Summary of Aging Management Evaluations in Chapter IV of NUREG-1801 for Reactor Vessel, Internals, and Reactor Coolant System [6] Table 3.1.1 Summary of Aging Management Evaluations in Chapter IV of NUREG-1801 for Reactor Vessel, Internals, and Reactor Coolant System [7] Table 3.1.1 Summary of Aging Management Evaluations for the Reactor Vessel, Internals, and Reactor Coolant System [8]	Commission [5] (1988) Arizona Public Service Co. [6] (2009) Northern States Power Co. [7] (2008) AmerGen Energy Company, LLC [8] (2008) NextEra Energy Point Beach, LLC [9] (2004)		

	Table 3.1.2-2 Reactor Coolant System - Reactor Vessel - Summary of Aging Management Evaluation [9]			
Instrumentation Tube Penetrations (Bottom Head)	Table 3.1.2-4 Reactor Vessel, Internals, and Reactor Coolant System - Reactor Vessel System - Summary of Aging Management Evaluation [7]	Northern States Power Co. [7] (2008)		Bottom mounted instrumentation weld failures could result in debris generation
Instrumentation Tube Penetrations (Top Head)	Table 3.1.2-4 Reactor Vessel, Internals, and Reactor Coolant System - Reactor Vessel System - Summary of Aging Management Evaluation [7]	Northern States Power Co. [7] (2008)		Top mounted (RV head) instrumentation weld failures could result in debris generation
Control Rod Drive Mechanism Nozzles	"Circumferential cracking in CRDM nozzles were identified at Oconee 2 and 3, and axial cracking in the J-groove weld in CRDM nozzles were identified at Oconee 1 and ANO 1 (i.e., B&W plants)." [10] "In 2002, the discovery of thinning of the vessel head wall at the Davis Besse nuclear power plant reactor indicated the possibility of an SBLOCA in the upper head of the reactor vessel as a result of	FirstEnergy [10] (2002) Universidad Politécnica de Madrid [11] (2011) Brookhaven National Laboratory [12] (2002)	"Two CRDMs had minor boron film running down from the above insulation. The insulation around the two CRDM nozzles and along nearby insulation seams had a heavier film of boron." [14]	CRDM nozzle weld failures could result in debris generation. The motor connections are not likely to result in significant jets due to the nature of the connection (threaded)

	circumferential cracking of a control rod drive mechanism penetration nozzle…" [11] "Primary water stress corrosion cracking (PWSCC) in the axial direction of control rod drive mechanism (CRDM) nozzles has previously been observed." [12] "In the updated histogram, Surry Unit 1 and North Anna Unit 1 remained in the most susceptible category, while Surry Unit 2 and North Anna Unit 2 remained in the intermediate category." [13]	AmerGen Energy Company, LLC [14] (2008) Virginia Electric & Power Co. [13] (2001)		
Control rod drive penetration nozzles	Table 3.1.1 Summary of Aging Management Evaluations in Chapter IV of NUREG-1801 for Reactor Vessel, Internals, and Reactor Coolant System [6] Table 3.1.1 Summary of Aging Management Evaluations in Chapter IV of NUREG-1801 for Reactor Vessel, Internals, and Reactor Coolant System [7] Table 3.1.1 Summary of Aging Management Evaluations for	Arizona Public Service Co. [6] (2009) Northern States Power Co. [7] (2008) AmerGen Energy Company, LLC [8] (2008)		

	the Reactor Vessel, Internals, and Reactor Coolant System[8]			
Control Rod Drive Nozzle	Table 3.1-1 Summary of Aging Management Program for Reactor Vessel, Internals, and Reactor Coolant System Evaluated in NUREG-1801 that are Relied on for FCS License Renewal [15] Table 3.2-1 Reactor Coolant System - Aging Management Programs Evaluated in NUREG-1801 that are Relied on for License Renewal [16]	Omaha Public Power District [15] (2002) R.E. Ginna Nuclear Power Plant, LLC [16] (2002)		Same as CRD penetration nozzle (Above) CRDM nozzle weld failures could result in debris generation (as opposed to motor connections)
Control Rod Drive Housing	Table 3.1-1 Summary of Aging Management Program for Reactor Vessel, Internals, and Reactor Coolant System Evaluated in NUREG-1801 that are Relied on for FCS License Renewal [15] Table 3.1.1 Summary of Aging Management Evaluations in Chapter IV of NUREG-1801 for Reactor Coolant System [3] Table 3.2-1 Reactor Coolant System - Aging Management Programs Evaluated in	Omaha Public Power District [15] (2002) Entergy Nuclear Operations, Inc. [3] (2005) R.E. Ginna Nuclear Power Plant, LLC [16] (2002)		CRDM housing failures, especially the drive shaft housing could result in debris generation

	NUREG-1801 that are Relied on for License Renewal [16]			
CRDM Housings	Table 3.1.2-2 Reactor Coolant System - Reactor Vessel - Summary of Aging Management Evaluation [9]	NextEra Energy Point Beach, LLC [9] (2004)		CRDM housing failures, especially the drive shaft housing could result in debris generation
Control Rod Drive Service Structure	Table 3.1.2-2 Reactor Vessel Summary of Aging Management Evaluation [8]	AmerGen Energy Company, LLC [8] (2008)		CRDM housing failures, especially the drive shaft housing could result in debris generation (not clear on what the service structure is)
CRDM Support	Table 3.1.2-1 Reactor Vessel, Internals, and Reactor Coolant System – Summary of Aging Management Evaluation – Reactor Vessel and Internals [17]	STP Nuclear Operating Co. [17] (2010)		CRDM housing failures, especially the drive shaft housing could result in debris generation
CRDM Housing Tubes	Table 3.1.2-4 Reactor Vessel, Internals, and Reactor Coolant System - Reactor Vessel System - Summary of Aging Management Evaluation [7]	Northern States Power Co. [7] (2008)		CRDM housing failures, especially the drive shaft housing could result in debris generation

CRDM Housing Tubes (Head Adapters)	Table 3.1.2-2 Reactor Coolant System - Reactor Vessel - Summary of Aging Management Evaluation [9]	NextEra Energy Point Beach, LLC [9] (2004)		CRDM housing failures, especially the drive shaft housing could result in debris generation
Reactor Vessel Head O-rings	"The procedure identifies the following areas as principal locations for possible leaks: ... Reactor Vessel Head O-rings" [10]	FirstEnergy [10] (2002)		Failures at the RV head flange could result in debris generation
Reactor Vessel Head Bolts	"At Turkey Point Unit 4, leakage of reactor coolant from the lower instrument tube seal on one of the incore instrument tubes resulted in corrosion of various components on the reactor vessel head including three reactor vessel bolts. The maximum depth of corrosion was 0.25 inches." [5]	U.S. Nuclear Regulatory Commission [5] (1988)		Failures at the RV head flange could result in debris generation
Valve Packing Follower Plate (Bolts)	"At San Onofre Unit 2, boric acid solution corroded nearly through the bolts holding the valve packing follow plate in the shutdown cooling system isolation valve. During an attempt to operate the valve, the bolts failed and the valve packing follow plate became	U.S. Nuclear Regulatory Commission [5] (1988)		Not sure what this valve is but it doesn't seem like it would be pressurized at power (plus, it looks like the experiment has been completed and it didn't block recirculation!).

	dislodged causing leakage of approximately 18,000 gallons of reactor coolant into the containment." [5]			
Reactor Vessel Head	"Corrosion by boric acid crystals was observed in Turkey Point Unit 4 where more than 500 pounds of boric acid crystals were found on the reactor vessel head." [5] "Recent industry events regarding reactor vessel head degradation required assessments at each site to ensure boric acid corrosion prevention programs are adequate and functioning effectively." [1]	U.S. Nuclear Regulatory Commission [5] (1988) Entergy Operations, Inc. [1] (2003)		Failures of the RV head could result in debris generation
Thimble Tubes	"… identified flow-induced vibration as a cause for wear (i.e., thinning) of the thimble tubes…" [12] "Flux thimble tubes are subject to loss of material at certain locations in the reactor vessel where flow-induced fretting causes wear at discontinuities in the path from the reactor vessel	Brookhaven National Laboratory [12] (2002) Entergy Nuclear Operations, Inc. [18] (2007)		Failure of thimble tube penetrations could result in debris generation

	instrument nozzle to the fuel assembly instrument guide tube." [18]			
Core Support Lugs	"…are not adequate for managing cracking of the core support lugs." [12]	Brookhaven National Laboratory [12] (2002)		Core support lugs would not cause debris generation (although they may result in a failure during seismic event).
Beltline Region * (Shell, Nozzles, and Welds)	"Another issue that is considered important for the reactor vessel is the loss of fracture toughness in the beltline region material due to both high neutron flux and high temperature conditions." [12] Table 3.1.1 Summary of Aging Management Evaluations in Chapter IV of NUREG-1801 for Reactor Coolant System [3] Table 3.1.1 Summary of Aging Management Evaluations in Chapter IV of NUREG-1801 for Reactor Vessel, Internals, and Reactor Coolant System [6]	Brookhaven National Laboratory [12] (2002) Entergy Nuclear Operations, Inc. [3] (2005) Arizona Public Service Co. [6] (2009) Northern States Power Co. [7] (2008)		RV Failures could result in debris generation Welded Center portion of the vessel directly adjacent to the fuel Highest embrittlement from neutrons

	Table 3.1.1 Summary of Aging Management Evaluations in Chapter IV of NUREG-1801 for Reactor Vessel, Internals, and Reactor Coolant System [7] "Based upon the materials and projected fluence levels, the only items expected to be susceptible to neutron embrittlement are the reactor vessel shell components in the beltline region immediately surrounding the core." [8] Table 3.2-1 Reactor Coolant System - Aging Management Programs Evaluated in NUREG-1801 that are Relied on for License Renewal [16]	AmerGen Energy Company, LLC [8] (2008) R.E. Ginna Nuclear Power Plant, LLC [16] (2002)		
Reactor Vessel Annulus		FNC Technology Co. Ltd [19] (2011)	Table 4 Volume Capture Type and Capture Fraction [19]	The RV annulus is internal to the vessel and would not result in debris generation. Cold water down comer around the fuel
RV Cooling Shroud	Table 3.2-1 Potential and Plausible ARDMS for the FHE and HLHC System [20]	Calvert Cliffs Nuclear Power Plant Inc. [20] (1998)		The RV cooling shroud is not pressurized and

				would not result in debris generation
Flow Skirt	Table 3.1-2 FCS Reactor Vessel, Internals, and Reactor Coolant System Component Types Subject to Aging Management not Evaluated in NUREG-1801 [15] Table 3.1.2-1: Reactor Vessel and CEDM Pressure Boundary [21] Table 3.1.2-1 Reactor Vessel, Internals, and Reactor Coolant System – Summary of Aging Management Evaluation – Reactor Vessel and Internals [6]	Omaha Public Power District [15] (2002) Entergy Operations, Inc. [21] (2003) Arizona Public Service Co. [6] (2009)		The flow skirt is not pressurized and would not result in debris generation
Thermal Shield (Positioning Pin & Bolt)	Table 3.1-3 Components in Reactor Vessel, Internals, and Reactor Coolant System not Evaluated in NUREG-1801 that rely on Aging Management Programs in NUREG-1801 for FCS License Renewal [15]	Omaha Public Power District [15] (2002)		RV internals would result in debris generation
Reactor Vessel Cladding	Table 3.1-3 Components in Reactor Vessel, Internals, and Reactor Coolant System not Evaluated in NUREG-1801 that	Omaha Public Power District [15] (2002)		RV cladding would no result in debris generation (although failure could result in

	rely on Aging Management Programs in NUREG-1801 for FCS License Renewal [15]			early failure due to boric acid corrosion)
Reactor Vessel Closure (Studs, Stud Assembly, Nuts, Bolts, and Washers)	Table 3.1.2-1: Reactor Vessel and CEDM Pressure Boundary [21] Table 3.4-1 Applicable Aging Effects for Reactor Coolant System Components & Class 1 Component Supports [2] Table 3.1.2-1 Reactor Vessel, Internals, and Reactor Coolant System – Summary of Aging Management Evaluation – Reactor Vessel and Internals [6] Table 3.1.2-1 Reactor Vessels [13] Table 3.1.2-2 Reactor Coolant System - Reactor Vessel - Summary of Aging Management Evaluation [9]	Entergy Operations, Inc. [21] (2003) Duke Energy Corp. [2] (1998) Arizona Public Service Co. [6] (2009) Virginia Electric & Power Co. [13] (2001) NextEra Energy Point Beach, LLC [9] (2004)		Failures at the RV head flange could result in debris generation

Reactor Head Closure Studs	"Minor nicks, scratches, gouges, and thread damage have occurred due to maintenance activities during refueling outages." [22]	Northern States Power Co. [22] (2008)		Failures at the RV head flange could result in debris generation
Reactor Vessel Nozzles Safe Ends (and Welds)	Table 3.1-1 Summary of Aging Management Program for Reactor Vessel, Internals, and Reactor Coolant System Evaluated in NUREG-1801 that are Relied on for FCS License Renewal [15] Table 3.1.2-1: Reactor Vessel, Internals, and Reactor Coolant System - Reactor Vessel - Aging Management Evaluation [23] Table 3.1.2-1: Reactor Vessel and CEDM Pressure Boundary [21] Table 3.1.2-2 Reactor Coolant System - Reactor Vessel - Summary of Aging Management Evaluation [3] Table 3.1.2-1 Reactor Vessel, Internals, and Reactor Coolant System – Summary of Aging	Omaha Public Power District [15] (2002) Dominion Nuclear Connecticut, Inc. [23] (2004) Entergy Operations, Inc. [21] (2003) Entergy Nuclear Operations, Inc. [3] (2005) Arizona Public Service Co. [6] (2009) AmerGen Energy Company, LLC [8] (2008)		Failures of nozzles could result in debris generation

	Management Evaluation – Reactor Vessel and Internals [6] Table 3.1.2-2 Reactor Vessel Summary of Aging Management Evaluation [8] Table 3.2-1 Reactor Coolant System - Aging Management Programs Evaluated in NUREG-1801 that are Relied on for License Renewal [16]	R.E. Ginna Nuclear Power Plant, LLC [16] (2002)		
Primary Nozzle Safe Ends	Table 3.1.2-2 Reactor Coolant System - Reactor Vessel - Summary of Aging Management Evaluation [9]	NextEra Energy Point Beach, LLC [9] (2004)		Failures of the RV nozzles could result in debris generation
RV Vent Nozzle	Table 3.1-3 Components in Reactor Vessel, Internals, and Reactor Coolant System not Evaluated in NUREG-1801 that rely on Aging Management Programs in NUREG-1801 for FCS License Renewal [15]	Omaha Public Power District [15] (2002)		Failures at RV nozzles could result in debris generation
Reactor Vessel Support Framing	Table 3.5.2-1 : Containment Buildings Structural Components and Commodities Summary of Aging Management Review [24]	Entergy Nuclear Operations, Inc. [24] (2007)		The external brackets are not pressurized and would not result in debris generation

	Table 3.5.2-1: Containment and Containment Internals [21]	Entergy Operations, Inc. [21] (2003)		
External Support Brackets	Table 3.1.2-4 Reactor Vessel, Internals, and Reactor Coolant System - Reactor Vessel System - Summary of Aging Management Evaluation [7] Table 3.1.2-2 Reactor Coolant System - Reactor Vessel - Summary of Aging Management Evaluation [9]	Northern States Power Co. [7] (2008) NextEra Energy Point Beach, LLC [9] (2004)		The external support brackets are not pressurized and would not result in debris generation
Reactor Vessel Column Support	Table 3.1.2-2 Reactor Coolant System - Reactor Vessel - Summary of Aging Management Evaluation [3]	Entergy Nuclear Operations, Inc. [3] (2005)		The RV column supports are not pressurized and would not result in debris generation
Reactor Vessel Support Skirt	Table 3.4-1 Applicable Aging Effects for Reactor Coolant System Components & Class 1 Component Supports [2] Table 3.1.2-2 Reactor Vessel Summary of Aging Management Evaluation [8]	Duke Energy Corp. [2] (1998) AmerGen Energy Company, LLC [8] (2008)		The RV column supports are not pressurized and would not result in debris generation
Support Flange	Table 3.4-1 Applicable Aging Effects for Reactor Coolant System Components & Class 1 Component Supports [2]	Duke Energy Corp. [2] (1998)		The RV support flange is not pressurized and

				would not result in debris generation
Closure head lifting lugs	Table 3.1.2-1: Reactor Vessel and CEDM Pressure Boundary [21] Table 3.1.2-1: Reactor Vessel, Internals, and Reactor Coolant System - Reactor Vessel - Aging Management Evaluation [23] Table 3.1.2-1: Reactor Vessel, Internals, and Reactor Coolant System - Reactor Vessel - Aging Management Evaluation [25] Table 3.1.2-2 Reactor Coolant System - Reactor Vessel - Summary of Aging Management Evaluation [3] Table 3.1.2-4 Reactor Vessel, Internals, and Reactor Coolant System - Reactor Vessel System - Summary of Aging Management Evaluation [7] Table 3.1.2-1 Reactor Vessels [13]	Entergy Operations, Inc. [21] (2003) Dominion Nuclear Connecticut, Inc. [23] (2004) Dominion Nuclear Connecticut, Inc. [25] (2004) Entergy Nuclear Operations, Inc. [3] (2005) Northern States Power Co. [7] (2008) Virginia Electric & Power Co. [13] (2001)		Failures of the RV flange could result in debris generation

	Table 3.1.2-2 Reactor Coolant System - Reactor Vessel - Summary of Aging Management Evaluation [9]	NextEra Energy Point Beach, LLC [9] (2004)		
Core stabilizing lugs	Table 3.1.2-1: Reactor Vessel and CEDM Pressure Boundary [21]	Entergy Operations, Inc. [21] (2003)		Core components are internal to the vessel and would not cause debris generation
Core Stop Lugs	Table 3.1.2-1: Reactor Vessel and CEDM Pressure Boundary [21] Table 3.1.2-1 Reactor Vessel, Internals, and Reactor Coolant System – Summary of Aging Management Evaluation – Reactor Vessel and Internals [6]	Entergy Operations, Inc. [21] (2003) Arizona Public Service Co. [6] (2009)		Core components are internal to the vessel and would not cause debris generation
Grayloc clamp studs and nuts	Table 3.1.2-1: Reactor Vessel and CEDM Pressure Boundary [21]	Entergy Operations, Inc. [21] (2003)		Grayloc clamps are to seal failed CRDM motor seal weld failures and are not expected to create debris
Reactor Vessel Support Pads	Table 3.1.2-1: Reactor Vessel and CEDM Pressure Boundary [21] Table 3.1.2-1 Reactor Vessel, Internals, and Reactor Coolant System – Summary of Aging	Entergy Operations, Inc. [21] (2003)		RV support pads are not expected to create debris

	Management Evaluation – Reactor Vessel and Internals [6]	Arizona Public Service Co. [6] (2009)		
Core Support Pads	Table 3.1.2-2 Reactor Coolant System - Reactor Vessel - Summary of Aging Management Evaluation [9]	NextEra Energy Point Beach, LLC [9] (2004)		Core components are internal to the vessel and would not cause debris generation
Nozzle Support Pads	Table 3.1.2-4 Reactor Vessel, Internals, and Reactor Coolant System - Reactor Vessel System - Summary of Aging Management Evaluation [7] Table 3.1.2-1 Reactor Vessels [13] Table 3.1.2-2 Reactor Coolant System - Reactor Vessel - Summary of Aging Management Evaluation [9]	Northern States Power Co. [7] (2008) Virginia Electric & Power Co. [13] (2001) NextEra Energy Point Beach, LLC [9] (2004)		Support pads are not expected to create debris
Shear Keys	Table 3.1.2-1 Reactor Vessel, Internals, and Reactor Coolant System – Summary of Aging Management Evaluation – Reactor Vessel and Internals [6]	Arizona Public Service Co. [6] (2009)		Shear keys would not create debi.

Shear Lugs	Table 3.1.2-1: Reactor Vessel and CEDM Pressure Boundary [21]	Entergy Operations, Inc. [21] (2003)		Shear lugs would not create debris.
Bottom head (torus, dome, and cladding)	Table 3.1.2-1: Reactor Vessel and CEDM Pressure Boundary [21] Table 3.1.2-1: Reactor Vessel, Internals, and Reactor Coolant System - Reactor Vessel - Aging Management Evaluation [23] Table 3.1.2-1: Reactor Vessel, Internals, and Reactor Coolant System - Reactor Vessel - Aging Management Evaluation [25] Table 3.1.2-2 Reactor Coolant System - Reactor Vessel - Summary of Aging Management Evaluation [3] Table 3.1.2-4 Reactor Vessel, Internals, and Reactor Coolant System - Reactor Vessel System - Summary of Aging Management Evaluation [7] Table 3.1.2-1 Reactor Vessels [13]	Entergy Operations, Inc. [21] (2003) Dominion Nuclear Connecticut, Inc. [23] (2004) Dominion Nuclear Connecticut, Inc. [25] (2004) Entergy Nuclear Operations, Inc. [3] (2005) Northern States Power Co. [7] (2008) Virginia Electric & Power Co. [13] (2001)		Failure of the bottom head would cause debris

	Table 3.1.2-2 Reactor Coolant System - Reactor Vessel - Summary of Aging Management Evaluation [9]	NextEra Energy Point Beach, LLC [9] (2004)		
Upper shell (and cladding) (and Flange)	Table 3.1.2-1: Reactor Vessel and CEDM Pressure Boundary [21] Table 3.1.2-1: Reactor Vessel, Internals, and Reactor Coolant System - Reactor Vessel - Aging Management Evaluation [23] Table 3.1.2-1: Reactor Vessel, Internals, and Reactor Coolant System - Reactor Vessel - Aging Management Evaluation [25] Table 3.1.2-2 Reactor Coolant System - Reactor Vessel - Summary of Aging Management Evaluation [3] Table 3.1.2-4 Reactor Vessel, Internals, and Reactor Coolant System - Reactor Vessel System - Summary of Aging Management Evaluation [7]	Entergy Operations, Inc. [21] (2003) Dominion Nuclear Connecticut, Inc. [23] (2004) Dominion Nuclear Connecticut, Inc. [25] (2004) Entergy Nuclear Operations, Inc. [3] (2005) Northern States Power Co. [7] (2008) AmerGen Energy Company, LLC [8] (2008)		RV internals would not create debris.

	Table 3.1.2-2 Reactor Vessel Summary of Aging Management Evaluation [8] Table 3.1.2-1 Reactor Vessels [13] Table 3.1.2-2 Reactor Coolant System - Reactor Vessel - Summary of Aging Management Evaluation [9]	Virginia Electric & Power Co. [13] (2001) NextEra Energy Point Beach, LLC [9] (2004)		
Reactor Vessel Upper Shell Flange	Table 3.1.2-2 Reactor Coolant System - Reactor Vessel - Summary of Aging Management Evaluation [3]	Entergy Nuclear Operations, Inc. [3] (2005)		Failures of the RV flange could result in debris generation
Reactor Vessel Closure Head (Including Studs, Nuts, & Washers)	Table 3.1.2-2 Reactor Coolant System - Reactor Vessel - Summary of Aging Management Evaluation [3] Table 3.1.2-1 Reactor Vessel, Internals, and Reactor Coolant System – Summary of Aging Management Evaluation – Reactor Vessel and Internals [6] "…manages cracking due to primary water stress corrosion cracking (PWSCC) and loss of material due to boric acid	Entergy Nuclear Operations, Inc. [3] (2005) Arizona Public Service Co. [6] (2009) Arizona Public Service Co. [26] (2009)		Failures of the RV flange could result in debris generation

	wastage in nickel-alloy pressure vessel head penetration nozzles and includes the reactor vessel closure head…" [26] Table 3.1.2-4 Reactor Vessel, Internals, and Reactor Coolant System - Reactor Vessel System - Summary of Aging Management Evaluation [7] Table 3.1.2-2 Reactor Vessel Summary of Aging Management Evaluation [8] "The Upper Head Nickel Alloy AMP provides for the management of cracking due to PWSCC in nickel-alloy vessel head penetration nozzles and includes the reactor vessel closure head, upper vessel head penetration nozzles and associated welds." [14]	Northern States Power Co. [7] (2008) AmerGen Energy Company, LLC [8] (2008) AmerGen Energy Company, LLC [14] (2008)		
Closure Head Bolts	Table 3.1.2-1 Reactor Vessel, Internals, and Reactor Coolant System – Summary of Aging Management Evaluation – Reactor Vessel and Internals [6]	Arizona Public Service Co. [6] (2009)		Failures of the RV flange could result in debris generation

Closure head dome (torus, dome, and cladding)	Table 3.1.2-1: Reactor Vessel and CEDM Pressure Boundary [21] Table 3.1.2-1: Reactor Vessel, Internals, and Reactor Coolant System - Reactor Vessel - Aging Management Evaluation [23] Table 3.1.2-1: Reactor Vessel, Internals, and Reactor Coolant System - Reactor Vessel - Aging Management Evaluation [25] Table 3.1.2-4 Reactor Vessel, Internals, and Reactor Coolant System - Reactor Vessel System - Summary of Aging Management Evaluation [7] Table 3.1.2-1 Reactor Vessels [13] Table 3.1.2-2 Reactor Coolant System - Reactor Vessel - Summary of Aging Management Evaluation [9]	Entergy Operations, Inc. [21] (2003) Dominion Nuclear Connecticut, Inc. [23] (2004) Dominion Nuclear Connecticut, Inc. [25] (2004) Northern States Power Co. [7] (2008) Virginia Electric & Power Co. [13] (2001) NextEra Energy Point Beach, LLC [9] (2004)		Failures of the RV headsw could result in debris generation

Closure Head Stud Assembly	Table 3.1.2-1: Reactor Vessel, Internals, and Reactor Coolant System - Reactor Vessel - Aging Management Evaluation [23] Table 3.1.2-1: Reactor Vessel, Internals, and Reactor Coolant System - Reactor Vessel - Aging Management Evaluation [25]	Dominion Nuclear Connecticut, Inc. [23] (2004) Dominion Nuclear Connecticut, Inc. [25] (2004)		Failures of the RV flange could result in debris generation
Closure head flange (and Cladding)	Table 3.1.2-1: Reactor Vessel and CEDM Pressure Boundary [21] Table 3.1.2-1: Reactor Vessel, Internals, and Reactor Coolant System - Reactor Vessel - Aging Management Evaluation [23] Table 3.1.2-1: Reactor Vessel, Internals, and Reactor Coolant System - Reactor Vessel - Aging Management Evaluation [25] Table 3.1.2-4 Reactor Vessel, Internals, and Reactor Coolant System - Reactor Vessel System - Summary of Aging Management Evaluation [7]	Entergy Operations, Inc. [21] (2003) Dominion Nuclear Connecticut, Inc. [23] (2004) Dominion Nuclear Connecticut, Inc. [25] (2004) Northern States Power Co. [7] (2008) Virginia Electric & Power Co. [13] (2001)		Failures of the RV flange could result in debris generation

	Table 3.1.2-1 Reactor Vessels [13] Table 3.1.2-2 Reactor Coolant System - Reactor Vessel - Summary of Aging Management Evaluation [9]	NextEra Energy Point Beach, LLC [9] (2004)		
Intermediate shell (and cladding)	Table 3.1.2-1: Reactor Vessel and CEDM Pressure Boundary [21] Table 3.1.2-1: Reactor Vessel, Internals, and Reactor Coolant System - Reactor Vessel - Aging Management Evaluation [23] Table 3.1.2-1: Reactor Vessel, Internals, and Reactor Coolant System - Reactor Vessel - Aging Management Evaluation [25] Table 3.1.2-2 Reactor Coolant System - Reactor Vessel - Summary of Aging Management Evaluation [3] Table 3.1.2-4 Reactor Vessel, Internals, and Reactor Coolant System - Reactor Vessel	Entergy Operations, Inc. [21] (2003) Dominion Nuclear Connecticut, Inc. [23] (2004) Dominion Nuclear Connecticut, Inc. [25] (2004) Entergy Nuclear Operations, Inc. [3] (2005) Northern States Power Co. [7] (2008)		Failures of the RV could result in debris generation

	System - Summary of Aging Management Evaluation [7] Table 3.1.2-1 Reactor Vessels [13] Table 3.1.2-2 Reactor Coolant System - Reactor Vessel - Summary of Aging Management Evaluation [9]	Virginia Electric & Power Co. [13] (2001) NextEra Energy Point Beach, LLC [9] (2004)		
Lower shell (and cladding)	Table 3.1.2-1: Reactor Vessel and CEDM Pressure Boundary [21] Table 3.1.2-1: Reactor Vessel, Internals, and Reactor Coolant System - Reactor Vessel - Aging Management Evaluation [23] Table 3.1.2-1: Reactor Vessel, Internals, and Reactor Coolant System - Reactor Vessel - Aging Management Evaluation [25] Table 3.1.2-2 Reactor Coolant System - Reactor Vessel - Summary of Aging Management Evaluation [3]	Entergy Operations, Inc. [21] (2003) Dominion Nuclear Connecticut, Inc. [23] (2004) Dominion Nuclear Connecticut, Inc. [25] (2004) Entergy Nuclear Operations, Inc. [3] (2005) Northern States Power Co. [7] (2008)		Failures of the RV heads could result in debris generation

	Table 3.1.2-4 Reactor Vessel, Internals, and Reactor Coolant System - Reactor Vessel System - Summary of Aging Management Evaluation [7] Table 3.1.2-1 Reactor Vessels [13] Table 3.1.2-2 Reactor Coolant System - Reactor Vessel - Summary of Aging Management Evaluation [9]	Virginia Electric & Power Co. [13] (2001) NextEra Energy Point Beach, LLC [9] (2004)		
Shell Bottom Head	Table 3.1.2-1 Reactor Vessel, Internals, and Reactor Coolant System – Summary of Aging Management Evaluation – Reactor Vessel and Internals [6]	Arizona Public Service Co. [6] (2009)		Failures of the RV head could result in debris generation
Primary inlet/outlet nozzles (and Cladding)	Table 3.1.2-1: Reactor Vessel and CEDM Pressure Boundary [21] Table 3.1.2-1: Reactor Vessel, Internals, and Reactor Coolant System - Reactor Vessel - Aging Management Evaluation [25] Table 3.1.2-4 Reactor Vessel, Internals, and Reactor Coolant System - Reactor Vessel	Entergy Operations, Inc. [21] (2003) Dominion Nuclear Connecticut, Inc. [25] (2004) Northern States Power Co. [7] (2008)		Failures of RV nozzless could result in debris generation

	System - Summary of Aging Management Evaluation [7] Table 3.1.2-1 Reactor Vessels [13] Table 3.1.2-2 Reactor Coolant System - Reactor Vessel - Summary of Aging Management Evaluation [9]	Virginia Electric & Power Co. [13] (2001) NextEra Energy Point Beach, LLC [9] (2004)		
Reactor Vessel Primary Coolant Nozzles	Table 3.1.2-2 Reactor Coolant System - Reactor Vessel - Summary of Aging Management Evaluation [3]	Entergy Nuclear Operations, Inc. [3] (2005)		Failures of RV nozzless could result in debris generation
Vessel Flange	Table 3.1.2-1: Reactor Vessel and CEDM Pressure Boundary [21] Table 3.1.2-1: Reactor Vessel, Internals, and Reactor Coolant System - Reactor Vessel - Aging Management Evaluation [23] Table 3.1.2-1: Reactor Vessel, Internals, and Reactor Coolant System - Reactor Vessel - Aging Management Evaluation [25]	Entergy Operations, Inc. [21] (2003) Dominion Nuclear Connecticut, Inc. [23] (2004) Dominion Nuclear Connecticut, Inc. [25] (2004)		Failures of the RV flange could result in debris generation

	Table 3.1.2-4 Reactor Vessel, Internals, and Reactor Coolant System - Reactor Vessel System - Summary of Aging Management Evaluation [7] Table 3.1.2-1 Reactor Vessels [13] Table 3.1.2-2 Reactor Coolant System - Reactor Vessel - Summary of Aging Management Evaluation [9]	Northern States Power Co. [7] (2008) Virginia Electric & Power Co. [13] (2001) NextEra Energy Point Beach, LLC [9] (2004)		
Threaded fasteners, reactor vessel support connections	Table 3.5.2-1: Containment and Containment Internals [21]	Entergy Operations, Inc. [21] (2003)		Failures of the RV flange could result in debris generation. Other external supports and so forth would cause debris generation
Core Support Ledge (and cladding)	Table 3.1.2-1: Reactor Vessel, Internals, and Reactor Coolant System - Reactor Vessel - Aging Management Evaluation [23] Table 3.1.2-1: Reactor Vessel, Internals, and Reactor Coolant System - Reactor Vessel - Aging Management Evaluation [25]	Dominion Nuclear Connecticut, Inc. [23] (2004) Dominion Nuclear Connecticut, Inc. [25] (2004)		This is internal to the vessel and would not cause debris

	Table 3.1.2-1 Reactor Vessels [13]	Virginia Electric & Power Co. [13] (2001)		
Reactor Vessel Seal Ledge Ring	Table 3.1.2-2 Reactor Coolant System - Reactor Vessel - Summary of Aging Management Evaluation [3]	Entergy Nuclear Operations, Inc. [3] (2005)		Not familiar but is probably referring to the flange seal which could cause debris generation
RPV Refueling Seal Ledge	Table 3.1.2-4 Reactor Vessel, Internals, and Reactor Coolant System - Reactor Vessel System - Summary of Aging Management Evaluation [7] Table 3.1.2-1 Reactor Vessels [13] Table 3.1.2-2 Reactor Coolant System - Reactor Vessel - Summary of Aging Management Evaluation [9]	Northern States Power Co. [7] (2008) Virginia Electric & Power Co. [13] (2001) NextEra Energy Point Beach, LLC [9] (2004)		Would not generate dbris
RVLIS Penetration Pipe Nozzle	Table 3.1.2-4 Reactor Vessel, Internals, and Reactor Coolant System - Reactor Vessel System - Summary of Aging Management Evaluation [7]	Northern States Power Co. [7] (2008)		Failures could result in debris generation Reactor Vessel Level Instrument System

Safety Injection Nozzles	Table 3.1.2-4 Reactor Vessel, Internals, and Reactor Coolant System - Reactor Vessel System - Summary of Aging Management Evaluation [7] Table 3.1.1 Summary of Aging Management Evaluations for the Reactor Vessel, Internals, and Reactor Coolant System [8]	Northern States Power Co. [7] (2008) AmerGen Energy Company, LLC [8] (2008)		Pressurized RCS-connected systems may result in debris generation
RCCA guide tube assemblies	Table 3.1.1 Summary of Aging Management Evaluations in Chapter IV of NUREG-1801 for Reactor Vessel, Internals, and Reactor Coolant System [6] Table 3.1.1 Summary of Aging Management Evaluations in Chapter IV of NUREG-1801 for Reactor Vessel, Internals, and Reactor Coolant System [7] Table 3.1.1 Summary of Aging Management Evaluations for the Reactor Vessel, Internals, and Reactor Coolant System [8]	Arizona Public Service Co. [6] (2009) Northern States Power Co. [7] (2008) AmerGen Energy Company, LLC [8] (2008)		The RCCA guide tube is internal to the vessel and would not cause debris generation Rod Control Cluster Assembly
RCCA Guide Tube Bolts	Table 3.1.2-3 Reactor Coolant System - Reactor Vessel Internals - Summary of Aging Management Evaluation [9]	NextEra Energy Point Beach, LLC [9] (2004)		The RCCA guide tube is internal to the vessel and would not cause debris generation

Upper internals assembly	Table 3.1.1 Summary of Aging Management Evaluations in Chapter IV of NUREG-1801 for Reactor Vessel, Internals, and Reactor Coolant System [6] Table 3.1.1 Summary of Aging Management Evaluations in Chapter IV of NUREG-1801 for Reactor Vessel, Internals, and Reactor Coolant System [7] Table 3.1.1 Summary of Aging Management Evaluations for the Reactor Vessel, Internals, and Reactor Coolant System [8]	Arizona Public Service Co. [6] (2009) Northern States Power Co. [7] (2008) AmerGen Energy Company, LLC [8] (2008)		The upper internals are internal to the vessel and would not cause debris generation
Lower internal assembly	Table 3.1.1 Summary of Aging Management Evaluations in Chapter IV of NUREG-1801 for Reactor Vessel, Internals, and Reactor Coolant System [6] Table 3.1.1 Summary of Aging Management Evaluations in Chapter IV of NUREG-1801 for Reactor Vessel, Internals, and Reactor Coolant System [7] Table 3.1.1 Summary of Aging Management Evaluations for the Reactor Vessel, Internals,	Arizona Public Service Co. [6] (2009) Northern States Power Co. [7] (2008) AmerGen Energy Company, LLC [8] (2008)		The lower internals are internal to the vessel and would not cause debris generation

	and Reactor Coolant System [8]			
CEA shroud assemblies	Table 3.1.1 Summary of Aging Management Evaluations in Chapter IV of NUREG-1801 for Reactor Vessel, Internals, and Reactor Coolant System [6] Table 3.1.1 Summary of Aging Management Evaluations in Chapter IV of NUREG-1801 for Reactor Vessel, Internals, and Reactor Coolant System [7] Table 3.1.1 Summary of Aging Management Evaluations for the Reactor Vessel, Internals, and Reactor Coolant System [8]	Arizona Public Service Co. [6] (2009) Northern States Power Co. [7] (2008) AmerGen Energy Company, LLC [8] (2008)		The CEA shroud would not cause debris generation
Core shroud assembly	Table 3.1.1 Summary of Aging Management Evaluations in Chapter IV of NUREG-1801 for Reactor Vessel, Internals, and Reactor Coolant System [6] Table 3.1.1 Summary of Aging Management Evaluations in Chapter IV of NUREG-1801 for Reactor Vessel, Internals, and Reactor Coolant System [7]	Arizona Public Service Co. [6] (2009) Northern States Power Co. [7] (2008) AmerGen Energy Company, LLC [8] (2008)		Internal to vessel, would not cause debris generation

	Table 3.1.1 Summary of Aging Management Evaluations for the Reactor Vessel, Internals, and Reactor Coolant System [8]			
Core support shield assembly	Table 3.1.1 Summary of Aging Management Evaluations in Chapter IV of NUREG-1801 for Reactor Vessel, Internals, and Reactor Coolant System [6] Table 3.1.1 Summary of Aging Management Evaluations in Chapter IV of NUREG-1801 for Reactor Vessel, Internals, and Reactor Coolant System [7]	Arizona Public Service Co. [6] (2009) Northern States Power Co. [7] (2008)		Internal, would not cause debris
Core barrel assembly	Table 3.1.1 Summary of Aging Management Evaluations in Chapter IV of NUREG-1801 for Reactor Vessel, Internals, and Reactor Coolant System [6] Table 3.1.1 Summary of Aging Management Evaluations in Chapter IV of NUREG-1801 for Reactor Vessel, Internals, and Reactor Coolant System [7]	Arizona Public Service Co. [6] (2009) Northern States Power Co. [7] (2008)		Internal, would not cause debris
Core Support Barrel Assembly	Table 3.1.2-1 Reactor Vessel, Internals, and Reactor Coolant System – Summary of Aging Management Evaluation – Reactor Vessel and Internals [6]	Arizona Public Service Co. [6] (2009)		Internal, would not cause debris

Core Support Barrel Snubber Assembly	Table 3.1.2-1 Reactor Vessel, Internals, and Reactor Coolant System – Summary of Aging Management Evaluation – Reactor Vessel and Internals [6]	Arizona Public Service Co. [6] (2009)		Internal, would not cause debris
Lower Support Structure Assembly	Table 3.1.2-1 Reactor Vessel, Internals, and Reactor Coolant System – Summary of Aging Management Evaluation – Reactor Vessel and Internals [6]	Arizona Public Service Co. [6] (2009)		Internal, would not cause debris
Lower grid assembly	Table 3.1.1 Summary of Aging Management Evaluations in Chapter IV of NUREG-1801 for Reactor Vessel, Internals, and Reactor Coolant System [6] Table 3.1.1 Summary of Aging Management Evaluations in Chapter IV of NUREG-1801 for Reactor Vessel, Internals, and Reactor Coolant System [7]	Arizona Public Service Co. [6] (2009) Northern States Power Co. [7] (2008)		Internal, would not cause debris
Flow distributor assembly	Table 3.1.1 Summary of Aging Management Evaluations in Chapter IV of NUREG-1801 for Reactor Vessel, Internals, and Reactor Coolant System [6]	Arizona Public Service Co. [6] (2009)		Internal, would not cause debris

	Table 3.1.1 Summary of Aging Management Evaluations in Chapter IV of NUREG-1801 for Reactor Vessel, Internals, and Reactor Coolant System [7]	Northern States Power Co. [7] (2008)		
Reactor vessel upper head (penetration?) nozzles	Table 3.1.1 Summary of Aging Management Evaluations in Chapter IV of NUREG-1801 for Reactor Vessel, Internals, and Reactor Coolant System [6] Table 3.1.1 Summary of Aging Management Evaluations in Chapter IV of NUREG-1801 for Reactor Vessel, Internals, and Reactor Coolant System [7] Table 3.1.1 Summary of Aging Management Evaluations for the Reactor Vessel, Internals, and Reactor Coolant System [8]	Arizona Public Service Co. [6] (2009) Northern States Power Co. [7] (2008) AmerGen Energy Company, LLC [8] (2008)		Failures of RV head nozzles would cause debris generation
Head vent pipe (top head)	Table 3.1.1 Summary of Aging Management Evaluations in Chapter IV of NUREG-1801 for Reactor Vessel, Internals, and Reactor Coolant System [6] Table 3.1.1 Summary of Aging Management Evaluations in Chapter IV of NUREG-1801 for Reactor Vessel, Internals, and Reactor Coolant System [7]	Arizona Public Service Co. [6] (2009) Northern States Power Co. [7] (2008)		Failures of RV head nozzles would cause debris generation

	Table 3.1.1 Summary of Aging Management Evaluations for the Reactor Vessel, Internals, and Reactor Coolant System [8]	AmerGen Energy Company, LLC [8] (2008)		
Head Vent Penetration	Table 3.1.2-1 Reactor Vessel, Internals, and Reactor Coolant System – Summary of Aging Management Evaluation – Reactor Vessel and Internals [6]	Arizona Public Service Co. [6] (2009)		Failures of RV head nozzles would cause debris generation
Vent Penetration Pipe Nozzle	Table 3.1.2-4 Reactor Vessel, Internals, and Reactor Coolant System - Reactor Vessel System - Summary of Aging Management Evaluation [7]	Northern States Power Co. [7] (2008)		Failures of RV head nozzles would cause debris generation
Surveillance capsule holders (and Tubes)	Table 3.1.2-1: Reactor Vessel and CEDM Pressure Boundary [21] Table 3.1.2-1 Reactor Vessel, Internals, and Reactor Coolant System – Summary of Aging Management Evaluation – Reactor Vessel and Internals [6] "The integrated reactor vessel material surveillance program was designed when the surveillance capsule holder tubes in a number of B&W reactors were damaged and	Entergy Operations, Inc. [21] (2003) Arizona Public Service Co. [6] (2009) AmerGen Energy Company, LLC [14] (2008)		Internal to vessel and would not cause debris

	could not be repaired without a complex and expensive repair program and considerable radiation exposure to personnel." [14]			
CEDM motor housing	Table 3.1.2-1: Reactor Vessel and CEDM Pressure Boundary [21]	Entergy Operations, Inc. [21] (2003)		Motor housing is unlikely to cause debris absent a catastrophic failure
RV CEDM Housing (Lower and Upper)	Table 3.1.2-1 Reactor Vessel, Internals, and Reactor Coolant System – Summary of Aging Management Evaluation – Reactor Vessel and Internals [6]	Arizona Public Service Co. [6] (2009)		Housings may cause debris
CEDM upper pressure housing	Table 3.1.2-1: Reactor Vessel and CEDM Pressure Boundary [21]	Entergy Operations, Inc. [21] (2003)		Housings may cause debris
Pressure housings	Table 3.1.2-2 Reactor Vessel Summary of Aging Management Evaluation [8]	AmerGen Energy Company, LLC [8] (2008)		Housings may cause debris
CEDM ball seal housing	Table 3.1.2-1: Reactor Vessel and CEDM Pressure Boundary [21]	Entergy Operations, Inc. [21] (2003)		Housings may cause debris
CEDM upper pressure housing upper fitting	Table 3.1.2-1: Reactor Vessel and CEDM Pressure Boundary [21]	Entergy Operations, Inc. [21] (2003)		Housings may cause debris
CEDM motor housing upper and lower end fittings	Table 3.1.2-1: Reactor Vessel and CEDM Pressure Boundary [21]	Entergy Operations, Inc. [21] (2003)		Housings may cause debris

CEDM upper pressure housing lower fitting	Table 3.1.2-1: Reactor Vessel and CEDM Pressure Boundary [21]	Entergy Operations, Inc. [21] (2003)		Housings may cause debris
CEDM nozzle	Table 3.1.2-1: Reactor Vessel and CEDM Pressure Boundary [21] Table 3.1.2-1 Reactor Vessel, Internals, and Reactor Coolant System – Summary of Aging Management Evaluation – Reactor Vessel and Internals [6]	Entergy Operations, Inc. [21] (2003) Arizona Public Service Co. [6] (2009)		Nozzle failures could cause debris generation
ICI nozzle tubes	Table 3.1.2-1: Reactor Vessel and CEDM Pressure Boundary [21]	Entergy Operations, Inc. [21] (2003)		Nozzle failures could cause debris generation
ICI Nozzle	Table 3.1.2-1 Reactor Vessel, Internals, and Reactor Coolant System – Summary of Aging Management Evaluation – Reactor Vessel and Internals [6]	Arizona Public Service Co. [6] (2009)		Nozzle failures could cause debris generation
CEDM steel ball	Table 3.1.2-1: Reactor Vessel and CEDM Pressure Boundary [21]	Entergy Operations, Inc. [21] (2003)		Failures could cause debris generation
ICI flange adapter/ seal plate	Table 3.1.2-1: Reactor Vessel and CEDM Pressure Boundary [21]	Entergy Operations, Inc. [21] (2003)		The seal table should be outside the containment building
Reactor Vessel Vent Pipe	Table 3.1.2-1: Reactor Vessel and CEDM Pressure Boundary [21]	Entergy Operations, Inc. [21] (2003)		Nozzle failures could cause debris generation

	Table 3.1.2-2 Reactor Coolant System - Reactor Vessel - Summary of Aging Management Evaluation [9]	NextEra Energy Point Beach, LLC [9] (2004)		
Reactor Vessel Vent Pipe Flange	Table 3.1.2-1: Reactor Vessel and CEDM Pressure Boundary [21]	Entergy Operations, Inc. [21] (2003)		Nozzle failures could cause debris generation
Grayloc clamp	Table 3.1.2-1: Reactor Vessel and CEDM Pressure Boundary [21]	Entergy Operations, Inc. [21] (2003)		Not likely to result in debris generation
ICI drive nuts	Table 3.1.2-1: Reactor Vessel and CEDM Pressure Boundary [21]	Entergy Operations, Inc. [21] (2003)		Not likely to result in debris generation
ICI spacer sleeves	Table 3.1.2-1: Reactor Vessel and CEDM Pressure Boundary [21]	Entergy Operations, Inc. [21] (2003)		Not likely to result in debris generation
CEA instrument tube	Table 3.1.2-2 Reactor Vessel Internals [21]	Entergy Operations, Inc. [21] (2003)		Internal components would not cause debris generation
CEA shroud adapter	Table 3.1.2-2 Reactor Vessel Internals [21]	Entergy Operations, Inc. [21] (2003)		Internal components would not cause debris generation
CEA shroud support	Table 3.1.2-2 Reactor Vessel Internals [21]	Entergy Operations, Inc. [21] (2003)		Would not cause debris generation
Ventilation Shroud Support Ring	Table 3.1.2-4 Reactor Vessel, Internals, and Reactor Coolant System - Reactor Vessel	Northern States Power Co. [7] (2008)		Would not cause debris generation

	System - Summary of Aging Management Evaluation [7] Table 3.1.2-1 Reactor Vessels [13] Table 3.1.2-2 Reactor Coolant System - Reactor Vessel - Summary of Aging Management Evaluation [9]	Virginia Electric & Power Co. [13] (2001) NextEra Energy Point Beach, LLC [9] (2004)		
Positioning plate	Table 3.1.2-2 Reactor Vessel Internals [21]	Entergy Operations, Inc. [21] (2003)		Would not cause debris generation
CEA shroud extension shaft guides, cylinders, and bases	Table 3.1.2-2 Reactor Vessel Internals [21]	Entergy Operations, Inc. [21] (2003)		Would not cause debris generation
CEA shroud base	Table 3.1.2-2 Reactor Vessel Internals [21]	Entergy Operations, Inc. [21] (2003)		Would not cause debris generation
CEA shroud flow channel	Table 3.1.2-2 Reactor Vessel Internals [21]	Entergy Operations, Inc. [21] (2003)		Would not cause debris generation
CEA shroud flow channel cap	Table 3.1.2-2 Reactor Vessel Internals [21]	Entergy Operations, Inc. [21] (2003)		Would not cause debris generation

CEA shroud shaft retention pin	Table 3.1.2-2 Reactor Vessel Internals [21]	Entergy Operations, Inc. [21] (2003)		Would not cause debris generation
CEA shroud retention block	Table 3.1.2-2 Reactor Vessel Internals [21]	Entergy Operations, Inc. [21] (2003)		Would not cause debris generation
External spanner nut	Table 3.1.2-2 Reactor Vessel Internals [21]	Entergy Operations, Inc. [21] (2003)		Would not cause debris generation
Internal spanner nut	Table 3.1.2-2 Reactor Vessel Internals [21]	Entergy Operations, Inc. [21] (2003)		
CEA shroud fasteners	Table 3.1.2-2 Reactor Vessel Internals [21]	Entergy Operations, Inc. [21] (2003)		
CEA shroud flow channel extension	Table 3.1.2-2 Reactor Vessel Internals [21]	Entergy Operations, Inc. [21] (2003)		
CEA shroud tube	Table 3.1.2-2 Reactor Vessel Internals [21]	Entergy Operations, Inc. [21] (2003)		
Core Shroud Plates	Table 3.1.2-2 Reactor Vessel Internals [21]	Entergy Operations, Inc. [21] (2003)		
Plates	Table 3.1.2-2 Reactor Vessel Internals [21]	Entergy Operations, Inc. [21] (2003)		

Ribs	Table 3.1.2-2 Reactor Vessel Internals [21]	Entergy Operations, Inc. [21] (2003)		
Intermediate Plates	Table 3.1.2-2 Reactor Vessel Internals [21]	Entergy Operations, Inc. [21] (2003)		
Core Shroud Guide Lugs	Table 3.1.2-2 Reactor Vessel Internals [21]	Entergy Operations, Inc. [21] (2003)		
CSB Alignment Keys	Table 3.1.2-2 Reactor Vessel Internals [21]	Entergy Operations, Inc. [21] (2003)		
CSB assembly dowel pin	Table 3.1.2-2 Reactor Vessel Internals [21]	Entergy Operations, Inc. [21] (2003)		
CSB lifting bolt insert	Table 3.1.2-2 Reactor Vessel Internals [21]	Entergy Operations, Inc. [21] (2003)		
CSB lower flange	Table 3.1.2-2 Reactor Vessel Internals [21]	Entergy Operations, Inc. [21] (2003)		
CSB lug	Table 3.1.2-2 Reactor Vessel Internals [21]	Entergy Operations, Inc. [21] (2003)		
CSB nozzle	Table 3.1.2-2 Reactor Vessel Internals [21]	Entergy Operations, Inc. [21] (2003)		
CSB cylinder	Table 3.1.2-2 Reactor Vessel Internals [21]	Entergy Operations, Inc. [21] (2003)		
CSB upper flange	Table 3.1.2-2 Reactor Vessel Internals [21]	Entergy Operations, Inc. [21] (2003)		

ICI Guide tubes	Table 3.1.2-2 Reactor Vessel Internals [21] Table 3.1.2-1 Reactor Vessel, Internals, and Reactor Coolant System – Summary of Aging Management Evaluation – Reactor Vessel and Internals [6]	Entergy Operations, Inc. [21] (2003) Arizona Public Service Co. [6] (2009)		May cause debris generation
Bottom Mounted Instrument Guide Tubes	Table 3.1.2-2 Reactor Coolant System - Reactor Vessel - Summary of Aging Management Evaluation [9]	NextEra Energy Point Beach, LLC [9] (2004)		May cause debris generation
Bottom Mounted Instrumentation Column	Table 3.1.2-3 Reactor Coolant System - Reactor Vessel Internals - Summary of Aging Management Evaluation [9]	NextEra Energy Point Beach, LLC [9] (2004)		May cause debris generation
ICI thimble support plate assembly	Table 3.1.2-2 Reactor Vessel Internals [21]	Entergy Operations, Inc. [21] (2003)		
ICI Support Structures	Table 3.1.2-1 Reactor Vessel, Internals, and Reactor Coolant System – Summary of Aging Management Evaluation – Reactor Vessel and Internals [6]	Arizona Public Service Co. [6] (2009)		
ICI support plate, grid, lifting support, lifting plate, column, plates, funnel	Table 3.1.2-2 Reactor Vessel Internals [21]	Entergy Operations, Inc. [21] (2003)		

ICI Pad, ring, nipple, hex bolt, spacer	Table 3.1.2-2 Reactor Vessel Internals [21]	Entergy Operations, Inc. [21] (2003)		
ICI Threaded rod, hex jam nut, thimble support nut, cap screws	Table 3.1.2-2 Reactor Vessel Internals [21]	Entergy Operations, Inc. [21] (2003)		
UGS CEA Shroud Assembly	Table 3.1.2-1 Reactor Vessel, Internals, and Reactor Coolant System – Summary of Aging Management Evaluation – Reactor Vessel and Internals [6]	Arizona Public Service Co. [6] (2009)		
UGS Holddown Ring	Table 3.1.2-1 Reactor Vessel, Internals, and Reactor Coolant System – Summary of Aging Management Evaluation – Reactor Vessel and Internals [6]	Arizona Public Service Co. [6] (2009)		
UGS Support Barrel Assembly	Table 3.1.2-1 Reactor Vessel, Internals, and Reactor Coolant System – Summary of Aging Management Evaluation – Reactor Vessel and Internals [6]	Arizona Public Service Co. [6] (2009)		
Lower Internals Assembly Bottom plate	Table 3.1.2-2 Reactor Vessel Internals [21]	Entergy Operations, Inc. [21] (2003)		
Lower Internals Assembly Bottom plate manhole cover	Table 3.1.2-2 Reactor Vessel Internals [21]	Entergy Operations, Inc. [21] (2003)		
Lower Internals Assembly Cylinder	Table 3.1.2-2 Reactor Vessel Internals [21]	Entergy Operations, Inc. [21] (2003)		

Lower Internals Assembly Core support column	Table 3.1.2-2 Reactor Vessel Internals [21]	Entergy Operations, Inc. [21] (2003)		
Lower Internals Assembly Core support plate	Table 3.1.2-2 Reactor Vessel Internals [21]	Entergy Operations, Inc. [21] (2003)		
Lower Internals Assembly Insert pins	Table 3.1.2-2 Reactor Vessel Internals [21]	Entergy Operations, Inc. [21] (2003)		
Lower Internals Assembly Support beam	Table 3.1.2-2 Reactor Vessel Internals [21]	Entergy Operations, Inc. [21] (2003)		
Lower Internals Assembly Support beam flange	Table 3.1.2-2 Reactor Vessel Internals [21]	Entergy Operations, Inc. [21] (2003)		
Upper Internals Assembly FAP plate	Table 3.1.2-2 Reactor Vessel Internals [21]	Entergy Operations, Inc. [21] (2003)		
Upper Internals Assembly FAP guide lug inserts	Table 3.1.2-2 Reactor Vessel Internals [21]	Entergy Operations, Inc. [21] (2003)		
Upper Internals Assembly Holddown ring	Table 3.1.2-2 Reactor Vessel Internals [21]	Entergy Operations, Inc. [21] (2003)		
Upper Internals Assembly Upper guide structure (UGS) support plate	Table 3.1.2-2 Reactor Vessel Internals [21]	Entergy Operations, Inc. [21] (2003)		
Upper Internals Assembly UGS cylinder	Table 3.1.2-2 Reactor Vessel Internals [21]	Entergy Operations, Inc. [21] (2003)		
Upper Internals Assembly UGS grid plate	Table 3.1.2-2 Reactor Vessel Internals [21]	Entergy Operations, Inc. [21] (2003)		

Upper Internals Assembly UGS flange	Table 3.1.2-2 Reactor Vessel Internals [21]	Entergy Operations, Inc. [21] (2003)		
Upper Internals Assembly UGS sleeve	Table 3.1.2-2 Reactor Vessel Internals [21]	Entergy Operations, Inc. [21] (2003)		
Upper Internals Assembly UGS lifting bolt insert	Table 3.1.2-2 Reactor Vessel Internals [21]	Entergy Operations, Inc. [21] (2003)		
Upper Internals Assembly UGS alignment keys	Table 3.1.2-2 Reactor Vessel Internals [21]	Entergy Operations, Inc. [21] (2003)		
Upper Internals Assembly UGS dowel pins	Table 3.1.2-2 Reactor Vessel Internals [21]	Entergy Operations, Inc. [21] (2003)		
Flow Venturi	Table 3.1.2-2 Reactor Vessel Summary of Aging Management Evaluation [8]	AmerGen Energy Company, LLC [8] (2008)		
Valve Body	Table 3.1.2-2 Reactor Vessel Summary of Aging Management Evaluation [8]	AmerGen Energy Company, LLC [8] (2008)		
Control rod guide tube assembly	Table 3.1.1 Summary of Aging Management Evaluations for the Reactor Vessel, Internals, and Reactor Coolant System [8]	AmerGen Energy Company, LLC [8] (2008)		
CRGT pipe and flange	Table 3.1.2-2 Reactor Vessel Summary of Aging Management Evaluation [8]	AmerGen Energy Company, LLC [8] (2008)		

CRGT rod guide sectors	Table 3.1.2-2 Reactor Vessel Summary of Aging Management Evaluation [8]	AmerGen Energy Company, LLC [8] (2008)		
CRGT rod guide tubes	Table 3.1.2-2 Reactor Vessel Summary of Aging Management Evaluation [8]	AmerGen Energy Company, LLC [8] (2008)		
CRGT spacer casting	Table 3.1.2-2 Reactor Vessel Summary of Aging Management Evaluation [8]	AmerGen Energy Company, LLC [8] (2008)		
CRGT spacer screws	Table 3.1.2-2 Reactor Vessel Summary of Aging Management Evaluation [8]	AmerGen Energy Company, LLC [8] (2008)		
Flange-to-upper grid screws	Table 3.1.2-2 Reactor Vessel Summary of Aging Management Evaluation [8]	AmerGen Energy Company, LLC [8] (2008)		
Baffle/former assembly	Table 3.1.2-2 Reactor Vessel Summary of Aging Management Evaluation [8]	AmerGen Energy Company, LLC [8] (2008)		

Baffle and Former Plates	Table 3.1.2-3 Reactor Coolant System - Reactor Vessel Internals - Summary of Aging Management Evaluation [9]	NextEra Energy Point Beach, LLC [9] (2004)		
Core Barrel Assembly	Table 3.1.1 Summary of Aging Management Evaluations for the Reactor Vessel, Internals, and Reactor Coolant System [8]	AmerGen Energy Company, LLC [8] (2008)		
Baffle/former bolts and screws	Table 3.1.2-2 Reactor Vessel Summary of Aging Management Evaluation [8] Table 3.1.2-3 Reactor Coolant System - Reactor Vessel Internals - Summary of Aging Management Evaluation	AmerGen Energy Company, LLC [8] (2008) NextEra Energy Point Beach, LLC [9] (2004)		
Core barrel cylinder (top and bottom flange)	Table 3.1.2-2 Reactor Vessel Summary of Aging Management Evaluation [8]	AmerGen Energy Company, LLC [8] (2008)		
Core barrel-to-thermal shield bolts	Table 3.1.2-2 Reactor Vessel Summary of Aging Management Evaluation [8]	AmerGen Energy Company, LLC [8] (2008)		

Lower Internals assembly-to-core barrel bolts	Table 3.1.2-2 Reactor Vessel Summary of Aging Management Evaluation [8]	AmerGen Energy Company, LLC [8] (2008)		
Core support shield assembly	Table 3.1.1 Summary of Aging Management Evaluations for the Reactor Vessel, Internals, and Reactor Coolant System [8]	AmerGen Energy Company, LLC [8] (2008)		
Core support shield cylinder (top and bottom flange)	Table 3.1.2-2 Reactor Vessel Summary of Aging Management Evaluation [8]	AmerGen Energy Company, LLC [8] (2008)		
Core support shield-to-core barrel bolts	Table 3.1.2-2 Reactor Vessel Summary of Aging Management Evaluation [8]	AmerGen Energy Company, LLC [8] (2008)		
Outlet and vent valve nozzles	Table 3.1.2-2 Reactor Vessel Summary of Aging Management Evaluation [8]	AmerGen Energy Company, LLC [8] (2008)		
Vent valve assembly locking device	Table 3.1.2-2 Reactor Vessel Summary of Aging Management Evaluation [8]	AmerGen Energy Company, LLC [8] (2008)		
Vent valve body	Table 3.1.2-2 Reactor Vessel Summary of Aging Management Evaluation [8]	AmerGen Energy Company, LLC [8] (2008)		

Vent valve retaining ring	Table 3.1.2-2 Reactor Vessel Summary of Aging Management Evaluation [8]	AmerGen Energy Company, LLC [8] (2008)		
Clamping ring	Table 3.1.2-2 Reactor Vessel Summary of Aging Management Evaluation [8]	AmerGen Energy Company, LLC [8] (2008)		
Flow distributor assembly	Table 3.1.1 Summary of Aging Management Evaluations for the Reactor Vessel, Internals, and Reactor Coolant System [8]	AmerGen Energy Company, LLC [8] (2008)		
Flow distributor head and flange	Table 3.1.2-2 Reactor Vessel Summary of Aging Management Evaluation [8]	AmerGen Energy Company, LLC [8] (2008)		
Incore guide support plate	Table 3.1.2-2 Reactor Vessel Summary of Aging Management Evaluation [8]	AmerGen Energy Company, LLC [8] (2008)		
Shell forging-to-flow distributor bolts	Table 3.1.2-2 Reactor Vessel Summary of Aging Management Evaluation [8]	AmerGen Energy Company, LLC [8] (2008)		

Lower grid assembly	Table 3.1.1 Summary of Aging Management Evaluations for the Reactor Vessel, Internals, and Reactor Coolant System [8]	AmerGen Energy Company, LLC [8] (2008)		
Fuel assembly support pads	Table 3.1.2-2 Reactor Vessel Summary of Aging Management Evaluation [8]	AmerGen Energy Company, LLC [8] (2008)		
Guide blocks	Table 3.1.2-2 Reactor Vessel Summary of Aging Management Evaluation [8]	AmerGen Energy Company, LLC [8] (2008)		
Guide blocks bolts	Table 3.1.2-2 Reactor Vessel Summary of Aging Management Evaluation [8]	AmerGen Energy Company, LLC [8] (2008)		
Incore guide tube spider castings	Table 3.1.2-2 Reactor Vessel Summary of Aging Management Evaluation [8]	AmerGen Energy Company, LLC [8] (2008)		
Lower grid and shell forgings	Table 3.1.2-2 Reactor Vessel Summary of Aging Management Evaluation [8]	AmerGen Energy Company, LLC [8] (2008)		
Lower grid flow distributor plate	Table 3.1.2-2 Reactor Vessel Summary of Aging Management Evaluation [8]	AmerGen Energy Company, LLC [8] (2008)		

Lower grid rib section	Table 3.1.2-2 Reactor Vessel Summary of Aging Management Evaluation [8]	AmerGen Energy Company, LLC [8] (2008)		
Lower grid rib-to-shell forging screws	Table 3.1.2-2 Reactor Vessel Summary of Aging Management Evaluation [8]	AmerGen Energy Company, LLC [8] (2008)		
Lower internals assembly-to-thermal shield bolts	Table 3.1.2-2 Reactor Vessel Summary of Aging Management Evaluation [8]	AmerGen Energy Company, LLC [8] (2008)		
Orifice plugs	Table 3.1.2-2 Reactor Vessel Summary of Aging Management Evaluation [8]	AmerGen Energy Company, LLC [8] (2008)		
Shock pads	Table 3.1.2-2 Reactor Vessel Summary of Aging Management Evaluation [8]	AmerGen Energy Company, LLC [8] (2008)		
Shock Pads Bolts	Table 3.1.2-2 Reactor Vessel Summary of Aging Management Evaluation [8]	AmerGen Energy Company, LLC [8] (2008)		

Support post pipes	Table 3.1.2-2 Reactor Vessel Summary of Aging Management Evaluation [8]	AmerGen Energy Company, LLC [8] (2008)		
Plenum cover and plenum cylinder	Table 3.1.1 Summary of Aging Management Evaluations for the Reactor Vessel, Internals, and Reactor Coolant System [8]	AmerGen Energy Company, LLC [8] (2008)		
Bottom flange-to-upper grid screws	Table 3.1.2-2 Reactor Vessel Summary of Aging Management Evaluation [8]	AmerGen Energy Company, LLC [8] (2008)		
Plenum cover assembly	Table 3.1.2-2 Reactor Vessel Summary of Aging Management Evaluation [8]	AmerGen Energy Company, LLC [8] (2008)		
Plenum cylinder	Table 3.1.2-2 Reactor Vessel Summary of Aging Management Evaluation [8]	AmerGen Energy Company, LLC [8] (2008)		
Reinforcing plates	Table 3.1.2-2 Reactor Vessel Summary of Aging Management Evaluation [8]	AmerGen Energy Company, LLC [8] (2008)		
Rib Pads	Table 3.1.2-2 Reactor Vessel Summary of Aging Management Evaluation [8]	AmerGen Energy Company, LLC [8] (2008)		

Top flange-to-cover bolts	Table 3.1.2-2 Reactor Vessel Summary of Aging Management Evaluation [8]	AmerGen Energy Company, LLC [8] (2008)		
Incore Guide Tube Gussets	Table 3.1.2-2 Reactor Vessel Summary of Aging Management Evaluation [8]	AmerGen Energy Company, LLC [8] (2008)		
Incore Guide Tube Nuts	Table 3.1.2-2 Reactor Vessel Summary of Aging Management Evaluation [8]	AmerGen Energy Company, LLC [8] (2008)		
Incore Guide Tube Spiders	Table 3.1.2-2 Reactor Vessel Summary of Aging Management Evaluation [8]	AmerGen Energy Company, LLC [8] (2008)		
Incore Guide Tubes	Table 3.1.2-2 Reactor Vessel Summary of Aging Management Evaluation [8]	AmerGen Energy Company, LLC [8] (2008)		
Thermal Shield	Table 3.1.2-2 Reactor Vessel Summary of Aging Management Evaluation [8]	AmerGen Energy Company, LLC [8] (2008)		

Upper grid assembly	Table 3.1.1 Summary of Aging Management Evaluations for the Reactor Vessel, Internals, and Reactor Coolant System [8]	AmerGen Energy Company, LLC [8] (2008)		
Rib-to-ring screws	Table 3.1.2-2 Reactor Vessel Summary of Aging Management Evaluation [8]	AmerGen Energy Company, LLC [8] (2008)		
Upper grid rib section	Table 3.1.2-2 Reactor Vessel Summary of Aging Management Evaluation [8]	AmerGen Energy Company, LLC [8] (2008)		
Upper grid ring forging	Table 3.1.2-2 Reactor Vessel Summary of Aging Management Evaluation [8]	AmerGen Energy Company, LLC [8] (2008)		
Instrumentation support structures	Table 3.1.2-2 Reactor Vessel Summary of Aging Management Evaluation [8]	AmerGen Energy Company, LLC [8] (2008)		
Control Rod Drive Flange	"During the Fall 2005 refueling outage, minor boric acid deposits were visible during the video inspection at three CRD flanges." [14]	AmerGen Energy Company, LLC [14] (2008)		
CRDM Flanges	Table 3.1.2-2 Reactor Coolant System - Reactor Vessel -	NextEra Energy Point Beach, LLC [9] (2004)		

	Summary of Aging Management Evaluation [9]			
Seal Table Fittings	Table 3.1.2-2 Reactor Coolant System - Reactor Vessel - Summary of Aging Management Evaluation [9]	NextEra Energy Point Beach, LLC [9] (2004)		
Clevis Insert Bolt Locking Mechanisms	Table 3.1.2-3 Reactor Coolant System - Reactor Vessel Internals - Summary of Aging Management Evaluation [9]	NextEra Energy Point Beach, LLC [9] (2004)		
Clevis Insert Bolts	Table 3.1.2-3 Reactor Coolant System - Reactor Vessel Internals - Summary of Aging Management Evaluation [9]	NextEra Energy Point Beach, LLC [9] (2004)		
Clevis Inserts	Table 3.1.2-3 Reactor Coolant System - Reactor Vessel Internals - Summary of Aging Management Evaluation [9]	NextEra Energy Point Beach, LLC [9] (2004)		
Core Barrel - Plates	Table 3.1.2-3 Reactor Coolant System - Reactor Vessel Internals - Summary of Aging Management Evaluation [9]	NextEra Energy Point Beach, LLC [9] (2004)		

Core Barrel Flange – ring forging, Core Barrel (guide key)	Table 3.1.2-3 Reactor Coolant System - Reactor Vessel Internals - Summary of Aging Management Evaluation [9]	NextEra Energy Point Beach, LLC [9] (2004)		
Core Barrel Outlet Nozzle - Nozzle forgings	Table 3.1.2-3 Reactor Coolant System - Reactor Vessel Internals - Summary of Aging Management Evaluation [9]	NextEra Energy Point Beach, LLC [9] (2004)		
RCCA Flexures	Table 3.1.2-3 Reactor Coolant System - Reactor Vessel Internals - Summary of Aging Management Evaluation [9]	NextEra Energy Point Beach, LLC [9] (2004)		
GT Support pin (split pin)	Table 3.1.2-3 Reactor Coolant System - Reactor Vessel Internals - Summary of Aging Management Evaluation [9]	NextEra Energy Point Beach, LLC [9] (2004)		
Flux Thimbles	Table 3.1.2-3 Reactor Coolant System - Reactor Vessel Internals - Summary of Aging Management Evaluation [9] Table 3.1.2-1 Reactor Vessel, Internals, and Reactor Coolant System – Summary of Aging Management Evaluation – Reactor Vessel and Internals [17]	NextEra Energy Point Beach, LLC [9] (2004) STP Nuclear Operating Co. [17] (2010)		

Head and Vessel Alignment Pins	Table 3.1.2-3 Reactor Coolant System - Reactor Vessel Internals - Summary of Aging Management Evaluation [9]	NextEra Energy Point Beach, LLC [9] (2004)		
Holddown Spring	Table 3.1.2-3 Reactor Coolant System - Reactor Vessel Internals - Summary of Aging Management Evaluation [9]	NextEra Energy Point Beach, LLC [9] (2004)		
Lower Core Plate	Table 3.1.2-3 Reactor Coolant System - Reactor Vessel Internals - Summary of Aging Management Evaluation [9]	NextEra Energy Point Beach, LLC [9] (2004)		
Lower Core Plate Fuel Alignment Pins	Table 3.1.2-3 Reactor Coolant System - Reactor Vessel Internals - Summary of Aging Management Evaluation [9]	NextEra Energy Point Beach, LLC [9] (2004)		
Lower Support Columns, Sleeves	Table 3.1.2-3 Reactor Coolant System - Reactor Vessel Internals - Summary of Aging Management Evaluation [9]	NextEra Energy Point Beach, LLC [9] (2004)		

Lower Support Forging	Table 3.1.2-3 Reactor Coolant System - Reactor Vessel Internals - Summary of Aging Management Evaluation [9]	NextEra Energy Point Beach, LLC [9] (2004)		
Lower Support Plate Column Bolts/Nuts	Table 3.1.2-3 Reactor Coolant System - Reactor Vessel Internals - Summary of Aging Management Evaluation [9]	NextEra Energy Point Beach, LLC [9] (2004)		
Radial Support Keys	Table 3.1.2-3 Reactor Coolant System - Reactor Vessel Internals - Summary of Aging Management Evaluation [9]	NextEra Energy Point Beach, LLC [9] (2004)		
RCCA Guide Tubes, Inserts, and Flow Downcomers	Table 3.1.2-3 Reactor Coolant System - Reactor Vessel Internals - Summary of Aging Management Evaluation [9]	NextEra Energy Point Beach, LLC [9] (2004)		
Secondary Core Support - base plate, energy absorber, Diffuser Plate (Flow Mixer Plate)	Table 3.1.2-3 Reactor Coolant System - Reactor Vessel Internals - Summary of Aging Management Evaluation [9]	NextEra Energy Point Beach, LLC [9] (2004)		
Secondary Core Support Assembly - guide post, housing	Table 3.1.2-3 Reactor Coolant System - Reactor Vessel Internals - Summary of Aging Management Evaluation [9]	NextEra Energy Point Beach, LLC [9] (2004)		

(Head-Cooling) Spray nozzle bodies, and nozzle tips	Table 3.1.2-3 Reactor Coolant System - Reactor Vessel Internals - Summary of Aging Management Evaluation [9]	NextEra Energy Point Beach, LLC [9] (2004)		
Thermal shield - plate material, flexures, Dowel Pin	Table 3.1.2-3 Reactor Coolant System - Reactor Vessel Internals - Summary of Aging Management Evaluation [9]	NextEra Energy Point Beach, LLC [9] (2004)		
Upper Core Plate	Table 3.1.2-3 Reactor Coolant System - Reactor Vessel Internals - Summary of Aging Management Evaluation [9]	NextEra Energy Point Beach, LLC [9] (2004)		
Upper Core Plate Alignment Pin	Table 3.1.2-3 Reactor Coolant System - Reactor Vessel Internals - Summary of Aging Management Evaluation [9]	NextEra Energy Point Beach, LLC [9] (2004)		
Upper Core Plate Fuel Alignment Pin	Table 3.1.2-3 Reactor Coolant System - Reactor Vessel Internals - Summary of Aging Management Evaluation [9]	NextEra Energy Point Beach, LLC [9] (2004)		
Upper Instrumentation Column, Conduit (tubing and supports), Spacers/Clamps	Table 3.1.2-3 Reactor Coolant System - Reactor Vessel Internals - Summary of Aging Management Evaluation [9]	NextEra Energy Point Beach, LLC [9] (2004)		

Upper Support Column and Bottom Nozzles	Table 3.1.2-3 Reactor Coolant System - Reactor Vessel Internals - Summary of Aging Management Evaluation [9]	NextEra Energy Point Beach, LLC [9] (2004)		
Upper Support Column-instr. Fittings- for installation of instrumentation	Table 3.1.2-3 Reactor Coolant System - Reactor Vessel Internals - Summary of Aging Management Evaluation [9]	NextEra Energy Point Beach, LLC [9] (2004)		
Upper Support Column-USC Base castings	Table 3.1.2-3 Reactor Coolant System - Reactor Vessel Internals - Summary of Aging Management Evaluation [9]	NextEra Energy Point Beach, LLC [9] (2004)		
Upper Support Column Bolts	Table 3.1.2-3 Reactor Coolant System - Reactor Vessel Internals - Summary of Aging Management Evaluation [9]	NextEra Energy Point Beach, LLC [9] (2004)		
Upper Support Plate, deep beam weldment, top plate, ribs, hollow rounds	Table 3.1.2-3 Reactor Coolant System - Reactor Vessel Internals - Summary of Aging Management Evaluation [9]	NextEra Energy Point Beach, LLC [9] (2004)		
Refueling Missile Shield	Table 3.1.2-1 Reactor Vessel, Internals, and Reactor Coolant System – Summary of Aging Management Evaluation – Reactor Vessel and Internals [17]	STP Nuclear Operating Co. [17] (2010)		

* Contains welds

References

[1] I. Entergy Operations, "License renewal application arkansas nuclear one - units 2 appendix B," U.S. Nuclear Regulatory Commission, October 2003.

[2] Duke Energy Corp., "Oconee nuclear station, units 1, 2 & 3- license renewal application volume II," U.S. Nuclear Regulatory Commission, June 1998.

[3] I. Entergy Nuclear Operations, "Palisades nuclear plant - application for renewed operating license," U.S. Nuclear Regulatory Commission, March 2005.

[4] M. Suzuki, T. Takeda, H. Asaka and H. Nakamura, "Effects of Secondary Depressurization on Core Cooling in PWR Vessel Bottom Small Break LOCA Experiments with HPI Failure and Gas Inflow," vol. 43, pp. 55-64, 2012.

[5] F. Miraglia, "Boric Acid Corrosion of Carbon Steel Reactor Pressure Boundary Components in PWR Plants (Generic Letter No. 88-05)," March, 17 1988.

[6] Arizona Public Service Co., "License renewal application palo verde nuclear generating station unit 1, unit 2, and Unit 3," U.S. Nuclear Regulatory Commission, 2009.

[7] Northern States Power Co., "Application for renewed operating licenses prairie island nuclear generating plant units 1 and 2," U.S. Nuclear Regulatory Commission, 2008.

[8] L. AmerGen Energy Company, "License renewal application three mile island nuclear station unit 1," U.S. Nuclear Regulatory Commission, 2008.

[9] NextEra Energy Point Beach, LLC, "Application for renewed operating licenses point beach nuclear plant units 1 & 2," U.S. Nuclear Regulatory Commission, 2004.

[10] S. A. Loehlin, "Root cause analysis report: Significant degradation of the reactor pressure vessel head," FirstEnergy Nuclear Operating Company, April, Tech. Rep. CR 2002-0891, 2002.

[11] C. Queral, J. González-Cadelo, G. Jimenez and E. Villalba, "Accident management actions in a upper-head small-break loss-of-coolant accident with high-pressure safety injection failed," Tech. Rep. 3, 2011.

[12] M. Subudhi, R. Morante and A. Lee, "Aging management of reactor coolant system mechanical components in pressurized water reactors for license renewal," in *ASME 2002 Pressure Vessels and Piping Conference*, 2002, pp. 41-49.

[13] Virginia Electric & Power Co., "Application for renewed operating licenses north anna power station units 1 and 2," U.S. Nuclear Regulatory Commission, 2001.

[14] L. AmerGen Energy Company, "License renewal application three mile island nuclear station unit 1 appendix B," U.S. Nuclear Regulatory Commission, 2008.

[15] Omaha Public Power District, "Fort calhoun station, unit 1- license renewal application section 3," U.S. Nuclear Regulatory Commission, January 2002.

[16] R.E. Ginna Nuclear Power Plant, LLC, "Application for renewed operating license R. E. ginna nuclear power plant," U.S. Nuclear Regulatory Commission, 2002.

[17] STP Nuclear Operating Co., "License renewal application south texas project unit 1 and unit 2," U.S. Nuclear Regulatory Commission, 2010.

[18] I. Entergy Nuclear Operations, "Indian point nuclear generating unit 2 and 3 - license renewal application appendix A," U.S. Nuclear Regulatory Commission, April 2007.

[19] J. Lee, J. Y. Lee, S. J. Hong, J. Y. Park, Y. Ryu and M. Kim, "Evaluation of recirculation sump performance for OPR1000 plant: Part I debris transport during the blow-down phase of LOCA," *Ann. Nucl. Energy*, vol. 38, pp. 681-693, 0, 2011.

[20] Calvert Cliffs Nuclear Power Plant Inc., "Calvert cliffs nuclear power plant, units 1 & 2 - license renewal application volume 1," U.S. Nuclear Regulatory Commission, April 1998.

[21] I. Entergy Operations, "License renewal application arkansas nuclear one - units 2," U.S. Nuclear Regulatory Commission, October 2003.

[22] Northern States Power Co., "Application for renewed operating licenses prairie island nuclear generating plant units 1 and 2 appendix B," U.S. Nuclear Regulatory Commission, 2008.

[23] I. Dominion Nuclear Connecticut, "Millstone nuclear power station, units 2 - license renewal application," U.S. Nuclear Regulatory Commission, January 2004.

[24] I. Entergy Nuclear Operations, "License renewal application indian point nuclear generating sections 1-4," U.S. Nuclear Regulatory Commission, April 2007.

[25] I. Dominion Nuclear Connecticut, "Millstone nuclear power station, units 3 - license renewal application," U.S. Nuclear Regulatory Commission, January 2004.

[26] Arizona Public Service Co., "License renewal application palo verde nuclear generating station unit 1, unit 2, and unit 3 supplement 1," U.S. Nuclear Regulatory Commission, Washington, D.C. 20555-0001, 2009.

EMERGENCY CORE COOLING SYSTEM

Component	Highlight	Author	GSI-191 Evidence	Expert Comments
CSS Heat exchanger (shell)	Table 3.2.2-2 Containment Spray System Summary of Aging Management (CSS Heat Exchanger (Shell) – Carbon Steel – Air (External) – Loss of Material) [1] Table 3.5-3 Applicable Aging Effects for Components of Emergency Core Cooling Systems (HPIS Heat Exchanger Shell - Stainless Steel – Borated Water – Loss of Material and Cracking) [2] TABLE 3.3-2 CONTAINMENT SPRAY (Containment Spray Pump Seal Water Heat Exchanger Shells – Cast Iron – Treated Water – Borated – Loss of Material) [3] TABLE 3.3-2 CONTAINMENT SPRAY (Containment Spray Pump Seal Water Heat Exchanger Covers - Cast Iron – Treated Water – Borated – Loss of Material) [3] Table 3.2.2-3 Engineered Safety Features, Emergency Core Cooling System – Summary of Aging Management Review (RHR Heat Exchanger (Shell) – Carbon Steel – Inside – Loss of Material – Borated Water Leakage Assessment and Evaluation Program) [4]	Entergy Operations, Inc. (2003) Duke Energy Corp. [2] (1998) Florida Power & Light Co. [3] (2000) Southern Nuclear Operating Co., Inc. [4] (2003) Southern Nuclear Operating Co., Inc. [5] (2007) Indiana Michigan Power Co. [6] (2003)		In some plants, the CSS does not use a heat exchanger for the pumped water. In this case, there is no effect. In plants where the CSS is pumped through the heat exchanger, plugging by debris needs to be checked. I think CSS HX is not part of Class 1 piping system pressure boundary. Additionally, if a leak/breach occurs, it would be an isolable LOCA without a significant contribution to the debris-clogging issue.

	Table 3.2.2-2 Emergency Core Cooling System: Summary of Aging Management Review (RHR Heat Exchanger (Shells) Carbon Steel – Air – Indoor (Exterior) (Borated Water Leakage) – Loss of Material (Boric Acid Corrosion Control Program)) [5] Table 3.2.2-3 Emergency Core Cooling System Summary of Aging Management Evaluation (Heat Exchanger (Shell) – Carbon Steel – Loss of Material (Boric Acid Corrosion Prevention)) [6]			
Tanks	Table 3.2.2-1 Emergency Core Cooling System Summary of Aging Management (Tank – Carbon Steel with Stainless Cladding - Treated Borated Water (Internal) – Loss of Material) [1] Table 3.2.2-3 Emergency Core Cooling System Summary of Aging Management Evaluation (Tank – Carbon Steel with Stainless Steel Cladding – Treated Water (Borated) (Internal) – Loss of Material) [6] Table : V ENGINEERED SAFETY FEATURES D1 Emergency Core Cooling System (PWR) [7] Table 3.2.2-2 Containment Spray System Summary of Aging Management (CSS Tank	Entergy Operations, Inc. [1] (2003) Indiana Michigan Power Co. [6] (2003) Nuclear Regulatory Commission [7] (2010) Duke Energy Corp. [2] (1998) Exelon Generation Co., LLC [8] (2008)		The RWST is need to inject borated water required for reactivity control during cool down. However, tank failure is not directly related to GSI-191 concerns I agree.

	- Stainless Steel – Treated Borated Water (Internal) – Loss of Material) [1] Table 3.2.2-1 Core Flooding System Summary of Aging Management Evaluation [8] Table 3.5-3 Applicable Aging Effects for Components of Emergency Core Cooling Systems (CFS Tank – Stainless Steel – Borated Water – Loss of Material and Cracking) [2] Table 3.5-3 Applicable Aging Effects for Components of Emergency Core Cooling Systems (High Pressure Injection System Tank – Stainless Steel – Borated Water – Loss of Material and Cracking) [2] Table 3.5-3 Applicable Aging Effects for Components of Emergency Core Cooling Systems (Low Pressure Injection System Tank – Carbon Steel (Lined) – Borated Water – Loss of Material) [2] Table 3.2.2-3 Engineered Safety Features, Emergency Core Cooling System – Summary of Aging Management Review (Refueling Water Storage Tank - Stainless Steel – Borated Water – loss of Material) [4] Table 3.2.2-2 Emergency Core Cooling System: Summary of Aging Management	Duke Energy Corp. [2] (1998) Southern Nuclear Operating Co., Inc. [4] (2003) Southern Nuclear Operating Co., Inc. [5] (2007)		

	Review (Eductors – RWST Mixing – Stainless Steel Borated Water (Interior) – Loss of Material) [5] Table 3.2.2-2 Emergency Core Cooling System: Summary of Aging Management Review (Tank – Boron Injection Tank (Unit 1 only) – Stainless Steel – Borated Water (Interior) – Loss of Material) [5] Table 3.2.2-2 Emergency Core Cooling System: Summary of Aging Management Review (Tank Liners (& internals) – RWST Liners – Stainless Steel – Borated Water (Interior) – Loss of Material) [5] Table 3.2.2-2 Emergency Core Cooling System: Summary of Aging Management Review (Tanks – SI Accumulator Tanks – Carbon Steel (with Stainless Steel Cladding) – Borated Water (Interior) – Loss of Material) [5]			
Bolting and Bearings	Table 3.2.2-1 Emergency Core Cooling System Summary of Aging Management (Bolting – Carbon Steel - Air (External) – Loss of Material – Boric Acid Corrosion Prevention) [1] Table 3.2.2-1 Core Flooding System Summary of Aging Management Evaluation (CFS Bolting – Carbon and Low Alloy Steel Bolting – Air with Borated Water Leakage	Entergy Operations, Inc. [1] (2003) Exelon Generation Co., LLC [8] (2008)		Typically, CSS pumps are low pressure and not connected to the RCS (high pressure) system. Failure of the CSS due to boron corrosion is not directly related to GSI-191 concerns.

	(External) – Loss of Material - Boric Acid Corrosion) [8] Table 3.2.2-3 Emergency Core Cooling System Summary of Aging Management Evaluation (Bolting – Carbon Steel – Air (External) – Loss of material (Boric Acid Corrosion Prevention) and Loss of mechanical Closure Integrity (Boric Acid Corrosion Prevention)) [6] Table 3.2.2-3 Engineered Safety Features, Emergency Core Cooling System – Summary of Aging Management Review (Closure Bolting – Alloy Steel and Carbon Steel – Inside and Outside – Loss of Material (Borated Water Leakage Assessment and Evaluation Program)) [4] Table 3.2.2-2 Emergency Core Cooling System: Summary of Aging Management Review (Closure Bolting – Carbon Steel – Air (Exterior) (Borated Water Leakage) – Loss of Material (Boric Acid Corrosion Control Program)) [5] Table 3.2.2-1 Emergency Core Cooling System Summary of Aging Management (Bearing Housing – Cast Iron – Air (External) – Loss of Material – Boric Acid Corrosion Prevention) [1]	Indiana Michigan Power Co. [6] (2003) Southern Nuclear Operating Co., Inc. [4] (2003) Southern Nuclear Operating Co., Inc. [5] (2007) U.S. Nuclear Regulatory Commission [9] (1982) Florida Power & Light Co. [3] (2000)		Other pumpsoperate at higher pressures but would not create debris (they are not located where insulation could be released to the sump) I think bolting/bearing might not be an issue itself; however leakage due to bolting/bearing might be a non-isolable LOCA issue. Please note my point is about Class 1 piping system pressure boundary. However, Class 1 SIS is between two valves off the RCS. This makes LOCA extremely unlikely.

	"Tests conducted by Durametallic on their safety back-up bushing show that the leakage rates under normal conditions for a 3 inch diameter bushing are about 80 gph at 60 psig for a ¼ inch long bushing and 47 gph for a 3/4 inch long bushing." [9] "Leakage tests on safety bushings typical of those used in RHR and CS pumps show that leakage rates are less than 100 gph." [9] Table 3.2.2-2 Containment Spray System Summary of Aging Management (CSS Bolting – Carbon Steel Air (External) – Loss of Material (Boric Acid Corrosion Prevention) and Loss of Mechanical Closure Integrity (Boric Acid Corrosion Prevention)) [1] TABLE 3.3-2 CONTAINMENT SPRAY (Containment Spray Bolting(mechanical closures) – Carbon Steel – Borated Water Leaks – Loss of Mechanical Closure Integrity) [3]			
Valves and Valve Bodies	Table 3.2.2-1 Emergency Core Cooling System Summary of Aging Management (Valve - Stainless Steel – Treated Borated Water (Internal) – Loss of Material) [1] Table 3.2.2-3 Engineered Safety Features, Emergency Core Cooling System – Summary of Aging Management Review	Entergy Operations, Inc. [1] (2003) Southern Nuclear Operating Co., Inc. [4] (2003)		Valve failures in RCS-connected systems can result in debris generation. The component would have to be in the first pressurized piping section

	(Valve Bodies - Stainless Steel – Borated Water – Cracking and Loss of Material) [4] Table 3.2.2-3 Emergency Core Cooling System Summary of Aging Management Evaluation (Valve – Carbon Steel – Air (Internal and External) and Treated Water (Borated) (Internal) – Loss of Material) [6] Table 3.2.2-2 Emergency Core Cooling System: Summary of Aging Management Review [5] "The crack resulted from high-cycle thermal fatigue that was caused by relatively cold water leaking through a closed globe valve at a pressure sufficient to open the check valve. The leaking globe valve is in the bypass pipe around the boron injection tank (BIT) as shown in Figure 2." [10] "At Tihange 1, the through-wall crack was in the base metal of the elbow. Other cracks at Tihange 1 were found in the pipe spool connected to one side of the elbow and in the body of the check valve connected to the other side." [11] Table 3.2.2-2 Containment Spray System Summary of Aging Management (CSS Valve - Stainless Steel – Treated Borated Water (Internal) – Loss of Material) [1]	Indiana Michigan Power Co. [6] (2003) Southern Nuclear Operating Co., Inc. [5] (2007) Nuclear Regulatory Commission [10] (1988) Nuclear Regulatory Commission [11] (1988) Florida Power & Light Co. [3] (2000) Duke Energy Corp. [2] (1998) U.S. Nuclear Regulatory Commission [12] (1998)		connected to the RCS. Is leak before break true for valves too? On the other hand valves in a piping system are designed based on the redundancy. This might mitigate LOCA probability extremely

	TABLE 3.3-2 CONTAINMENT SPRAY (Containment Spray Valves, Piping/fittings and Tubing/fittings – Stainless Steel – Treated Water – Borated – Loss of Material) [3] Table 3.5-3 Applicable Aging Effects for Components of Emergency Core Cooling Systems (CFS Valve Bodies - Stainless Steel – Borated Water – Loss of Material) [2] Table 3.5-3 Applicable Aging Effects for Components of Emergency Core Cooling Systems (HPIS Valve Bodies - Stainless Steel – Borated Water – Loss of Material and Cracking) [2] Table 3.5-3 Applicable Aging Effects for Components of Emergency Core Cooling Systems (LPIS Valve Bodies - Stainless Steel – Borated Water – Loss of Material and Cracking) [2] "In LER 96-007, the licensee for Diablo Canyon Nuclear Power Plant, Unit 1, reported a radiograph inspection finding that openings in the Diablo Canyon plant's 3.81-cm (1-1/2 in.) centrifugal-charging pump run-out-protection manual throttle valves and in the 5.08-cm (2 in.) safety-injection (SI) to cold-leg manual throttle valves were less than the 0.673-cm (0.265 in.) diagonal			

	opening in the containment recirculation sump debris screen." [12] "After reviewing an Institute of Nuclear Power Operations (INPO) operational experience report on this event, the licensee for Millstone Nuclear Station, Unit 2, determined that eight throttle valves in the high pressure safety injection (HPSI) system injection lines were susceptible to the failure mechanism described in Diablo Canyon Nuclear Power Plant LER 96-007." [12]			
Tubing	Table 3.2.2-1 Emergency Core Cooling System Summary of Aging Management (Tubing – Stainless Steel – Treated Borated Water (Internal) – Loss of Material) [1] Table 3.2.2-3 Emergency Core Cooling System Summary of Aging Management Evaluation (Tubing – Stainless steel – Treated Water (Borated) (Internal) – Loss of Material) [6] Table 3.2.2-2 Containment Spray System Summary of Aging Management (CSS Tubing - Stainless Steel – Treated Borated Water (Internal) – Loss of Material) [1] TABLE 3.3-2 CONTAINMENT SPRAY [3] Table 3.5-3 Applicable Aging Effects for Components of Emergency Core Cooling Systems (CFS Tubing - Stainless Steel –	Entergy Operations, Inc. [1] (2003) Indiana Michigan Power Co. [6] (2003) Florida Power & Light Co. [3] (2000) Duke Energy Corp. [2] (1998) Southern Nuclear Operating Co., Inc. [5] (2007)		Tubing failures are small enough that they can be mitigated without recirculation. Some small tubing failures can be repaired at power This part of piping is off the RCS and between the first and second valves. Therefore, LOCA might be highly small.

	Borated Water – Loss of Material and Cracking) [2] Table 3.5-3 Applicable Aging Effects for Components of Emergency Core Cooling Systems (HPIS Tubing - Stainless Steel – Borated Water – Loss of Material and Cracking) [2] Table 3.5-3 Applicable Aging Effects for Components of Emergency Core Cooling Systems (LPIS Tubing - Stainless Steel – Borated Water – Loss of Material and Cracking) [2] Table 3.2.2-2 Emergency Core Cooling System: Summary of Aging Management Review (Seal Water Coolers (RHR Pumps Tubes) – Carbon Steel – Air – Indoor (Exterior) (Borated Water Leakage) – Loss of Material (Boric Acid Corrosion Control Program)) [5] Table 3.5-3 Applicable Aging Effects for Components of Emergency Core Cooling Systems (LPIS Annular Tube - Stainless Steel – Borated Water – Loss of Material and Cracking) [2]			

Strainers, Suction, Grating, and Sump	Table 3.2.2-3 Emergency Core Cooling System Summary of Aging Management Evaluation (Strainer Housing - Stainless Steel – Treated Water (Borated) (Internal) – Loss of Material) [6] "Problems have also been found with the material condition of sumps and suction strainers. These problems, potentially impairing the operation of the ECCS or safety-related CSS, include deformed suction strainers and unintentional flow paths created by missing grout." [12] "1.Operator found debris in the sump." [12] "2.Five 208 L (55-gallon) drums of sludge removed from ECCS sump. Also, plastic sheeting, nuts, and bolts, tie wraps, and pencils." [12] "1.Construction debris discovered in containment recirculation spray system (RSS) containment sump and in RSS suction lines" [12] "Other concerns related to debris generated during postulated accidents are beyond the scope of the GSI-191 study and the parametric analyses presented in this report. Examples of such concerns include...(b) structural failure of sump screens as a result	Indiana Michigan Power Co. [6] (2003) U.S. Nuclear Regulatory Commission [12] (1998) U.S. Nuclear Regulatory Commission [13] (2002) U.S. Nuclear Regulatory Commission [14] (2003)		If the ECCS suction strainers are weakened by corrosion or have additional buildup of corrosion prior to the need for recirculation, they could fail mechanically (allowing excess debris bypass to the core) or collapse and prevent pumping. I think these parts are key components in ECCS. Any deterioration in their performance could have a substantiate effect on GSI-191 issue.

	of l6ads from debris or direct jet impingement." [13] "Sump failure is likely to occur for sumps in this configuration because of cavitation within the pump housing when head loss caused by debris accumulation exceeds the NPSHMagn." - Fully Submerged Sump Screens [13] "Failure can occur for sumps in this configuration in one of two ways: by pump cavitation as explained above or when head loss caused by debris buildup prevents sufficient water from entering the sump." - Partially Submerged Sump Screens [13] "structural failure of the sump screens as a result of loads from debris or direct jet impingement." [14] "4.Bolts and clips missing from the vortex suppression grating." [12]			
Seals	"In the event of increased leakage of the shaft seals due to wear, the seal safety bushings limit leakage to less than 0.1% of pump flow rates." [9] "In pumps with mechanical shaft seals, debris could cause clogging or excessive wear, leading to increased seal leakage. However, catastrophic failure of a shaft seal	U.S. Nuclear Regulatory Commission [9] (1982) U.S. Nuclear Regulatory Commission [14] (2003)		ECCS equipment requiring seals would not result in debris generation that would cause sump blockage if you consider that SIS piping system is located between two

	as a result of debris ingestion was considered unlikely." [14] "Durametallic Corp. [42] has also conducted tests of their seals for nuclear power plant auxiliary and cooldown pumps. They report that seal life is shortened due to high temperatures, pressures and the presence of boric acid." [9]	U.S. Nuclear Regulatory Commission [9] (1982)		valves, you would not evaluate seal failure LOCA's a significant issue
Nozzles	Table 3.2.2-1 Emergency Core Cooling System Summary of Aging Management (Nozzle – Inconel – Treated Borated Water (Internal) – Loss of Material) [1] Table 3.2.2-2 Containment Spray System Summary of Aging Management (CSS Nozzle - Stainless Steel – Treated Borated Water (Internal) – Loss of Material) [1] Table 3.5-3 Applicable Aging Effects for Components of Emergency Core Cooling Systems (HPIS Flow Nozzle - Stainless Steel – Borated Water – Loss of Material and Cracking) [2]	Entergy Operations, Inc. [1] (2003) Duke Energy Corp. [2] (1998)		Containment spray nozzles should not be affected by GSI-191 concerns because of the hole size compared to the ECCS screen hole size The same as seals.
Orifices	Table 3.2.2-1 Emergency Core Cooling System Summary of Aging Management (Orifice – Stainless Steel – Treated Borated Water (Internal) – Loss of Material) [1] Table 3.2.2-3 Emergency Core Cooling System Summary of Aging Management Evaluation (Orifice – Stainless Steel –	Entergy Operations, Inc. [1] (2003) Indiana Michigan Power Co. [6] (2003)		Orifices are large diameter and should not be affected by debris. The flow measuring orifices may indicate properly if debris collects around ports

	Treated Water (Borated) (Internal) – Loss of Material/Erosion) [6] Table 3.2.2-2 Containment Spray System Summary of Aging Management (CSS Orifice - Stainless Steel – Treated Borated Water (Internal) – Loss of Material) [1] TABLE 3.3-2 CONTAINMENT SPRAY (Containment Spray Orifices – Stainless Steel – Treated Water – Borated – Loss of Material) [3] Table 3.5-3 Applicable Aging Effects for Components of Emergency Core Cooling Systems (HPIS Orifice - Stainless Steel – Borated Water – Loss of Material and Cracking) [2] Table 3.5-3 Applicable Aging Effects for Components of Emergency Core Cooling Systems (LPIS Orifice - Stainless Steel – Borated Water – Loss of Material and Cracking) [2] Table 3.2.2-3 Engineered Safety Features, Emergency Core Cooling System – Summary of Aging Management Review (Charging/SI Pump Mini-Flow Orifices – Stainless Steel – Borated Water – Loss of Material) [4]	Florida Power & Light Co. [3] (2000) Duke Energy Corp. [2] (1998) Southern Nuclear Operating Co., Inc. [4] (2003) Nuclear Regulatory Commission [7] (2010) Southern Nuclear Operating Co., Inc. [5] (2007)		one point that should be explained is if these components are studied for debris generation by itself or how do these parts perform in a pressure boundary break? If there is no LOCA in pressure boundary, it would be hard to assign any number to these subcomponent other than a minimum. However, if there is a LOCA in pressure boundary, any issue in ECCS might be important.

	Table : V ENGINEERED SAFETY FEATURES D1 Emergency Core Cooling System (PWR) [7] Table 3.2.2-3 Engineered Safety Features, Emergency Core Cooling System – Summary of Aging Management Review (Flow Orifice/Element - Stainless Steel – Borated Water – Cracking and Loss of Material) [4] Table 3.2.2-2 Emergency Core Cooling System: Summary of Aging Management Review (Flow Orifice/Element - Stainless Steel – Borated Water (Interior) – Loss of Material) [5]			
Thermowell	Table 3.2.2-1 Emergency Core Cooling System Summary of Aging Management (Thermowell - Stainless Steel – Treated Borated Water >270 °F (Internal) – Loss of Material) [1] Table 3.2.2-3 Emergency Core Cooling System Summary of Aging Management Evaluation (Thermowell – Stainless Steel – Treated Water (Borated) >270°F (Internal) – Cracking/Fatigue, Cracking, and Loss of Material) [6] Table 3.2.2-2 Containment Spray System Summary of Aging Management (CSS Thermowell - Stainless Steel – Treated	Entergy Operations, Inc. [1] (2003) Indiana Michigan Power Co. [6] (2003)		Pressurized, RCS-conneted thermowell failure has the potential for creating debris as I said in my previous comment, does this mean there is no breach in pressure boundary? In other words, is debris generated concurrently with debris generation in pressure boundary? I am not sure

	Borated Water (Internal) – Loss of Material) [1]			thermowell has any potential for debris generation
Filters	Table 3.2.2-2 Containment Spray System Summary of Aging Management (CSS Filter Housing – Stainless Steel – Treated Borated Water (Internal) – Loss of Material) [1] Table 3.2.2-3 Emergency Core Cooling System Summary of Aging Management Evaluation (Filter Housing – Carbon Steel – Air (External) – Loss of Material (Boric Acid Corrosion Prevention)) [6] Table 3.2.2-2 Emergency Core Cooling System: Summary of Aging Management Review (Filter Housings – Carbon Steel – Air (Ecterior0 (Borated Water Leakage) – Loss of Material (Boric Acid Corrosion Control Program)) [5] Table 3.5-3 Applicable Aging Effects for Components of Emergency Core Cooling Systems (HPIS Filter - Stainless Steel – Borated Water – Loss of Material and Cracking) [2]	Entergy Operations, Inc. [1] (2003) Indiana Michigan Power Co. [6] (2003) Southern Nuclear Operating Co., Inc. [5] (2007) Duke Energy Corp. [2] (1998)		ECCS filter failures would not create debris (although they could become clogged) I agree.
Heater Housing	Table 3.2.2-3 Emergency Core Cooling System Summary of Aging Management Evaluation (Heater Housing – Stainless Steel – Treated Water (Borated) (Internal) – Loss of Material) [6]	Indiana Michigan Power Co. [6] (2003) Southern Nuclear Operating Co., Inc. [5] (2007)		Heaters would not cause GSI-191-related issues or debris I agree.

	Table 3.2.2-2 Emergency Core Cooling System: Summary of Aging Management Review (Electric Heater Housings – Stainless Steel – Borated Water (Interior) – Loss of Material) [5] Table 3.2.2-2 Containment Spray System Summary of Aging Management (CSS Heater Housing - Stainless Steel – Treated Borated Water (Internal) – Loss of Material) [1]	Entergy Operations, Inc. [1] (2003)		
Oil Cooler Shell and Channel Head	Table 3.2.2-3 Engineered Safety Features, Emergency Core Cooling System – Summary of Aging Management Review (Oil Cooler (Shell) (for High Head Safety Injection Pump) – Inside – Loss of Material (Borated Water Leakage Assessment and Evaluation Program)) [4] Table 3.2.2-3 Engineered Safety Features, Emergency Core Cooling System – Summary of Aging Management Review (Oil Cooler (Channel Head) (for High Head Safety Injection Pump) – Inside – Loss of Material (Borated Water Leakage Assessment and Evaluation Program))[4]	Southern Nuclear Operating Co., Inc. [4] (2003)		Oil cooler failure would not result in debris generation
Spray System	"Most of the coating in the torus is unqualified, which could affect the operability of the low-pressure coolant injection and core spray systems." [12]	U.S. Nuclear Regulatory Commission [12] (1998)		Coatings failures are a concern related to ECCS screen head loss.

	"1.Construction debris discovered in containment recirculation spray system (RSS) containment sump and in RSS suction lines" [12]			I am not sure this is a category for us. Torus is a subcomponent in BWR's.
Flex Hose	Table 3.2.2-3 Emergency Core Cooling System Summary of Aging Management Evaluation (Flex Hose – Stainless Steel – Treated Water (Borated) (Internal) – Loss of Material) [6] Table 3.5-3 Applicable Aging Effects for Components of Emergency Core Cooling Systems (HPIS Flex Hose - Stainless Steel – Borated Water – Loss of Material and Cracking) [2]	Indiana Michigan Power Co. [6] (2003) Duke Energy Corp. [2] (1998)		Flex hose is related to any GSI-191 concerns I agree.
High Pressure Injection System	Table 3.5-3 Applicable Aging Effects for Components of Emergency Core Cooling Systems (HPIS Demineralizer - Stainless Steel – Borated Water – Loss of Material and Cracking) [2] Table 3.5-3 Applicable Aging Effects for Components of Emergency Core Cooling Systems (HPIS Flow Meter - Stainless Steel – Borated Water – Loss of Material and Cracking) [2] Table 3.5-3 Applicable Aging Effects for Components of Emergency Core Cooling Systems (HPIS Mechanical Expansion Joint	Duke Energy Corp. [2] (1998)		Pressurized RCS-connected ECCS componenets have the potential to creat debris I agree.

	- Stainless Steel – Borated Water – Loss of Material and Cracking) [2]			
Structural and Coating	"Seven unscreened holes found in masonry grout below screen assembly of ECCS sump. Could potentially degrade both trains of HPSI and containment spray. Had previously inspected sump because of IN 89-77; did not discover problem. NRC estimate of incremental increase in core damage: 3 X10-04." [12] "There have been no changes made specifically to address particular aging-related or coating-related problems or failures." [16] "Most of the coating in the torus is unqualified, which could affect the operability of the low-pressure coolant injection and core spray systems." [12]	U.S. Nuclear Regulatory Commission [12] (1998) Calvert Cliffs Nuclear Power Plant Inc. [16] (1998) Northern States Power Co. – Minnesota [17] (2008) Florida Power & Light Co. [3] (2000)	"The issue is based on containment sump strainer design and on the identification of new potential sources of debris, including failed containment coatings that have the potential to block the sump strainers." [17] "Coatings qualified for use in the Turkey Point Units 3 and 4 Containments are adequate to resist exposures due to both normal operating and design basis accident conditions. These exposures include ionizing radiation, high temperature and pressure, impingement from	Coatings failures are a concern related to ECCS screen head loss. I think this category is related to BWR's

			jets or sprays, and abrasion due to traffic." [3]	
Pump Casings	Table 3.2.2-1 Emergency Core Cooling System Summary of Aging Management (Pump Casing – Stainless Steel – Treated Borated Water (Internal) – Loss of Material)[1] Table 3.2.2-3 Emergency Core Cooling System Summary of Aging Management Evaluation (Pump Casing – Carbon Steel with Stainless Steel Cladding – Treated Water (Borated) (Internal) – Cracking and Loss of Material) [6] Table : V ENGINEERED SAFETY FEATURES D1 Emergency Core Cooling System (PWR) [7] Table 3.2.2-2 Containment Spray System Summary of Aging Management (CSS Pump Casing – Cast Stainless Steel – Treated Borated Water (Internal) – Loss of Material) [1] Table 3.5-3 Applicable Aging Effects for Components of Emergency Core Cooling Systems (HPIS Pump Casing - Stainless Steel – Borated Water – Loss of Material and Cracking) [2]	Entergy Operations, Inc. [1] (2003) Indiana Michigan Power Co. [6] (2003) Nuclear Regulatory Commission [7] (2010) Duke Energy Corp. [2] (1998) Nuclear Regulatory Commission [18] (2008) Southern Nuclear Operating Co., Inc. [4] (2003) Southern Nuclear Operating Co., Inc. [5] (2007)		ECCS pump casings would not cause debris (in recirculation) My understanding is that pump casing should be important and in fact would cause debris. Unless they are sitting in an isolated place.

	"In May 1997, at Oconee Nuclear Station Unit 3, hydrogen ingestion during plant cooldown damaged and rendered nonfunctional two high-pressure injection (HPI) pumps." "In February 2005, an HPI pump at Indian Point Energy Center Unit 2 was found inoperable because the pump casing was filled with gas."[18] Table 3.5-3 Applicable Aging Effects for Components of Emergency Core Cooling Systems (LPIS Pump Casing - Stainless Steel – Borated Water – Loss of Material and Cracking) [2] Table 3.2.2-3 Engineered Safety Features, Emergency Core Cooling System – Summary of Aging Management Review (High Head and RHR Pump Casings – Carbon Steel/Stainless Steel Clad – Borated Water – Loss of Material) [4] Table 3.2.2-2 Emergency Core Cooling System: Summary of Aging Management Review (Pump Casing (Centrifugal Charging Pumps) - Stainless Steel – Borated Water (Interior) – Loss of Material) [5] Table 3.2.2-2 Emergency Core Cooling System: Summary of Aging Management Review (Pump Casing (RHR Pumps) -			

	Stainless Steel – Borated Water (Interior) – Loss of Material) [5] Table 3.2.2-2 Emergency Core Cooling System: Summary of Aging Management Review (Pump Casing (Safety Injection Pumps) - Stainless Steel – Borated Water (Interior) – Loss of Material) [5] Table 3.2.2-2 Emergency Core Cooling System: Summary of Aging Management Review (Pump Casing (Sludge Mixing Pumps) - Stainless Steel – Borated Water (Interior) – Loss of Material) [5]			
Pumps	"At Surry Units 1 and 2, some of the debris was large enough to cause pump damage or flow degradation." [12] "In addition, extended operation at low flow or severe cavitation may cause mechanical damage to the pump which can lead to pump failure during the long-term recirculation phase." [9] "Test data on the mechanical wear of pumps indicate that the estimated quantity of debris expected in the recirculating fluid is too small to seriously impair long-term pump operation as a result of material erosion." [9] "The principal concerns are interrelated. They involve those factors which have the potential to affect the short or long term	U.S. Nuclear Regulatory Commission [12] (1998) U.S. Nuclear Regulatory Commission [9] (1982) Florida Power & Light Co. [3] (2000) U.S. Nuclear Regulatory Commission [19] (1986)		ECCS pump casings would not cause debris (in recirculation) Please see previous comment. Also, should “pump casing” read “pump” above.

	ability of the pumps to provide adequate cooling to the core and containment. These factors have been identified as:...mechanical erosion or failure of the pumps caused by debris." [9] TABLE 3.3-2 CONTAINMENT SPRAY (Containment Spray Pump – Stainless Steel – Treated Water – Borated – Loss of Material) [3] "September 18, 1992: During Technical Specification inservice inspection testing of the A containment spray pump the pump was declared inoperable. A foam rubber plug was blocking pump suction. Plug removed and pump tested satisfactorily. One train of Unit 2 residual heat removal, safety injection, and containment spray systems inoperable for entire operating cycle. Plug was part of a cleanliness barrier." [12] "Containment spray and HPSI pumps declared inoperable." [12] "Experimental data and pump and seal manufacturers' experience agree that for the types and quantities of debris present, hydraulic performance degradation of RHR and CS pumps should be negligible." [9] "Experimental data and pump and seal manufacturers' experience agree that for the	Calvert Cliffs Nuclear Power Plant Inc. [20] (1998)		

	types and quantities of debris present, hydraulic performance degradation of RHR and CS pumps should be negligible." [9] "The malfunction of the pumps was apparently caused by boric acid crystallization blocking pump suction and by possible gas binding of the pumps." [19] "In that event, two of the three SI pumps were rendered inoperable as a result of boric acid crystallization." [19] Table F.2-2 SUMMARY OF CCNPP SAMAs CDF Improvement of 2.7% [20]			
Heat Exchanger (Channel Heads and Coils	Table 3.5-3 Applicable Aging Effects for Components of Emergency Core Cooling Systems(HPIS Heat Exchanger Coil - Stainless Steel – Borated Water - Cracking) [2] Table 3.5-3 Applicable Aging Effects for Components of Emergency Core Cooling Systems (LPIS Heat Exchanger Channel Heads - Stainless Steel – Borated Water – Loss of Material and Cracking) [2] Table 3.2.2-3 Engineered Safety Features, Emergency Core Cooling System – Summary of Aging Management Review (RHR Heat Exchanger (Channel Head) -	Duke Energy Corp. [2] (1998) Southern Nuclear Operating Co., Inc. [4] (2003) Southern Nuclear Operating Co., Inc. [5] (2007)		ECCS heat exchangers would not cause debris (in recirculation) due to their location

	Stainless Steel – Borated Water – Loss of Material) [4] Table 3.2.2-2 Emergency Core Cooling System: Summary of Aging Management Review (RHR Hat Exchanger (Channel Head) - Stainless Steel – Borated Water (Interior) – Loss of Material) [5]			
Heat Exchanger (Tubes and Tubesheets/Tube Shields)	Table 3.2.2-1 Emergency Core Cooling System Summary of Aging Management (Heat Exchanger (Tubes) – Stainless Steel – Treated Borated Water (Internal) – Loss of Material) [1] Table 3.2.2-3 Emergency Core Cooling System Summary of Aging Management Evaluation (Heat Exchanger (Tubes) - Stainless Steel – Treated Water (Borated) >270 °F (Internal) – Cracking/Fatigue, Cracking, and Loss of Material) [6] Table 3.2.2-2 Containment Spray System Summary of Aging Management (CSS Heat Exchanger (Tubes) – Ferritic Stainless Steel – Treated Borated Water (Internal) – Loss of Material) [1] Table 3.5-3 Applicable Aging Effects for Components of Emergency Core Cooling Systems (HPIS Heat Exchanger Tubes - Stainless Steel – Borated Water – Loss of Material and Cracking) [2]	Entergy Operations, Inc. [1] (2003) Indiana Michigan Power Co. [6] (2003) Duke Energy Corp. [2] (1998) Florida Power & Light Co. [3] (2000) Southern Nuclear Operating Co., Inc. [4] (2003) Southern Nuclear Operating Co., Inc. [5] (2007)		ECCS heat exchanger failures would not cause debris (in recirculation) due to their location

	Table 3.5-3 Applicable Aging Effects for Components of Emergency Core Cooling Systems (LPIS Heat Exchanger Tubes - Stainless Steel – Borated Water – Loss of Material and Cracking) [2] Table 3.5-3 Applicable Aging Effects for Components of Emergency Core Cooling Systems (LPIS Heat Exchanger Tubesheet - Stainless Steel – Borated Water – Loss of Material and Cracking) [2] TABLE 3.3-2 CONTAINMENT SPRAY (Containment Spray Pump Seal Water Heat Exchanger Tube Shields - Brass – Treated Water – Borated – Loss of Material) [3] TABLE 3.3-2 CONTAINMENT SPRAY (Containment Spray Pump Seal Water Heat Exchanger Tubes (inside diameter) – Stainless Steel - Treated Water – Borated – Loss of Material and Fouling) [3] Table 3.2.2-3 Engineered Safety Features, Emergency Core Cooling System – Summary of Aging Management Review (RHR Heat Exchanger (Tube sheet) – Carbon Steel/ Stainless Steel (clad on tube side only) – Borated Water – Cracking and Loss of Material) [4]			

	Table 3.2.2-2 Emergency Core Cooling System: Summary of Aging Management Review (RHR Heat Exchanger (Tubesheets) – Carbon Steel (with Stainless Steel Cladding) – Borated Water (Interior) – Loss of Material) [5] Table 3.2.2-3 Engineered Safety Features, Emergency Core Cooling System – Summary of Aging Management Review (RHR Heat Exchanger (Tubes) - Stainless Steel – Borated Water – Loss of Material) [4] Table 3.2.2-2 Emergency Core Cooling System: Summary of Aging Management Review (RHR Heat Exchanger (Tubes) - Stainless Steel – Borated Water (Interior) – Loss of Material) [5] Table 3.5-3 Applicable Aging Effects for Components of Emergency Core Cooling Systems (HPIS Heat Exchange Tubesheet - Stainless Steel – Borated Water – Loss of Material and Cracking) [2]			

References

[1] I. Entergy Operations, "License renewal application arkansas nuclear one - units 2," U.S. Nuclear Regulatory Commission, October 2003.

[2] Duke Energy Corp., "Oconee nuclear station, units 1, 2 & 3- license renewal application volume II," U.S. Nuclear Regulatory Commission, June 1998.

[3] Florida Power & Light Co., "Application for renewed operating licenses turkey point units 3 & 4," U.S. Nuclear Regulatory Commission, 2000.

[4] Southern Nuclear Operating Co., Inc., "Joseph M. farley license renewal application," U.S. Nuclear Regulatory Commission, September 2003.

[5] Southern Nuclear Operating Co., Inc., "Vogtle electric generating plant units 1 and 2 license renewal application," U.S. Nuclear Regulatory Commission, 2007.

[6] Indiana Michigan Power Co., "License renewal application donald C cook nuclear plant," U.S. Nuclear Regulatory Commission, October 2003.

[7] Nuclear Regulatory Commission, "Generic Aging Lessons Learned GALL Report," *NUREG-1801*, 2010.

[8] L. AmerGen Energy Company, "License renewal application three mile island nuclear station unit 1," U.S. Nuclear Regulatory Commission, 2008.

[9] P. S. Kamath, T. J. tantillo and W. L. Swift, "An assessment of residual heat removal and containment spray pump performance under air and debris ingesting conditions," U.S. Nuclear Regulatory Commission, Washington, D.C. 20555, Tech. Rep. NUREG/CR-2792; CREARE TM-825, 1982.

[10] C. E. Rossi, "Bulletin 88-08: Thermal Stresses in Piping Connected to Reactor Coolant System," 1988.

[11] C. E. Rossi, "Bulletin 88-08: Supplement 2, Thermal Stresses in Piping Connected to Reactor Coolant Systems," 1988.

[12] J. W. Roe, "Potential for Degradation of the Emergency Core Cooling System and the Containment Spray System after a Loss-of-Coolant-Accident Because of Construction and Protective Coating Deficiencies and Foreign Material in Containment (GENERIC LETTER NO. 98-04)," 1998.

[13] D. V. Rao, B. C. Letellier, C. Shaffer, S. Ashbaugh and L. S. Bartlein, "GSI-191 technical assessment: Parametric evaluations for pressurized water reactor recirculation sump performance," U.S. Nuclear Regulatory Commission, Washington, DC 20555-0001, Tech. Rep. NUREG/CR-6762, Vol. 1; LA-UR-01-4083, 2002.

[14] D. V. Rao, C. J. Shaffer, M. T. Leonard and K. W. Ross, "Knowledge base for the effect of debris on pressurized water reactor emergency core cooling sump performance," U.S. Nuclear Regulatory Commission, Washington, DC 20555-0001, Tech. Rep. NUREG/CR-6808; LA-UR-03-0880, 2003.

[15] C. E. Rossi, "Bulletin 88-08: Supplement 1, Thermal Stresses in Piping Connected to Reactor Coolant Systems," 1998.

[16] Calvert Cliffs Nuclear Power Plant Inc., "Calvert cliffs nuclear power plant, units 1 & 2 - license renewal application volume 1," U.S. Nuclear Regulatory Commission, April 1998.

[17] Northern States Power Co., "Application for renewed operating licenses prairie island nuclear generating plant units 1 and 2," U.S. Nuclear Regulatory Commission, 2008.

[18] M. J. Case, "Managing Gas Accumulation in Emergency Core Cooling, Decay Heat Removal, and Containment Spray System (Generic Letter 2008-01)," 2008.

[19] E. L. Jordan, "Information Notice No. 86-63: Loss of Safety Injection Capability," 1986.

[20] Calvert Cliffs Nuclear Power Plant Inc., "Calvert cliffs nuclear power plant, units 1 & 2 - license renewal application volume 3," U.S. Nuclear Regulatory Commission, April 1998.

CHEMICAL AND VOLUME CONTROL SYSTEM

Component	Highlight	Author	GSI-191 Evidence	Expert Comments
Valve and Bodies	Table 3.3.2-10 Chemical and Volume Control and Boron Recycle Systems: Summary of Aging Management Review (Valve Bodies - Stainless Steel – Borated Water (Interior) – Loss of Material) [1] Table 3.3.2-3 Chemical and Volume Control System Summary of Aging Management Evaluation (Valve Body – CASS – Treated Borated Water (Internal) – Loss of Material) [2] Table 3.3.2-7 Auxiliary Systems – Summary of Aging Management Evaluation - Chemical and Volume Control System (Valve - Stainless Steel – Reactor Coolant (Int) – Loss of Material) [3] TABLE 3.3-1 CHEMICAL AND VOLUME CONTROL (Valves - Stainless Steel – Treated Water Borated – Loss of Material and Cracking) [7] Table 3.3.2-6-IP2 Chemical and Volume Control Summary of Aging Management Review (Valve Body – CASS – Treated Borated Water (Int) – Loss of Material) [4] Table 3.3.2-5 Chemical and Volume Control System Summary of Aging Management	Southern Nuclear Operating Co. [1] (2007) NextEra Energy Seabrook, LLC [2] (2010) Wolf Creek Nuclear Operating Corp. [3] (2008) Florida Power & Light Co. [7] (2001) Entergy Nuclear Operations, Inc [4] (2007) Entergy Nuclear Operations, Inc [5] (2003) Arizona Public Service Co. [6] (2009) Dominion Nuclear Connecticut, Inc. [9] (2004)		Some CVCS equipment and piping is connected to RCS pressurized systems. This equipment could create debris. CVCS is another system located out of RCS pressure boundary between the first and second valves. The potential for debris generation could be an issue, but they are isolable-LOCA.

	Evaluation (Valve - Stainless Steel – Treated Borated Water (Internal) – Cracking and Loss of Material) [5] Table 3.3.2-10 Auxiliary Systems – Summary of Aging Management Evaluation – Chemical and Volume Control System (Valve - Stainless Steel - Reactor Coolant (Int) - Cracking and Loss of Material) [6] Table 3.3.2-15: Auxiliary Systems - Chemical and Volume Control - Aging Management Evaluation (Valves - Carbon Steel - Borated Water Leakage - Loss of Material - Boric Acid Corrosion) [9]			
Housings	TABLE 3.3-1 CHEMICAL AND VOLUME CONTROL (Suction Stabilizers Housings - Stainless Steel – Treated Water Borated – Loss of Material and Cracking) [7] TABLE 3.3-1 CHEMICAL AND VOLUME CONTROL (Pulsation Dampers Housings - Stainless Steel – Treated Water Borated – Loss of Material and Cracking) [7] Table 3.3.2-6-IP2 Chemical and Volume Control Summary of Aging Management Review (Pulsation Dampener Housing - Stainless Steel – Treated Borated Water (Int) – Loss of Material) [4] TABLE 3.3-1 CHEMICAL AND VOLUME CONTROL (Purification Filters Housings -	Florida Power & Light Co. [7] (2001) Entergy Nuclear Operations, Inc [4] (2007)		Some CVCS equipment and piping is connected to RCS pressurized systems. This equipment could create debris. Please note that LOCA might happen in primary path with no effect on CVCS subcomponents. If a component of CVCS fails it

	Stainless Steel – Treated Water Borated – Loss of Material and Cracking) [7] TABLE 3.3-1 CHEMICAL AND VOLUME CONTROL (Ion Exchangers Housings - Stainless Steel – Treated Water Borated – Loss of Material and Cracking) [7]			might not even actuate ECCS.
Thermowell	Table 3.3.2-3 Chemical and Volume Control System Summary of Aging Management Evaluation (Thermowell - Stainless Steel – Treated Borated Water (Internal) – Loss of Material) [2] TABLE 3.3-1 CHEMICAL AND VOLUME CONTROL (Thermowells - Stainless Steel – Treated Water Borated – Loss of Material and Cracking) [7] Table 3.3.2-6-IP2 Chemical and Volume Control Summary of Aging Management Review (Thermowell - Stainless Steel – Treated Borated Water (Int) – Loss of Material) [4] Table 3.3.2-5 Chemical and Volume Control System Summary of Aging Management Evaluation (Thermowell - Stainless Steel – Treated Borated Water >270 270°F (Internal) – Cracking-fatigue and Loss of Material) [5]	NextEra Energy Seabrook, LLC [2] (2010) Florida Power & Light Co. [7] (2001) Entergy Nuclear Operations, Inc [4] (2007) Entergy Nuclear Operations, Inc [5] (2003)		Some CVCS equipment and piping is connected to RCS pressurized systems. This equipment could create debris. extremely unlikely to generate debris with a significant contribution to clogging issue of strainer.
Gauges and Indicators	Table 3.3.2-10 Auxiliary Systems – Summary of Aging Management Evaluation – Chemical and Volume Control System (Flow Indicator -	Arizona Public Service Co. [6] (2009)		Some CVCS equipment and piping is connected to RCS

	Stainless Steel - Treated Borated Water (Int) - Loss of Material) [6] Table 3.3.2-10 Auxiliary Systems – Summary of Aging Management Evaluation – Chemical and Volume Control System (Sight Gauge - Stainless Steel - Treated Borated Water (Int) - Loss of Material) [6] Table 3.3.2-15: Auxiliary Systems - Chemical and Volume Control - Aging Management Evaluation (CS Manifolds (Level Indicators - Carbon Steel - Borated Water Leakage - Loss of Material - Boric Acid Corrosion) [9]	Dominion Nuclear Connecticut, Inc. [9] (2004)		pressurized systems. This equipment could create debris. as above.
Vessels, Accumulators, and Reservoirs	Table 3.3.2-10 Chemical and Volume Control and Boron Recycle Systems: Summary of Aging Management Review (Demineralizer Vessels – Stainless Steel – Borated Water (Interior) – Loss of Material) [1] Table 3.3.2-10 Auxiliary Systems – Summary of Aging Management Evaluation – Chemical and Volume Control System (Demineralizer - Stainless Steel - Treated Borated Water (Int) - Loss of Material) [6] Table 3.3.2-15: Auxiliary Systems - Chemical and Volume Control - Aging Management Evaluation (CS Manifolds (Lube Oil Reservoirs - Carbon Steel - Borated Water Leakage - Loss of Material - Boric Acid Corrosion) [9]	Southern Nuclear Operating Co. [1] (2007) Arizona Public Service Co. [6] (2009) Dominion Nuclear Connecticut, Inc. [9] (2004)		Some CVCS equipment and piping is connected to RCS pressurized systems. This equipment could create debris. please see previous notes. All these reservoirs are isolated from pressure boundary.

	Table 3.3.2-10 Auxiliary Systems – Summary of Aging Management Evaluation – Chemical and Volume Control System (Accumulator - Stainless Steel - Treated Borated Water (Int) - Loss of Material) [6]			
Pumps and Cases	"Cracking of stainless steel pump casings in the CVCS system" [1] Table 3.3.2-3 Chemical and Volume Control System Summary of Aging Management Evaluation (Pump Casing - Stainless Steel – Treated Borated Water (Internal) – Loss of Material) [2] Table 3.3.2-7 Auxiliary Systems – Summary of Aging Management Evaluation - Chemical and Volume Control System (Pump – Carbon Steel – Plant Indoor Air (Ext) – Loss of Material) [3] Table 3.3.2-6-IP2 Chemical and Volume Control Summary of Aging Management Review (Pump Casing - Stainless Steel – Treated Borated Water (Int) – Loss of Material) [4] Table 3.3.2-5 Chemical and Volume Control System Summary of Aging Management Evaluation (Pump Casing - Stainless Steel – Treated Borated Water (Internal) – Cracking-fatigue and Loss of Material-wear) [5]	Southern Nuclear Operating Co. [1] (2007) NextEra Energy Seabrook, LLC [2] (2010) Wolf Creek Nuclear Operating Corp. [3] (2008) Entergy Nuclear Operations, Inc [4] (2007) Entergy Nuclear Operations, Inc [5] (2003) Arizona Public Service Co. [6] (2009) Florida Power & Light Co. [7] (2001)		The CVCS pumps are not susceptible to failure that would cause debris I agree

	Table 3.3.2-10 Auxiliary Systems – Summary of Aging Management Evaluation – Chemical and Volume Control System (Pump - Stainless Steel - Treated Borated Water (Int) - Cracking and Loss of Material) [6] Table 3.3.2-10 Chemical and Volume Control and Boron Recycle Systems: Summary of Aging Management Review (Pump Casings – Boric Acid Transfer Pumps - Stainless Steel – Borated Water (Interior) – Loss of Material) [1] Table 3.3.2-10 Chemical and Volume Control and Boron Recycle Systems: Summary of Aging Management Review (Pump Casings – CVCS Recycle Feed Pumps - Stainless Steel – Borated Water (Interior) – Loss of Material) [1] Table 3.3.2-10 Chemical and Volume Control and Boron Recycle Systems: Summary of Aging Management Review (Pump Casings – Normal Charging Pumps - Stainless Steel – Borated Water (Interior) – Loss of Material) [1] Table 3.3.2-3 Chemical and Volume Control System Summary of Aging Management Evaluation (Pump Casing (High Head Centrifugal Pump) - Stainless Steel – Treated	Dominion Nuclear Connecticut, Inc. [8] (2004) Dominion Nuclear Connecticut, Inc. [9] (2004)		

	Borated Water (Internal) – Loss of Material) [2] TABLE 3.3-1 CHEMICAL AND VOLUME CONTROL (Boric Acid Makeup Pumps - Stainless Steel – Treated Water Borated – Loss of Material) [7] TABLE 3.3-1 CHEMICAL AND VOLUME CONTROL (Charging Pumps - Stainless Steel – Treated Water Borated – Loss of Material and Cracking) [7] Table 3.3.2-10: Auxiliary Systems - Chemical and Volume Control - Aging Management Evaluation (Pumps (Charging Pump Lube Oil) – Carbon Steel - Borated Water Leakage – Loss of Material – Boric Acid Corrosion) [8] Table 3.3.2-15: Auxiliary Systems - Chemical and Volume Control - Aging Management Evaluation (Charging Pump Lube Oil Coolers (Channel Head) - Carbon Steel - - Borated Water Leakage - Loss of Material - Boric Acid Corrosion) [9] Table 3.3.2-15: Auxiliary Systems - Chemical and Volume Control - Aging Management Evaluation (Charging Pump Lube Oil Coolers (Shell) - Carbon Steel - Borated Water Leakage - Loss of Material - Boric Acid Corrosion) [9]			

	Table 3.3.2-15: Auxiliary Systems - Chemical and Volume Control - Aging Management Evaluation (CS Manifolds (Pumps) - Carbon Steel - Borated Water Leakage - Loss of Material - Boric Acid Corrosion) [9] Table 3.3.2-10: Auxiliary Systems - Chemical and Volume Control - Aging Management Evaluation (Lube Oil Reservoirs (Charging Pump) –Carbon Steel - Borated Water Leakage – Loss of Material – Boric Acid Corrosion) [8] Table 3.3.2-15: Auxiliary Systems - Chemical and Volume Control - Aging Management Evaluation (CS Manifolds (Charging Pump LO) - Carbon Steel - Borated Water Leakage - Loss of Material - Boric Acid Corrosion) [9] Table 3.3.2-10 Chemical and Volume Control and Boron Recycle Systems: Summary of Aging Management Review (Motor Coolers – Normal Charging Pumps (Shells) – Carbon Steel – Air Indoor (Exterior) – Loss of Material – Borated Water Leakage) [1]			
Bolting and Fasteners	Table 3.3.2-10 Chemical and Volume Control and Boron Recycle Systems: Summary of Aging Management Review (Closure Bolting – Carbon Steel – Air Indoor (Exterior) – Loss of Material – Borated Water Leakage) [1]	Southern Nuclear Operating Co. [1] (2007) Wolf Creek Nuclear Operating Corp. [3] (2008)		Some CVCS equipment and piping is connected to RCS pressurized systems. This

	"NUREG-1800 item 3.3.2.2.4 (4) relates to cracking of high strength closure bolting for chemical and volume control system bolting exposed to steam or water leakage." [1] Table 3.3.2-7 Auxiliary Systems – Summary of Aging Management Evaluation - Chemical and Volume Control System (Closure Bolting – Carbon Steel – Plant Indoor Air (Ext) – Loss of Material) [3] Table 3.3.2-10 Auxiliary Systems – Summary of Aging Management Evaluation – Chemical and Volume Control System (Closure Bolting - Carbon Steel - Borated Water Leakage (Ext) - Loss of Preload (Bolting Integrity) and Loss of Material) [6] Table 3.3.2-3 Chemical and Volume Control System Summary of Aging Management Evaluation (Bolting – Steel – Air With Borated Water Leakage (Exterior) – Loss of Material) [2] TABLE 3.3-1 CHEMICAL AND VOLUME CONTROL (Bolting (Mechanical Closures) – Carbon Steel – Borated Water Leaks – Loss of Mechanical Closure Integrity) [7] Table 3.3.2-6-IP2 Chemical and Volume Control Summary of Aging Management Review (Bolting – Carbon Steel – Air Indoor	Arizona Public Service Co. [6] (2009) NextEra Energy Seabrook, LLC [2] (2010) Florida Power & Light Co. [7] (2001) Entergy Nuclear Operations, Inc [4] (2007) Entergy Nuclear Operations, Inc [5] (2003) Dominion Nuclear Connecticut, Inc. [8] (2004) Dominion Nuclear Connecticut, Inc. [9] (2004) Entergy Nuclear Operations, Inc. [10] (2004)		equipment could create debris. any leakage due to bolting and fasteners should be quickly recognized and isolated.

	(Ext) – Loss of Material – Boric Acid Corrosion Prevention) [4] Table 3.3.2-5 Chemical and Volume Control System Summary of Aging Management Evaluation (Bolting Carbon Steel – Air (External) – Loss of Material – Boric Acid Corrosion Prevention) [5] Table 3.3.2-10: Auxiliary Systems - Chemical and Volume Control - Aging Management Evaluation (Bolting – Low-Alloy Steel – Borated Water Leakage – Loss of Material – Boric Acid Corrosion) [8] Table 3.3.2-15: Auxiliary Systems - Chemical and Volume Control - Aging Management Evaluation (Bolting - Low-Alloy Steel - Borated Water Leakage - Loss of Material - Boric Acid Corrosion) [9] Table 3.3.2-1 Auxiliary Systems - Chemical and Volume Control System - Summary of Aging Management Evaluation (Fasteners - Stainless Steel - Containment Air (Ext) - Loss of Preload - Bolting Integrity Program) [10]			
Filters and Strainers	Table 3.3.2-10 Chemical and Volume Control and Boron Recycle Systems: Summary of Aging Management Review (Filter Housings – Stainless Steel – Borated Water (Interior) – Loss of Material) [1]	Southern Nuclear Operating Co. [1] (2007) NextEra Energy Seabrook, LLC [2] (2010)		CVCS filters and strainers are generally not connected to pressurized RCS piping. They

	Table 3.3.2-3 Chemical and Volume Control System Summary of Aging Management Evaluation (Filter Housing – Stainless Steel – Treated Borated Water (Internal) – Loss of Material) [2] Table 3.3.2-7 Auxiliary Systems – Summary of Aging Management Evaluation - Chemical and Volume Control System (Filter – Carbon Steel – Plant Indoor Air (Ext) – Loss of Material) [3] Table 3.3.2-6-IP2 Chemical and Volume Control Summary of Aging Management Review (Filter Housing – Stainless Steel – Treated Borated Water (Int) – Loss of Material) [4] Table 3.3.2-10 Auxiliary Systems – Summary of Aging Management Evaluation – Chemical and Volume Control System (Filter - Stainless Steel - Treated Borated Water (Int) - Loss of Material) [6] Table 3.3.2-10: Auxiliary Systems - Chemical and Volume Control - Aging Management Evaluation (Filter/Strainers (Housing – Charging Pump Lube Oil) – Carbon Steel - Borated Water Leakage – Loss of Material – Boric Acid Corrosion) [8] TABLE 3.3-1 CHEMICAL AND VOLUME CONTROL (Strainer Elements - Stainless	Wolf Creek Nuclear Operating Corp. [3] (2008) Entergy Nuclear Operations, Inc [4] (2007) Arizona Public Service Co. [6] (2009) Dominion Nuclear Connecticut, Inc. [8] (2004) Florida Power & Light Co. [7] (2001)		should not cause debris generation I agree.

	Steel – Treated Water Borated – Loss of Material) [7] Table 3.3.2-10 Auxiliary Systems – Summary of Aging Management Evaluation – Chemical and Volume Control System (Strainer - Stainless Steel - Treated Borated Water (Int) - Loss of Material) [6] TABLE 3.3-1 CHEMICAL AND VOLUME CONTROL (Charging Pump Strainers Housings - Stainless Steel – Treated Water Borated – Loss of Material and Cracking) [7] TABLE 3.3-1 CHEMICAL AND VOLUME CONTROL (Let Down Strainers Housings - Stainless Steel – Treated Water Borated – Loss of Material and Cracking) [7] TABLE 3.3-1 CHEMICAL AND VOLUME CONTROL (Boric Acid Suction Strainers Housings - Stainless Steel – Treated Water Borated – Loss of Material and Cracking) [7] Table 3.3.2-6-IP2 Chemical and Volume Control Summary of Aging Management Review (Strainer Housing - Stainless Steel – Treated Borated Water (Int) – Loss of Material) [4] Table 3.3.2-10 Chemical and Volume Control and Boron Recycle Systems: Summary of Aging Management Review (Piping			

	Components – Pipe Spools for Startup Strainers - Stainless Steel – Borated Water (Interior) – Loss of Material) [1]			
Tanks	Table 3.3.2-3 Chemical and Volume Control System Summary of Aging Management Evaluation (Tank - Stainless Steel – Treated Borated Water (Internal) – Loss of Material) [2] Table 3.3.2-7 Auxiliary Systems – Summary of Aging Management Evaluation - Chemical and Volume Control System (Tank – Carbon Steel – Plant Indoor Air (Ext) – Loss of Material) [3] Table 3.3.2-6-IP2 Chemical and Volume Control Summary of Aging Management Review (Tank - Stainless Steel – Treated Borated Water (Int) – Loss of Material) [4] Table 3.3.2-5 Chemical and Volume Control System Summary of Aging Management Evaluation (Tank - Stainless Steel – Treated Borated Water (Internal) – Cracking and Loss of Material) [5] Table 3.3.2-10 Auxiliary Systems – Summary of Aging Management Evaluation – Chemical and Volume Control System (Tank - Stainless Steel - Treated Borated Water (Int) - Loss of Material) [6]	NextEra Energy Seabrook, LLC [2] (2010) Wolf Creek Nuclear Operating Corp. [3] (2008) Entergy Nuclear Operations, Inc [4] (2007) Entergy Nuclear Operations, Inc [5] (2003) Arizona Public Service Co. [6] (2009) Southern Nuclear Operating Co. [1] (2007) Florida Power & Light Co. [7] (2001)		CVCS tanks are not directly connected to RCS piping and should not cause debris generation please see previous notes

	Table 3.3.2-10 Chemical and Volume Control and Boron Recycle Systems: Summary of Aging Management Review (Tanks – Boric Acid Batching Tanks - Stainless Steel – Borated Water (Interior) – Loss of Material) [1] Table 3.3.2-10 Chemical and Volume Control and Boron Recycle Systems: Summary of Aging Management Review (Tanks – Boric Acid Storage Tanks - Stainless Steel – Borated Water (Interior) – Loss of Material) [1] Table 3.3.2-10 Chemical and Volume Control and Boron Recycle Systems: Summary of Aging Management Review (Tanks – Boron Meter Tanks - Stainless Steel – Borated Water (Interior) – Loss of Material) [1] Table 3.3.2-10 Chemical and Volume Control and Boron Recycle Systems: Summary of Aging Management Review (Tanks – Chemical Mixing Tanks - Stainless Steel – Borated Water (Interior) – Loss of Material) [1] Table 3.3.2-10 Chemical and Volume Control and Boron Recycle Systems: Summary of Aging Management Review (Tanks – Recycle Holdup Tanks - Stainless Steel – Borated Water (Interior) – Loss of Material) [1]			

	Table 3.3.2-10 Chemical and Volume Control and Boron Recycle Systems: Summary of Aging Management Review [1] TABLE 3.3-1 CHEMICAL AND VOLUME CONTROL (Voluem control Tanks - Stainless Steel – Treated Water Borated – Loss of Material and Cracking) [7] TABLE 3.3-1 CHEMICAL AND VOLUME CONTROL (Boric Acid Makeup Tanks – Stainless Steel – Treated Water Borated – Loss of Material) [7] Table 3.3.2-10 Auxiliary Systems – Summary of Aging Management Evaluation – Chemical and Volume Control System (Tank Liner - Stainless Steel - Treated Borated Water (Int) - Loss of Material) [6]			
Orifices and Elements	Table 3.3.2-10 Chemical and Volume Control and Boron Recycle Systems: Summary of Aging Management Review (Flow Orifice/Elements - Stainless Steel – Borated Water (Interior) – Loss of Material) [1] Table 3.3.2-6-IP2 Chemical and Volume Control Summary of Aging Management Review (Flow Element - Stainless Steel – Treated Borated Water (Int) – Loss of Material) [4] Table 3.3.2-10 Auxiliary Systems – Summary of Aging Management Evaluation – Chemical	Southern Nuclear Operating Co. [1] (2007) Entergy Nuclear Operations, Inc [4] (2007) Arizona Public Service Co. [6] (2009)		CVCS orifices and other instrumentation would not cause debris generation I agree.

	and Volume Control System (Flow Element - Stainless Steel - Treated Borated Water (Int) - Loss of Material) [6] Table 3.3.2-3 Chemical and Volume Control System Summary of Aging Management Evaluation (Orifice - Stainless Steel – Treated Borated Water (Internal) – Loss of Material) [2] TABLE 3.3-1 CHEMICAL AND VOLUME CONTROL (Orifices - Stainless Steel – Treated Water Borated – Loss of Material and Cracking) [7] Table 3.3.2-10 Auxiliary Systems – Summary of Aging Management Evaluation – Chemical and Volume Control System (Orifice - Stainless Steel - Treated Borated Water (Int) - Loss of Material) [6] Table 3.3.2-10 Chemical and Volume Control and Boron Recycle Systems: Summary of Aging Management Review (Letdown Orifices - Stainless Steel – Borated Water (Interior) – Loss of Material) [1] Table 3.3.2-3 Chemical and Volume Control System Summary of Aging Management Evaluation (Instrumentation Element – Copper Alloy >15% Zn – Air With Borated Water Leakage (External) – Loss of Material) [2]	NextEra Energy Seabrook, LLC [2] (2010) Florida Power & Light Co. [7] (2001)		

Piping, Hoses, and Fittings	Table 3.3.2-3 Chemical and Volume Control System Summary of Aging Management Evaluation (Piping And Fittings – Steel – Air With Borated Water Leakage (External) – Loss of Material) [2] Table 3.3.2-7 Auxiliary Systems – Summary of Aging Management Evaluation - Chemical and Volume Control System (Class 1 Piping <= 4in – Stainless Steel – Reactor Coolant (Int) – Loss of Material) [3] TABLE 3.3-1 CHEMICAL AND VOLUME CONTROL (Piping/Fittings - Stainless Steel – Treated Water Borated – Loss of Material and Cracking) [7] Table 3.3.2-6-IP2 Chemical and Volume Control Summary of Aging Management Review (Piping – Stainless Steel – Treated Borated Water (Int) – Loss of Material) [4] Table 3.3.2-5 Chemical and Volume Control System Summary of Aging Management Evaluation (Piping – Stainless Steel – Treated Borated Water (Internal) – Cracking and Loss of Material) [5] Table 3.3.2-10 Auxiliary Systems – Summary of Aging Management Evaluation – Chemical and Volume Control System (Piping - Stainless Steel - Reactor Coolant (Int) - Cracking and Loss of Material) [6]	NextEra Energy Seabrook, LLC [2] (2010) Wolf Creek Nuclear Operating Corp. [3] (2008) Florida Power & Light Co. [7] (2001) Entergy Nuclear Operations, Inc [4] (2007) Entergy Nuclear Operations, Inc [5] (2003) Arizona Public Service Co. [6] (2009) Dominion Nuclear Connecticut, Inc. [9] (2004)		Some CVCS piping is connected to pressurized RCS systems. If not isolated, they may could contribute to debris generation It would be good to investigate if there is any piping in CVCS that is not isolable.

	Table 3.3.2-15: Auxiliary Systems - Chemical and Volume Control - Aging Management Evaluation (CS Manifolds (Pipe - Carbon Steel - Borated Water Leakage - Loss of Material - Boric Acid Corrosion) [9] TABLE 3.3-1 CHEMICAL AND VOLUME CONTROL (Tubing/Fittings - Stainless Steel – Treated Water Borated – Loss of Material and Cracking) [7] Table 3.3.2-6-IP2 Chemical and Volume Control Summary of Aging Management Review (Tubing - Stainless Steel – Treated Borated Water (Int) – Loss of Material) [4] Table 3.3.2-5 Chemical and Volume Control System Summary of Aging Management Evaluation (Tubing - Stainless Steel – Treated Borated Water (Internal) – Cracking and Loss of Material) [5] Table 3.3.2-10 Auxiliary Systems – Summary of Aging Management Evaluation – Chemical and Volume Control System (Tubing - Stainless Steel - Treated Borated Water (Int) - Loss of Material) [6] Table 3.3.2-3 Chemical and Volume Control System Summary of Aging Management Evaluation (Flexible Hose – Nickel Alley –			

	Treated Borated Water (Internal) – Loss of Material) [2]			
Heat Exchanger (Channel Heads and Covers)	Table 3.3.2-3 Chemical and Volume Control System Summary of Aging Management Evaluation (Heat Exchangers Components (CS E-2 Channel Head) - Stainless Steel – Treated Borated Water (Internal) – Loss of Material) [2] Table 3.3.2-10 Chemical and Volume Control and Boron Recycle Systems: Summary of Aging Management Review (Heat Exchangers – Excess Letdown HXs (Channel Heads) - Stainless Steel – Borated Water (Interior) – Loss of Material) [1] Table 3.3.2-10 Chemical and Volume Control and Boron Recycle Systems: Summary of Aging Management Review (Heat Exchangers – Letdown Chillers (Channel Heads) - Stainless Steel – Borated Water (Interior) – Loss of Material) [1] Table 3.3.2-10 Chemical and Volume Control and Boron Recycle Systems: Summary of Aging Management Review (Heat Exchangers – Letdown HXs (Channel Heads) - Stainless Steel – Borated Water (Interior) – Loss of Material) [1]	NextEra Energy Seabrook, LLC [2] (2010) Southern Nuclear Operating Co. [1] (2007) Florida Power & Light Co. [7] (2001) Dominion Nuclear Connecticut, Inc. [9] (2004)		The CVCS heat exchangers are generally operated at lower pressures (shell side) and located where they should not cause debris generation I agree. Also, in industry HX is a system usually isolated.

	TABLE 3.3-1 CHEMICAL AND VOLUME CONTROL (Letdown Heat Exchanger Channel Heads and Covers - Stainless Steel – Treated Water Borated – Loss of Material and Cracking) [7] Table 3.3.2-10 Chemical and Volume Control and Boron Recycle Systems: Summary of Aging Management Review (Heat Exchangers – Letdown Reheat HXs (Channel Heads) - Stainless Steel – Borated Water (Interior) – Loss of Material) [1] Table 3.3.2-10 Chemical and Volume Control and Boron Recycle Systems: Summary of Aging Management Review (Heat Exchangers – Moderating HXs (Channel Heads) - Stainless Steel – Borated Water (Interior) – Loss of Material) [1] Table 3.3.2-10 Chemical and Volume Control and Boron Recycle Systems: Summary of Aging Management Review (Heat Exchangers – Regenerative HXs (Channel Heads) - Stainless Steel – Borated Water (Interior) – Loss of Material) [1] Table 3.3.2-10 Chemical and Volume Control and Boron Recycle Systems: Summary of Aging Management Review (Heat Exchangers – Seal Water HXs (Channel Heads) - Stainless Steel – Borated Water (Interior) – Loss of Material) [1]			

	Table 3.3.2-3 Chemical and Volume Control System Summary of Aging Management Evaluation (Heat Exchanger Components (CS-P-128 Fluid Drive Cooler Channel Head) – Air With Borated Water Leakage (External) – Loss of Material) [2] Table 3.3.2-3 Chemical and Volume Control System Summary of Aging Management Evaluation (Heat Exchanger Components (CS-P-128 Pump Oil Cooler Channel Head) – Gray Cast Iron – Air With Borated Water Leakage (External) – Loss of Material) [2] Table 3.3.2-15: Auxiliary Systems - Chemical and Volume Control - Aging Management Evaluation (Thermal Regeneration Chiller Compressor Oil Cooler (Channel Head) - Carbon Steel - Borated Water Leakage - Loss of Material - Boric Acid Corrosion) [9] Table 3.3.2-15: Auxiliary Systems - Chemical and Volume Control - Aging Management Evaluation (Thermal Regeneration Chiller Condenser (Channel Head) - Carbon Steel - Borated Water Leakage - Loss of Material - Boric Acid Corrosion) [9]			
Heat Exchanger (Shell)	Table 3.3.2-3 Chemical and Volume Control System Summary of Aging Management Evaluation (Heat Exchanger Components (CS-E-2 Shell) - Stainless Steel – Treated	NextEra Energy Seabrook, LLC [2] (2010)		The CVCS heat exchangers are generally operated at lower pressures (shell

	Borated Water (Internal) – Loss of Material) [2] Table 3.3.2-7 Auxiliary Systems – Summary of Aging Management Evaluation - Chemical and Volume Control System (Heat Exchanger Shell Side (HX #41,42,43) – Carbon Steel – Plant Indoor Air (Ext) – Loss of Material) [3] Table 3.3.2-10 Chemical and Volume Control and Boron Recycle Systems: Summary of Aging Management Review (Heat Exchangers – Excess Letdown HXs (Shells) – Air Indoor (Exterior) – Loss of Material – Borated Water Leakage) [1] Table 3.3.2-15: Auxiliary Systems - Chemical and Volume Control - Aging Management Evaluation (Excess Letdown Heat Exchanger (Shell) - Carbon Steel - Borated Water Leakage - Loss of Material - Boric Acid Corrosion) [9] Table 3.3.2-10 Chemical and Volume Control and Boron Recycle Systems: Summary of Aging Management Review (Heat Exchangers – Letdown Chiller (Shells) – Air Indoor (Exterior) – Loss of Material – Borated Water Leakage) [1] Table 3.3.2-10 Chemical and Volume Control and Boron Recycle Systems: Summary of Aging Management Review (Heat	Wolf Creek Nuclear Operating Corp. [3] (2008) Southern Nuclear Operating Co. [1] (2007) Dominion Nuclear Connecticut, Inc. [9] (2004) Dominion Nuclear Connecticut, Inc. [8] (2004) Entergy Nuclear Operations, Inc. [10] (2004) Entergy Nuclear Operations, Inc [5] (2003)		side) and located where they should not cause debris generation I agree.

	Exchangers – Letdown HXs (Shells) – Air Indoor (Exterior) – Loss of Material – Borated Water Leakage) [1] Table 3.3.2-10: Auxiliary Systems - Chemical and Volume Control - Aging Management Evaluation (Letdown Heat Exchanger (Shell) – Carbon Steel - Borated Water Leakage – Loss of Material – Boric Acid Corrosion) [8] Table 3.3.2-1 Auxiliary Systems - Chemical and Volume Control System - Summary of Aging Management Evaluation (Letdown Heat Exchanger Shell - Carbon Steel - Containment Air (Ext) - Loss of Material - Boric Acid Corrosion Program) [10] Table 3.3.2-10 Chemical and Volume Control and Boron Recycle Systems: Summary of Aging Management Review (Heat Exchangers – Letdown Reheat HXs (Shells) - Stainless Steel – Borated Water (Interior) – Loss of Material) [1] Table 3.3.2-10 Chemical and Volume Control and Boron Recycle Systems: Summary of Aging Management Review (Heat Exchangers – Moderating HXs (Shells) - Stainless Steel – Borated Water (Interior) – Loss of Material) [1] Table 3.3.2-10 Chemical and Volume Control and Boron Recycle Systems: Summary of			

	Aging Management Review (Heat Exchangers – Regenerative HXs (Shells) - Stainless Steel – Borated Water (Interior) – Loss of Material) [1] Table 3.3.2-10 Chemical and Volume Control and Boron Recycle Systems: Summary of Aging Management Review (Heat Exchangers – Seal Water HXs (Shells) – Carbon Steel – Air Indoor (Exterior) – Loss of Material – Borated Water Leakage) [1] Table 3.3.2-3 Chemical and Volume Control System Summary of Aging Management Evaluation (Heat Exchanger Components (CS-p-128 Fluid Drive Cooler Shell) – Steel – Air With Borated Water Leakage (External) – Loss of Material) [2] Table 3.3.2-3 Chemical and Volume Control System Summary of Aging Management Evaluation (Heat Exchanger Components (CS-P-128 Pump Oil Cooler Shell – Copper Alloy >15% Zn – Air With Borated Water Leakage (External) – Loss of Material) [2] Table 3.3.2-5 Chemical and Volume Control System Summary of Aging Management Evaluation (Heat Exchanger (Shell) Stainless Steel – Treated Borated Water >270 °F (Internal) – Cracking, Cracking-Fatigue, and Loss of Material) [5]			

	Table 3.3.2-15: Auxiliary Systems - Chemical and Volume Control - Aging Management Evaluation (CS Manifolds (Letdown Chiller Heat Exchanger (Shell) - Carbon Steel - Borated Water Leakage - Loss of Material - Boric Acid Corrosion) [9] Table 3.3.2-15: Auxiliary Systems - Chemical and Volume Control - Aging Management Evaluation (CS Manifolds (Letdown Heat Exchanger (Shell) - Carbon Steel - Borated Water Leakage - Loss of Material - Boric Acid Corrosion) [9] Table 3.3.2-15: Auxiliary Systems - Chemical and Volume Control - Aging Management Evaluation (CS Manifolds (Seal Water Heat Exchanger (Shell) - Carbon Steel - Borated Water Leakage - Loss of Material - Boric Acid Corrosion) [9] Table 3.3.2-15: Auxiliary Systems - Chemical and Volume Control - Aging Management Evaluation (Thermal Regeneration Chiller Compressor Oil Cooler (Shell) - Carbon Steel - Borated Water Leakage - Loss of Material - Boric Acid Corrosion) [9] Table 3.3.2-15: Auxiliary Systems - Chemical and Volume Control - Aging Management Evaluation (Thermal Regeneration Chiller Condenser (Shell) - Carbon Steel - Borated			

	Water Leakage - Loss of Material - Boric Acid Corrosion) [9] Table 3.3.2-15: Auxiliary Systems - Chemical and Volume Control - Aging Management Evaluation (Thermal Regeneration Chiller Evaporator (Shell) - Carbon Steel - Borated Water Leakage - Loss of Material - Boric Acid Corrosion) [9]			
Heat Exchanger (Tubes and Tubesheets)	Table 3.3.2-3 Chemical and Volume Control System Summary of Aging Management Evaluation (Heat Exchanger Components (CS-E-2 Tubes) - Stainless Steel – Treated Borated Water (Internal) – Loss of Material) [2] Table 3.3.2-6-IP2 Chemical and Volume Control Summary of Aging Management Review (Heat Exchanger (Tubes) Stainless Steel – Treated Borated Water > 140 °F (Int) – Loss of Material) [4] Table 3.3.2-3 Chemical and Volume Control System Summary of Aging Management Evaluation (Heat Exchanger Components (CS-E-2 Tube Sheet) - Stainless Steel – Treated Borated Water (Internal) – Loss of Material) [2] Table 3.3.2-10 Chemical and Volume Control and Boron Recycle Systems: Summary of Aging Management Review (Heat Exchangers – Excess Letdown HXs (Tubes &	NextEra Energy Seabrook, LLC [2] (2010) Entergy Nuclear Operations, Inc [4] (2007) Southern Nuclear Operating Co. [1] (2007) Florida Power & Light Co. [7] (2001)		The CVCS heat exchangers are generally operated at lower pressures (shell side) and located where they should not cause debris generation please see previous notes.

	Tubesheets) - Stainless Steel – Borated Water (Interior) – Loss of Material) [1] Table 3.3.2-10 Chemical and Volume Control and Boron Recycle Systems: Summary of Aging Management Review (Heat Exchangers – Letdown Chillers (Tubes) - Stainless Steel – Borated Water (Interior) – Loss of Material) [1] Table 3.3.2-10 Chemical and Volume Control and Boron Recycle Systems: Summary of Aging Management Review (Heat Exchangers – Letdown HXs (Tubes & Tubesheets) - Stainless Steel – Borated Water (Interior) – Loss of Material) [1] TABLE 3.3-1 CHEMICAL AND VOLUME CONTROL (Letdown Heat Exchanger Tubes and Tubesheets - Stainless Steel – Treated Water Borated – Loss of Material and Cracking) [7] Table 3.3.2-10 Chemical and Volume Control and Boron Recycle Systems: Summary of Aging Management Review (Heat Exchangers – Letdown Reheat HXs (Tubes & Tubesheets) - Stainless Steel – Borated Water (Interior) – Loss of Material) [1] Table 3.3.2-10 Chemical and Volume Control and Boron Recycle Systems: Summary of			

	Aging Management Review (Heat Exchangers – Moderating HXs (Tubes & Tubesheets) - Stainless Steel – Borated Water (Interior) – Loss of Material) [1] Table 3.3.2-10 Chemical and Volume Control and Boron Recycle Systems: Summary of Aging Management Review (Heat Exchangers – Regenerative HXs (Tubes & Tubesheets) - Stainless Steel – Borated Water (Interior) – Loss of Material) [1] TABLE 3.3-1 CHEMICAL AND VOLUME CONTROL (Regenerative Heat Exchangers (Including Tubes) - Stainless Steel – Treated Water Borated – Loss of Material and Cracking) [7] Table 3.3.2-10 Chemical and Volume Control and Boron Recycle Systems: Summary of Aging Management Review (Heat Exchangers – Seal Water HXs (Tubes & Tubesheets) - Stainless Steel – Borated Water (Interior) – Loss of Material) [1]			

References

[1] Southern Nuclear Operating Co., Inc., "Vogtle electric generating plant units 1 and 2 license renewal application," U.S. Nuclear Regulatory Commission, 2007.

[2] L. NextEra Energy Seabrook, "Seabrook station license renewal application," U.S. Nuclear Regulatory Commission, 2010.

[3] Wolf Creek Nuclear Operating Corp., "License renewal application wolf creek generating station unit 1," 2008.

[4] I. Entergy Nuclear Operations, "License renewal application indian point nuclear generating sections 1-4," U.S. Nuclear Regulatory Commission, April 2007.

[5] I. Entergy Operations, "License renewal application arkansas nuclear one - units 2," U.S. Nuclear Regulatory Commission, October 2003.

[6] Arizona Public Service Co., "License renewal application palo verde nuclear generating station unit 1, unit 2, and Unit 3," U.S. Nuclear Regulatory Commission, 2009.

[7] Florida Power & Light Co., "License renewal application st lucie units 1 & 2," U.S. Nuclear Regulatory Commission, 2001.

[8] I. Dominion Nuclear Connecticut, "Millstone nuclear power station, units 2 - license renewal application," U.S. Nuclear Regulatory Commission, January 2004.

[9] I. Dominion Nuclear Connecticut, "Millstone nuclear power station, units 3 - license renewal application," U.S. Nuclear Regulatory Commission, January 2004.

[10] I. Entergy Nuclear Operations, "Palisades nuclear plant - application for renewed operating license," U.S. Nuclear Regulatory Commission, March 2005.

APPENDIX C: OVERVIEW OF RENEWAL PROCESS THEORY

C.1. INTRODUCTION

Understanding and modeling system or component availability is a critical part of reliability and risk analysis for high consequence industries such as the nuclear power generation industry. One common approach taken by analysts is to model the failure mechanisms that lead to unavailability of an item (i.e., component or system). However, for complex engineering systems, failure mechanisms only tell part of the story. Complex engineering systems have maintenance programs that are designed, to the most possible extent, to optimize system performance and prevent failure. To develop accurate item unavailability estimations, it is critical to incorporate the effects of maintenance mechanisms.

As failure mechanisms work to degrade a component or system, maintenance mechanisms work to reduce the effects of the failure mechanisms, or to return the item to a less degraded state. Perfect repair mechanisms would return the component or system to an "as good as new" state. Perfect repair is modeled by the renewal process (RP). RP theory considers successive failure times that are independently and identically distributed random variables. At the moment of each failure, the system is immediately restored to the "as good as new" condition [1, 2].

The perfect repair assumption is not realistic. This is because it is not reasonable to expect to have a perfect repair for every repair in an entire system. Therefore, the minimal repair assumption is implemented to return the system to an "as bad as old" condition. The "as bad as old" condition assumes that the failed item is replaced with an identical item and the system is returned to the state it was in immediately before failure occurred. This concept of minimal repair was modeled in [3, 4] in order to find the optimal time between preventive maintenance for cost optimization. This concept has been advanced to consider optimal repair times using the Non-Homogenous Poisson Process (NHPP) [1, 2, 5-11].

Perfect repair and minimal repair assumptions are insufficient for modeling many systems, as many repairs fall somewhere in-between (or exceed) these two conditions. In order to capture a combination of both assumptions[12], a bivariate method, where perfect repair has a probability of p and imperfect repair (minimal repair) has a probability of $q=1-p$, is developed. The authors also introduced the concept of effective age. The effective age is the time elapsed since the component was perfectly repaired. The bivariate p and q concept was extended by [13] to include time dependency.

The authors of [14] consider a multivariate imperfect repair concept, where p represents the probability that a repair is unsuccessful and the item is scrapped (replaced), and $q=1-p$ represents the probability that a minimal repair will occur. This research considers the case when only one component at a time can fail and then generalizes the model for multiple simultaneous component failures.

In [15], the authors establish the concept of a degree of repair, A_n. This concept will be elaborated in detail in next section of this appendix, when the generalized renewal process (GRP) is explained. However, it is mentioned here to set the framework for the literature that builds off that fundamental concept, but does not utilize the GRP.

The bivariate concept of repair was expanded upon, and sometimes referenced as a geometric process by multiple papers including [16], which examines the problem from the angle of both working age (residual age) and failure numbers. This concept is accompanied by [17] which investigates an optimization of replacement policy implementing both analytical and numerical solutions. The concept is then extended for a multistate degenerative system in [18].

The concept of imperfect maintenance was implemented in a cumulative damage shock model by [19] for optimization of preventive maintenance periods that minimized the expected cost rate. In this paper, the imperfect repair reduces the damage to the system by $100(1-b)\ \%$, where b is the degree of effectiveness of the maintenance action. The authors expand upon the model to include minimal repairs at the point where the system fails due to the cumulative damage accrued from periodic (according to a Poisson process) shocks to the system in [20].

All the renewal models discussed until now have assumed repair or maintenance actions to be point processes with a negligible time. This assumption is relaxed by [21], who develops unavailability steady state fractions.

C.2. GENERALIZED RENEWAL PROCESS THEORY

The classical renewal theory focuses on associated counting processes, $N(t)$. [22] focuses on the renewal function (g-renewal function), $H(t)=E[N(t)]$, and the renewal density function (g-renewal density), $h(t)=(d/dt)H(t)$. The theory defines intervals between failures as a Markov process in discrete times of non-negative real numbers which is temporally and spatially homogenous.

The concept of a virtual age is introduced in [23], a paper that considers periodic system replacement as well as failure replacement. Then, in [15], the general repair models for repairable systems using the concept of virtual age are established. This is the paper that lays the foundation for the modern GRP literature.

Until [15], the stochastic behavior of repairable systems assumed either perfect or minimal repair. The new GRP utilizes the concept of virtual age. If the virtual age of the system is $V_{n-1}=y$ immediately after the (n-1)th repair, then the nth failure time X_n is distributed as:

$$\Pr[X_n \le x \,|\, V_{n-1} = y] = \frac{F(x+y)-F(y)}{1-F(y)} \tag{C.1}$$

Here F(x) is the failure time distribution of a system with virtual age $V_0=0$, or a "new" system. The authors define A_n as the "degree" (or quality) of the nth repair. Two possible models are developed by the authors and, in recent publications, remain relevant.

The first model, which will be referred to as KIJIMA I, assumes that the nth repair cannot remove the damage (age) incurred before the (n-1)th repair. The additional age added to the virtual age of the system is reduced from X_n to A_n* X_n. Therefore, the virtual age after the nth repair is:

$$V_n = V_{n-1} + A_n X_n \tag{C.2}$$

The second model, which will be referred to as KIJIMA II, assumes that the nth repair can remove the damage (age) that has been accumulated before the (n-1)th repair. The second model shows a virtual age after the nth repair as:

$$V_n = A_n (V_{n-1} + X_n) \tag{C.3}$$

In both KIJIMA models, A_n is a random variable with values of the range [0,1]. If $A_n=0$, then the models represent the special case of perfect repair. If $A_n=1$, the models represent the special case of minimal repair.

The development of the generalized renewal theory set the groundwork for the expansion from renewal models that considered two repair types (perfect or minimal repair), which resulted in two post-repair conditions ("as good as new" and "as bad as old") to renewal models that considered five post-repair conditions: "as good as new", "as bad as old", "better than old, but worse than new", "worse than old", and "better than new".

The "better than old, but worse than new" post-repair condition is a result of a repair that has a degree, A_n, somewhere between (0,1). This means that the repair was better than minimal repair, but not as effective as perfect repair. This is intuitively a very common post-repair condition, as there are many cases where it is unrealistic for actions applied to a complex system to repair the entire system perfectly, but where the repair actions still do improve the condition of the system more than the minimal repair assumption indicates. The "worse than old" post-repair condition is a result of a repair that has a degree $A_n>1$. This means that the "repair" damaged or aged the system further instead bringing it to a "newer" or less-degraded state. Such an event can occur when a maintenance worker is improperly trained and causes damage to the system instead of rejuvenating the system. Finally, the "better than new" post-repair condition is a result of a repair that has a degree, $A_n<0$. This can occur when the resulting repair action brings the system to a state that is less aged or degraded than when the system originated. Such an action could potentially include a situation where a repair mitigates some underlying failure mechanism of the system; thus, producing a slower rate of degradation and a reduced likelihood of failure for the system.

The expected number of failures from the time when the system is put in operation (t=0) until an arbitrary time, T, is given by the solution of the G-renewal equation:

$$\mathrm{H(t)}=\int_0^T\left(g\left(\theta \mid 0\right)+\int_0^T h(x)g(\theta-x \mid x)dx\right)d\theta \tag{C.4}$$

where:

$$\mathrm{g}\left(t \mid x\right)=\frac{f\left(t+qx\right)}{1-F\left(qx\right)} \tag{C.5}$$

represents the conditional probability density function; q is the parameter or rejuvenation or quality of repair[23]. The closed form solution of Equation (C.4) is not available for an underlying Weibull distribution. A Monte Carlo simulation numerical approach is discussed in [24]. This Monte Carlo approach to estimation is applied for warranty data analysis for data collected over 18 months and used to estimate the parameters of the Weibull distribution to be used in the GRP modeling.

C.3. GENERALIZED RENEWAL PROCESS APPLICATIONS

Having been introduced approximately 25 years ago, the GRP is still very young. A large part of the literature regarding the GRP is focused on the development of the process itself and the assumptions that surround the process and the different techniques used to find solutions (analytical or numerical) for the GRP. This section discusses some of the areas where the GRP has been applied.

A replacement model with general repair is used to develop an optimal replacement policy for the expected average cost per unit time in [25]. The benefit that can be derived from an item as a function of its virtual age is explored in [26]. The paper considers an item than can only be repaired N times and which continuously yields a benefit at a rate which is a function only of its virtual age. The model takes into consideration costs for maintenance and explores the total benefit of the item.

Most applications of the GRP utilized a maximum likelihood estimation of the parameters for the model. However, [27] demonstrated that even when there is a relatively small amount of data, a Bayesian approach can be sufficient for estimation of the parameters and the model can still accurately describe the failure data.

The behavior of the KIJIMA I and KIJIMA II models with underlying Weibull time-to-failure distributions is explored in [28]. This paper explores the sensitivity of the GRP models for the degree of repair as well as the shape and scale parameters of the underlying Weibull distributions. The decision between performing preventive replacement or renewal maintenance is explored in [29]. The various decision variables are taken into consideration including the time between preventive replacements. The model utilizes the KIJIMA II type general or imperfect repair, as well as random failure times to decide the optimal method for renewal.

Time dependent scale transformation of the underlying distribution function is explored and compared to the virtual age processes proposed by Kijima in [30]. Both KIJIMA I and KIJIMA II models are used to compute a mean cost function in order to determine optimal preventive maintenance schedules in [31]. The authors found that KIJIMA I models required optimal preventive maintenance periods to be more uniformly spread out over the life of the system, whereas in the KIJIMA II models the required optimal preventive maintenance periods between required actions quickly decreased. One important observation that the authors make at the end of this paper is that maintenance not only reduces the occurrence of failures, but also increases the efficiency of the system. Therefore, cost optimization methods should account for this increase in efficiency in future lifetime cost optimization work.

A point process model, known as the geometric process, models the “better than new” post-repair condition using the maximum likelihood estimation of the model for the case of the Exponential and Weibull underlying distributions in [32]. The Monte Carlo simulation approach, combined with a semi-Markov chain theory, allowed for an accurate estimation for an underlying failure distribution function of Weibull in [33].

The authors of [34] discuss systems whose state cannot be known without inspection of the system. Such inspections have an associated cost that is incorporated into the optimization maintenance strategy using an iterative algorithm to minimize the mean long-run cost rate. The author of [35] points out that the cost-centric optimization methods ignore “the value dimension” of maintenance. This paper explores general repair optimization incorporating semi-Markov decision methods, discounted cash flow techniques, and dynamic programming.

Three of the most popular maintenance policies are studied in [36]. For a Weibull failure time distribution function for the g-renewal Kijima models, the authors developed two efficient solutions: an approximate solution previously developed in [37] and a Monte Carlo simulation method. The authors examine the sensitivity of each model with respect to the restoration factor (degree of repair) to benchmark other approximate methods for solving g-renewal equations.

The GRP literature largely focuses on cost optimization work for maintenance. The most common decision variable explored is the length of time between preventive maintenance activities. The models are built based on point estimates developed from maximum likelihood approaches. GRP literature generally focuses on single failure modes for system optimization analysis. As is pointed out in [38], some models are considered "black box" models where the main goal is simply to fit the model to data. Therefore, it becomes difficult to consider multiple failure modes. However, to most accurately represent a system and optimize it for cost or availability, it is important to consider all the possible failure modes.

REFERENCES

1. Modarres, M., *Risk Analysis in Engineering: Techniques, Tools, and Trends*. 2006, Boca Rator, FL: Taylor & Francis Group, LLC.
2. Modarres, M., M. Kaminskiy, and V. Krivtsov, *Reliability Engineering and Risk Analysis: A Practical Guide*. Second ed. 2010, Boca Raton, FL: Taylor & Francis Group.
3. Nakagawa, T., *Imperfect Preventive-Maintenance.* IEEE Transactions on Reliability, 1979. **R-28**(5).
4. Nakagawa, T., *Optimum Policies When Preventive Maintenance is Imperfect.* IEEE Transactions on Reliability, 1979. **R-28**(4): p. 331-332.
5. Engelhardt, M. and L.J. Bain, *On the Mean Time Between Failures For Repairable Systems.* IEEE Transactions on Reliability, 1986. **R-35**(4): p. 419-422.
6. Hartler, G., *THE NONHOMOGENEOUS POISSON PROCESS - A MOEL FOR THE RELIABILITY OF COMPLEX REPAIRABLE SYSTEMS.* Microelectronics Reliability, 1989. **29**(3): p. 381-386.
7. Coetzee, J., *The role of NHPP models in the practical analysis of maintenance failure data.* Reliability Engineering & System Safety, 1997. **56**: p. 161-168.
8. Rausand, M. and A. Hoyland, *System Reliability Theory: Models, Statistical Methods, and Applications*. Second ed. 2004, Hoboken, NJ: John Wiley & Sons, Inc.
9. Krivtsov, V.V., *Practical extensions to NHPP application in repairable system reliability analysis.* Reliability Engineering & System Safety, 2007. **92**(5): p. 560-562.
10. Muralidharan, K., *A review of repairable systems and point process models.* ProbStat Forum, 2008. **1**: p. 26-49.

11. Huynh, K.T., et al., *Modeling age-based maintenance strategies with minimal repairs for systems subject to competing failure modes due to degradation and shocks.* European Journal of Operational Research, 2012. **1**: p. 140-151.

12. Brown, M. and F. Proschan, *Imperfect Repair.* Applied Probability Trust, 1983. **20**(4): p. 851-859.

13. Block, H.W., W.S. Borges, and T.H. Savits, *Age-Dependent Minimal Repair.* Journal of Applied Probability, 1985. **22**(2): p. 370-385.

14. Shaked, M. and J.G. Shanthikumar, *Multivariate Imperfect Repair.* Operations Research, 1986. **34**(3): p. 437-448.

15. Kijima, M., *Some Results for Repairable Systems with General Repair.* Journal of Applied Probability, 1989. **26**(1): p. 89-102.

16. Yeh, L., *A Note on the Optimal Replacement Problem.* Advances in Applied Probability, 1988. **20**(2): p. 479-482.

17. Yeh, L., *GEOMETRIC PROCESSES AND REPLACEMENT PROBLEM.* Acta Mathematicae Applicatae Sinica, 1988. **4**(4): p. 366-377.

18. Lam, Y., Y.L. Zhang, and Y.H. Zheng, *A geometric process equivalent model for a multistate degenerative system.* European Journal of Operational Research, 2002. **142**: p. 21-29.

19. Kijima, M. and T. Nakagawa, *A Cumulative Damage Shock Model with Imperfect Preventive Maintenance.* Naval Research Logistics, 1991. **38**: p. 145-156.

20. Kijima, M. and T. Nakagawa, *Replacement policies of a shock model with imperfect preventive maintenance.* European Journal of Operational Research, 1992. **57**: p. 100-110.

21. Iyer, S., *Availability Results for Imperfect Repair.* Sankhya: The Indian Journal of Statistics, Series B (1960-2002), 1992. **54**(2): p. 249-256.

22. Kijima, M. and U. Sumita, *A Useful Generalization of Renewal Theory: Counting Processes Governed by Non-Negative Markovian Increments.* Journal of Applied Probability, 1986. **23**(1): p. 71-88.

23. Kijima, M., H. Morimura, and Y. Suzuki, *Periodical Replacement Problem Without Assuming Minimal Repair.* European Journal of Operational Research, 1988. **37**: p. 194-203.

24. Kaminskiy, M. and V. Krivtsov, *A Monte Carlo Approach To Estimation Of G-Renewal Process in Warranty Data Analysis.* Reliability: Theory & Applications, 2006. **1**: p. 29-31.

25. Makis, V. and A.K.S. Jardine, *A note on optimal replacement policy under general repair.* European Journal of Operational Research, 1993. **63**: p. 75-82.

26. Scarsini, M. and M. Shaked, *On the value of an item subject to general repair or maintenance.* European Journal of Operational Research, 2000. **122**: p. 625-637.

27. Yanez, M., F. Joglar, and M. Modarres, *Generalized renewal process for analysis of repairable systems with limited failure experience.* Reliability engineering and System Safety, 2002. **77**: p. 167-180.

28. Jacopino, A., F. Groen, and A. Mosleh. *Behavioural Study of the General Renewal Process*. in *Annual Reliability and Maintainability Symposium*. 2004. IEEE.

29. Shirmohammadi, A.H., Z.G. Zhang, and E. Love, *A Computational Model for Determining the Optimal Preventive Maintenance Policy With Random Breakdowns and Imperfect Repairs.* IEEE Transactions on Reliability, 2007. **56**(2): p. 332-339.

30. Sevcik, J. *Repairable systems with general repair*. in *15th European Young Statisticians Meeting*. 2007. Castro Uriales (Spain).

31. Bartholomew-Biggs, M., M.J. Zuo, and X. Li, *Modelling and optimizing sequential imperfect preventive maintenance.* Reliability Engineering & System Safety, 2009. **94**(1): p. 53-62.

32. Kaminskiy, M.P. and V.V. Krivtsov, *G1-Renewal Process as Repairable System Model.* arXiv, 2010. **1006.3718**.

33. Yevkin, O., *A Monte Carlo approach for evaluation of availability and failure intensity under g-renewal process model*. Advances in Safety, Reliability and Risk Management. 2012, London: Taylor & Francis Group.

34. Le, M.D. and C.M. Tan, *Optimal maintenance strategy of deteriorating system under imperfect maintenance and inspection using mixed inspectionscheduling.* Reliability Engineering & System Safety, 2013. **113**: p. 21-29.

35. Marais, K.B., *Value maximizing maintenance policies under general repair.* Reliability Engineering & System Safety, 2013. **119**: p. 76-87.

36. Yevkin, O. and V. Krivtsov, *Comparative Analysis of Optimal Maintenance Policies Under General Repair With Underlying Weibull Distributions.* IEEE Transactions on Reliability, 2013. **62**(1): p. 82-91.

37. Yevkin, O. and V. Krivtsov, *An Approximate Solution to the G-Renewal Equation With an Underlying Weibull Distribution.* IEEE Transactions on Reliability, 2012. **61**(1): p. 68-73.

38. Lindqvist, B.H. *Repairable systems with general repair*. in *European Safety and Reliability Conference*. 1999. Munich, Germany.

APPENDIX D: MATLAB CODES FOR CRACK PROPAGATION SIMULATION OF ALLOY 690 AND STAINLESS STEEL

D.1 PITTING TO CRACK TRANSITION CODE FOR DEVELOPMENT OF NEW TO FLAW TRANSITION RATE FOR ALLOY 690

```
% LHS SCC Pit Growth Propagation Code for Alloy 690
% Developer: Nick O'Shea
% Date: 7.6.16
%
==================================================================
%
==================================================================
% SECTION 1: Initialization
%
==================================================================
%
==================================================================
%Simulation Conditions
p = parpool('local', 2);
numsamp = 50;
deltagrowthtime = 1;                    %step-time in [s] (3600s = 1hr)
Maxruntimeinyears = 60;                 %max run time for the code in years
% myCluster=parcluster('local');
% myCluster.NumWorkers = 20;
% saveProfile(myCluster);
% parpool(myCluster, 20);
%parpool('size');
%Variable initialization
minpit = 2.5E-5;                        %min pit size
alphamin = 9.59166E-09;
alphamax = 2.82489E-07;
beta = 0.5;                             %initialize beta parameter for sample growth size of pits
CW=2;                                   %[percent] CW by Rolling for exp trans region
sigma_ys = (CW*20.283)+296.61;          %[MPa] calculate yield strength
sigma_app = 430;                        %[MPa] total effective stress (applied+residual) exp trans
region
%SCC Constants
SIFthreshold = 9;                       %[MPasqrt(m)] SIF when SCC crack propagation begins
Tref = 598.15;                          %[Kelvin] Normalize to 325C
Q = 120;                                %kJ/mol for Alloy 690
R = 0.008314;                           %[kJ/mol-K] Boltzmann constant
H2 = 26;                                %[cc/kg] Hydrogen concentration of primary water environment
temp = 598.15;                          %[K] temperature of primary water 325
C690pittable = nan(numsamp,1);
n690pittable = nan(numsamp,1);
```

```
m690pittable = nan(numsamp,1);
B690pittable = nan(numsamp,1);
alpha690pittable = nan(numsamp,1);
beta690pittable = nan(numsamp,1);
prefail690pittable = nan(numsamp,1);
toosmall690pittable = nan(numsamp,1);
numcrack690pittable = nan(numsamp,1);
TTCtable = nan(numsamp,1);              %data matrix for TTF tracking
initpittable = nan(numsamp,1);          %data matrix for initial pit size
cracktranstable = nan(numsamp,1);       %data matrix for tracking transition size of flaw/crack
initpitvaluetable = nan(numsamp,1);
Maximumruntime = Maxruntimeinyears*365.25*24*60*60;
%years*days*hours*minutes*seconds
%Fitting Weibull distribution to Turnbull Data at 15,402 hours
numbin = [5,16,33,22,19,10,3,2,2,1];
binbounds = [20,40,60,80,100,120,140,160,180,200,220];      %microns
totalinitpits = sum(numbin);
initpitdatatable = nan(max(size(numbin)),max(numbin));
for pout = 1:max(size(numbin))
    for pin = 1:numbin(pout)
        initpitdatatable(pout,pin) = (binbounds(pout)+(rand*(binbounds((pout+1))-
binbounds(pout))))*(1E-6);
    end
end
initpitdatatablecolumn = initpitdatatable(:);
initpitdatatablecolumn(isnan(initpitdatatablecolumn)) = [];
pdW=fitdist(initpitdatatablecolumn,'Weibull');
WeibullA = 1/((pdW.A)^(pdW.B));
WeibullB = pdW.B;
%
==========================================================================
%
==========================================================================
% SECTION 2: Generate Samples
%
==========================================================================
%
==========================================================================
%Crack model parameters
load('Alloy690params.mat');     %#,C,m,n,B,s
[datalength, ~] = size(Alloy690params);
alphadist = makedist('Uniform','lower',alphamin,'upper',alphamax);
randalphadist = random(alphadist,datalength,1);
Alloy690params = [Alloy690params randalphadist];
randpitdist = random(pdW,datalength,1);
Alloy690params = [Alloy690params randpitdist];
```

```
[datalength, numvar] = size(Alloy690params);
rng shuffle;
randnummatrix = rand(numsamp,numvar);
samplematrix = zeros(numsamp,numvar);
for j = 1:numvar
   idx = randperm(numsamp)';
   Pmatrix = ((idx-randnummatrix(:,j))/numsamp).*100;
   samplematrix(:,j) = prctile(Alloy690params(:,j),Pmatrix); %#,C,m,n,Beta(CPR),s,alpha,initpit
end
parfor samp = 1:numsamp
   remainder = rem(samp,10);
   if remainder == 0
      fprintf('Sample: %d\n',samp)
   end
   dt = deltagrowthtime;
   prefail = 0;            %reset too large sample counter
   toosmall = 0;
   numcrack = 0;
   growthtime = 0;         %reset growth time for each sample
   checker = 0;
   cracksize = nan;
   alpha = samplematrix(samp,7);
   C690 = samplematrix(samp,2);
   m690 = samplematrix(samp,3);
   n690 = samplematrix(samp,4);
   B690 = samplematrix(samp,5);
   %record model parameter selection
   C690pittable(samp) = C690;
   n690pittable(samp) = n690;
   m690pittable(samp) = m690;
   B690pittable(samp) = B690;
   alpha690pittable(samp) = alpha;
   beta690pittable(samp) = beta;
   pitsize = samplematrix(samp,8);
   initpitvaluetable(samp,1) = pitsize;
   SIF = sigma_app*sqrt(pi()*pitsize);
   pitgrowthrate = (beta*(alpha^(1/beta))*(pitsize^(1-(1/beta)))); %[m/s]
   dadt690 = (C690*exp(-(Q/R)*((1/temp)-(1/Tref)))*(sigma_ys^m690)*((SIF-
SIFthreshold)^n690)*(H2^B690)); %calc dadt [m/s]
   %Check for Initial Pit Out of Acceptable Range
   if ((abs(real(dadt690)) >= pitgrowthrate) && (SIF >= SIFthreshold))
      %if ((dadt690 >= pitgrowthrate) && (SIF >= SIFthreshold))
      prefail = prefail+1;
   end
   %pit propagation loop
   if prefail == 0
```

```
    while (growthtime < Maximumruntime)
      pitgrowth = pitgrowthrate*dt;
      pitsize = pitsize+pitgrowth;
      growthtime = growthtime+dt;
      if (growthtime>=1*3600) && (growthtime<(1*3600+3600))
        dt = 1800;
        %fprintf('dt: %d\n',dt)
      elseif (growthtime>=240*3600) && (growthtime<(240*3600+10800))
        dt = 5400;
        %fprintf('dt: %d\n',dt)
      elseif (growthtime>=720*3600) && (growthtime<(720*3600+21600))
        dt = 10800;
        %fprintf('dt: %d\n',dt)
      elseif (growthtime>=4320*3600) && (growthtime<(4320*3600+43200))
        dt = 21600;
        %fprintf('dt: %d\n',dt)
      elseif (growthtime>=8640*3600) && (growthtime<(8640*3600+86400))
        dt = 43200;
        %fprintf('dt: %d\n',dt)
      end
      pitgrowthrate = (beta*(alpha^(1/beta))*(pitsize^(1-(1/beta))));
      SIF = sigma_app*sqrt(pi()*pitsize);
      dadt690 = (C690*exp(-(Q/R)*((1/temp)-(1/Tref)))*(sigma_ys^m690)*((SIF-
SIFthreshold)^n690)*(H2^B690)); %calc dadt [m/s]
      if (SIF >= SIFthreshold)
        if (dadt690 >= pitgrowthrate)
          TTCtable(samp) = growthtime/3600;      %convert to hours
          numcrack = numcrack+1;
          cracksize = pitsize;
          cracktranstable(samp)=cracksize;
          break
        end
      end
    end
  end
  prefail690pittable(samp) = prefail;
  % toosmall690pittable(samp) = toosmall;
  numcrack690pittable(samp) = numcrack;
end
%Fraction of pits that propagate to cracks
totalprefails = sum(prefail690pittable);
fprintf('Number of Prefails = %d\n',totalprefails)
% totaltoosmalls = sum(toosmall690pittable);
% fprintf('Number of Toosmalls = %d\n',totaltoosmalls)
totalnumcracks = sum(numcrack690pittable);
totalnumpits = numsamp-totalprefails;
```

```
percentage = (totalnumcracks/totalnumpits)*100;
fprintf('There were %d cracks out of %d pits, which is %6.2f percent of pits\n',totalnumcracks,
totalnumpits, percentage);
%TTF distribution of transition from N to F stage
TTCtablecolumn = TTCtable(:);
TTCtablecolumn(isnan(TTCtablecolumn)) = [];
TTCmean = mean(TTCtablecolumn);
TTCvary = var(TTCtablecolumn);
%pdf development for 1 set of model parameters
%pd1=fitdist(TTCtablecolumn,'Normal');
%pd1=fitdist(TTCtablecolumn,'Exponential');
pd1=fitdist(TTCtablecolumn,'Kernel','Kernel','epanechnikov');
%LAMBDAN2F=1/(pd1.mu);
fprintf('Mean TTC = %f [hours] \n',TTCmean)
fprintf('TTC Variance = %f [hours] \n',TTCvary)
%fprintf('Crack Rate from New Stage = %f [1/hours] \n',LAMBDAN2F)
%fprintf('STD TTC= %f \n',pd1.sigma)
% addition for mean and variance for convergence check
alphavalue = 0.05;
gammavalue = 0.05;
statt = tinv(1-(alphavalue/2),(numsamp-1));
GAMMAFRAC=gammavalue/(1+gammavalue);
numsamplesreq=TTCvary*(statt^2)/((GAMMAFRAC*TTCmean)^2);
fprintf('Number of required simulations for time from flaw = %d\n',numsamplesreq);
delete(gcp('nocreate'));
```

D.2 PITTING TO CRACK TRANSITION CODE FOR DEVELOPMENT OF NEW TO FLAW TRANSITION RATE FOR STAINLESS STEEL

```
% LHS SCC Pit Growth Propagation Code
% Developer: Nick O'Shea
% Date: 7.6.16
%
==========================================================================
%
==========================================================================
% SECTION 1: Initialization
%
==========================================================================
%
==========================================================================
%Simulation Conditions
%p = parpool('local', 2);
numsamp = 500;
deltagrowthtime = 1;               %step-time in [s] (3600s = 1hr)
Maxruntimeinyears = 60;               %max run time for the code in years
```

```
myCluster=parcluster('local');
myCluster.NumWorkers = 2;
saveProfile(myCluster);
parpool(myCluster, 2);
%parpool('size');
%Variable initialization
minpit = 2.5E-5;                    %min pit size
alphamin = 9.59166E-09;
alphamax = 2.82489E-07;
beta = 0.5;                         %initialize beta parameter for sample growth size of pits
%[percent] CW by Rolling for exp trans region
sigma_ys = 263.75;          %[MPa] calculate yield strength
sigma_app = 430;                    %[MPa] total effective stress (applied+residual) exp trans
region
%SCC Constants
SIFthreshold = 10;                  %[MPasqrt(m)] SIF when SCC crack propagation begins
Tref = 598.15;                      %[Kelvin] Normalize to 325C
Q = 84;                             %kJ/mol for Alloy 690
R = 0.008314;                       %[kJ/mol-K] Boltzmann constant
temp = 598.15;                      %[K] temperature of primary water 325
CSSpittable = nan(numsamp,1);
nSSpittable = nan(numsamp,1);
mSSpittable = nan(numsamp,1);
alphaSSpittable = nan(numsamp,1);
betaSSpittable = nan(numsamp,1);
prefailSSpittable = nan(numsamp,1);
toosmallSSpittable = nan(numsamp,1);
numcrackSSpittable = nan(numsamp,1);
TTCtable = nan(numsamp,1);              %data matrix for TTF tracking
initpittable = nan(numsamp,1);          %data matrix for initial pit size
cracktranstable = nan(numsamp,1);       %data matrix for tracking transition size of flaw/crack
initpitvaluetable = nan(numsamp,1);
Maximumruntime = Maxruntimeinyears*365.25*24*60*60;
%years*days*hours*minutes*seconds
%Fitting Weibull distribution to Turnbull Data at 15,402 hours
numbin = [5,16,33,22,19,10,3,2,2,1];
binbounds = [20,40,60,80,100,120,140,160,180,200,220];      %microns
totalinitpits = sum(numbin);
initpitdatatable = nan(max(size(numbin)),max(numbin));
for pout = 1:max(size(numbin))
   for pin = 1:numbin(pout)
      initpitdatatable(pout,pin) = (binbounds(pout)+(rand*(binbounds((pout+1))-
binbounds(pout))))*(1E-6);
   end
end
initpitdatatablecolumn = initpitdatatable(:);
```

```
initpitdatatablecolumn(isnan(initpitdatatablecolumn)) = [];
pdW=fitdist(initpitdatatablecolumn,'Weibull');
WeibullA = 1/((pdW.A)^(pdW.B));
WeibullB = pdW.B;
%
==================================================================
%
==================================================================
% SECTION 2: Generate Samples
%
==================================================================
%
==================================================================
%Crack model parameters
load('SSparams.mat');     %#,C,m,n,B,s
[datalength, ~] = size(SSparams);
alphadist = makedist('Uniform','lower',alphamin,'upper',alphamax);
randalphadist = random(alphadist,datalength,1);
SSparams = [SSparams randalphadist];
randpitdist = random(pdW,datalength,1);
SSparams = [SSparams randpitdist];
[datalength, numvar] = size(SSparams);
rng shuffle;
randnummatrix = rand(numsamp,numvar);
samplematrix = zeros(numsamp,numvar);
for j = 1:numvar
   idx = randperm(numsamp)';
   Pmatrix = ((idx-randnummatrix(:,j))/numsamp).*100;
   samplematrix(:,j) = prctile(SSparams(:,j),Pmatrix); %#,C,m,n,Beta(CPR),s,alpha,initpit
end
parfor samp = 1:numsamp
   remainder = rem(samp,10);
   if remainder == 0
      fprintf('Sample: %d\n',samp)
   end
   dt = deltagrowthtime;
   prefail = 0;              %reset too large sample counter
   toosmall = 0;
   numcrack = 0;
   growthtime = 0;            %reset growth time for each sample
   checker = 0;
   cracksize = nan;
   alpha = samplematrix(samp,7);
   CSS = samplematrix(samp,2);
   mSS = samplematrix(samp,3);
   nSS = samplematrix(samp,4);
```

```
    %record model parameter selection
    CSSpittable(samp) = CSS;
    nSSpittable(samp) = nSS;
    mSSpittable(samp) = mSS;
    alphaSSpittable(samp) = alpha;
    betaSSpittable(samp) = beta;
    pitsize = samplematrix(samp,8);
    initpitvaluetable(samp,1) = pitsize;
    SIF = sigma_app*sqrt(pi()*pitsize);
    pitgrowthrate = (beta*(alpha^(1/beta))*(pitsize^(1-(1/beta)))); %[m/s]
    dadt_SS = (CSS*exp(-(Q/R)*((1/temp)-(1/Tref)))*(sigma_ys^mSS)*((SIF-
SIFthreshold)^nSS)); %calc dadt [m/s]
    %Check for Initial Pit Out of Acceptable Range
    if ((abs(real(dadt_SS)) >= pitgrowthrate) && (SIF >= SIFthreshold))
        %if ((dadt690 >= pitgrowthrate) && (SIF >= SIFthreshold))
        prefail = prefail+1;
    end
    %pit propagation loop
    if prefail == 0
        while (growthtime < Maximumruntime)
            pitgrowth = pitgrowthrate*dt;
            pitsize = pitsize+pitgrowth;
            growthtime = growthtime+dt;
            if (growthtime>=1*3600) && (growthtime<(1*3600+3600))
                dt = 3600;
                %fprintf('dt: %d\n',dt)
            elseif (growthtime>=240*3600) && (growthtime<(240*3600+10800))
                dt = 10800;
                %fprintf('dt: %d\n',dt)
            elseif (growthtime>=720*3600) && (growthtime<(720*3600+21600))
                dt = 21600;
                %fprintf('dt: %d\n',dt)
            elseif (growthtime>=4320*3600) && (growthtime<(4320*3600+43200))
                dt = 43200;
                %fprintf('dt: %d\n',dt)
            elseif (growthtime>=8640*3600) && (growthtime<(8640*3600+86400))
                dt = 86400;
                %fprintf('dt: %d\n',dt)
            elseif (growthtime>=17280*3600) && (growthtime<(17280*3600+172800))
                dt = 172800;
                %fprintf('dt: %d\n',dt)
            end
            pitgrowthrate = (beta*(alpha^(1/beta))*(pitsize^(1-(1/beta))));
            SIF = sigma_app*sqrt(pi()*pitsize);
            dadt_SS = (CSS*exp(-(Q/R)*((1/temp)-(1/Tref)))*(sigma_ys^mSS)*((SIF-
SIFthreshold)^nSS)); %calc dadt [m/s]
```

```
            if (SIF >= SIFthreshold)
                if (dadt_SS >= pitgrowthrate)
                    TTCtable(samp) = growthtime/3600;         %convert to hours
                    numcrack = numcrack+1;
                    cracksize = pitsize;
                    cracktranstable(samp)=cracksize;
                    break
                end
            end
        end
    end
    prefailSSpittable(samp) = prefail;
    % toosmall690pittable(samp) = toosmall;
    numcrackSSpittable(samp) = numcrack;
end
%Fraction of pits that propagate to cracks
totalprefails = sum(prefailSSpittable);
fprintf('Number of Prefails = %d\n',totalprefails)
% totaltoosmalls = sum(toosmall690pittable);
% fprintf('Number of Toosmalls = %d\n',totaltoosmalls)
totalnumcracks = sum(numcrackSSpittable);
totalnumpits = numsamp-totalprefails;
percentage = (totalnumcracks/totalnumpits)*100;
fprintf('There were %d cracks out of %d pits, which is %6.2f percent of pits\n',totalnumcracks,
totalnumpits, percentage);
%TTF distribution of transition from N to F stage
TTCtablecolumn = TTCtable(:);
TTCtablecolumn(isnan(TTCtablecolumn)) = [];
TTCmean = mean(TTCtablecolumn);
TTCvary = var(TTCtablecolumn);
%pdf development for 1 set of model parameters
%pd1=fitdist(TTCtablecolumn,'Normal');
%pd1=fitdist(TTCtablecolumn,'Exponential');
pd1=fitdist(TTCtablecolumn,'Kernel','Kernel','epanechnikov');
%LAMBDAN2F=1/(pd1.mu);
fprintf('Mean TTC = %f [hours] \n',TTCmean)
fprintf('TTC Variance = %f [hours] \n',TTCvary)
%fprintf('Crack Rate from New Stage = %f [1/hours] \n',LAMBDAN2F)
%fprintf('STD TTC= %f \n',pd1.sigma)
% addition for mean and variance for convergence check
alphavalue = 0.05;
gammavalue = 0.05;
statt = tinv(1-(alphavalue/2),(numsamp-1));
GAMMAFRAC=gammavalue/(1+gammavalue);
numsamplesreq=TTCvary*(statt^2)/((GAMMAFRAC*TTCmean)^2);
fprintf('Number of required simulations for time from flaw = %d\n',numsamplesreq);
```

```
delete(gcp('nocreate'));
```

D.3 STRESS CORROSION CRACKING PROPAGATION CODE FOR DEVELOPING FLAW TO LEAK, FLAW TO RUPTURE, AND LEAK TO RUPTURE TRANSITION RATES FOR ALLOY 690

```
% Crack Propagation MATLAB Code for SCC Alloy 690 using LHS
% Developer: Nick O'Shea
% Date: 6.27.16
%
=====================================================================
%
=====================================================================
% SECTION 1: Initialization
%
=====================================================================
%
=====================================================================
% Simulation conditions
% p = parpool('local', 2);
numsamp = 100;
myCluster = parcluster('local');
myCluster.NumWorkers = 2;
saveProfile(myCluster);
parpool(myCluster, 2);
timestep = 3600;                    % seconds to one loop 3600 = 1 hour
prefailtable = nan(numsamp,1);
noproptable = nan(numsamp,1);
NOFAILtable = nan(numsamp,1);
numF2Ltable = nan(numsamp,1);
numF2Rtable = nan(numsamp,1);
numL2Rtable = nan(numsamp,1);
LNORtable = nan(numsamp,1);
datamean = nan(numsamp,1);
difftable = nan(numsamp,1);
datamean2 = nan(numsamp,1);
difftable2 = nan(numsamp,1);
datatable = nan(numsamp,1);     % data matrix for TTF tracking
L2Rtable = nan(numsamp,1);      % data matric for L2R time storage
%temp_L2Rtable = zeros(numsamp,1);
maxtime = 60*365.25*24*60*60;               % max time set to 60 years
%Steam Generator Tube Information
thickness = 0.002;                  %[m] thickness of tube
Radius = 0.0155/2;                  %[m] tube inside radius for use in failure code
CW = 2;                             %[percent] CW by Rolling for exp trans region
sigma_ys = (CW*20.283)+296.61;          %[MPa] calculate yield strength
```

```
sigma_uts = 709;                %[MPa] ultimate tensile stress
sigma_app = 430;        %[MPa] total effective stress (applied+residual) exp trans region
%Primary Coolant Information
H2 = 26;                %[cc/kg] Hydrogen concentration of primary water environment
temp = 598.15;                  %[K] temperature of primary water 325
p_pressure = 17.24;             %[MPa] primary side pressure
s_pressure = 5.67;              %[MPa] secondary side pressure
d_pressure = p_pressure - s_pressure;     %[MPa] pressure differential
% SCC Constants
Kth = 9;                        %[MPaROOT(m)] threshold SCC intensity factor
Tref = 598.15;                  %[Kelvin] Normalize to 325C
Q = 120;                        %kJ/mol for Alloy 690
R = 0.008314;                   %[kJ/mol-K] Boltzmann constant
%
==========================================================================
%
==========================================================================
% SECTION 2: Generate Samples
%
==========================================================================
%
==========================================================================
% Load model parameter distributions for Alloy 690
load('Alloy690params.mat');   %#,C,m,n,B,s,adding crack size
[datalength, ~] = size(Alloy690params);
initcrackdist = makedist('Gamma','a',3.393,'b',1.395);
maxcracklength = 2*(2/0.24);   %mm (2*c=length)(2mm max crack depth)(0.24 max aspect
ratio(a/c))
truncinitcrackdist = truncate(initcrackdist,0,maxcracklength);     %[mm]
randinitcrackdist = random(truncinitcrackdist,datalength,1);
randinitcrackdist = randinitcrackdist./1000;   %convert to m
randinitcrackdist = randinitcrackdist./2;      %convert to half length
Alloy690params = [Alloy690params randinitcrackdist];
[datalength, numvar] = size(Alloy690params);
rng shuffle;
randnummatrix = rand(numsamp,numvar);
samplematrix = zeros(numsamp,numvar);
for j = 1:numvar
   idx = randperm(numsamp)';
   Pmatrix = ((idx-randnummatrix(:,j))/numsamp).*100;
   samplematrix(:,j) = prctile(Alloy690params(:,j),Pmatrix); %#,C,m,n,Beta,s, c_initial
end
%
==========================================================================
%
==========================================================================
```

```
% SECTION 3: Building Time-To-100%TW Iteration Loop
%
===========================================================================
%
===========================================================================
parfor samp = 1:numsamp
    remainder = rem(samp,10);
    if remainder == 0
        fprintf('Sample: %d\n',samp);
    end
    prefail = 0;             % number of flaws that already failed
    noprop = 0;              % number of flaws that do not propagate via SCC
    NOFAIL = 0;              % number of flaws that propagate but do not fail in 60 years
    numfail_F2L = 0;         % number of flaws that fail by leak
    numfail_F2R = 0;         % number of flaws that fail by rupture
    numfail_L2R = 0;         % number of flaws that fail by leak and then rupture
    LNOR = 0;                % number of flaws that fail by leak but not rupture
    fail_F2L = 0;
    fail_F2R = 0;
    fail_L2R = 0;
    L2Rtime  = 0;
    C690 = samplematrix(samp,2);
    m690 = samplematrix(samp,3);
    n690 = samplematrix(samp,4);
    B690 = samplematrix(samp,5);
    c_initial = samplematrix(samp,7);
    aspectratio=random('unif',0.24,0.35);
    a_initial=c_initial*aspectratio;
    fail = checkFail690(a_initial,c_initial,sigma_ys,thickness,sigma_uts,d_pressure,Radius);
    K_initial=(sigma_app*sqrt(pi()*a_initial));
    if fail == 1
        prefail = prefail+1;
    elseif K_initial<Kth
        noprop = noprop+1;
        fail = 1;      %sample does not fail, but done to avoid propagation loop
    end
    time = 0;
    dt = timestep;
    a = a_initial;
    c = c_initial;
    %Crack propagation loop
    while(fail==0)
        K=sigma_app*sqrt(pi()*a);
        dadt_690 = (C690*exp(-(Q/R)*((1/temp)-(1/Tref)))*(sigma_ys^m690)*((K-
Kth)^n690)*(H2^B690)); %calc dadt [m/s]
        random_ac=random('unif',0.24,0.35);
```

```
        dcdt=dadt_690/random_ac;
        da=dadt_690*dt;
        dc=dcdt*dt;
        a=a+da;
        c=c+dc;
        time=time+dt;
        if (time>=(10000*3600)) && (time<(10000*3600)+10800)
          dt = 10800;           %increase step time to 3 hours
        elseif (time>=(20000*3600)) && (time<(20000*3600)+21600)
          dt = 21600;           %increase step time to 6 hours
        elseif (time>=(40000*3600)) && (time<(40000*3600)+43200)
          dt = 43200;           %increase step time to 12 hours
        elseif (time>=(80000*3600)) && (time<(80000*3600)+86400)
          dt = 86400;           %increase step time to 24 hours
        elseif (time>=(100000*3600)) && (time<(100000*3600)+172800)
          dt = 172800;          %increase step time to 48 hours
        end
        if (time >= maxtime)
          NOFAIL=NOFAIL+1;
          break
        end
        [fail_F2L, fail_F2R,
fail]=checkFailure_690(a,c,sigma_ys,thickness,sigma_uts,d_pressure,Radius);
        %Enter the Leak to Rupture Simulation
        if (fail_F2L == 1)
          numfail_F2L = numfail_F2L + 1;
          fail_L2R = 0;
          time_L2R = 0;
          dt = timestep;
          K = sigma_app*sqrt(pi()*a);          %calculate K with a=thickness
          dadt_690 = (C690*exp(-(Q/R)*((1/temp)-(1/Tref)))*(sigma_ys^m690)*((K-Kth)^n690));
%calc dadt [m/s]
          while (fail_L2R==0)
            random_ac = random('unif',0.24,0.35);
            dcdt = dadt_690/random_ac;
            dc = dcdt*dt;
            c = c + dc;
            time_L2R = time_L2R + dt;
            if (time_L2R>=(10000*3600)) && (time_L2R<(10000*3600)+10800)
              dt = 10800;          %increase step time to 3 hours
            elseif (time_L2R>=(20000*3600)) && (time_L2R<(20000*3600)+21600)
              dt = 21600;          %increase step time to 6 hours
            elseif (time_L2R>=(40000*3600)) && (time_L2R<(40000*3600)+43200)
              dt = 43200;          %increase step time to 12 hours
            elseif (time_L2R>=(80000*3600)) && (time_L2R<(80000*3600)+86400)
              dt = 86400;          %increase step time to 24 hours
```

```
            elseif (time_L2R>=(100000*3600)) && (time_L2R<(100000*3600)+172800)
                dt = 172800;            %increase step time to 48 hours
            end
            if time_L2R>(maxtime-time)
                LNOR=LNOR + 1;
                break
            end
            fail_L2R = checkfail_L2R_690(c,sigma_ys,thickness,sigma_uts,d_pressure,Radius);
        end
        if (fail_L2R==1)
            numfail_L2R = numfail_L2R +1;
        end
        L2Rttf = time_L2R/3600;
        L2Rtable(samp) = L2Rttf;
    end
    if (fail_F2R == 1)
        numfail_F2R = numfail_F2R + 1;
    end
  end
  if (prefail == 1)||(noprop == 1)
    datatable(samp) = nan;
  else
    ttf=(time/3600);                %convert time to hours
    datatable(samp)=ttf;
  end
  prefailtable(samp)=prefail;
  noproptable(samp)=noprop;
  NOFAILtable(samp)=NOFAIL;
  numF2Ltable(samp)=numfail_F2L;
  numF2Rtable(samp)=numfail_F2R;
  numL2Rtable(samp)=numfail_L2R;
  LNORtable(samp)=LNOR;
end
prefailtotal=sum(prefailtable);
noproptotal=sum(noproptable);
NOFAILTOTAL=sum(NOFAILtable);
totalleaks=sum(numF2Ltable);
totalruptures=sum(numF2Rtable);
totalL2R=sum(numL2Rtable);
totalLnotR=sum(LNORtable);
fprintf('Total Number of Prefails: %d\n',prefailtotal);
fprintf('Total Number of Noprops: %d\n',noproptotal);
fprintf('Total Number of Non-failures: %d\n',NOFAILTOTAL);
fprintf('Total Number of Ruptures: %d\n',totalruptures);
fprintf('Total Number of Leaks: %d\n',totalleaks);
fprintf('Total Number of Leaks to Ruptures: %d\n',totalL2R);
```

```
fprintf('Total Number of Leaks never Rupture: %d\n',totalLnotR);
datatablecolumn=datatable(:);
datatablecolumn(isnan(datatablecolumn))=[];
totalmean = mean(datatablecolumn);
% Cumulative/Aggregated PDF
pd2=fitdist(datatablecolumn,'Exponential');
LAMBDA=1/(pd2.mu);
fprintf('Aggregated Mean TTF = %f [hours] \n',pd2.mu)
fprintf('Aggregated Failure Rate from Flaw Stage = %f [1/hours] \n',LAMBDA)
if (totalleaks > 0)
   %PDF of times for L2R
   L2Rtablecolumn=L2Rtable(:);
   L2Rtablecolumn(isnan(L2Rtablecolumn))=[];
   L2Rtotalmean = mean(L2Rtablecolumn);
   pd3=fitdist(L2Rtablecolumn,'Exponential');
   LAMBDAL2R=1/(pd3.mu);
   fprintf('Mean TTR Given Leak State = %f [hours] \n',pd3.mu)
   fprintf('Rupture Rate from Leak Stage = %f [1/hours] \n',LAMBDAL2R)
end
% addition for mean and variance for convergence check
finalsamp = numsamp-(prefailtotal+noproptotal);
varianceoutput = var(datatablecolumn);
varianceoutput2 = var(L2Rtablecolumn);
fprintf('Mean of TTF data out of F = %f hours\n',totalmean);
fprintf('Variance of TTF data out of F = %f \n',varianceoutput);
fprintf('Mean of TTF L2R data out of F = %f hours\n',L2Rtotalmean);
fprintf('Variance of TTF L2R data out of F = %f \n',varianceoutput2);
alphavalue = 0.05;
gammavalue = 0.05;
statt = tinv(1-(alphavalue/2),(numsamp-1));
GAMMAFRAC=gammavalue/(1+gammavalue);
numsamplesreq=varianceoutput*(statt^2)/((GAMMAFRAC*totalmean)^2);
fprintf('Number of required simulations for time from flaw = %d\n',numsamplesreq);
numsamplesreq2=varianceoutput2*(statt^2)/((GAMMAFRAC*L2Rtotalmean)^2);
fprintf('Number of required simulations for L2R = %d\n',numsamplesreq2);
delete(gcp('nocreate'));
```

D.4 STRESS CORROSION CRACKING PROPAGATION CODE FOR DEVELOPING FLAW TO LEAK, FLAW TO RUPTURE, AND LEAK TO RUPTURE TRANSITION RATES FOR STAINLESS STEEL

```
% Crack Propagation MATLAB Code for SCC SS using LHS
% Developer: Nick O'Shea
% Date: 6.28.16
%
==================================================================
```

```
%
==================================================================
% SECTION 1: Initialization
%
==================================================================
%
==================================================================
% Simulation conditions
% p = parpool('local', 2);
numsamp = 10;
myCluster = parcluster('local');
myCluster.NumWorkers = 2;
saveProfile(myCluster);
parpool(myCluster, 2);
timestep = 3600;                          % seconds to one loop 3600 = 1 hour
prefailtable = nan(numsamp,1);
noproptable = nan(numsamp,1);
NOFAILtable = nan(numsamp,1);
numF2Ltable = nan(numsamp,1);
numF2Rtable = nan(numsamp,1);
numL2Rtable = nan(numsamp,1);
LNORtable = nan(numsamp,1);
datamean = nan(numsamp,1);
difftable = nan(numsamp,1);
datamean2 = nan(numsamp,1);
difftable2 = nan(numsamp,1);
datatable = nan(numsamp,1);      % data matrix for TTF tracking
L2Rtable = nan(numsamp,1);       % data matric for L2R time storage
maxtime = 60*365.25*24*60*60;                 % max time set to 60 years
%Steam Generator Tube Information
thickness = 0.002;                        %[m] thickness of tube
Radius = 0.0155/2;                        %[m] tube inside radius for use in failure code
%CW = 2;                                  %[percent] CW by Rolling for exp trans region
%sigma_ys = (CW*20.283)+296.61;            %[MPa] calculate yield strength
sigma_ys = 263.75;                        %[MPa] calculate yield strength from Table 3 Terachi paper
sigma_uts = 709;                          %[MPa] ultimate tensile stress
sigma_app = 430;           %[MPa] total effective stress (applied+residual) exp trans region
%Primary Coolant Information
H2 = 26;                   %[cc/kg] Hydrogen concentration of primary water environment
temp = 598.15;                            %[K] temperature of primary water 325
p_pressure = 17.24;                       %[MPa] primary side pressure
s_pressure = 5.67;                        %[MPa] secondary side pressure
d_pressure = p_pressure - s_pressure;       %[MPa] pressure differential
% SCC Constants
Kth = 10;                                 %[MPaROOT(m)] threshold SCC intensity factor
Tref = 598.15;                            %[Kelvin] Normalize to 325C
```

```
Q = 84;                                %kJ/mol for Alloy 690
R = 0.008314;                          %[kJ/mol-K] Boltzmann constant
%
==========================================================================
%
==========================================================================
% SECTION 2: Generate Samples
%
==========================================================================
%
==========================================================================
% Load model parameter distributions for Alloy 690
load('SSparams.mat');     %#,C,m,n,~,s,adding crack size
[datalength, ~] = size(SSparams);
initcrackdist = makedist('Gamma','a',3.393,'b',1.395);
maxcracklength = 2*(2/0.24);    %mm (2*c=length)(2mm max crack depth)(0.24 max aspect
ratio(a/c))
truncinitcrackdist = truncate(initcrackdist,0,maxcracklength);        %[mm]
randinitcrackdist = random(truncinitcrackdist,datalength,1);
randinitcrackdist = randinitcrackdist./1000;    %convert to m
randinitcrackdist = randinitcrackdist./2;        %convert to half length
SSparams = [SSparams randinitcrackdist];
[datalength, numvar] = size(SSparams);
rng shuffle;
randnummatrix = rand(numsamp,numvar);
samplematrix = zeros(numsamp,numvar);
for j = 1:numvar
   idx = randperm(numsamp)';
   Pmatrix = ((idx-randnummatrix(:,j))/numsamp).*100;
   samplematrix(:,j) = prctile(SSparams(:,j),Pmatrix); %#,C,m,n,Beta,s, c_initial
end
%
==========================================================================
%
==========================================================================
% SECTION 2: Building Time-To-100%TW Iteration Loop
%
==========================================================================
%
==========================================================================
parfor samp = 1:numsamp
   remainder = rem(samp,10);
   if remainder == 0
      fprintf('Sample: %d\n',samp);
   end
   prefail = 0;               % number of flaws that already failed
```

```
    noprop = 0;                 % number of flaws that do not propagate via SCC
    NOFAIL = 0;                 % number of flaws that propagate but do not fail in 60 years
    numfail_F2L = 0;            % number of flaws that fail by leak
    numfail_F2R = 0;            % number of flaws that fail by rupture
    numfail_L2R = 0;            % number of flaws that fail by leak and then rupture
    LNOR = 0;                   % number of flaws that fail by leak but not rupture
    fail_F2L = 0;
    fail_F2R = 0;
    fail_L2R = 0;
    L2Rtime  = 0;
    CSS = samplematrix(samp,2);
    mSS = samplematrix(samp,3);
    nSS = samplematrix(samp,4);
    c_initial = samplematrix(samp,7);
    aspectratio=random('unif',0.24,0.35);
    a_initial=c_initial*aspectratio;
    fail = checkFailSS(a_initial,c_initial,sigma_ys,thickness,d_pressure,Radius,sigma_uts);
    K_initial=(sigma_app*sqrt(pi()*a_initial));
    if fail == 1
       prefail = prefail+1;
    elseif K_initial<Kth
       noprop = noprop+1;
       fail = 1;      %sample does not fail, but done to avoid propagation loop
    end
    time = 0;
    dt = timestep;
    a = a_initial;
    c = c_initial;
    %Crack propagation loop
    while(fail==0)
       K=sigma_app*sqrt(pi()*a);
       dadt_SS = (CSS*exp(-(Q/R)*((1/temp)-(1/Tref)))*(sigma_ys^mSS)*((K-Kth)^nSS)); %calc
dadt [m/s]
       random_ac=random('unif',0.24,0.35);
       dcdt=dadt_SS/random_ac;
       da=dadt_SS*dt;
       dc=dcdt*dt;
       a=a+da;
       c=c+dc;
       time=time+dt;
       if (time>=(10000*3600)) && (time<(10000*3600)+10800)
          dt = 10800;                %increase step time to 3 hours
       elseif (time>=(20000*3600)) && (time<(20000*3600)+21600)
          dt = 21600;                %increase step time to 6 hours
       elseif (time>=(40000*3600)) && (time<(40000*3600)+43200)
          dt = 43200;                %increase step time to 12 hours
```

```
    elseif (time>=(80000*3600)) && (time<(80000*3600)+86400)
      dt = 86400;            %increase step time to 24 hours
    elseif (time>=(100000*3600)) && (time<(100000*3600)+172800)
      dt = 172800;           %increase step time to 48 hours
    end
    if (time >= maxtime)
      NOFAIL=NOFAIL+1;
      break
    end
    [fail_F2L, fail_F2R,
fail]=checkFailure_SS(a,c,sigma_ys,thickness,sigma_uts,d_pressure,Radius);
    %Enter the Leak to Rupture Simulation
    if (fail_F2L == 1)
      numfail_F2L = numfail_F2L + 1;
      fail_L2R = 0;
      time_L2R = 0;
      dt = timestep;
      K = sigma_app*sqrt(pi()*a);          %calculate K with a=thickness
      dadt_SS = (CSS*exp(-(Q/R)*((1/temp)-(1/Tref)))*(sigma_ys^mSS)*((K-Kth)^nSS));
%calc dadt [m/s]
      while (fail_L2R==0)
        random_ac = random('unif',0.24,0.35);
        dcdt = dadt_SS/random_ac;
        dc = dcdt*dt;
        c = c + dc;
        time_L2R = time_L2R + dt;
        if (time_L2R>=(10000*3600)) && (time_L2R<(10000*3600)+10800)
          dt = 10800;          %increase step time to 3 hours
        elseif (time_L2R>=(20000*3600)) && (time_L2R<(20000*3600)+21600)
          dt = 21600;          %increase step time to 6 hours
        elseif (time_L2R>=(40000*3600)) && (time_L2R<(40000*3600)+43200)
          dt = 43200;          %increase step time to 12 hours
        elseif (time_L2R>=(80000*3600)) && (time_L2R<(80000*3600)+86400)
          dt = 86400;          %increase step time to 24 hours
        elseif (time_L2R>=(100000*3600)) && (time_L2R<(100000*3600)+172800)
          dt = 172800;         %increase step time to 48 hours
        end
        if time_L2R>(maxtime-time)
          LNOR=LNOR + 1;
          break
        end
        fail_L2R = checkfail_L2R_SS(a,c,sigma_ys,thickness,sigma_uts,d_pressure,Radius);
      end
      if (fail_L2R==1)
        numfail_L2R = numfail_L2R +1;
      end
```

```
            L2Rttf = time_L2R/3600;
            L2Rtable(samp) = L2Rttf;
        end
        if (fail_F2R == 1)
            numfail_F2R = numfail_F2R + 1;
        end
    end
    if (prefail == 1)||(noprop == 1)
        datatable(samp) = nan;
    else
        ttf=(time/3600);                    %convert time to hours
        datatable(samp)=ttf;
    end
    prefailtable(samp)=prefail;
    noproptable(samp)=noprop;
    NOFAILtable(samp)=NOFAIL;
    numF2Ltable(samp)=numfail_F2L;
    numF2Rtable(samp)=numfail_F2R;
    numL2Rtable(samp)=numfail_L2R;
    LNORtable(samp)=LNOR;
end
prefailtotal=sum(prefailtable);
noproptotal=sum(noproptable);
NOFAILTOTAL=sum(NOFAILtable);
totalleaks=sum(numF2Ltable);
totalruptures=sum(numF2Rtable);
totalL2R=sum(numL2Rtable);
totalLnotR=sum(LNORtable);
fprintf('Total Number of Prefails: %d\n',prefailtotal);
fprintf('Total Number of Noprops: %d\n',noproptotal);
fprintf('Total Number of Non-failures: %d\n',NOFAILTOTAL);
fprintf('Total Number of Ruptures: %d\n',totalruptures);
fprintf('Total Number of Leaks: %d\n',totalleaks);
fprintf('Total Number of Leaks to Ruptures: %d\n',totalL2R);
fprintf('Total Number of Leaks never Rupture: %d\n',totalLnotR);
datatablecolumn=datatable(:);
datatablecolumn(isnan(datatablecolumn))=[];
totalmean = mean(datatablecolumn);
% Cumulative/Aggregated PDF
pd2=fitdist(datatablecolumn,'Exponential');
LAMBDA=1/(pd2.mu);
fprintf('Aggregated Mean TTF = %f [hours] \n',pd2.mu)
fprintf('Aggregated Failure Rate from Flaw Stage = %f [1/hours] \n',LAMBDA)
if (totalleaks > 0)
    %PDF of times for L2R
    L2Rtablecolumn=L2Rtable(:);
```

```
    L2Rtablecolumn(isnan(L2Rtablecolumn))=[];
    L2Rtotalmean = mean(L2Rtablecolumn);
    pd3=fitdist(L2Rtablecolumn,'Exponential');
    LAMBDAL2R=1/(pd3.mu);
    fprintf('Mean TTR Given Leak State = %f [hours] \n',pd3.mu)
    fprintf('Rupture Rate from Leak Stage = %f [1/hours] \n',LAMBDAL2R)
end
% addition for mean and variance for convergence check
finalsamp = numsamp-(prefailtotal+noproptotal);
varianceoutput = var(datatablecolumn);
varianceoutput2 = var(L2Rtablecolumn);
fprintf('Mean of TTF data out of F = %f hours\n',totalmean);
fprintf('Variance of TTF data out of F = %f \n',varianceoutput);
fprintf('Mean of TTF L2R data out of F = %f hours\n',L2Rtotalmean);
fprintf('Variance of TTF L2R data out of F = %f \n',varianceoutput2);
alphavalue = 0.05;
gammavalue = 0.05;
statt = tinv(1-(alphavalue/2),(numsamp-1));
GAMMAFRAC=gammavalue/(1+gammavalue);
numsamplesreq=varianceoutput*(statt^2)/((GAMMAFRAC*totalmean)^2);
fprintf('Number of required simulations for time from flaw = %d\n',numsamplesreq);
numsamplesreq2=varianceoutput2*(statt^2)/((GAMMAFRAC*L2Rtotalmean)^2);
fprintf('Number of required simulations for L2R = %d\n',numsamplesreq2);
delete(gcp('nocreate'));
```

D.5 STRESS CORROSION CRACKING PROPAGATION FAILURE FUNCTIONS FOR TESTING SAMPLE TRANSITION BETWEEN FLAW, LEAK, AND RUPTURE STATES FOR ALLOY 690

```
% checkFail() determines if the tube has failed 100%TW
%
==========================================================================
function fail = checkFail690(a,c,sigma_ys,thickness,sigma_uts,d_pressure,Radius)
% Steam Generator Assumptions/Constants
sigma_bar = 0.5*(sigma_uts+sigma_ys);
Pb = sigma_bar*log(1+(thickness/Radius)); % failure pressure for unflawed tube
% determine pressure required to fail remaining ligament. does not
% mean that the tube will burst (fish-mouth) at this pressure
Rm = Radius+(thickness/2);
lamda = (1.82*c)/sqrt(Rm*thickness);
m1 = 0.614 + 0.481*lamda + 0.386*exp(-1.25*lamda);
alpha = 1 + 0.9*(a/thickness)*(a/thickness)*(1 - 1/m1);
mp = (1-(alpha*a/(m1*thickness)))/(1-(a/thickness));
Pcr = Pb/m1;
Psc = Pb/mp;
%ASME Burst (NUREG-6365)
```

```
m2 = sqrt(1 + 1.61*(c*c)/(Radius*thickness));
exp1 = ((thickness/a) - 1)/((thickness/a) - (1/m2));
Pb_ASME = (thickness/Radius)*(3*sigma_bar)*exp1;
if (a > thickness)
   fail = 1;
end
if (a <= thickness)
   if (Psc < d_pressure)
      fail = 1;
   elseif (Pcr < d_pressure)
      fail = 1;
   elseif (Pb_ASME < d_pressure)
      fail = 1;
   else
      fail = 0;
   end
end
end

% checkFailure_690 determines if the tube has failed (leak or rupture) for Alloy 690
% Date: 3/23/16
%
=================================================================
function [fail_F2L, fail_F2R, fail] =
checkFailure_690(a,c,sigma_ys,thickness,sigma_uts,d_pressure,Radius)
% Steam GeneRadiusator Assumptions/Constants
sigma_bar = 0.5*(sigma_uts+sigma_ys);
Pb = sigma_bar*log(1+(thickness/Radius)); % failure pressure for unflawed tube
% determine pressure required to fail remaining ligament. does not
% mean that the tube will burst (fish-mouth) at this pressure
Rm = Radius+(thickness/2);
lamda = (1.82*c)/sqrt(Rm*thickness);
m1 = 0.614 + 0.481*lamda + 0.386*exp(-1.25*lamda);
alpha = 1 + 0.9*(a/thickness)*(a/thickness)*(1 - 1/m1);
mp = (1-(alpha*a/(m1*thickness)))/(1-(a/thickness));
Pcr = Pb/m1;
Psc = Pb/mp;
%ASME Burst (NUREG-6365)
m2 = sqrt(1 + 1.61*(c*c)/(Radius*thickness));
exp1 = ((thickness/a) - 1)/((thickness/a) - (1/m2));
Pb_ASME = (thickness/Radius)*(3*sigma_bar)*exp1;
% check for burst to rupture
if(Pb_ASME < d_pressure)
   fail_F2R = 1;
   fail_F2L = 0;
   fail = 1;
```

```
elseif (Pb_ASME >= d_pressure)
   fail_F2R = 0;
   %check for ligament pressure
   if(Psc < d_pressure)
      fail_F2L = 1;
      fail = 1;
      if (Pcr < Psc)
         fail_F2R = 1;
         fail_F2L = 0;
      end
   elseif (Psc >= d_pressure)
      fail_F2L = 0;
      fail = 0;
   end
end
end

% checkfail_L2R_690 determines if the tube has failed (leak or rupture) for Alloy 690
% Date: 3/29/16
%
==========================================================================
function [fail_L2R] = checkfail_L2R_690(c,sigma_ys,thickness,sigma_uts,d_pressure,Radius)

sigma_bar = 0.5*(sigma_uts+sigma_ys);
Pb = sigma_bar*log(1+(thickness/Radius)); % failure pressure for unflawed tube
% determine pressure required to fail remaining ligament. does not
% mean that the tube will burst (fish-mouth) at this pressure
Rm = Radius+(thickness/2);
lamda = (1.82*c)/sqrt(Rm*thickness);
m1 = 0.614 + 0.481*lamda + 0.386*exp(-1.25*lamda);
Pcr = Pb/m1;

if(Pcr < d_pressure)
   fail_L2R = 1;
elseif (Pcr > d_pressure)
   fail_L2R = 0;
end

end
```

D.6 STRESS CORROSION CRACKING PROPAGATION FAILURE FUNCTIONS FOR TESTING SAMPLE TRANSITION BETWEEN FLAW, LEAK, AND RUPTURE STATES FOR STAINLESS STEEL

```
% checkFail() determines if the tube has failed 100%TW
```

```
%
==============================================================================
function fail = checkFailSS(a,c,sigma_ys,thickness,d_pressure,Radius,sigma_uts)
%Modified B31G Rupture
DDD = 2.0*(Radius + thickness);
GGG = (c^4)/(DDD*thickness);
if( GGG <= 50)
   MMM = sqrt(1 + 0.6275*GGG - 0.003375*(GGG^2));
elseif( GGG > 50)
   MMM = 0.032*GGG + 3.3;
end
PfB31G =  2*(sigma_ys + 68.95)*thickness*((1 - 0.85*a/thickness)/(1 -
0.85*a/thickness/MMM))/DDD;
%Shell-92 L2R
M92=sqrt(1+((0.805*(c^4))/(DDD*thickness)));
Pf92=((1.8*thickness*sigma_uts)/DDD)*((1-(a/thickness))/(1-(a/(thickness*M92))));
%remaining ligament bursts leading to leak
sigma_bar = 0.5*(sigma_uts+sigma_ys);
Pb = sigma_bar*log(1+(thickness/Radius)); % failure pressure for unflawed tube
% determine pressure required to fail remaining ligament. does not
% mean that the tube will burst (fish-mouth) at this pressure
Rm = Radius+(thickness/2);
lamda = (1.82*c)/sqrt(Rm*thickness);
m1 = 0.614 + 0.481*lamda + 0.386*exp(-1.25*lamda);
alpha = 1 + 0.9*(a/thickness)*(a/thickness)*(1 - 1/m1);
mp = (1-(alpha*a/(m1*thickness)))/(1-(a/thickness));
Psc = Pb/mp;

if (a > thickness)
   fail = 1;
end
if (a <= thickness)
   if (PfB31G < d_pressure)
      fail = 1;
   elseif (Pf92 < d_pressure)
      fail = 1;
   elseif (Psc < d_pressure)
      fail = 1;
   else
      fail = 0;
   end
end
end

% checkFailure_SS determines if the tube has failed (leak or rupture) for Alloy 690
% Date: 5/25/16
```

```
% All rupture conditions for SS are modeled the same as 690 (different
% equations), but F=>L is simply using the a >= thickness condition as per
% NUREG-6986
%
================================================================
function [fail_F2L, fail_F2R, fail] =
checkFailure_SS(a,c,sigma_ys,thickness,sigma_uts,d_pressure,Radius)
%Modified B31G Rupture
DDD = 2.0*(Radius + thickness);
GGG = (c^4)/(DDD*thickness);
if( GGG <= 50)
   MMM = sqrt(1 + 0.6275*GGG - 0.003375*(GGG^2));
elseif( GGG > 50)
   MMM = 0.032*GGG + 3.3;
end
PfB31G =  2*(sigma_ys + 68.95)*thickness*((1 - 0.85*a/thickness)/(1 -
0.85*a/thickness/MMM))/DDD;
%Shell-92 L2R
M92=sqrt(1+((0.805*(c^4))/(DDD*thickness)));
Pf92=((1.8*thickness*sigma_uts)/DDD)*((1-(a/thickness))/(1-(a/(thickness*M92))));
%remaining ligament bursts leading to leak
%sigma_bar = 0.5*(sigma_uts+sigma_ys);
%Pb = sigma_bar*log(1+(thickness/Radius)); % failure pressure for unflawed tube
% determine pressure required to fail remaining ligament. does not
% mean that the tube will burst (fish-mouth) at this pressure
%Rm = Radius+(thickness/2);
%lamda = (1.82*c)/sqrt(Rm*thickness);
%m1 = 0.614 + 0.481*lamda + 0.386*exp(-1.25*lamda);
%alpha = 1 + 0.9*(a/thickness)*(a/thickness)*(1 - 1/m1);
%mp = (1-(alpha*a/(m1*thickness)))/(1-(a/thickness));
%Psc = Pb/mp;

if (PfB31G < d_pressure) || (Pf92 < d_pressure)
   fail_F2R = 1;
   fail_F2L = 0;
   fail = 1;
elseif (PfB31G >= d_pressure) && (Pf92 >= d_pressure)
   fail_F2R = 0;
%     if (Psc < d_pressure)
   if (a >= thickness)
      fail_F2L = 1;
      fail = 1;
   else
      fail_F2L = 0;
      fail = 0;
   end
```

```
end
end

% checkfail_L2R_SS determines if the tube has failed (leak or rupture) for
% SS
% Date: 3/29/16
%
=======================================================================
function [fail_L2R] = checkfail_L2R_SS(a,c,sigma_ys,thickness,sigma_uts,d_pressure,Radius)

%Modified B31G Rupture
DDD = 2.0*(Radius + thickness);
GGG = (c^4)/(DDD*thickness);
if( GGG <= 50)
   MMM = sqrt(1 + 0.6275*GGG - 0.003375*(GGG^2));
elseif( GGG > 50)
   MMM = 0.032*GGG + 3.3;
end
PfB31G =  2*(sigma_ys + 68.95)*thickness*((1 - 0.85*a/thickness)/(1 -
0.85*a/thickness/MMM))/DDD;
%Shell-92 L2R
M92=sqrt(1+((0.805*(c^4))/(DDD*thickness)));
Pf92=((1.8*thickness*sigma_uts)/DDD)*((1-(a/thickness))/(1-(a/(thickness*M92))));

if (PfB31G < d_pressure) || (Pf92 < d_pressure)
   fail_L2R = 1;
else
   fail_L2R = 0;
end
end
```